PB86-159480

REPORT NO.
UCB/EERC-85/13
DECEMBER 1985

EARTHQUAKE ENGINEERING RESEARCH CENTER

A METHODOLOGY FOR COMPUTER-AIDED DESIGN OF EARTHQUAKE-RESISTANT STEEL STRUCTURES

by

M. A. AUSTIN
K. S. PISTER
S. A. MAHIN

Report to the National Science Foundation

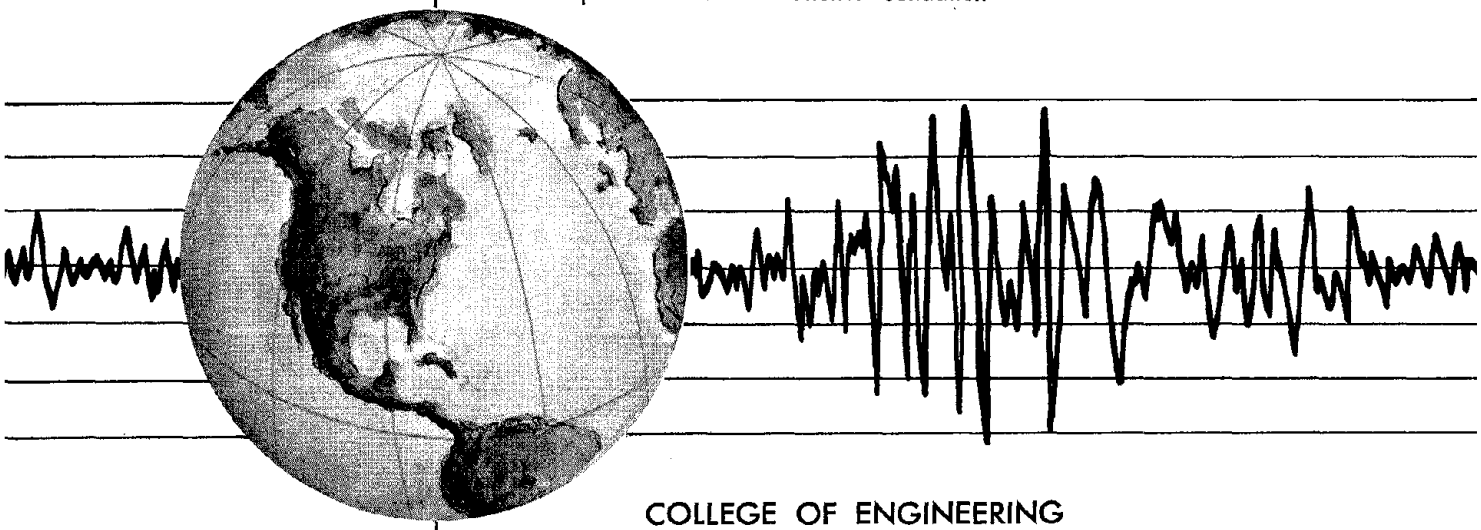

COLLEGE OF ENGINEERING

UNIVERSITY OF CALIFORNIA · Berkeley, California

For sale by the National Technical Information Service, U.S. Department of Commerce, Springfield, Virginia 22161.

See back of report for up to date listing of EERC reports.

A METHODOLOGY FOR COMPUTER-AIDED DESIGN OF EARTHQUAKE-RESISTANT STEEL STRUCTURES

by

M. A. Austin

K. S. Pister

and

S. A. Mahin

Report to the

National Science Foundation

Report No. UCB/EERC-85/13
Earthquake Engineering Research Center
College of Engineering
University of California
Berkeley, California

December 1985

i.a

ABSTRACT

This report focuses on the development and preliminary testing of a methodology for the probabilistic limit states design of seismic-resistant steel structures. Emphasis is placed on the formulation of a mechanism which allows a designer to include the effects of uncertainties and multiple design objectives in an optimization-based design process.

Sources of uncertainty in the seismic design environment are identified and described. The concept of [GOOD,BAD] and [HIGH,LOW] preference pairs is proposed as a mechanism for allowing a designer to impart aspects of his or her engineering judgement and intuitive knowledge to the design process. Scaling procedures for combining the aforementioned effects, and the statistics of frame response into a single design entity called *designer dissatisfaction* are given.

The design method is demonstrated via the design of a three story, single bay, moment resistant steel frame using a computer-aided design system called DELIGHT.STRUCT. Linear and non-linear time history analyses are built into the design procedure itself rather than serving as a check at the end of the design process. The frame's performance is assessed on the basis of its statistical response to gravity loads alone, gravity loads plus a family of moderate earthquakes and finally gravity loads combined with an ensemble of rare severe earthquake ground motions. Design objectives include the frame volume, minimum story drifts and maximum hysteretically dissipated energy. The Phase I-II-III Method of Feasible Directions is used to solve the constrained optimization problem. Examples are presented to demonstrate the proposed method for a selection of single design objective and multiple design objective problems having various design parameter layouts.

ACKNOWLEDGEMENTS

The study reported herein was supported by the National Science Foundation under grants PFR-7908261 and ENG-7810992. This support is gratefully acknowledged. The views presented in the report are those of the authors and not necessarily those of the National Science Foundation.

The authors would also like to acknowledge the many useful and enjoyable discussions held with the Structural Engineering and Structural Mechanics (SESM) faculty and staff, the Electrical Engineering and Computer Sciences (EECS) faculty, and students during this period of research. Professor R. L. Taylor, Professor E. Polak, G. Dilley, C. Thewalt, J. Landers, Jo Ann Kim, L. Vu-Quoc, D. Coster, T. Wuu, J. Higgins, W. Nye and A. Heunis provided many suggestions during the project. Bill Nye deserves a special word of thanks for his helpful assistance with the computational aspects of this work.

Table of Contents

ABSTRACT i
ACKNOWLEDGEMENTS ii
Table of Contents iii
CHAPTER 1 - INTRODUCTION 1
1. Nature of the Problem 1
1.1 Optimization-based Seismic-Resistant Design 4
1.2 A Historical Review 7
1.3 Objectives and Scope of this Study. 9
CHAPTER 2 - UNCERTAINTIES AND RISK IN SEISMIC-RESISTANT DESIGN 11
2. Introduction 11
2.1 Types of Uncertainty and Response Variation 12
2.1.1 Material Strengths 13
2.1.2 Dead and Live Gravity Loads 13
2.1.3 Earthquake Loads 14
2.1.4 Frame Response 15
2.2 A Hierarchy of Design Environment Uncertainties 16
2.3 Identifying Suitable Analysis Techniques 16
2.4.1 Proposed Design Method 18
2.5 Modeling for the Effects of Uncertainty 18
2.6 Performance Zones 20
2.7 Summary 20
CHAPTER 3 - FORMULATING MULTIPLE CRITERIA PROBLEMS 22
3. Introduction 22
3.1 Optimization Background 23
3.2 Procedure for Formulating the Design Problem 25
3.3 The Design Parameters 25
3.3.1 Scaling the Design Parameters : the nominal variation. 25
3.4 The Design Constraints. 26
3.4.1 Constraint Types 27
3.4.2 Procedure for Constraint Evaluation. 28
3.5 The Design Objectives 29
3.5.1 Procedure for Design Objective Evaluation 29
3.6 Interpreting the Dissatisfaction Equation 30
3.6.1 Frame Response Enhancement Factors due to Uncertainty 31
3.7 A Procedure for Setting-up the Design Problem 32
3.7.1 Algorithm ACTION Given a Design's CONDITION 33

CHAPTER 4 - THE DESIGN EXAMPLE 35
4. Introduction 35
4.1 Frame Geometry, Gravity Loads, and Boundary Conditions 35
4.2 Element Modeling 36
4.3 Loadings 36
4.3.1 Gravity Loads 36
4.3.2 Ground Motions 37
4.4 The Frame Simulation Assumptions 41
4.4.1 Gravity Loads Alone 41
4.4.2 Gravity Loads plus Moderate Earthquake Loading 41
4.4.3 Gravity Loads plus Severe Earthquake Loading 43
4.5 The Optimization Problem Assumptions 44
4.5.1 Design Parameters 44
4.5.2 Design Constraints 46
4.5.2.1 Box Constraints 46
4.5.2.2 Constraints Under Gravity Loads Alone 47
4.5.2.3 Constraints Under Combined Gravity and Moderate Quake Loads 50
4.5.2.4 Constraints Under Combined Gravity and Severe Quake Loads 54
4.5.3 Design Objectives 57
4.5.3.1 Volume of Structural Elements 57
4.5.3.2 Story Drifts 58
4.5.3.3 Energy Based Design 59
4.5.3.4 Parameter Settings for the Energy Based Design 66
CHAPTER 5 - PRELIMINARY ANALYSIS 68
5. Introduction 68
5.1 Additional Frame Simulation Assumptions 68
5.2 Simulation Results 70
5.2.1 Design Objectives 71
5.2.2 Box Constraints 73
5.2.3 Limit State 1 : Gravity Loads Alone 73
5.2.4 Limit State 2 : Gravity Loads + Moderate Earthquake Loading 75
5.2.4 Limit State 3 : Gravity Loads + Severe Earthquake Loading 78
5.3 Hierarchy of Frame Performance Attributes 80
5.4 Summary 82
CHAPTER 6 - OPTIMAL DESIGN PROBLEMS 84
6. Introduction 84
6.1 Single Objective Designs 85
6.1.1 Minimum Volume Designs 85
6.1.2 Minimum Story Drift Designs 86
6.1.3 Maximum Dissipated Energy Designs 88

6.2 Multiple-Objective Design 91
6.2.1 Sensitivity of Design Performance to Design parameter Lay-out 92
6.2.2 A Combined Volume, Story Drifts and Energy Based Design 94
6.2.3 A Comparison of Initial and Final Design Responses 98
6.2.3.1 Design Objectives 98
6.2.3.2 Box Constraints 100
6.2.3.3 Limit State 1 : Gravity Loads Alone 100
6.2.3.4 Limit State 2 : Gravity Loads + Moderate Earthquake Loading 101
6.2.3.4 Limit State 3 : Gravity Loads + Severe Earthquake Loading 102
6.2.3 Sensitivity of Dissatisfactions to Limit State Reliability 104
6.3 A Summary and Assessment of the Optimal Design Problems 105
CHAPTER 7 - CONCLUSIONS AND FUTURE RESEARCH 112
7. Introduction 112
7.1 Recommendations for Further Work 114
REFERENCES 119
APPENDIX 1 126
APPENDIX 2 130
APPENDIX 3 132
APPENDIX 4 144

CHAPTER 1

INTRODUCTION

> The strongest test of any system is not how well its features conform to anticipated needs but how well it performs when one wants to do something the designer did not foresee. It is a question less of possibility than perspicuity[35].

1. Nature of the Problem

The design of structures to resist earthquake loading presents one of the most challenging problems facing structural engineers. This problem is complicated by the large uncertainty in predicting the spatial and temporal nature of future seismic events. Further uncertainties are introduced due to the limited ability of analytical models to properly describe the nonlinear response of structures under severe earthquake excitations. Consequently, designers have difficulty in making quantitative decisions regarding the adequacy of a design, and in choosing rationally among different design alternatives.

The decision making process is further complicated by the fact that performance criteria are usually multi-tiered and related to notions of acceptable risk. For example, the Structural Engineers' Association of California[54] has recommended a three-tiered seismic design criterion that has become the "accepted design philosophy" for the design of seismic-resistant buildings. They stipulate that a conventional structure should resist frequently occurring minor earthquakes without any damage, and possess sufficient strength to assure complete protection against structural damage from moderate ground shakings. In the event of an unusually severe earthquake, extensive structural damage without collapse is accepted. However, explicit satisfaction of all of these criteria in the face of uncertainties in loading and resistance is a formidable task at best.

To facilitate the design of conventional buildings, most current codes approach the design problem indirectly by means of simplified "equivalent" loads, approximate analysis methods, and prescriptive detailing requirements. The Uniform Building Code[63], for example, stipulates a set of pseudo-static equivalent lateral loads with the intention of providing adequate strength against structural damage under moderate ground shaking, and excessive inelastic deformations during severe seismic excitations. Load and resistance factors are introduced to deal implicitly with variations in seismicity, a structure's gravity loads, and material properties. Design codes impose drift limits to constrain nonstructural damage during minor and moderate earthquakes, and to avoid structural instability during severe shaking. Finally, nominal detailing and other requirements are prescribed to achieve an adequate ductility capacity. It is important to note that codes set minimum standards for public safety, and that the numerous load factors and special requirements are based on observed performance of structures during past earthquakes, theoretical considerations and test results. Consequently, the seismic performance of conventional structures designed according to the codes is expected to be satisfactory.

Experienced designers often contend that when conventional structures are being designed, analyses need only have sufficient complexity to permit the essential features of the response to be evaluated in terms of the "accepted design philosophy." Detail beyond this objective is usually considered unwarranted for design because future seismic events are not deterministic. Therefore, elastic analyses are used in practice. They are relatively simple to apply, and result in member forces of the correct order.

Nonetheless, the relationship of the simplified method to the accepted design philosophy is tenuous. While design analyses give the implication that

the structure will respond elastically to the design loadings, the accepted design criteria rely on extensive inelastic deformations to absorb energy under severe earthquake excitations. The cases where these discrepancies are likely to cause difficulties include:

(a) complex or irregular structural systems. Simplified loading procedures may no longer be adequate.

(b) innovative or unusual structural systems, or those employing new structural materials or details. Because there may be no prior seismic experience in such cases, code provisions may not apply.

(c) situations where considerations of economics or post earthquake functionality necessitate more specific performance criteria and a closer evaluation of structural response. The accepted design philosophy may not apply to these cases.

(d) situations where the availability of site specific information on input excitations makes more explicit analyses desirable.

(e) locations where unusual seismic conditions might be expected due to local soil conditions or the proximity to causitive faults.

Designers may have little experience in these specific cases and consequently find it difficult to assess the quality of a final design. Most designers compensate for the additional uncertainty in these situations by merely increasing the design load factors. Typically, this is followed by a trial and error design process in which elastic analyses are used. The use of inelastic time history analyses in the design process has always been dismissed as being too costly, except for special structures[4,68]. Even more recent recommendations, such as the ATC draft provisions[6], tend to refine the details of such elastic deterministic design procedures rather than addressing the problems of

explicitly satisfying the various performance criteria with an acceptable risk. For some special structures, however, ensembles of records have been used in analysis to evaluate performance criteria established for various levels of excitation. The difficulties in doing such explicit time-history analyses are formidable and time consuming. In addition, it is often difficult to identify the design changes necessary to improve the performance of a structure, especially when the effects of uncertainty in the response and loads are taken into account. Trial and error approaches to design that incorporate explicit analysis procedures can be both uneconomical and ineffective. Consequently, there is a need to use advanced numerical methods and optimization theory to develop a design procedure that will assist a designer with the evaluation of a design, and suggest possible improvements.

While such explicit procedures are unlikely to be practicable for conventional structures, the increasing computational capabilities of modern computers indicates a need to develop a methodology which is capable of achieving structural designs that are consistent with specified performance criteria. Ideally, a computer-based design environment of this type should integrate appropriate dynamic analysis and optimization techniques with methods accounting for uncertainties in structural behavior, structural modeling, and earthquake excitations. It should enable the engineer to explicitly set special performance criteria for unique structures, and assist the designer in making decisions based on likely structural performance versus design criteria and expected costs.

1.1 Optimization-based Seismic-Resistant Design

Seismic design may be viewed as a multiple-level decision making process in which tradeoffs among alternatives and options of various types occur. The

key steps in the design process include (a) the specification of design requirements, (b) the selection of a structural configuration, and (c) the determination of element sizes. In order to complete steps (a) and (b) of the design process, a designer should first estimate the performance, cost, and reliability of each alternative structural system before comparing their relative merits. Completing this task in a consistent manner is sometimes impossible because the design attributes are frequently incommensurable, conflicting in nature, or subject to uncertainty in their tradeoff information. In fact, it is because problems of this type have so far eluded a step-by-step solution procedure that researchers have made little progress in the development of tools which provide a designer with computer assistance during stages (a) and (b) of the design process. Consequently, the selection of a structural layout is usually left to the creativity of an experienced designer, and the use of optimization techniques in seismic design primarily restricted to the optimal proportioning and sizing of structural members.

A key step in the formulation of these problems is the transformation of the initial practical design problem into a non-linear programming problem. The design objectives and constraints are cast into mathematical statements that describe structural performance attributes and all the ways in which a structure may fail to fulfill its intended purpose. Ideally these mathematical statements should have sufficient complexity to capture the details of practical design problem, yet be sufficiently straightforward to be handled by existing optimization algorithms. Nevertheless, the resulting mathematical descriptions for the design objectives and constraints are often nonlinear. They must be maximized while simultaneously satisfying multiple nonlinear and sometimes nonconvex constraints.

Optimization methods in the present context are divided into two general

classes[19]. The first and simpler case can be accomplished with deterministic optimization and is known as *Nominal design*. The structural topology is fixed *a priori* in a typical formulation of this type. The optimization problem is cast by assigning values to a set of parameters that are not subject to statistical variation. Thus, the design is optimized when a set of specifications is maximized while satisfying all of the problem's constraints. The second and more difficult problem class deals with *Statistical design*. In this problem class the design variables and objectives can be subject to statistical variation. Monte Carlo techniques may be used to estimate a structure's reliability.

Frequent objections to the use of optimization include "real design problems are not this simple" or "real design problems have more than one objective." Many designers also contend that they cannot express everything they know about a good design in a mathematical formulation because design often implies functional and aesthetic factors as well as technical, economic and political ones. Nonetheless, the potential benefits of casting a seismic-design problem into an optimization format are significant. As the problems become increasingly complex, formulations of this type provide insight that would otherwise be difficult to perceive. They may be employed during the latter stages of the design procedure to find both an improved design and the sensitivity of performance objectives with respect to perturbations in the design parameters. They can also facilitate interaction between the structural analysis and performance assessment phases of design. Indeed, when information is presented accurately, and in a not-too-overwhelming manner, judgements may be made more conveniently and accurately than would otherwise be possible. If the optimal and preliminary designs are similar, the former may be asserted to be capable of giving both a practicable and economic design. Conversely, the preliminary design method may be deficient for structures that are dynamically

irregular. Optimization methods may suggest a feasible solution in such cases, however.

1.2 A Historical Review

Prior to the mid 1960's the body of knowledge required to handle the design of systems having dynamic constraints was largely undeveloped. Researchers in the area of structural design were concentrating on the design of structures for static loads only[61]. It wasn't until the late 1960's that the theory required to handle problems having dynamic constraints was developed[50]. And then, problems were formulated as one of optimal control or one of mathematical programming. In the area of structural optimization, the latter formulation has predominated in the various approaches to the design of seismic-resistant structures. For example, Ray et al.[53] captured the essential features of the newly developed optimization theory in their development of a methodology for the optimal design of multi-story shear buildings. Earthquake loads were modeled with a design response spectrum. In a following contribution, Vitiello and Pister[65] developed a reliability-based methodology for incorporating in the decision-making process of design the explicit consideration of possible future performance of the designed structure in the presence of uncertainties in both loading and structural design parameters. Merit functions for a design consisted of the structure's initial cost plus a term describing the cost of expected structural damage during the structure's lifetime. Design examples for simplified structural models were presented to demonstrate the method.

Our perception of how the design process should be approached has also changed during the last 20 years. Until recently it was commonly believed that development of these techniques would allow complete automation of the

design process. The notion of a *black-box* approach to optimization-based design being sufficient is clearly conveyed by the partial quotation:

> methodology of *automated* or *hands-off* design, where the *algorithm* replaces *insight*....[21]

With this attitude it is no wonder the early optimization-based design programs provided little feedback when their developers did not perceive the needs or advantages of an interactive computing environment, nor did they even expect the designer to be part of the design process. Fortunately, this attitude has changed; it is now expected that a designer and computer should be complementary as they work together to complete an optimal design.

At Berkeley, the thrust of the most recent work in this area has been directed towards the development of a computer-aided design environment for the seismic-resistant design of steel frames. The name of this environment is DELIGHT.STRUCT[13]. DELIGHT is an interactive computer system that was developed to provide engineers from various disciplines with a working environment in which optimization techniques could be applied to engineering design[44]. The DELIGHT.STRUCT software is the union of (a) DELIGHT, (b) a dynamic nonlinear general purpose structural analysis package named ANSR[41], (c) a library of optimization algorithms with corresponding interfaces for use in structural design, and (d) specialized software for the design of seismic-resistant planar steel frames. Within the DELIGHT.STRUCT environment, structural performance is measured by partitioning the specifications into limit states that are consistent with currently accepted seismic design philosophies. As a result, the temporal aspects of different magnitudes of ground motions are not explicitly included in the design process. Rather designs are conditional upon all limit states being activated during the structure's lifetime.

DELIGHT.STRUCT has been used for the design of planar steel

frames[12,14], where designs based on minimization of story drift and dissipated energy under strong ground motion were compared with code-based designs. Further, a study of friction-braced frames under seismic loading was conducted[10], examining and extending design concepts described by Pall and Marsh[47]. Experience with the software system is summarized in [9].

1.3 Objectives and Scope of this Study.

The long term goal of this research program is to formulate a design methodology and develop computer-aided design software that will help engineers (a) achieve designs that are more consistent with the accepted design philosophy and (b) make rational decisions while designing seismic-resistant structures.

Unfortunately, it may be many years before a designer is provided with effective computer assistance of this type during all stages of the design process. The reasons for this are due, in part, to the diversity of areas to be integrated; structural analysis and design, earthquake engineering, decision analysis, statistics, interactive computer graphics, and optimization are all disciplines which are currently applicable. In future research efforts, techniques and ideas emanating from the frontiers of knowledge engineering, artificial intelligence, expert systems and database management are anticipated to play roles of increasing importance. Because no single person or group is likely to have the diversity to tackle this problem in its entirety, solution strategies to problems of this nature are incremental, with the scope of each contribution being restricted to a specialized extension to previously developed ideas and software. Moreover, our perspective of what constitutes a reasonable amount of computation is rapidly changing as improved hardware becomes available. Objections to design methods currently perceived as being computationally

intensive will no longer be relevant by the time most of the required developments have been completed. Consequently, the aim of this study is to formulate an improved design methodology that mitigates some of the most significant current deficiences, irrespective of the computation required.

The DELIGHT.STRUCT system reported in reference [13] is capable of dealing with design problems that are deterministic. In this investigation, the capabilities of the DELIGHT.STRUCT software system are extended to include probabilistic limit states design. Emphasis is placed on the development of a mechanism that allows a designer to include the effects of uncertainties and multiple design objectives in an optimization-based design process. Scaling procedures for combining the aforementioned effects, and the statistics of frame response into a single design entity called ***designer dissatisfaction*** are given. Sources of uncertainty in the seismic design environment are identified and described, together with the objectives and constraints relevant to the design of moment-resistant steel frames.

A principal deficiency of the previous studies has been the optimum design process itself. Because convenient design improvements could only be based on single objectives (see refs [10],[14] and [17]), the design process typically considered the influence of multiple design criteria by dividing the design process into segments and sequentially working through modifications of the design with different objectives. Fortunately, this stepwise procedure is no longer necessary because the recently developed Phase I-II-III Method of Feasible Directions has the capability of simultaneously considering multiple objectives. This algorithm is added to the optimization algorithm library of DELIGHT.STRUCT. An example is presented to demonstrate and evaluate the effectiveness of the proposed method for a moment-resistant steel frame designed with both single and multiple design objectives.

CHAPTER 2

UNCERTAINTIES AND RISK IN SEISMIC-RESISTANT DESIGN

2. Introduction

Variations in a structure's loading and resistance quantities are the main reason that absolute structural safety and integrity over a structure's lifetime cannot be assured. Indeed, economic considerations generally prohibit the design of structures for which absolute safety and performance are even close to being assured. In Chapter 1 it was explained that while the traditional approaches to seismic design result in satisfactory performance for a large class of structures, the shortcomings of the traditional methods become significant when a new problem area is being studied. The designer has little experience in these cases and consequently finds it difficult to assess the quality of a final design. Therefore, it was proposed to mitigate these deficiencies by developing a design method which explicitly captures the effects of the most significant variations in seismic design. This chapter begins by posing the following questions that are related to the research goal:

(a) What are the important sources and types of uncertainty in seismic design?

(b) What is the contribution of each component to the final variation in a structure's response?

(c) What statistical distributions best describe these variations?

(d) Can the same statistical distributions and parameters be used for all response quantities, structural system types and configurations?

(e) How sensitive are the parameters of the statistical distribution to different structural systems and frame geometries?

(f) How is a structure's risk of failure affected by the magnitude of these variations?

(g) What levels of risk constitute *safe* performance?

(h) What accuracy of modeling is needed in order to elicit the design information with a required level of confidence?

(i) What techniques are currently available for assessing the effects of uncertainty in seismic design?

Answering these questions in an absolute sense is impossible; it is beyond the scope of this work to even try. Instead, it is first noted that a design's performance is usually based on the magnitude and variation of the response output, not the input. Variations in the frame response output may be due to variations in the external loading, or variations in the frame's properties. Our goal is to identify those features of the design environment which contribute to the response output. For the purposes of this investigation, the sources of variation are limited to material properties, dead and live gravity loads, and earthquake loads. Statistical distributions of frame response quantities frequently of interest in design are also identified. The reliability in predicting each component is assessed and a hierarchy of uncertainty magnitudes is formed. Finally, a design method which deals explicitly with the largest variations and their consequences is proposed. A procedure for dealing with variations of lesser magnitude is also given.

2.1 Types of Uncertainty and Response Variation

Uncertainties are generally divided into three types. Inherent randomness intrinsic to a phenomenon cannot be reduced by the collection of additional data. For instance, the variation of a material's yield stress, the randomness of

live load and indeed, the variation in earthquake lateral loads all fall into this classification. The second type of uncertainty is known as prediction error. Prediction error is used to describe uncertainty in values of the model parameters produced by lack of sufficient model parameter data. The uncertainty in predicting modeling parameters can be reduced by gathering additional data. Finally, modeling error is related to the choice of a model. It can be reduced by using a model which provides a better description of reality, thereby reducing bias in the output of the model[5].

2.1.1 Material Strengths

This investigation is confined to the behavior of wide-flange economy hot-rolled steel sections.

A material's yield stress f_y under dynamic loads is typically higher than under static loads. In fact, the average ratio of the former to the latter lies in the interval [1.06-1.12] with high ratios generally valid for low yield strengths and vice-versa[28]. The yield strength referred to by most building codes is the standardized minimum yield strength guaranteed by the manufacturing mill. The quality of manufacture generally controls the dispersion of yield strength. With excellent quality control a coefficient of variation [0.05-0.075] is typical. This may rise to [0.075-0.10] for good quality control. Hence from a probabilistic standpoint, one can roughly say that the ratio "minimum guaranteed [or dependable] yield strength" to "mean yield strength" covers the interval [0.8-0.9].

2.1.2 Dead and Live Gravity Loads

Dead loads remain relatively constant throughout a structure's lifetime. They include the weight of the structure, its partitions, installations, floor cov-

erings and roofing. Investigators usually assume that the mean load equals the nominal dead load with a coefficient of variation covered by the interval 0.06-0.15. A typical value is 0.1 [1].

Live loads include the weight of the occupants, their possessions, furniture, movable partitions and portable fixtures. They can conveniently be thought of as composed of two parts. The first is an "arbitrary point-in-time component" that remains relatively constant with time. The second is an extraordinary component that arises from an infrequent clustering of load above normal loading. Both the arbitrary point-in-time live loading and the maximum anticipated live load over the life time of the structure are of interest in design. Reference[1] indicates that the arbitrary point-in-time live load is a function of the area of influence and can vary from 0.2 to 0.89 of the basic unreduced (nominal) design live load. Maximum live loads during the structure's lifetime may be due to changes in occupancy; the expected maximum live load is a function of the influence area and typically varies from 1.18-1.38 of the nominal live loading. The coefficient of variation (c.o.v.) is almost independent of influence area and is approximately equal to 0.25[1].

2.1.3 Earthquake Loads

Earthquake loads can only be predicted with large uncertainty due to significant variations in the spatial and temporal nature of ground motion occurrences, and the sensitivity of ground motion details to source and propagation mechanisms that are currently poorly understood. Cornell[22] employed elementary considerations from seismicity to show that peak ground acceleration follows a type II extreme value distribution[1]. Its cumulative distribution is

[1] Note that the tail of the type II distribution decays with polynomial order. Type I extreme distributions decay exponentially[32]. A larger scatter is implied by the former distribution.

given by:

$$F_A(a) = e^{-\left[\frac{a}{u}\right]^k} \tag{2.1}$$

with parameters u and k. Assuming that k = 2.3-3.3, the coefficient of variation ranges over the interval 0.57-1.38 [25]. Shah and Dong[58] point out that this variation could be even larger if the effects of earthquake duration and frequency content are also considered.

2.1.4 Frame Response

Ruiz and Penzien[56] were among the earliest researchers to investigate the statistical nature of frame response. They studied the response variability of several idealized multistory shear-type structures subjected to an ensemble of strong ground motions. Frame response quantities identified as significant include the distribution of local peaks in the story drift, peak story ductilities and energy dissipation at each story level. Story ductilities were found to be in good agreement with the extreme type I distribution. No attempt was made to fit probability distributions to the remaining response parameters. Instead, confidence intervals for the expected frame response were constructed by using the student-t distribution and assuming the response parameter to be normally distributed. In a later investigation Murakami and Penzien[42] studied the hysteretic response of several spring type models excited by 100 different artificially generated accelerograms. The Gumbel Type I extreme distribution was once again found to accurately describe the response distribution.

In more recent investigations, Shah and Dong[59] report that the cumulative distribution of curvature ductility for the frame members is well fitted to

the Gumbel Type I extreme distribution. Similarly, Lashkari and Krawinkler[37] carried out a statistical analysis of bilinear single degree of freedom systems excited by 6 ground motion inputs. They found that the lognormal distribution represented the normalized plastic deformations for individual frame responses. Maximum plastic deformations were similarly found to be adequately described by the Type I extreme distribution.

It is concluded that the exponential type I distribution provides a good fit to peak member and story ductilities. Distributions for other frame response parameters are not well defined. This result is somewhat expected since the ability of frame members to deform beyond the elastic range is an intrinsic material property. Peak story drifts, elastic bending moments and frame sway on the other hand are dependent on structural configuration and layout. Assuming that these response quantities follow a particular distribution has no significance because each structure's building-wide properties are different.

2.2 A Hierarchy of Design Environment Uncertainties

Of all the factors considered in Sections 2.1.1-2.1.4 it is evident that the largest dispersion occurs due to earthquake loading. Its coefficient of variation covers the interval [0.57-1.38] while the remaining effects range over the interval [0.05-0.25].

2.3 Identifying Suitable Analysis Techniques

The identification and selection of analysis techniques for the design procedure is a crucial step in its development. With respect to the structural simulations, it is assumed *a priori* that linear and nonlinear time-history analysis techniques will be built into the design procedure itself. Additionally employed techniques used to capture the effects of uncertainty should be compatible.

Unfortunately, random vibration theory seems practically limited to elastic systems. The commonly used extension for modeling the nonlinear response of structures is to assume an equivalently-damped linear system [11,46,67]. This assumption is not consistent with the requirement of using linear and nonlinear time-history analyses within the design process, and therefore will not be used.

Current reliability techniques rely on calculating the risk of failure due to parameter variations that are characterized with high confidence. Satisfying this criterion in the seismic design environment is sometimes impossible because a portion of the design information may be imperfect, scarce, unavailable, or poorly understood. For example, failure of the severe earthquake loading limit state is not related to the behavior of a single component, but rather some less well defined building-wide behavior (such as collapse).

Although general procedures for using the first-order second-moment reliability method in the analysis of seismic resistant structures have only been developed for elastic frames subject to a pseudo-static lateral loads[23], there appears to be no conceptual reason why the framework of the method cannot be extended to nonlinear structures. Giannini[29] reports on the modifications required for extending the first-order second-moment reliability method to nonlinear structures; a very simple nonlinear structure loaded with an elastic response spectrum is presented as an example. However, the development of reliability methods for handling general nonlinear structures is by no means complete. With our current knowledge, calculating the reliability of a general nonlinear structure is only possible using Monte-Carlo simulation techniques. Brayton et al.[19] indicate that the amount of computation is independent of both the number of parameters and the shape of the feasible domain. The main shortcoming of this approach is that hundreds of simulations are normally required to obtain a reasonable estimate of the frame's reliability.

2.4.1 Proposed Design Method

A design method which allows the use of time-history analyses, and incorporates the effects of uncertainty of the types described in Section 2.1 is now proposed. Reliability-based ideas are included in the design method by first ordering the design factors and parameters into a hierarchy of increasing variability. Statistical techniques are used to model those parameters exhibiting the largest variability. For those parameters that can be predicted with greater accuracy, it is assumed that the parameters take their mean values. Their variability is implicitly accounted for in the setting of design factors.

As the gravity loads and material properties have the lowest coefficient of variation their behavior is modeled deterministically. The scatter in earthquake loads is explicitly accounted for by generating a family of ground motion records and providing these as input to the structure. Simulations of the structure are completed for each input. Mean values and standard deviations of relevant frame response quantities are then calculated. The allowable frame response parameters are set to account indirectly for the secondary effects of material and gravity load variability.

2.5 Modeling for the Effects of Uncertainty

A simple formulation is proposed to account for uncertainties. It is assumed that all of the significant uncertainties arising in design can be encompassed by one of the following two groups:

(a) The first source of uncertainty is related to measurement of the frame performance. Some user-specified constraints describe the frame's performance in a qualitative manner and may only be an approximate measure of the effect to be controlled (for example, story drift is often used as an

indirect measure of structural damage potential). Enforcing a rigid constraint boundary is unwarranted and the designer should only be expected to provide bounds on the acceptable frame performance. It is expected that the most active constraints of an effective design would lie within this region.

The user-specified bounds on frame response are called the GOOD and BAD values. From the standpoint of implementation, the GOOD frame response value corresponds to a *dependable* level of system performance. By contrast the BAD frame performance could represent a threshold at which undesirable performance is almost assured if exceeded.

(b) The second source of uncertainty is related to the structure's reliability. Using statistics one may design so that the probability of the peak frame response exceeding a particular quantity is no more than a prescribed value, say 5% (for example, see Chapter 11 of Rao[52]). However, while it is easy for a designer to specify an exact tolerance it is much more difficult to justify its choice compared to an alternative value located nearby. This is particularly true for problem areas in which the designer has little experience, or for which limited data is available. At best, the designer can only supply ballpark estimates of desired protection.

This phenomenon is modeled herein by having the designer designate HIGH and LOW exceedance probabilities. The HIGH exceedance probability represents the lowest level of reliability the designer is prepared to accept when the limit state is actived. By contrast, the LOW exceedance probability represents a level of safety which the designer considers to border on *conservative safety* against failure for the limit state.

2.6 Performance Zones

The previous section defined two general sets of criteria for assessing overall frame performance. In this section further assumptions are made in order to allow linking of the [GOOD,BAD] and [HIGH,LOW] pairs to form a single performance criterion.

In terms of the previously defined criteria, a designer is assumed to be completely satisfied with a measure of frame performance when the probability of peak frame response exceeding the GOOD frame response is less than the LOW exceedance probability. Conversely, the designer is certainly dissatisfied when the probability of the peak frame response being larger than the BAD frame response is greater than the HIGH exceedance probability. In this instance, the frame response is measured in two ways and is unfavorable on both counts. Table [2.1] shows how these criteria can be used to map each constraint and design objective's performance to one of three performance zones.

2.7 Summary

This chapter has identified the significant sources of uncertainty and variation in the seismic environment, and a mechanism for accounting for these sources of uncertainty has been proposed. Now a procedure for linking the various sources of uncertainty into a single design entity that can be handled by an optimization-based design procedure needs to be defined. Chapter 3 reports on the development of such a procedure.

ZONE 1	is known as the *infeasible domain*. Measures of frame performance that are clearly unsatisfactory are assigned to this region. This occurs when
$P[$ *Peak Response* $>$ *BAD Frame Response* $] >$ *HIGH Exceedance Probability*	
ZONE 3	is known as the *feasible domain*. Measures of frame performance that are clearly satisfactory are assigned to this region. For the purposes of this simulation package, satisfactory performance occurs when
$P[$ *Peak Response* $>$ *GOOD Frame Response* $] <$ *LOW Exceedance Probability*	
ZONE 2	is a region within which the designer is neither clearly satisfied, nor, clearly dissatisfied with a constraint's performance. This *fuzzy region* lies between zones 1 and 3 and is bounded by the inequalities
$P[$ *Peak Response* $\geq$ *BAD Frame Response* $] \leq$ *HIGH Exceedance Probability*	
and	
$P[$ *Peak Response* $\geq$ *GOOD Frame Response* $] \geq$ *LOW Exceedance Probability*	

Table[2.1] : Design Constraint and Objective Performance Zones

CHAPTER 3

FORMULATING MULTIPLE CRITERIA PROBLEMS

3. Introduction

Multi-objective problems arise naturally in seismic design because an effective structure balances the attributes of cost, reliability and performance in some optimal manner[1]. Design alternatives may be defined by decision variables, or simply as a list of choices. In the former case, the criterion upon which decisions are based is given in terms of the multiple objectives, which are themselves functions of the design variables (or the decision variables). If the problem is cast, however, as a list of ranked alternatives the choices play the roles of both the variables and the attributes. While a need exists for research in this area (see reference [15]), this investigation will be confined to problems cast with design variables.

The basic ingredients in a design variable formulation are (a) a set of quantifiable objectives, (b) a set of well defined constraints, and (c) a process for obtaining tradeoff information among objectives. Constituents (a) and (b) define the scope of most optimization problems. Component (c) contains a decision rule that enables the best compromise to be made among multiple criteria. Collectively these criteria should be capable searching for feasible solutions, evaluating alternatives, and providing recommendations for further action.

This chapter begins with a review of optimization problem formulations. Alternative techniques for scaling the constraints and objectives in multiple criteria problems are described. The Phase I-II-III Method of Feasible Directions is discussed. An interpretation of the dissatisfaction equation is provided,

[1] Comprehensive discussions on this topic may also be found in Goicoechea et al.[30], by Dlesk and Leibman[24], and Brayton et al.[19].

together with modifications for incorporating the performance zones defined in Chapter 2. A step-by-step procedure is given for evaluating the constraints and design objectives. The chapter concludes with a summary of recommended algorithm ACTION following the verification of a problem's CONDITION.

3.1 Optimization Background

The standard form of the constrained nonlinear programming problem may be stated as:

$$\min_{x} \; [\, cost(x) \,] \tag{3.1}$$

$$subject\ to\ \ eq(x) = 0\ \ and\ \ ineq(x) \leq 0$$

where $cost(x)$ is the objective function to be minimized, and eq and $ineq$ are equality and inequality conventional constraint functions of the design vector x. Equality constraints are not considered further in this investigation for two reasons; most engineering design problems do not involve them, and second, they cannot be handled in a simple manner.

Unfortunately, equation (3.1) must be modified before it can be used to solve many of the problems that arise in engineering applications. For instance, (3.1) cannot handle constraints which must be satisfied over the range of an independent parameter such as time or frequency. Such specifications are called functional constraints. Extensions to (3.1) are also necessary for problems that cannot be described by a single design objective. The most common approach is to combine multiple criteria into a single objective with a weighted sum. A second approach is to cast the design problem into a constrained minimax optimization format.

When the functional inequality constraints are included in the minimax optimization format, a semi-infinite nonlinear programming problem of the

form:

$$\min_{x} \left[\max_{i} w_i cost_i(x) : i = 1,2..l \right] \tag{3.2}$$

$$\begin{aligned} \textit{subject to} \quad & g_j(x) \leq 0 : j = 1,2..m \ ] \\ \textit{and} \quad & f_k(x,t) \leq 0 \ \forall \ t \in [T_b, T_e] : k = 1,2..n \ ] \end{aligned}$$

results. In (3.2), w_i is the weighting coefficient for the i^{th} goal of l objective functions, $g_j(x)$ the j^{th} entity of m conventional constraints, and $f_k(x,t)$ the k^{th} member of n functional inequality constraints. The parameters T_b and T_e bound the range of the independent parameter t.

It is important to note that techniques for including multiple criteria tend to be ad hoc, irrespective of the method used. Typically, the designer begins by assigning a weighting which reflects the relative importance of minimizing each cost. As one proceeds through several iterations of optimization, this process has the shortcoming of hiding the changing importance of each term. Furthermore, without continually updating the coefficients, weightings can only be chosen to normalize various objectives and constraints for a single degree of satisfaction. Nye and Tits[45] indicate that a preferable case would be to have the values of normalized objectives and constraints coincide for any degree of satisfaction.

The weighted sum approach has the added deficiency of frequently requiring the combination of objectives that have incommensurable units. As a result, the physical interpretation of those weighting coefficients having unfamiliar units may become difficult, if not impossible. This shortcoming may be mitigated by using single weighting functions that normalize each objective to eliminate units with which the designer is working.

3.2 Procedure for Formulating the Design Problem

In this study the practical seismic design problem is recast into a nonlinear programming problem which can be solved with the Phase I-II-III Method of Feasible Directions developed by Nye and Tits[45]. This algorithm has the desirable attributes of (a) always producing a feasible design if one exists, (b) guaranteeing that the design is improved with each iteration, and (c) requiring only first order derivatives.

3.3 The Design Parameters

In this formulation the frame topology is fixed, and the optimization is cast by assigning values to a set of parameters that are not subject to variation. To simplify the design analyses, the frame elements are assumed to take their mean values. Modeling of the design parameter variations is accounted for implicitly within the constraint parameter settings.

3.3.1 Scaling the Design Parameters : the Nominal Variation.

The efficiency of most optimization algorithms is heavily penalized if the design vector enters a steep valley; ie, the eps-active[2] constraints have gradients of widely differing magnitude. A preferable case is for the algorithm to see the most active design objectives and constraints as isotropically as possible. In response to this need Nye and Tits[45] have introduced the concept of the nominal variation and applied it to what they call the *uniform parameter influence rule*. This rule states that "a change in each parameter by its nominal variation should influence the most binding objectives and constraints to roughly the same degree." Thus a scaled design parameter is obtained by dividing the raw design value by its nominal variation;

[2] A constraint is known as eps-active if its maximum value is greater than the maximum value over all the constraints minus the width of the eps-active bandwidth. In such cases the gradients of the constraint with respect to the design parameters is included in the direction vector phase of the Phase I-II-III Method of Feasible Directions.

$$X\_scaled = \left\lfloor \frac{X\_raw}{Nominal\ Variation} \right\rfloor \tag{3.3}$$

Parameter scaling may be automatic or manual. Automatic scaling has the disadvantage of not allowing the designer to supplement the algorithm with his or her intuitive knowledge. By contrast, manual control may become too cumbersome for design problems having a large number of parameters. Section 4.5.1. describes the way in which the software of DELIGHT.STRUCT has been set up to handle this problem.

3.4 The Design Constraints.

The purpose of design constraints is to discourage the design parameters from taking values that are impractical, and from moving into a region that has an unacceptably high level of risk of unsatisfactory frame performance.

The uniform satisfaction/dissatisfaction rule is used to scale the objectives and constraints. In its original form, this rule states that the objectives and constraints may be scaled to coincide for two levels of satisfaction by assuming that the designer is uniformly satisfied by all constraints and design objectives when they reach their GOOD value. Conversely, the designer is uniformly dissatisfied when constraints and objectives reach their BAD values[45]. Zone 2 of the designer dissatisfaction is mapped onto the [0,1] interval with the transformation:

$$D(response\_value) = \begin{cases} 0 \text{ for } [\, actual\_resp - GOOD \,] < 0 : otherwise \\ \left\lfloor \dfrac{response\_value - GOOD}{BAD - GOOD} \right\rfloor \end{cases} \tag{3.4}$$

For this investigation, the uniform satisfaction/dissatisfaction rule is modified to account for the performance zone requirements of Section 2.6. In a manner analogous to the above formulation the boundary contours between zones 1 and 2, and zones 2 and 3, are assumed to provide constant contours of satisfac-

tion and dissatisfaction. These additional features are incorporated by modifying equation (3.4) to give:

$$D(const_i) = \begin{cases} 0 \text{ for } [\, LOW\_resp - GOOD \,] < 0 : \text{otherwise} \\ \left[\dfrac{LOW\_resp - GOOD}{(LOW\_resp - HIGH\_resp) + (BAD - GOOD)} \right] \end{cases} \tag{3.5}$$

where : LOW_resp = frame response corresponding to LOW exceedance probability.
HIGH_resp = frame response corresponding to HIGH exceedance probability.
$const_i$ = i^{th} constraint.

The boundary between zones 1 and 2 is reached when the frame response corresponding to the LOW exceedance probability equals the GOOD frame performance. Similarly, the boundary between zones 2 and 3 is located where the frame response corresponding to the HIGH exceedance probability equals the BAD frame response. Notice that a singularity in equation (3.5) cannot occur when the GOOD frame response is strictly less than the BAD frame response.

3.4.1 Constraint Types

Two attributes are allocated to each constraint. Those constraints that do not depend on time or some other independent parameter are termed conventional, while those which depend on time are termed functional (see equation (3.2)).

In addition each constraint is given either a HARD or SOFT attribute. HARD constraints are ones that the designer wishes the algorithm to give the greatest emphasis, and once satisfied [ie; better than the GOOD design value], the designer wishes to remain satisfied and not to take part in subsequent tradeoffs. SOFT constraints are those that the designer is interested in conveniently trading off against one another and against the performance objectives in an optimization run. They include desired or target values that the design should try to attain; however no further gain would be obtained when the

specification over-achieves its target value.

Figure [3.1] shows that conventional constraints are bounded by zero response, and a single pair of [GOOD,BAD] performance values for maximum frame response. It plots the "dissatisfaction" vs "peak frame response" for the special case of peak frame response having zero variation. Box constraints ensure that the design parameters lie within a specified interval. They have a [GOOD,BAD] frame performance pair at each end of the interval, as shown in Figure [3.2]. The [GOOD,BAD] and [HIGH,LOW] performance pair components for a frame response quantity having non-zero variation is shown in Figure [3.3].

3.4.2 Procedure for Constraint Evaluation.

The following step-by-step procedure is required for the evaluation of each constraint.

STEP 1 Specify the [GOOD,BAD] and [HIGH,LOW] pairs for each constraint.

STEP 2 Simulate the frame response for the appropriate limit state.

STEP 3 Identify the appropriate frame response quantities. Calculate the mean and standard deviation of the response quantities and plot a histogram of the results.

STEP 4 Assume a probability distribution and calculate its parameters from the data provided.

STEP 5 Calculate the characteristic values on frame response [HIGH_resp , LOW_resp] corresponding to the HIGH and LOW exceedance probabilities specified at STEP 1.

STEP 6 Substitute into (3.5) to get the designer's dissatisfaction.

Notice that in this process of performance evaluation, only one point is contributed to the histogram of peak constraint quantities from each response simu-

lation. In other words, the time dependent characteristics of the functional constraints are swept out when the individual frame responses are combined into the overall constraint dissatisfaction. During the direction finding phase of an optimization iteration, however, the eps-active local maxima of time-dependent responses should also be considered so that the generalized gradients of the frame response quantities with respect to the design parameters remains continuously differentiable[3].

3.5 The Design Objectives.

The design objectives are those aspects of the design problem that quantify its performance. They are controlled by the design variables, and should provide the motivation and direction for moving towards a better design.

The design objectives are evaluated in a manner similar to the constraints. The main difference is that only GOOD and BAD values are used for the objectives. HIGH and LOW response values are not used because they describe the probability of the design being feasible. If the design already has sufficient reliability, only GOOD and BAD objective values are needed to provide a general direction for change to a better design.

3.5.1 Procedure for Design Objective Evaluation.

The calculation procedure for the design objectives is:

STEP 1 Identify the design objectives relevant to the problem at hand.

STEP 2 Specify GOOD and BAD values for each design objective.

STEP 3 Simulate the frame response for the appropriate limit state.

---

[3] Further comments on this aspect of the optimization procedure are given in Chapter 7.

STEP 4 Identify the relevant frame response parameters and calculate the appropriate statistics of frame performance.

STEP 5 Substitute frame performance response quantities into (3.5) to get the designer dissatisfaction.

3.6 Interpreting the Dissatisfaction Equation.

This section examines the behavior of the dissatisfaction function as a function of its parameters. The process is expedited by defining the following dimensionless parameters:

$$ramp = \left[\frac{GOOD\ allowable\ frame\ response}{BAD\ \ allowable\ frame\ response} \right] \tag{3.6}$$

$$mean = \left[\frac{Mean\ frame\ response}{BAD\ \ allowable\ frame\ response} \right] \tag{3.7}$$

$$cov = \left[\frac{Standard\ deviation\ of\ frame\ response}{Mean\ frame\ response} \right] \tag{3.8}$$

In addition, the distributions of peak frame response quantities is assumed to be described by either the normal distribution, the lognormal distribution, or the Gumbel Type I extreme distribution. Both the second and third distributions are skewed to the left, as is typically the case for statistical distributions describing extreme events. Coefficients in the calculations for the extreme type 1 distribution are based on a sample size that is very large. Note that Penzien and Murakami[42] looked at the coefficient of variation of ductility factors for various combinations of earthquake and frame strength and found the coefficient of variation for the mean ductility factor to lie in the interval [0.1-0.95]. Typically the coefficient of variation is 0.4[49]; however, this may increase to above unity for structures having a very short fundamental period. Figures [3.4] to [3.12] show the "dissatisfaction function" plotted against "coefficient of variation of frame response" over the interval [0.0-1.0], since this

is expected to cover the variations of most practical cases. The following points are noted:

(a) For all three statistical distributions the "dissatisfaction" decreases for decreasing mean frame response. It increases for increasing coefficient of variation of frame response. As the coefficient of variation of frame response increases, however, the difference between the HIGH and LOW frame responses is accentuated and is the cause of the gradient reduction for increasing ratios of *cov*. This effect is particularly noticeable for the positively skewed lognormal distribution.

(b) The frame response is deterministic when its coefficient of variation equals zero. In such cases the behavior of the dissatisfaction function is primarily dependent on *ramp*. For a fixed frame response the dissatisfaction function decreases for decreasing *ramp*. Moreover, the slope of the dissatisfaction function tends towards infinity as *ramp* approaches 1. A singularity in the dissatisfaction function occurs in the limit indicating convergence of the boundaries separating zones 1 and 2, and zones 2 and 3. In these cases a design is either totally feasible, or totally infeasible.

(c) For a fixed level of reliability the mean frame response decreases as the coefficient of variation increases. In other words, as the variation in response increases a more conservative design will be required to ensure a target reliability. This trend is in agreement with the observations of Briseghella[20] and Frangopol[27].

3.6.1 Frame Response Enhancement Factors due to Uncertainty

The ratios:

$$E_1 = \left[\frac{HIGH\_resp}{Mean\ Frame\ Response} \right] \text{ and } E_2 = \left[\frac{LOW\_resp}{Mean\ Frame\ Response} \right] \qquad (3.9)$$

depend on the mean frame response, its c.o.v. and its statistical distribution type. Both ratios are of interest because they place approximate bounds on the required mean frame response enhancement necessary to compensate for the effects of frame response scatter, and achieve a target reliability. Ratio E_1 places the lower bound on the required enhancement, and E_2 an upper bound.

The minimum value of the enhancement factors occurs for deterministic response because the mean value corresponds to the frame response quantity required to achieve all levels of reliability. In these cases the enhancement factor equals unity. Otherwise, the enhancement factor increases monotonically both with increasing scatter and increased limit state reliability. From a practical standpoint, these factors can be compared to code load factors imposed to compensate for uncertainties. This provides a rough means of comparing the conservatism implied implicitly by the code to the reliability calculated explicitly by this design method.

3.7 A procedure for Setting-up the Design Problem.

The design problem is cast by working through the following step-by-step procedure:

STEP 1 The designer must decide whether each performance goal is to be considered as an objective or a constraint. From the algorithm's perspective, the main difference between constraints and objectives is that constraints are not pushed after they achieve their GOOD values whereas objectives continue to be pushed beyond their GOOD values.

STEP 2 HIGH and LOW exceedance probabilities are designated for each constraint.

STEP 3 HARD and SOFT attributes are assigned to each constraint.

STEP 4 GOOD and BAD frame performance quantities are designated for all design objectives and constraints.

STEP 5 The system's performance is calculated. The designer checks that the hierarchy of dissatisfactions calculated with the uniform satisfaction/dissatisfaction rule (equations (3.4) and (3.5)) corresponds to his or her feelings about a the design's performance. If the answer is YES, the designer can proceed to STEP 6. However, if the answer is NO, then an iterative procedure must be entered. The designer adjusts the [GOOD,BAD] and [HIGH,LOW] preference pairs and recalculates the frame's performance until the first test is satisfied.

STEP 6 The designer proceeds to find an improved design.

3.7.1 Algorithm ACTION Given a Design's CONDITION

An essential feature of an effective optimization algorithm is the ability to ascertain a problem's condition, and provide recommendations for continued action. Table[3.5] summarizes the ACTION recommended by the Phase I-II-III Method of Feasible Directions after the CONDITION of a problem has been ascertained.

CONDITION	
PHASE I	At least one HARD constraint is not satisfied.
PHASE II	All HARD constraints are satisfied. At least one SOFT constraint is not satisfied or one performance objective is worse than its GOOD value.
PHASE III	All HARD and SOFT constraints are satisfied and all performance objectives are at their GOOD values or better.
ACTION	
PHASE I	Try to satisfy all the HARD constraints that are not satisfied. One constructs a descent direction for the maximum HARD violation, possibly also trying to decrease the highest costs and soft constraints.
PHASE II	Try to improve both the performance objectives and the SOFT constraints while simultaneously keeping the HARD constraints satisfied. This is done by constructing a descent direction for the highest costs and SOFT constraints, as well as for the eps-active hard constraints.
PHASE III	Try to improve further the performance objectives while keeping all constraints satisfied, in particular, SOFT constraints better than their GOOD values.

Table[3.5] : System performance zones

CHAPTER 4

THE DESIGN EXAMPLE

4. Introduction

As was mentioned in Chapter 1, the scope of applications used in this study to demonstrate the proposed methodology is limited to the design of moment-resistant steel frames. This chapter introduces the example design problem. The practical design problem is translated into a set of mathematical statements that describe the design parameters, constraints and objectives. Initial parameter settings for desirable frame performance are specified. Techniques used for selecting the *design earthquake ground motion* and for scaling ground motion input records are explained. The frame simulation assumptions for each design limit state are also given. Frame performance is evaluated by comparing the frame's response to the designer specified constraints and objectives.

4.1 Frame Geometry, Gravity Loads, and Boundary Conditions

A simple three-story, one-bay, moment-resistant steel frame, shown in Figure[4.1], is employed as the design example to demonstrate the application of the proposed design methodology. It is assumed to be one of many similar frames spaced at $20ft$ centers in a three dimensional structure. Dead and live gravity loads are $80psf$ and $40psf$ on all floors and the roof, respectively. Initial beam and column sizes were obtained by manually designing the frame according to the UBC[63] for Seismic Zone 4. This structure is large enough to illustrate the capabilities of the proposed procedures, but small enough to facilitate interpretation of results and minimize computational effort. A summary of each frame's initial beam and column moments of inertia, and applied gravity loads is shown in Figure[4.2].

The frame's geometry, mass, and boundary conditions are fixed throughout the design process. Each frame is modeled as a two-dimensional structure with its mass lumped at the nodes. The column bases are assumed to be fixed and torsional effects are ignored in the design. Finally, soil-structure interaction effects are ignored.

4.2 Element Modeling

The beam and column elements are bare wide flange sections and are modeled using the lumped-plasticity parallel-component elements in ANSR[41]. These sections are assumed compact, and sufficiently restrained so that lateral and local buckling failures are delayed until after the development of required plastic hinge rotations. Shearing deformation and out-of-plane deformations were not considered in order to simplify the analysis. Likewise the finite size of the beam-column joints was disregarded as were panel zone deformations. Moreover, σ_y was set to 36 *ksi*, E to 29000 *ksi* and the strain hardening ratio, S, to 0.05. For the columns, geometric nonlinearities were taken into account, and an AISC based axial load vs bending moment interaction relation [hexagonal] was used. The parameters for the column and girder interaction relationships are shown in Figure[4.3].

4.3 Loadings

Frame loads are composed of dead and live gravity loads plus lateral seismic loading. Wind, snow and vertical ground accelerations are neglected for simplicity. In the sections that follow each loading type is discussed, together with an explanation of the loading model adopted for the design examples.

4.3.1 Gravity Loads

Based on information provided in Chapters 2 and 3, dead and live gravity

loads are considered to be deterministic. For the limit state defined by *gravity loads alone*, gravity loads consist of the structure's dead load plus the maximum probable live load over the duration of the structure's lifetime; the latter live load is modeled as the nominal design live load. When an earthquake occurs, it is assumed that the instantaneous live load corresponds to its mean lifetime value. Thus, for simulation purposes column axial forces are calculated for dead plus a reduced nominal live load. As a final note, the mass matrix for the structure's horizontal degrees of freedom is based on the dead load only because the live load may not be rigidly attached to the frame structure.

4.3.2 Ground Motions

Ground motion ensembles may be generated by several procedures. One possibility is to scale other ground motion records (having similar epicentral distances and site characteristics) to possess approximately the same probability of exceedance as the target design ground motion. Selecting appropriate scaling parameters is a complicated and difficult step in itself because parameters that are capable of describing a ground motion's potential to cause structural damage with high confidence have yet to be identified[2,38]. Peak values (peak absolute ground acceleration, effective ground acceleration, and velocity), spectral content (spectral intensity and Fourier amplitude), and time related factors such as duration of shaking and Arias intensity are all recommended indices of structural damage potential. Similarly, various measures of ductility have also been suggested. No single measure or scaling procedure by itself has been demonstrated to be completely reliable. In particular, Kennedy[36] notes that isolated high intensity short duration spikes of peak ground acceleration may have little effect on the response spectra of an elastic structure. The smoothed response spectrum for SDOF systems is an improvement because it provides a qualitative description of the intensity and

frequency content of a ground motion. Reliable inelastic design response spectra may be constructed if information on a ground motion's intensity, frequency content and duration can be supplied. This information is used to estimate maximum inelastic deformations. Smoothed inelastic response spectra may be obtained from statistical studies of inelastic response spectra of structures with different strengths and damping ratios. Nonetheless, a deficiency of both the elastic and inelastic spectra techniques is that they can only provide qualitative guidelines and are incapable of incorporating duration effects.

The commentary for ATC[7] suggests that a better method might be to use a set of four or more acceleration time histories within the design process itself. While each ground motion is scaled to the same overall intensity and frequency content, the individual earthquake records are assumed to differ in some potentially important detail of time sequences. The intent of scaling each record is neither to normalize every record to cause exactly the same structural damage, nor to eliminate the various ways in which this damage may be caused. Indeed, a significant scatter in some of the frame response quantities is expected after scaling of the ground motions. An important advantage of this approach is that the limit states may be described in probabilistic terms, thereby smoothing out the influence of individual ground motion irregularities on the design.

Table[4.1] summarizes the library of ground motion records used in this study. They are digitized at 0.02 second intervals. The scaled design ground motions were obtained by working through the following procedure:

(a) The worst ten second sample of each record was subjectively isolated[1]. This was done solely to reduce the required calculation and is not essential

[1] This step was in fact done by Balling et al.[14].

RECORD	COMP	DESCRIPTION
E1	S00E	El Centro Site Imperial Valley Irrigation District. May 18,1940
E2	S90W	El Centro Site Imperial Valley Irrigation District. May 18,1940
E3	S00W	El Centro Site Imperial Valley Irrigation District. Dec 30,1934
E4	S90W	El Centro Site Imperial Valley Irrigation District. Dec 30,1934
E5	N50E	El Centro Community Hospital on Keystone Road. Oct 15,1979
E6	N40W	El Centro Community Hospital on Keystone Road. Oct 15,1979

Table[4.1] : Library of Earthquake Records

to the methodology proposed. Graphs of each ten second ground motion sample are shown in Figure[4.4].

(b) Each record was translated along the y-axis to remove residual velocity effects.

(c) A family of moderate design ground motions was obtained by scaling each record to have the same spectral intensity [**SI** (*in*)] [at 5% damping] over the interval [0.1-2.61] seconds, while simultaneously constraining the mean peak ground acceleration [**PGA** (*g*)] over the family of ground motions to 0.15g.

(d) A family of maximum credible ground motions was employed for severe earthquake lateral loading. Given that an event of this magnitude occurs, the structure is expected to respond by cycling well into the inelastic range without a significant loss of strength. Because the design criteria are energy based it was decided to constrain each ground motion to have equal Arias intensity [**AI** (*in / sec*)] [8] while simultaneously ensuring an average peak ground acceleration of 0.5g across the group. Notice, however, that since the ground motion samples have the same duration, Arias

intensity is equivalent to the root mean square (a_{rms}) ground acceleration. This scaling procedure is recommended by Kennedy[36].

Before Scaling				After Scaling			
Record	**PGA**	**SI**	**AI**	**SCALE**	**PGA**	**SI**	**AI**
E1	0.3463	59.16	44.70	1.672	0.579	98.92	125.00
				0.419	0.145	24.75	7.84
E2	0.2110	44.73	27.98	2.114	0.446	94.56	125.00
				0.554	0.117	24.75	8.58
E3	0.1608	20.17	16.04	2.792	0.449	56.32	125.00
				1.227	0.197	24.75	24.14
E4	0.1621	15.64	13.67	3.024	0.551	47.29	125.00
				1.583	0.288	24.75	34.25
E5	0.1741	46.54	19.46	2.534	0.436	117.93	125.00
				0.532	0.093	24.75	5.51
E6	0.2249	62.46	24.83	2.244	0.505	140.16	125.00
				0.396	0.089	24.75	3.89

Table [4.2] : Ground Motion Scaling Factors

The ground motion scaling factors are shown in Table [4.2]. The severe and moderate scaling factors range over the intervals [1.67-3.02], and [0.396-1.583] with mean values of 2.39 and 0.78 respectively. The c.o.v. of the peak ground accelerations for the severe and moderate scaled ground motions is 0.122 and 0.49, respectively. Since all of the scaling factors for the severe lateral loading are greater than one, this family of ground motions is a reasonable candidate for modeling the maximum credible ground motion. Figure[4.5a] illustrates the spectral velocities of the six unscaled records. Spectral velocities of the same six records after they have been scaled are shown in Figure[4.5b]. Similarly, the Arias Intensity of the six ground motion records before and after scaling the severe earthquake intensity are shown in Figures[4.6a] and [4.6b], respectively.

4.4 The Frame Simulation Assumptions

The general purpose structural analysis program ANSR[41] is used to compute structural response for each limit state. For those limit states requiring dynamic analysis, structural response is computed one second beyond the end of the 10 second ground motion samples.

Path dependent state determination is used in all analyses. The maximum allowable nodal displacements is unlimited, convergence tolerance on force norm vectors is set to 0.01, and the next load or time step is applied regardless of convergence in the previous step. In addition, the following modeling assumptions are made for the individual limit state analyses:

4.4.1 Gravity Loads Alone

A Newton-Raphson iteration scheme is employed to execute a nonlinear static analysis. Gravity load are applied in a series of five load steps. The maximum number of iterations permitted at any load step is 20, and the stiffness matrix is reformed at each iteration. In addition, the frame is modeled with two translational (x and y) plus one rotational degree of freedom at each nodal point. This accounts for axial deformations in both the columns and girders. Under these assumptions the example frame is modeled with 18 degrees of freedom, as illustrated in Figure[4.7].

4.4.2 Gravity Loads plus Moderate Earthquake Loading

Simulation for this limit state requires a static linear analysis under gravity loads only followed by dynamic linear analysis under moderate quake loading. Both analyses are simplified by neglecting axial deformations in the columns and girders and by assuming a linear elastic response.

The latter requirement is ensured in the program by increasing the model yield moments and forces by a factor of 1000 and allowing only one iteration per time step. Thus, only one static load step is required to represent the gravity loads before the moderate earthquake ground motion loads are applied. Each frame node has a maximum of two degrees of freedom; the x translational plus the ϑ rotational degree of freedom. The translational degrees of freedom at each floor level are slaved. Hence Figure[4.8] shows that the example frame is modeled with 9 degrees of freedom. The damping matrix is modeled as a linear combination of the mass and stiffness matrices. This Rayleigh damping matrix has the form:

$$\left[C \right] = a_1 \left[M \right] + a_2 \left[K \right] \tag{4.1}$$

where : $\left[C \right]$ = *damping matrix*

$\left[M \right]$ = *mass matrix*

$\left[K \right]$ = *stiffness matrix*

$$a_1 = \left[\frac{2 \lambda w_1 w_2}{w_1 + w_2} \right]$$

$$a_2 = \left[\frac{2 \lambda}{w_1 + w_2} \right]$$

w_1, w_2 = *first and second natural circular frequencies*

λ = *percentage of critical damping in the 1st and 2nd modes*

In order to maintain constant damping values in the first and second modes the coefficients a_1 and a_2 are updated for each current design at the beginning of the calculations for this limit state. First, ANSR is employed to form the mass and stiffness matrices (including geometric stiffness effects) for the present design. A subspace iteration routine extracted from the program FEAP[69] is called to calculate the frame's natural periods of vibration corresponding to the non-zero mass degrees of

freedom.

A damping ratio of 2% critical is applicable to frames of this type for low amplitude motions where it is assumed that all stresses remain within working stress load limits. The damping may increase to 5-7% for larger amplitude motions during which yielding at the joints may occur[43]. Moreover, localized inelastic deformations in multi-degree of freedom structures may reduce the system's apparent vibrational frequencies (indicating, in part, a loss of stiffness) and an increase the participation factor of the fundamental mode[55,64]. It is clear that any particular value of Rayleigh damping can only be an approximation to the structure's actual damping. If the adopted damping value is too large, the decreased response will result in a non-conservative design. Consequently, 3% damping in the first and second modes was chosen as being most realistic in modeling the frame's response. Additional damping during large amplitude motions is taken into account by including the material's hysteretic behavior in a nonlinear time-history analysis.

4.4.3 Gravity Loads plus Severe Earthquake Loading

Simulation for this limit state requires a static nonlinear analysis under gravity loads only followed by a dynamic nonlinear analysis under severe earthquake loading. The nonlinear static and dynamic analyses use Newton Raphson iteration. As with the previous limit state, each frame node is modeled with two degrees of freedom. Column and girder axial deformations are ignored. Gravity loads are applied in five static load steps; this is followed by the severe earthquake time-history analysis. The stiffness matrix is reformulated at each iteration in each load or time step and the maximum number of iterations within each timestep or load incre-

ment is 20.

4.5 The Optimization Problem Assumptions

The design parameters, constraints and objectives are now outlined. Parameter settings are given along with their initial values.

4.5.1 Design Parameters

The frame elements are each modeled by a single section property parameter. Moment of inertia is the primary section property parameter used for the beam and column elements, and cross-sectional area for truss elements. Element properties of secondary importance such as radius of gyration and element depth are obtained from empirical relations derived by Walker[66] for economy wide flange steel sections. These are (in English Units):

$$\textit{for columns}\quad I \le 429\ in^4 \qquad (4.2)$$
$$d = 1.47 I^{0.368}$$
$$r = 0.39 d^{1.04}$$

$$\textit{when}\quad I > 429\ in^4$$
$$d = 10.5 I^{0.0436}$$
$$r = 0.39 d^{1.04}$$

$$\textit{for girders}\quad d = 2.66 I^{0.287}$$
$$r = 0.52 I^{0.92}$$

The section area and plastic moment can then be computed as:

$$A = \frac{I}{r^2} \qquad (4.3)$$

$$M_p = \left[\frac{Ad}{8} + \frac{3I}{2d}\right]\sigma_y \qquad (4.4)$$

$$\textit{for braces}\quad I = 0.169 A^3$$

Frame members may be subject to design or fixed at their initially chosen values. In addition, frame element sizes can be clustered into groups that are either equally or proportionally constrained. From a practical standpoint, repetition of equally sized elements implies both economical construction and a reduction in the computational work needed for each iteration of optimization. Proportional constraints are more general and allow element repetition while locally imposing a desirable ratio of frame element sizes. This facility enables various member proportioning philosophies to be investigated economically. The main disadvantage of constraint proportioning is that section sizes are bounded by the most critical constraint within the group. Therefore, a balance in criteria is desirable; grouping should retain flexibility in the optimal design while simultaneously keeping the problem practical in terms of element repetition and amount of calculation required.

The process of allocating frame elements to a group and designating members as ***designed*** or ***not designed*** tends to be subjective. In spite of the aforementioned guidelines, the selection of the best design parameter ***arrangement***, or ***layout***, is still subjective. Figure[4.9] shows the three arrangements of design element groupings to be considered in this investigation. The column and beam members are constrained to a single parameter in the first arrangement. The first element in the group (Column 1) is called the ***leading element***. The remaining elements are proportionally constrained to the leader (see Appendix 1) and are called ***tracking elements***. In the second arrangement the girders and columns are modeled by independent design parameters. The third arrangement permits a variation of stiffness over the height of the structure while locally constraining the relative strength of adjacent columns and girders. All of the frame ele-

ments are subject to design in each of the parameter arrangements.

Parameter scaling can be handled either automatically or manually. A disadvantage of automatic scaling is that it fails to account for the designer's intuition in dealing with the problem at hand. Fully manual control maybe too cumbersome. DELIGHT.STRUCT strives for a balance by initially handling parameter scaling automatically, but providing the user with a manual user over-ride during the optimization stages.

Since most designers will have little idea what the most binding constraints will be at the beginning of the design process, DELIGHT.STRUCT provides initial values for the *Nominal Variation* in equation (3.3). They are obtained by first assuming that a perturbation in any frame element size will have the same effect on the most binding constraints. However, a single design parameter is frequently used to represent several frame elements. Thus, the starting *Nominal Variation* is estimated by counting the number of elements within the frame group and dividing it by the total number of elements in the frame. The designer may modify these values as the need arises.

4.5.2 Design Constraints

Appendix 1 shows that the example problem has 18 box constraints, 46 conventional constraints and 25 functional constraints. Those corresponding to each limit state are now outlined:

4.5.2.1 Box Constraints

Box constraints (written as pairs of conventional constraints) ensure that the beam and column section moments of inertia lie within the intervals [50,100] and [2500,3000] in^4, respectively (see Figure[3.2]).

PARAMETER	TYPE	DESCRIPTION
Const_type_Lowbox	HARD	Low box constraint
Const_type_Upbox	HARD	Upper box constraint

Table[4.3] : Box Constraint Type Parameters

Table [4.3] shows that the box parameter constraint types are set to HARD. Hence, during the initial iterations of optimization priority is given to satisfying box constraints that do not lie within the feasible domain. The algorithm achieves this goal by pushing the design vector until all of its components are better than the GOOD value of the box constraint.

4.5.2.2 Constraints Under Gravity Loads Alone

The following conventional constraints apply to the beams, columns and braces under gravity loading alone:

$$[\ \textit{column axial force}\ ] < \textit{Colax} \times \textit{Column axial force} \quad (4.5)$$

$$[\ \textit{column end moment}\ ] < \textit{Colgra} \times \textit{Column yield moment} \quad (4.6)$$

$$[\ \textit{girder end moment}\ ] < \textit{Girgra} \times \textit{Girder yield moment} \quad (4.7)$$

$$[\ \textit{girder midspan deflection under live load}\ ] < \textit{Girdef} \times \textit{Girder span} \quad (4.8)$$

PARAMETER	VALUE	DESCRIPTION
Good_Colax	.5000	good gravity column axial force factor
Bad_Colax	.6000	bad gravity column axial force factor
Good_Colgra	.6000	good gravity column yield factor
Bad_Colgra	.8000	bad gravity column yield factor
Good_Girgra	.6000	good gravity girder yield factor
Bad_Girgra	.8000	bad gravity girder yield factor

Table[4.4] : Gravity Loads Alone Constraint Parameters

A convention of nomenclature introduced in equations (4.5) to (4.8) is now explained. The parameters *Colax*, *Colgra* and so on should be interpreted as a shortened notation for the GOOD and BAD performance (or

preference) pair settings discussed in Section 4.2. For example, the GOOD value of the column axial force constraint described by (4.5) is simply the dependable column axial force factor, *Good_Colax* shown in Table[4.4], multiplied by the column axial force required to cause either yielding in tension, or Euler buckling in compression. The GOOD value is set to 0.5. This corresponds to a safety factor of two against Euler buckling of a pin-ended column, or a somewhat lower level of conservatism against instability of frames that have no resistance to sidesway. It is also the approximate level of loading at which nonlinear effects due to residual stresses start to become important. 0.6 is chosen as the BAD value. This seems reasonable since a frame's lateral degrees of freedom will be partially restrained in practice, and the probable material yield stress may well exceed the modeling yield stress. The American Institute of Steel Construction's recommended allowable stress factor for bending is 0.6[3].

PARAMETER	VALUE	DESCRIPTION
Good_Girdef	4.170e-3 [1/240]	good girder midspan deflection
Bad_Girdef	4.570e-3 [1/219]	bad girder midspan deflection

Table[4.5] : Girder Deflection Constraint Parameters

Calculations for the midspan girder deflections are based on a uniform dead plus reduced live gravity loading plus the additional deflections due to rotations of the frame joints. With respect to an allowable deflection the AISC commentary states that:

> "there is no single way by which the limit of tolerable deflection can be defined... the most satisfactory solution rests with the sound judgement of qualified engineers."

Consequently, the GOOD girder deflection is set to the Uniform Building Codes recommended value. The BAD girder mid-span deflection, shown

in Table[4.5], is just an arbitrarily increased value.

A constraint may also be placed on the maximum volume of the design elements. The maximum volume constraint is usually employed when a balance among multiple design objectives is required (see Chapter 6). In the meantime, however, this constraint is effectively removed by adjusting the GOOD and BAD parameter values to those shown in Table[4.6].

PARAMETER	VALUE	DESCRIPTION
Good_Volmax	1.000e+5	good volume maximum
Bad_Volmax	1.200e+5	bad volume maximum

Table[4.6] : Maximum Volume Constraint Parameters

PARAMETER	VALUE	DESCRIPTION
High_Colax_prob	.2000	high gravity column axial force factor
Low_Colax_prob	.1000	low gravity column axial force factor
High_Colgra_prob	.2000	high gravity column yield factor
Low_Colgra_prob	.1000	low gravity column yield factor
High_Girgra_prob	.2000	high gravity girder yield factor
Low_Girgra_prob	.1000	low gravity girder yield factor
High_Girdef_prob	.2000	high girder midspan deflection
Low_Girdef_prob	.1000	low girder midspan deflection
High_Volmax_prob	.2000	high volmax probability
Low_Volmax_prob	.1000	low volmax probability

Table[4.7] : Constraint Exceedance Probabilities

Table[4.7] shows the exceedance probabilities adopted for the gravity loads alone limit state constraints. The variation in computed frame response is zero for this limit state because the gravity loads are assumed to be deterministic. Thus the HIGH and LOW frame response values effectively cancel. Furthermore, Table[4.8] shows that this limit state's constraints are set to SOFT; they may be traded off against one another and against design objectives during the optimization.

PARAMETER	TYPE	DESCRIPTION
Const_type_Colax	SOFT	gravity column axial force factor
Const_type_Colgra	SOFT	gravity column yield factor
Const_type_Girgra	SOFT	gravity girder yield factor
Const_type_Girdef	SOFT	girder midspan deflection
Const_type_Volmax	SOFT	volume maximum

Table[4.8] : Gravity Loads Constraint Types

4.5.2.3 Constraints Under Combined Gravity and Moderate Quake Loads

Under this loading condition non-structural damage should be limited with only superficial structural damage. Two measures of frame response are used to identify nonstructural damage. Damage to frame members, windows, partitions and other architectural elements is related to relative frame displacements. These are controlled by enforcing a constraint[2] on story drifts of the form:

$$[\ story\ drift\ ]_{max\ over\ time} < Drift \times story\ height \qquad (4.9)$$

Similarly floor acceleration is used as a measure of damage to a structure's contents, equipment, and elements attached to the floors. The form of this constraint is:

$$[\ absolute\ floor\ acceleration\ ]_{max\ over\ time} < Accel \times acc'n\ of\ gravity \qquad (4.10)$$

Very few references quantify expected structural damage as a function of the above parameters. The parameter usually used to describe structural damage is called the *damage ratio*. A damage ratio of zero corresponds to negligible damage, while a damage ratio of greater than or equal to one signifies total damage or complete collapse. Ferrito[26]

[2] Components of story drift consist of (a) column bending, (b) girder bending, (c) joint rotations and (d) bending of the frame as a whole due to column axial deformations. The latter component is neglected in this formulation.

reports that the damage ratio for windows and steel frames is negligible for an effective story drift of 0.001, 0.3 for story drift of 0.005, 0.8 for drift of 0.01, and 1 for a drift of 0.02. Damage ratios of building contents associated with floor accelerations range from 0.05 at 0.08g to 1.0 at 1.4g. Damage to building contents at 0.5g is 0.6 and 0.9 at 1.2g. Effective values for response prediction were taken as 65% of the peak values in both instances. Guangquian et al.[31] confirm that no damage should be expected for story drifts less than or equal to the ratio [1/300-1/200] in framed construction. Slight structural damage can be expected for story drifts within the interval [0.005-0.004], severe damage for the ratio 0.01 and collapse as the drift approaches 0.02. The Uniform Building Code[63] stipulates that 0.5% (story drift ratio = 0.005) story drift is permissible for moderate lateral seismic loading.

Mahin and Bertero[40] indicate that while story drift is used to measure damage, there is in fact little data available to make these estimates more than qualitative. Indeed, the same could be said of the floor accelerations. The boundary between *satisfactory* and *unsatisfactory* frame performance cannot be sharply defined; this is reflected in the large relative difference between the GOOD and BAD frame response parameters shown in Table[4.9].

PARAMETER	VALUE/TYPE	DESCRIPTION
Good_Drift	4.500e-3	good max moderate story drift
Bad_Drift	8.000e-3	bad max moderate story drift
Good_Accel	0.700	good max moderate floor accel in gs
Bad_Accel	1.400	bad max moderate floor accel in gs
Const_type_Drift	SOFT	max moderate story drift
Const_type_Accel	SOFT	max moderate floor accel in gs

Table[4.9] : Drift and Acceleration Constraint Parameters

The frame should also possess sufficient strength so that under moderate lateral loads structural damage is minimal. Inelastic deformations are discouraged by ensuring that the frame response satisfies the following constraints:

$$[\ \textit{column end moments}\ ]_{\textit{max over time}} < \textit{Colyld} \times \textit{column yield moments} \qquad (4.11)$$

$$[\ \textit{girder end moments}\ ]_{\textit{max over time}} < \textit{Giryld} \times \textit{girder yield moments} \qquad (4.12)$$

PARAMETER	VALUE/TYPE	DESCRIPTION
Good_Colyld	.8500	good moderate column yield factor
Bad_Colyld	1.100	bad moderate column yield factor
Good_Giryld	.9000	good girder yield factor
Bad_Giryld	1.100	bad girder yield factor
Const_type_Colyld	SOFT	moderate column yield factor
Const_type_Giryld	SOFT	girder yield factor

Table[4.10] : Element Yielding Constraint Parameters

The GOOD element yielding parameter values shown in Table[4.10] may be viewed as stress reduction factors. Their purpose is (a) to allow for the probability of understrength in the frame elements due to variations in member strengths, (b) to allow for inaccuracies in modeling, and (c) to reflect the importance of a member in the structure. A lower GOOD value is used for the columns than for the beams because columns carry axial loads and have displacements that are comparatively more sensitive to the details of individual ground motions. The BAD yield factors can be attributed to several factors. First, the probable yield stress of steel under dynamic loading may well exceed the ideal yield stress (see Section 2.2). Hence, even if the calculations indicate yielding in the members of the frame, a real structure may still be elastic. In any case, even though an entirely elastic response is desirable, a few minor excursions of the critical regions into the inelastic range can often be tolerated without reaching an

unacceptable level of structural damage.

Several difficulties arise with setting the HIGH and LOW exceedance probability parameters. Their purpose is to provide a level of reliability to each limit state that reflects the consequences of failure when sufficient information is available to describe the parameter fluctuations with statistical regularity. The Applied Technology Council[7] provides guidelines in its commentary on the expected number of failures for ground motions exceeding the *design ground motion*. Its estimates are approximate. Indeed, achieving consistency with the design criteria in absolute terms would appear unobtainable because an acceptable level of risk is often affected by intangibles.

Identifying an acceptable risk level requires experience and judgement. Because the problem studied here is the first to be examined with this methodology, the author has little experience to draw upon. Consequently, the best that can be achieved is to set the parameters to values which seem reasonable, and concentrate on developing the design example for comparison with more familiar design techniques.

A similar problem exists for the identification of a suitable statistical distribution to describe each frame response quantity. When only a small number of samples is used to approximate the variation in each frame response quantity, the statistical distributions of frame response quantities have to be assumed before the calculations begin. However, in Section 2.5 it was shown that information obtained from analytical studies can provide useful guidelines for selecting an appropriate distribution for only some of the frame response quantities. Thus, for the initial design computations all of the response quantities relating to material behavior, such as peak member ductilities, are assumed to be Extreme Type I distributed.

Where information is not available, it is assumed that the parameter is normally distributed. The same HIGH and LOW exceedance probabilities are assumed for all constraint types within a single limit state.

Specifying a rigid boundary on acceptable level of frame risk cannot be justified for a number of reasons. First, the actual (or real) level of frame risk will differ from the calculated level of frame risk. With accurate modeling one can hope that the actual and real frame risks are close. The designer cannot specify a rigid level of frame risk in the absence of experience. Experience requires hindsight; because both are absent at this stage all that can be done is to specify risk levels that appear reasonable. After a few examples have been completed the risk explicitly set in this method may be compared to the conservatism implicitly set by other approaches such as the UBC Code[63]. Consequently, we begin with a relatively wide difference between the HIGH and LOW exceedance probabilities, as shown in Table[4.11].

PARAMETER	VALUE	DESCRIPTION
High_Drift_prob	.2000	high max moderate story drift
Low_Drift_prob	.1000	low max moderate story drift
High_Accel_prob	.2000	high max moderate floor accel in gs
Low_Accel_prob	.1000	low max moderate floor accel in gs
High_Colyld_prob	.2000	high moderate column yield factor
Low_Colyld_prob	.1000	low moderate column yield factor
High_Giryld_prob	.2000	high girder yield factor
Low_Giryld_prob	.1000	low girder yield factor

Table[4.11] : Constraint Exceedance Probability Parameters

4.5.2.4 Constraints Under Combined Gravity and Severe Quake Loads

The currently accepted design philosophy permits major structural damage, possibly beyond repair, resulting from a severe earthquake.

Frame collapse and loss of life are nevertheless discouraged. Constraints are divided into two categories reflecting frame behavior at the global level and frame behavior at the element level.

Global frame instability is generally attributed to enhanced bending moments due to P-delta effects when large lateral frame displacements act in conjunction with high axial forces. This type of behavior is prohibited herein by placing an upper bound on allowable peak frame displacements. For the purposes of this study large displacements at the top of the frame are used as an approximate measure of the possibility of collapse. The parameter *Sway* is defined as the maximum relative horizontal displacement at the top of the frame divided by the frame height and the constraint is described as follows:

$$[\ frame\ sway\ ]_{max\ over\ time} < Sway \times frame\ height \qquad (4.12)$$

PARAMETER	VALUE/TYPE	DESCRIPTION
Good_Sway	1.400e-2 [0.14%]	good structure sway max
Bad_Sway	2.000e-2 [0.20%]	bad structure sway max
High_Sway_prob	.2000	high structure sway max
Low_Sway_prob	.1000	low structure sway max
Const_type_Sway	SOFT	structure sway max

Table[4.12] : Frame Sway Constraint Parameters

As mentioned in Section 4.5.2.3 collapse can occur for peak story drifts approaching 0.02. The Uniform Building Code tacitly implies that lateral frame deflections of 1.5% are acceptable for severe lateral loads. Table[4.12] shows the frame sway constraint parameters adopted for this study.

Structural damage at the material level is closely related to the extent

of inelastic deformations. One reversed cycle at a high ductility range may cause damage equivalent to many cycles at a lower ductility range. Experimental results[51] indicate that this behavior is characteristic of low cycle fatigue. A constraint on allowable energy dissipation is formulated by assuming that the total hysteretic energy dissipated under an arbitrarily changing deformation history may be equated to the energy dissipated by a monotonic load moving through an equivalent displacement to ultimate failure. Kato[34] reports that this assumption is reasonable. The allowable energy dissipation in the latter mechanism is used to form the constraint, namely:

$$E_d < E_y \times f(\mu, S) \tag{4.13}$$

where $f(\mu, S) = [\mu - 1][1 - S][2 + S[\mu - 1]]$

E_d = *Inelastic dissipated energy.*
E_y = *Elastic strain energy at yield.*
μ = *Allowable rotational ductility factor.*
S = *Strain hardening ratio.*

PARAMETER	VALUE/TYPE	DESCRIPTION
Good_Colduc	3.000	good column ductility
Bad_Colduc	4.000	bad column ductility
Good_Girduc	4.000	good girder ductility
Bad_Girduc	6.000	bad girder ductility
High_Colduc_prob	.2000	high column ductility
Low_Colduc_prob	.1000	low column ductility
High_Girduc_prob	.2000	high girder ductility
Low_Girduc_prob	.1000	low girder ductility
Const_type_Colduc	SOFT	column ductility
Const_type_Girduc	SOFT	girder ductility

Table[4.13] : Element Ductility Constraint Parameters

In equation (4.13) the allowable rotational ductility is defined as the maximum end rotation ϑ_{max} divided by the rotation ϑ_y at incipient yielding. In

calculating ϑ_y, anti-symmetrical double curvature is assumed for the member[3]. Table[4.13] summarizes the beam and column ductility factors. The conventional constraints represented by equation (4.13) are:

$$\textit{Column end inelastic energy dissipation} < E_y \times f(\textit{Colduc}, S) \qquad (4.14)$$

$$\textit{Girder end inelastic energy dissipation} < E_y \times f(\textit{Girduc}, S) \qquad (4.15)$$

No checks are made on a section's lateral and local buckling failure modes.

4.5.3 Design Objectives

This section outlines the design objective alternatives. The capabilities of the DELIGHT.STRUCT software are briefly explained together with the desirable attributes for the performance of each design objective function. Particular attention is given to energy based designs. Initial values of the design parameters are given for the example frame for subsequent use.

4.5.3.1 Volume of Structural Elements

Utilizing minimum volume as a design objective reflects a typical design philosophy. Although volume is correlated to material cost, a modest material saving may be of lesser importance than other possible objective functions when considering the structure's lifetime performance and cost. Nonetheless, minimum volume is often used as the starting point for optimization inasmuch as it reflects the minimum initial material cost of the structure.

The DELIGHT.STRUCT preprocessor allows the designer tc specify

---

[3] The validity of this assumption is only good when girder gravity load bending moments are small compared to those caused by the seismic loads. Similarly, the position of contraflexure in the columns can be moved significantly due to the influence of dynamic forces and the higher modes[48].

which frame elements should be included into the design volume calculation. In the example problem all of the frame elements are included in the volume calculation[4], with Table[4.14] showing the GOOD and BAD design objective values.

PARAMETER	VALUE	DESCRIPTION
Good_Costvol	1.800e+4	good volume objective
Bad_Costvol	2.400e+4	bad volume objective

Table[4.14] : Volume Design Objective Constraint Parameters

4.5.3.2 Story Drifts

Drift control generally ensures structural integrity and the control of non-structural damage. Any reasonable control of drift will ensure structural stability. In some cases, however, partitions and ceilings may be very vulnerable to distortions. Teal[62] reports that their collapse may kill people directly or block the use of essential life safety services. Hence minimizing non-structural damage via control of story drifts may not only be a necessary economic consideration, but in some instances, essential to assuring life safety.

DELIGHT.STRUCT handles story drift constraints and design objectives in different ways. First, the story levels considered for the design objective evaluation may correspond to, or be a subset of the story levels subject to constraint. Intermediate design objectives are calculated for each story level by comparing the mean peak story drift to the GOOD and BAD story drift design objectives (see Table[4.15]).

Overall design objective performance is taken as the mean of the

[4] The total volume of frame elements for the initial design is 21470 in^2.

PARAMETER	VALUE	DESCRIPTION
Good_Costdri	2.000e-3 [0.2%]	good drift objective
Bad_Costdri	4.000e-3 [0.4%]	bad drift objective

Table[4.15] : Story Drift Design Objective Parameters

intermediate dissatisfactions calculated for the individual story levels. The main advantage of this formulation is that the design objectives and constraints are measured with the same units and unscaled numbers. Moreover, because the GOOD and BAD values are specified for both the constraints and objectives, the latter can be used to encourage an improvement in the overall frame behavior while the constraints ensure that the displacements are not excessive at any particular story level.

4.5.3.3 Energy Based Design

Although it is possible to design a structure to resist severe lateral earthquake loads elastically, economic factors usually dictate that it is more feasible to design a system having the largest energy dissipation capacity that is consistent with tolerable deformations[7]. The frame should survive these motions with reasonable predictability, which usually implies that a frame should reach full plastic yielding before the maximum lateral frame displacements are reached.

The term *energy based* is given to those design methods that account for inelasticity by including energy concepts into the design process. These methods have been around for many years, and typically incorporate a number of empirical shortcuts based on energy ideas[16,18,33]. One of the essential ingredients in this type of formulation is the energy balance equation; it reduces a conglomerate of complex mechanical information distributed in both space and time into a time-dependent scalar equation

of the form:

$$W = E_k + D + E_e + E_i \tag{4.15}$$

where E_k = *kinetic energy*

D = *damped energy at the element level*

E_e = *Elastic energy*

E_i = *Inelastic or dissipated energy*

W = *total input energy (or work done) by externally applied loads*

Energy is fed into the base of the structure throughout the duration of a ground motion. It is important to know how the energy is distributed among the terms in the energy balance equation, and how each term is related to the physical characteristics of structural behavior. Input energy is the scalar product of the base shear force (plus all external loads) moving through an incremental displacement at each timestep integrated over time. This quantity is a function of the structure's properties, including its mass, damping, and stiffness. With respect to structural behavior, input energy generally decreases and becomes less sensitive to ground motion frequency content for structures that have a low yield level. Structures with high yield values primarily dissipate energy through element damping, whereas structures with low yield values dissipate energy through inelastic cycling. The contribution of the elastic and kinetic energy terms are usually of secondary importance in the balance equation.

Attention is now focused on structural behavior at the element level. The spatial and temporal distribution of column interstory displacements, inelastic deformations and ductility ratios are of concern because these are known to be extremely sensitive to the details of different ground motions. In the worst cases excessive lateral displacements may lead to the development of a soft story mechanism and collapse. Performance of this type in multi-story moment resistant frames may be discouraged by

ensuring that dependable column strengths exceed the overstrengths of adjacent beams. This design criterion is called the weak-beam strong-column proportioning philosophy, and is preferred because plastic hinging is forced into elements that have a greater capacity for energy dissipation.

A qualitative design objective is needed that seeks a structure which not only satisfies the constraints, but performs well under severe lateral loads. As already indicated, the contribution of each term in the energy balance equation depends on the structure itself. As a general guideline, however, safely minimizing input energy and maximizing the percentage of energy dissipated through inelastic internal energy results in good overall performance because the structure attracts smaller quantities of energy, and distributes it to as many elements as possible without violating constraints. In other words, over the duration of the earthquake we aim to optimize the criterion:

$$\begin{aligned} &\textit{minimize } W \\ \textit{and} \quad &\textit{maximize } \left[\frac{E_i}{W}\right] \end{aligned} \tag{4.16}$$

A similar description is given by Pall and Marsh[47]. They suggest that a *good design* will result if the energy available to cause large deformations is minimized. This idea is equivalent to extracting kinetic energy from a body, and the optimal design problem is viewed as minimizing the difference between the total input energy and the frame dissipated energy. However, this design objective fails to relate explicitly the energy dissipated by the structure to its capacity for energy dissipation; the latter is usually cast as a constraint. The problem of optimally allocating a fixed quantity of resources is another design objective of practical interest. In the context of seismic design, this can be viewed as determining the

member proportioning of a structure's elements which maximizes frame performance reliability for a fixed structure volume (or initial cost). All of these design objectives are distinct; the important point to note is that the choice of an appropriate energy function is not unique, and in fact tends to be subjective.

DELIGHT.STRUCT has the capability of assessing frame performance with three distinct types of energy based design objectives. During the preprocessor stage the designer designates energy group number attributes for selected frame elements. The basic idea in completing this procedure is to distinguish the elements of the frame that are capable dissipating large quantities of energy from those that are less capable of dissipating excessive quantities of inelastic energy without adverse consequences to the overall integrity of a structure. This separation of criteria is achieved by describing the performance of each energy group with two design objectives. Input energy at the frame base is considered as the third energy-based design objective. Each of these design objectives is now explained in more detail.

Design Objective 1 in each energy group is calculated by first dividing the energy dissipated at each node in the group by the corresponding element's ability (taken as the GOOD constraint value) to dissipate energy. Then, the mean value of the normalized ratios summed over both the energy group's nodes and all of the ground motion records is computed. The level of design objective dissatisfaction is obtained directly by substituting the mean normalized ratio and the [GOOD,BAD] preference pairs into equation (3.4). From a physical standpoint this design objective gives an overall measure of the average energy dissipation demand compared to the energy group's ability to dissipate energy. Notice that the design

objective is not just the mean dissipated energy since it fails to account for *equitable sharing*; large frame elements are capable of dissipating more energy than smaller frame elements. A high value of design objective 1 is desirable for groups of frame elements that are capable of dissipating energy without adverse consequences to overall frame performance since this indicates that energy dissipation is well shared among frame elements in the group. Frame performance generally improves as the design objective approaches unity because each of the frame elements dissipates an amount of hysteretic energy that becomes increasingly closer to its dependable capacity. Notice, however, that the objective only measures the mean value; the variation of energy dissipation at each node is expected to be well described by the extreme type 1 distribution[49]. By noting that energy dissipation can only be positive and that this distribution is positively skewed, this implies that the distribution of energy dissipation will be accompanied by a high coefficient of variation. Consequently, it is unlikely that a mean value of unity would ever be obtained before causing a constraint violation at one or more of the group's nodes. This is reflected in the setting of the GOOD values for this design objective (see Tables [4.16] and [4.17]).

The calculation for second design objective in each energy group begins by computing the coefficient of variation of the aforementioned normalized energy ratios for each ground motion input. The response quantity used for the frame performance assessment is the maximum value of the coefficients of variation calculated. Again, the corresponding level of designer dissatisfaction is computed with equation (3.4). The physical interpretation of this design objective is less obvious. As an overall measure, it places a lower bound on the group's effectiveness in always sharing

the burden of energy dissipation equitably among its nodes. In the ideal case design objective 2 equals zero; that is, each frame node within a group always dissipates a constant proportion of energy in relation to its capacity to dissipate energy. This implies that the frame response is uncoupled from the time-dependent details of individual earthquakes, and that the magnitude of total energy dissipation is only a function of the overall ground motion intensity. In practice, however, this objective will not be attained because a structure cannot completely isolate itself from the details of ground motion. For example, near-field ground motion inputs are of particular concern to moment-resistant and braced frames because they frequently contain long duration pulses that feed a large quantity of energy into the structure in a relatively short period of time[60]. This may lead to a concentration of energy dissipation at the frame base (accompanied by the formation of a soft story mechanism) due to the inability of the input energy to distribute itself over the vertical height of the structure. The total input energy of other record types may be equal, but distributed more uniformly in terms of time. Therefore, the goal of Design Objective 2 is to encourage a redistribution of frame element strengths when an undesirable concentration of hysteretically dissipated energy is detected within an energy group.

Suppose, for example, that the columns of a frame at the ground level constitute one energy group, with the remaining columns in the frame defining a second energy group. Conservative performance of the first energy group is detected by zero energy dissipation at the frame base; ie, low values of design objective 1 and design objective 2. Good performance of this energy group occurs when some of the nodes at the frame base dissipate energy; in other words, this corresponds to a low value of design

objective 1 and a high value of design objective 2. The likely formation of a soft story collapse mechanism at the first floor of a frame would be detected with a low value of design objective 2 and a high value of design objective 1. Because the frame elements in the second energy group are essentially required to remain elastic, low values of design objective 1 and design objective 2 are desirable. Initially it would seem that an incremental solution strategy is best for problems of this nature. One could begin by modifying a design to achieve desirable values of design objective 1. If it becomes apparent that the starting allocation of elements to the energy groups could be improved, then this should be done as an intermediate step in the design process. Further improvements might then be encouraged by emphasizing a redistribution of element sizes which improves the performance of design objective 2.

Design objective 3 is the mean value of the input energy at the frame base computed for each of the ground motion inputs. Recall that input energy at the frame base of an undamped system is the scalar product of the base shear moving through an incremental displacement at each timestep integrated over time[5]. The primary use for this objective is in the design of base isolation systems, since lowering the yield level at the frame base decreases the total input energy. Decreasing the input energy has its limits, however, because displacements increase as the yield level is decreased (up until the frame has a fundamental period of about 0.5 seconds). In these design cases, inelastic deformations are expected to be confined to the base of the frame, with the remainder of the structure remaining elastic even for the most severe lateral loads. Thus, the design criterion constitutes an enhanced design philosophy, which will not be

[5] Additional input energy occurs at the frame base if the system has element damping.

pursued further in this report.

4.5.3.4 Parameter Settings for the Energy Based Design

In the example problem all of the frame elements were allocated to one of two energy groups. The columns form the first group; as already noted, conservative performance (but still satisfactory) for this energy group occurs when the columns remain completely elastic. Less conservative performance occurs when a limited quantity of hysteretic energy is dissipated only at the frame base. Table[4.16] summarizes the design objective parameters used to encourage this type of behavior. The second energy group consists of the frame's girders. The coefficients in this group are set to encourage a high mean energy dissipation throughout the group, as shown in Table[4.17]. Notice that the GOOD and BAD values for design objective 2 in both energy groups have been set initially to remove this objective from affecting the frame performance; this emphasizes an initial improvement of design objective 1.

PARAMETER	VALUE	DESCRIPTION
Group1_gmean_dis	0.00	Group1 - mean dissipated energy
Group1_bmean_dis	0.15	
Group1_gvar_dis	3.00	Group1 - energy variation
Group1_bvar_dis	5.00	

Table[4.16] : Design Objective Parameters for Energy Group 1

PARAMETER	VALUE	DESCRIPTION
Group2_gmean_dis	0.50	Group2 - mean dissipated energy
Group2_bmean_dis	0.00	
Group2_gvar_dis	1.00	Group2 - energy variation
Group2_bvar_dis	3.00	

Table[4.17] : Design Objective Parameters for Energy Group 2

CHAPTER 5

PRELIMINARY ANALYSIS

5. Introduction

This Chapter reports on a preliminary analysis for the example frame. Additional assumptions are stated for the frame simulation and constraint evaluation. The parameter settings discussed in Chapter 4 are used to evaluate the frame constraints for two sets of ground motion inputs. A hierarchy of ranked frame performance attributes is constructed. The Chapter concludes with a discussion of the overall frame performance.

5.1 Additional Frame Simulation Assumptions

One of the difficult issues characteristic of a probabilistic limit states design method that uses time-history analyses with the design procedure itself is "how many design ground motions are needed to estimate the frame performance?" Brayton et al.[19] report that the width of the confidence interval for estimating the reliability of a system using Monte Carlo simulation techniques is proportional to $N^{-\frac{1}{2}}$, where N = total number of simulations. Hundreds of simulations may be required to obtain reliability estimates of high accuracy. A trade-off situation develops because computational effort is proportional to N; one must therefore decide upon a level at which the gain in increased accuracy is balanced by additional computational effort.

In any case, calculating frame performance based on hundreds of time history analyses is beyond the scope and capabilities of this study. The commentary for the Applied Technology Council[7] suggests that design methods of this type should use a minimum of 4 design ground motion records. The maximum number of ground motions that can be considered in this investigation is six, since this is the number of records in the ground motion library discussed in

Section 4.3.2. Thus, given these computational bounds, this section presents frame performance results for two sets of ground motion inputs. The frame performance is first evaluated using the complete library of ground motions. Although this option corresponds to an upper bound on the available accuracy (in this investigation at least), it also requires the maximum amount of computation. A second frame performance evaluation is then computed using a subset of 4 ground motion inputs subjectively taken from the library. The second family of ground motions is shown in Table[5.1].

RECORD	COMP	DESCRIPTION
E1	S00E	El Centro Site Imperial Valley Irrigation District. May 18,1940
E3	S00W	El Centro Site Imperial Valley Irrigation District. Dec 30,1934
E5	N50E	El Centro Community Hospital on Keystone Road. Oct 15,1979
E2	S90W	El Centro Site Imperial Valley Irrigation District. May 18,1940

Table[5.1] : Family of Four Earthquake Records

The frame performance evaluated in this case represents a lower bound on permissible computation, and gives the wider confidence interval for the reliability estimates. A comparison of the two frame performances is made in order to determine the sensitivity of the mean extreme frame response quantities and their scatter to the number of ground motion inputs.

With respect to the frame's response, peak story drifts, floor accelerations, elastic bending moments, and the maximum frame sway constraints are statistically described by the normal distribution. The scatter in frame response quantities such as cumulative energy dissipation (described by ductility), which are somewhat intrinsic to the frame material, are modeled with the Gumbel Extreme Type 1 distribution[32]. The exceedance probability for this

distribution is given by:

$$P[\,\mu\,] = 1 - e^{\left[-e^{-\alpha(\mu-u)}\right]} \tag{5.1}$$

where μ = maximum response measured in terms of the response parameter, and α and u are parameters that depend on the sample size, the average of μ, and its standard deviation. For small sample sizes less than 8, α and μ are approximately given by:

$$\alpha = \left[\frac{0.9043}{\sigma_\mu}\right] \tag{5.2}$$

$$and\ u = \bar{\mu} - 0.5356 \times \sigma_\mu$$

where $\bar{\mu}$ and σ_μ are the mean and standard deviation of the sampled response values.

5.2 Simulation Results

The designer's goal during the initial stages of simulation is to tune the [GOOD,BAD] preference pair settings specified in Chapter 4 until the relative design objective and frame constraint performances are correctly represented by a hierarchy of ranked dissatisfactions. This process is expedited if the designer can interact freely with the design program. Its efficiency is also increased when the designer has a good idea of what constitutes adequate reliability and constraint performance before a particular design process begins. Code recommendations and technical papers, together with experience, can be used to this end. Ascertaining GOOD and BAD values for the design objectives is, however, more difficult because the design objectives tend to be less well defined, often assuming values which are strongly related to a structure's size and configuration. For instance, the initial cost of the frame will not be known until the volume of design elements has been calculated. This requires a simu-

lation and it provides the designer with an additional item of information. Achieving the desired goal may, indeed, require several performance evaluations because no absolute scale exists with which to anchor the dissatisfactions. Moreover, because designer perception is subjective, several conceptual revisions of what constitutes GOOD and BAD performance may occur before a satisfactory hierarchy is obtained. Only then can an algorithm be expected to encourage design modifications that are consistent with the designer's intents.

The results presented in the section have evolved through two or three previous design appraisals of the type discussed. Parameters modified from their initial values in Chapter 4 are mentioned where appropriate. Presentation of the results is divided into the following sections; design objectives, box constraints, and limit state constraints.

5.2.1 Design Objectives

Levels of designer dissatisfaction for the example problem's six design objectives are summarized in Table[5.2].

OBJECT	RECORDS	DISSAT.	MDO	STD	GDO	BDO
1	-	0.7185	21470	0.000	15000	24000
2	4 records	0.000	0.000	0.000	0.000	0.150
	6 records	0.000	0.000	0.000	0.000	0.150
3	4 records	0.000	0.000	0.000	3.000	5.000
	6 records	0.000	0.000	0.000	3.000	5.000
4	4 records	0.7530	0.1235	0.000	0.500	0.000
	6 records	0.6896	0.1552	0.000	0.500	0.000
5	4 records	0.2565	1.513	0.000	1.000	3.000
	6 records	0.2565	1.513	0.000	1.000	3.000
6	4 records	0.0000	0.1811%	0.0571%	0.2%	0.4%
	6 records	0.0667	0.2014%	0.0868%	0.2%	0.4%

Table [5.2] : Summary of Design Objective Performance

Design Objective 1 is the total volume of the frame elements. A moderate amount of dissatisfaction results from the GOOD and BAD parameter settings[1]. Notice that the GOOD and BAD values for this design goal have been changed. Design objectives 2 and 3 measure the mean and coefficient of variation of hysteretic energy dissipation in the columns (recall that the columns were allocated to energy group 1). For both simulations the mean dissipated energy is zero with a corresponding zero variation in energy dissipation. The columns remain elastic; this still constitutes GOOD frame performance even though limited plastic deformations at the frame base are permitted. Design objectives 4 and 5 measure the mean energy dissipation and the coefficient of variation of hysteretic energy dissipation for the girders (recall that the girders were allocated to energy group 2). After a severe earthquake, the elements of this group are deemed to have performed well when the ratio of energy dissipated by each element divided by its dependable capacity for energy dissipation approaches 0.5. Design objective 4 registers a moderate amount of dissatisfaction because the mean hysteretic energy dissipation is only 15% of each frame node's dependable capacity for inelastic energy dissipation. Relatively high values for the GOOD and BAD variation parameters have been chosen for design objective 5. The primary effect of this action is to de-emphasize the importance of the poor variation of energy dissipation during the initial stages of design. Finally, design objective 6 measures the mean frame story drift under combined gravity loads plus moderate earthquake loading. Table[5.2] shows that in both cases the level of discontent for this design objective is minor.

---

[1] The symbols used are MDO = mean design objective, STD = response standard deviation, HPE = high exceedance probability, LPE = low exceedance probability, MFR = mean frame response, GFR = GOOD or dependable frame response, BFR = BAD frame response, HFR = frame response corresponding to the HIGH exceedance probability, LFR = frame response corresponding to the LOW exceedance probability, GDO = good design value for the frame response, and finally BDO = bad design value for the frame response.

5.2.2 Box Constraints

9 box constraints are enforced to control the range of permissible section sizes. The boundaries of these constraints are shown in Table [5.3].

CONSTRAINT	DISSAT.	MRF	STD	GFR	BFR
HARD_BOX(1) - HARD_BOX(9)	0.000	720	0.000	100	50
HARD_BOX(10) - HARD_BOX(18)	0.000	720	0.000	2500	3000

Table [5.3] : Upper and Lower Box Constraints

5.2.3 Limit State 1 : Gravity Loads Alone

This limit state is based on the frame's response to dead loads plus the maximum expected live loading during the lifetime of the structure. In this study maximum lifetime live load is taken as the unreduced live loading. Only a single simulation is required to evaluate the frame performance because the gravity loads are assumed to be deterministic. Consequently, the standard deviation of the frame responses equals zero; this also implies that the mean frame responses are identical to the HIGH and LOW frame responses. The latter pair is not shown. Table [5.4] indicates that the GOOD and BAD values were set to remove this constraint from influencing the design. Consequently, the designer dissatisfaction for the maximum volume constraint is zero.

Constraint No	MFR	STD	HFR	LFR	GFR	BFR
SOFT_INEQ(1)	21470	0.000	21470	21470	100000	120000

Table [5.4] : Statistics of the Maximum Volume Constraint

Table[5.5] shows that the column axial force constraints are all less than their allowable values. For the purposes of comparison, axial forces for the dead plus reduced live loading case are shown in brackets. The differences are small, mainly because of the high live load reduction factor (see Appendix 2)

Constraint No	MFR (kip)	GFR (kip)	BFR (kip)
SOFT_INEQ(2)	54.00 [51.84]	352.6	423.1
SOFT_INEQ(3)	54.00 [51.84]	352.6	423.1
SOFT_INEQ(4)	36.00 [34.56]	352.6	423.1
SOFT_INEQ(5)	36.00 [34.56]	352.6	423.1
SOFT_INEQ(6)	18.00 [17.28]	352.6	423.1
SOFT_INEQ(7)	18.00 [17.28]	352.6	423.1

Table [5.5] : Column axial forces

resulting from the example problem's small tributary floor areas.

Constraint No	MFR (kip-in)	GFR (kip-in)	BFR (kip-in)
SOFT_INEQ(8)	105.5	2408	3210
SOFT_INEQ(9)	208.3	2408	3210
SOFT_INEQ(10)	105.5	2408	3210
SOFT_INEQ(11)	208.3	2408	3210
SOFT_INEQ(12)	263.2	2408	3210
SOFT_INEQ(13)	208.4	2408	3210
SOFT_INEQ(14)	263.2	2408	3210
SOFT_INEQ(15)	208.4	2408	3210
SOFT_INEQ(16)	285.1	2408	3210
SOFT_INEQ(17)	415.4	2408	3210
SOFT_INEQ(18)	285.1	2408	3210
SOFT_INEQ(19)	415.4	2408	3210

Table [5.6] : Column Bending Moments

Conventional constraint numbers 8 to 19 measure the column end moments under gravity loads only. These are summarized in Table[5.6]. The mean values are all well less than the GOOD response values. Furthermore, notice that the GOOD and BAD constraint values remain constant over the height of the structure. This indicates that the column axial loads are low; they do not exceed 0.15 of the force required to cause yielding in the columns. Conventional constraint numbers 20-25 measure the girder end moments.

The girder midspan deflections under live loading are all much less than their GOOD values, as summarized in Table [5.8]. Notice that the dissatisfaction is zero for the constraints in this group; they are unlikely to become active during the iterations of optimization.

Constraint No	MFR (kip-in)	GFR (kip-in)	BFR (kip-in)
SOFT_INEQ(20)	471.5	1974	2632
SOFT_INEQ(21)	471.5	1974	2632
SOFT_INEQ(22)	502.2	1974	2632
SOFT_INEQ(23)	502.2	1974	2632
SOFT_INEQ(24)	415.4	1974	2632
SOFT_INEQ(25)	415.4	1974	2632

Table [5.7] : Girder Bending Moments

Constraint No	MFR (in)	GFR (in)	BFR (in)
SOFT_INEQ(26)	0.1329e-1	.7506	.8226
SOFT_INEQ(27)	0.7331e-2	.7506	.8226
SOFT_INEQ(28)	0.2417e-1	.7506	.8226

Table [5.8] : Maximum Girder Midspan Deflections

5.2.4 Limit State 2 : Gravity Loads + Moderate Earthquake Loading

A frame's response to moderate lateral loads should be essentially elastic with only a few minor excursions into the inelastic range. The frame's modal periods of vibration and eigenvectors are shown in Table [5.9].

mode no	period (sec)	dof/mode	1	2	3
mode 1	0.3437	1	0.3037	1.0000	1.0000
mode 2	0.1022	4	0.7217	0.7633	-0.9127
mode 3	0.0561	7	1.0000	-0.8546	0.3549

Table [5.9] : Frame Eigenvalues and Modal Periods

Table [5.10] summarizes the statistics of response for the constraint which encourages an elastic frame response by limiting the peak column and girder end moments. The GOOD and BAD column bending moments are (0.85 and 1.1 times the ideal yielding moment) 3411 and 4414 $kip-in$ respectively. Notice that none of the constraints in this group is active. The c.o.v. generally decreases with increasing height up the structure. The LOW frame response is well below the GOOD frame response for all constraints in the group. Similarly,

the GOOD and BAD girder end moments are 2961 and 3620 $kip-in$. The statistics of response are summarized in Table[5.11].

Constraint No	4 Records				6 Records			
	MFR	STD	HFR	LFR	MFR	STD	HFR	LFR
SOFT_FINEQ(1)	1175	329	1452	1597	1287	529	1732	1965
SOFT_FINEQ(2)	718	159	852	922	767	250	978	1088
SOFT_FINEQ(3)	1231	382	1553	1721	1326	500	1747	1967
SOFT_FINEQ(4)	743	185	899	980	791	243	996	1103
SOFT_FINEQ(5)	893	219	1077	1173	971	342	1258	1408
SOFT_FINEQ(6)	920	238	1120	1225	996	362	1301	1460
SOFT_FINEQ(7)	906	210	1084	1176	970	300	1223	1355
SOFT_FINEQ(8)	947	245	1153	1261	1012	333	1292	1439
SOFT_FINEQ(9)	572	98	655	699	614	165	753	826
SOFT_FINEQ(10)	918	172	1063	1138	989	249	1229	1355
SOFT_FINEQ(11)	563	86	635	673	600	132	711	769
SOFT_FINEQ(12)	920	161	1055	1126	979	237	1178	1283
c.o.v.	range = [0.15 - 0.31] average = 0.23				range = [0.22 - 0.41] average = 0.31			
E_1	range = [1.12 - 1.26] average = 1.18				range = [1.18 - 1.34] average = 1.26			
E_2	range = [1.19 - 1.39] average = 1.29				range = [1.28 - 1.57] average = 1.40			

Table [5.10] : Maximum Column Moments

Constraint No	4 Records				6 Records			
	MFR	STD	HFR	LFR	MFR	STD	HFR	LFR
SOFT_FINEQ(13)	1589	366	1879	2058	1712	572	2194	2446
SOFT_FINEQ(14)	1638	397	1972	2146	1740	530	2186	2419
SOFT_FINEQ(15)	1471	327	1746	1890	1594	524	2034	2265
SOFT_FINEQ(16)	1492	326	1766	1909	1594	461	1982	2185
SOFT_FINEQ(17)	918	172	1063	1138	990	285	1229	1355
SOFT_FINEQ(18)	920	161	1055	1126	979	237	1178	1283
c.o.v.	range = [0.17 - 0.24] average = 0.21				range = [0.24 - 0.33] average = 0.30			
E_1	range = [1.14 - 1.20] average = 1.17				range = [1.20 - 1.28] average = 1.25			
E_2	range = [1.22 - 1.31] average = 1.27				range = [1.31 - 1.43] average = 1.38			

Table [5.11] : Maximum Column Moments

Bounds are also placed on the frame story drifts and peak absolute floor accelerations in order to control implicitly the extent of non-structural

damage. Since each floor level has the same height, the GOOD and BAD values are $0.54in$ and $0.96in$ for all constraints. The statistics of response are summarized in Table[5.11].

Constraint No	4 Records				6 Records			
	MFR	STD	HFR	LFR	MFR	STD	HFR	LFR
SOFT_FINEQ(19)	.2014	.0638	.2551	.2832	.2200	.0909	.2965	.3364
SOFT_FINEQ(20)	.2721	.0856	.3442	.3819	.3015	.1297	.4107	.4677
SOFT_FINEQ(21)	.1784	.0562	.2257	.2505	.2034	.0921	.2809	.3215
c.o.v.	range = [0.314 - 0.316] average = 0.315				range = [0.41 - 0.45] average = 0.43			
E_1	range = [1.26 - 1.26] average = 1.26				range = [1.34 - 1.38] average = 1.36			
E_2	range = [1.40 - 1.40] average = 1.40				range = [1.53 - 1.58] average = 1.55			

Table [5.12] : Peak Story Drifts

Constraint No	4 Records				6 Records			
	MFR	STD	HFR	LFR	MFR	STD	HFR	LFR
SOFT_FINEQ(22)	101	24	121	132	113	51	156	178
SOFT_FINEQ(23)	171	52	214	238	186	73	248	281
SOFT_FINEQ(24)	218	71	277	308	250	115	348	398
c.o.v.	range = [0.24 - 0.33] average = 0.29				range = [0.39 - 0.46] average = 0.43			
E_1	range = [1.19 - 1.27] average = 1.24				range = [1.33 - 1.39] average = 1.37			
E_2	range = [1.31 - 1.41] average = 1.37				range = [1.51 - 1.59] average = 1.56			

Table [5.13] : Peak Absolute Floor Accelerations

Figure[5.1] shows the "floor acceleration" vs "time" for the structure's three floor levels. The GOOD and BAD constraint values are 270 an 540 $in\,\mathrm{sec}^{-2}$, and the statistics of response are displayed in Table [5.13]. It is noted from this table that the average c.o.v. on peak ground acceleration is 0.326 and 0.494 for the 4 and 6 ground motion suites. The variation in the peak floor accelerations is less; one therefore deduces that the structure is partially isolated from the spikes in peak ground acceleration. The mean peak floor acceleration

increases with height up the structure. Accordingly, constraints 23 and 24 (see Appendix 1) have non-zero dissatisfaction, while the first floor acceleration constraint is not active.

5.2.4 Limit State 3 : Gravity Loads + Severe Earthquake Loading

As already mentioned in Chapter 4, currently accepted design criteria permit major structural damage, possibly beyond repair, as the result of gravity loads plus a severe lateral earthquake loading. The adopted HIGH and LOW exceedance probabilities are 20% and 10% respectively. Also, the scatter in peak frame sways is described by the normal distribution, and the Extreme Type 1 distribution used to describe the variation in the energy based constraints.

The GOOD and BAD values of energy dissipation for the column elements are 30.77 and 47.25 *kip –in*. The columns remain elastic for all ground motion inputs (constraints 29-40). Similarly, the GOOD and BAD energy dissipation values for the girders are 47.66 and 83.13 *kip –in*, respectively.

Constraint No	4 Records				6 Records			
	MFR	STD	HFR	LFR	MFR	STD	HFR	LFR
SOFT_INEQ(41)	14.20	11.28	26.87	36.83	18.90	11.80	32.15	41.94
SOFT_INEQ(42)	17.11	12.28	30.90	41.09	19.17	11.45	32.03	41.52
SOFT_INEQ(43)	1.866	1.934	4.038	5.643	3.371	2.893	6.620	9.021
SOFT_INEQ(44)	2.124	1.443	3.745	4.942	2.935	1.705	4.850	6.265
SOFT_INEQ(45)	0.000	0.000	0.000	0.000	0.000	0.000	0.000	0.000
SOFT_INEQ(46)	0.000	0.000	0.000	0.000	0.000	0.000	0.000	0.000
c.o.v.	range = [0.68 - 1.04] average = 0.81				range = [0.58 - 0.85] average = 0.66			
E_1	range = [1.76 - 2.16] average = 1.90				range = [1.65 - 1.96] average = 1.76			
E_2	range = [2.33 - 3.02] average = 2.59				range = [2.13 - 2.67] average = 2.32			

Table [5.14] : Girder Hysteretic Energy Dissipation

The statistics of girder hysteretic energy dissipation, for those nodes dissipating non-zero energy are summarized in Table [5.14]. Conventional constraints 45 and 46 indicate that the roof girders remain elastic. Because energy dissipation is only defined for non-negative values, one can deduce that the distribution of energy dissipation is positively skewed. The mean energy dissipation responses are enhanced by factors of 2.24 and 2.04 for the 4 and 6 ground motion simulations. Hence it would also appear that the extreme type 1 statistical distribution provides a better description of the variation of energy dissipation than the normal distribution. In view of this result, setting the GOOD girder energy dissipation to 0.5 is reasonable.

Record Name	Input Energy	Hysteretic Energy	Work Done By Loads	Damped Energy
E1	0.144e+03	0.202e+02	0.319e+01	0.123e+03
E2	0.174e+03	0.766e+01	0.385e+00	0.162e+03
E3	0.261e+03	0.385e+02	0.164e+01	0.216e+03
E4	0.370e+03	0.774e+02	0.336e+01	0.282e+03
E5	0.225e+03	0.748e+02	0.364e+01	0.151e+03
E6	0.209e+03	0.476e+02	0.336e+01	0.159e+03

record name	E1	E2	E3	E4	E5	E6
energy group 1	0.0	0.0	0.0	0.0	0.0	0.0
energy group 2	20.2	7.6	38.5	77.4	74.8	47.6

Table [5.15] : Energy Balance for the Initial Design

In addition, Table[5.15] summarizes terms from the energy balance equation[2]; included are the total work done by loads, and input energy, along with hysteretic dissipated energy. The corresponding time history responses for the Input Energy, Hysteretic Dissipated Energy, Element Damped Energy, and Kinetic Energy are shown in Figures[5.2a] to Figure[5.2d], respectively. This set of figures clearly shows that the rate of element energy dissipation by damping

[2] Reference [14] reports on the energy balance equation used in DELIGHT.STRUCT. Input energy is the work done by the base shear of the frame as it moves through the ground displacement. Hysteretic energy is that dissipated by inelastic deformation of the elements. The remainder of the dissipated energy is through internal element damping. The "work done by loads" represents work done by the externally applied loads.

tends to be constant, whereas hysteretically dissipated energy occurs in short impulses. From a statistical viewpoint the mean and standard deviation pairs for the total input energy (Input Energy + Work Done By Loads) and Hysteretic energy are [232.6,79.7] and [44.8,28.3] respectively. Among the records the c.o.v. on the input energy is significantly less than for the dissipated energy. The majority (81% average) of the input energy is dissipated by damping at the element level. The remaining energy is dissipated via hysteretic deformations. Hysteretic energy is not, however, directly correlated to input energy since a threshold on input energy exists for which no hysteretic energy will be dissipated. Moreover, given two ground motion acceleration components recorded at the same site from a single event, one cannot even say that dissipated energy increases with increasing input energy (for example, see records E1 and E2).

Constraint No	4 Records				6 Records			
	MFR	STD	HFR	LFR	MFR	STD	HFR	LFR
SOFT_FINEQ(25)	2.002	.1544	2.132	2.200	2.070	.1694	2.212	2.287
c.o.v.	average = 0.077				average = 0.082			
E_1	average = 1.06				average = 1.06			
E_2	average = 1.09				average = 1.10			

Table [5.16] : Peak Frame Sway

Table [5.16] summarizes the statistics of peak frame sway displacements. The GOOD and BAD values of frame sway are set at 5.04 and 6.12 *in*. The scatter for this constraint appears to be unusually low.

5.3 Hierarchy of Frame Performance Attributes

The term *active* is used to describe those frame performance attributes that have non-zero dissatisfaction. The group of constraints and design objectives having this attribute are of importance because they are the most binding criteria on a design. They are summarized in Table [5.17].

Constraint or Objective	Dissatisfaction 4 records	6 records
OBJEC(1)	0.7185	0.7185
OBJEC(4)	0.7530	0.6896
OBJEC(5)	0.2560	0.2564
OBJEC(6)	0.0000	0.0667
SOFT_FINEQ(23)	0.0000	0.0363
SOFT_FINEQ(24)	0.1262	0.4000

Table[5.17] : Active Frame Performance Attributes

The reader is referred to Appendix 1 for a summary of the purpose of each constraint and design objective. If an iteration of optimization leads to large changes in a design, those constraints which are nearly active at the beginning of the design process may become so, and are therefore also of interest to the designer. A second group of non-active constraints is considered. Our criterion for inclusion is to test whether or not the LOW frame response exceeds 70% of the GOOD frame response. The constraints and objectives falling into this second category are shown in Table [5.18].

Constraint or Objective	4 records LFR	6 records LFR	GFR
SOFT_FINEQ(13)	2058	2446	2961
SOFT_FINEQ(14)	2146	2419	2961
SOFT_FINEQ(15)	1890	2265	2961
SOFT_FINEQ(16)	1909	2185	2961
SOFT_FINEQ(20)	0.38	0.47	0.54
SOFT_INEQ(41)	36.8	41.9	47.6
SOFT_INEQ(42)	41.1	41.5	47.6

Table[5.18] : Nearly-Active Frame Performance Attributes

In particular, the capacity of the frame girders for energy dissipation is excessive. An equivalent level of discontent is also registered for the frame volume. Table [5.17] indicates that the maximum constraint dissatisfaction belongs to the gravity loads plus moderate lateral loads limit state. Indeed, the

sizing of the frame elements in the initial design using the UBC[63] lateral loading was controlled by story drift considerations, not collapse under severe lateral loads. The columns remain elastic for all 6 ground motion inputs. While behavior of this type is satisfactory, improved performance for a frame of this type would be accompanied by limited plastic hinging at the column bases. It is concluded that the initial design is too conservative.

The gravity loads alone limit state constraints are not active. As indicated in Table[5.17], the constraint having the maximum dissatisfaction is the peak absolute roof acceleration under moderate lateral loads. Although none of the other moderate lateral loads limit state constraints is active, the girder elastic bending moments under moderate loads are nearly-active. The average value of the ratio "mean frame response for 6 ground motion inputs" divided by "mean frame response for 4 ground motion inputs" is 1.08. In addition, the frame response coefficients of variation range over the intervals [0.15 - 0.33] and [0.22 - 0.46] for the families of 4 and 6 ground motion inputs, respectively. The average values of the enhancement factors cover the intervals [1.17-1.40] and [1.25-1.56] for the 4 and 6 record inputs respectively. Finally, the average enhancement factors for the energy dissipation constraints are bounded by the intervals [1.9-2.59] and [1.76-2.32] for the four and six ground motion input frame responses. The corresponding coefficients of variation of response are significantly larger than other response measures and cover the intervals [0.68, 1.04] and [0.58, 0.85]. Table[5.14] shows that the mean dissipated energy for the six ground motions input frame response is 25% higher than when four records are used.

5.4 Summary

The overall mean and scatter of the frame performance is greater for the 6

ground motion ensemble than the 4 record input. This is reflected in larger coefficients of variation and mean frame response values. Nonetheless the ranking order of constraints and design objectives is the same for both simulations. Of the active constraints, only the roof acceleration constraint registers a marked variation. The largest level of discontent lies equally with the frame volume and girder energy dissipation design objectives.

Because the design problem is cast in a minimax format, the Phase I-II-III Method of Feasible Directions will emphasize a reduction of the most active dissatisfactions. Thus 4 ground motions need only be used in the initial stages of optimization. This option is desirable on two counts. First, the 4 ground motion input has the larger level of maximum dissatisfaction and therefore will be more conservative. This option also requires the least calculation. It is noted, however, that there is no guarantee that 4 ground motions will give the more conservative design as modifications are made. Consequently, the number of simulations should be increased to 6 when more accurate reliability estimates are required for tradeoff analyses among competing performance criteria.

CHAPTER 6

OPTIMAL DESIGN PROBLEMS

6. Introduction

This chapter reports on the sensitivity and behavior of the *example* frame when each of the design parameter arrangements discussed in Section 4.5.1 is optimized according to the design criteria specified in Section 4.5.3. The chapter is divided into three sections.

The purpose of the first section is to test the behavior of the optimal designs for the individual design criteria of minimum volume, minimum mean story drifts and maximum dissipated energy. In each case the starting design is taken as the preliminary design discussed in Chapters 4 and 5. No member proportioning philosophies are assumed *a priori*. Four ground motion records are used for the seismic input. Three iterations of optimization are calculated for each of the nine permutations of the three design objectives and three design parameter distributions outlined in Chapter 4. This section concludes with a comparison of the performance and practicality of the different optimal design results.

The second section begins with an optimization problem that balances the multiple design attributes of volume, story drift and maximum dissipated energy. The mean frame response and the accuracy with which reliability estimates are calculated is improved by increasing the number of ground motion inputs used for the frame performance evaluation to six. Three iterations of optimization are calculated. A sample output from an iteration of optimization is shown in Appendix 3. The design reached at the end of iteration three is designated as the *final* design. A comparison of response variability for the initial and final designs, and the governing limit states for various levels of perfor-

mance reliability is given in Sections 6.2.3 and 6.2.4.

The chapter concludes with a summary and assessment of the proposed design method.

6.1 Single Objective Designs

Minimum volume, minimum story drifts and the maximum dissipated energy design objectives are tested for each of the design parameter layouts discussed in Section 4.5.1.

6.1.1 Minimum Volume Designs

Figures [6.1a],[6.2a] and [6.3a] graph the "frame section inertia" vs "iteration no." for the three design parameter distributions shown in Figure[4.9] In each case contours of the lower GOOD and BAD box constraints are also shown. The corresponding plots of "peak cost function dissatisfaction", "soft constraint group dissatisfaction", and "hard constraint group dissatisfaction" vs "iteration no" are graphed in Figures [6.1b], [6.2b] and [6.3b].

The maximum dissatisfaction level for the initial design is associated with the frame volume design objective. It registers a value of 0.7185, as shown in Figures[6.1b], [6.2b] and [6.3b]. Because the optimization problem is cast in a mini-max format, the initial objective of the Phase I-II-III Method of Feasible Directions is to recommend design changes which minimize the frame volume. The only design constraint registering non-zero discontent (at 0.1256) is the peak absolute roof acceleration.

A significant decrease in frame volume is obtained for all three design parameter layouts during the first iteration of optimization. The volume decrease is accompanied by an increase in all of the frame's natural periods and a reduction in the level of discontent for the peak roof acceleration.

Further volume reductions during second and third iterations are accompanied by a slight decrease in the cost dissatisfaction, and a significant increase in the peak soft dissatisfaction as the dissipated energy constraint at the first floor level becomes active. Figures [6.1a] and [6.2a] show that during iterations two and three, the one design parameter and two design parameter layouts (see Figure[4.9]) are bound by this pair of conflicting design attributes. However, the behavior of the three design parameter problem is significantly different because it allows an independent increase in the first story member moments of inertia. At the end of the first iteration the first floor dissipated energy constraints are almost active. In fact, this constraint group lies inside the eps-active bandwidth for iteration two; it is included in the direction vector calculation together with the active volume design objective. A decrease in the peak soft constraint value due to an increase in the energy dissipation capacity of the girders at the first floor level is the main change in frame performance as one moves along the direction vector from the design at the end of iteration one. This modification permits further volume reductions at the second and third floor levels. Minor adjustments to the frame member sizes take place at iteration three. Figure[6.4] shows that the volume reductions as a percentage of the initial frame volume are 19%, 18%, and 23% for the one, two, and three design parameter layouts, respectively.

6.1.2 Minimum Story Drift Designs

The second cost function that is investigated is minimum story drifts. In Section 4.5.3 the GOOD and BAD mean story drift design objective parameters were set at 2.000e-3 [0.2%] and 4.000e-3 [0.4%], respectively. Unfortunately the behavior of the story drifts cost function cannot be tested with this parameter setting because it results (see Section 5.2.1) in only a minor level of

design dissatisfaction. Hence the initial GOOD and BAD parameters were artificially adjusted to 0.000e-3 [0.0%] and 2.000e-3 [0.2%] in order to force the story drifts design objective to have the maximum problem dissatisfaction.

Plots of the "peak cost function dissatisfaction", "soft constraint group dissatisfaction", and "hard constraint group dissatisfaction" vs "iteration no" are graphed in Figures[6.5b], [6.6b] and [6.7b]. They show that the adjusted maximum design objective dissatisfaction is 0.9053. The only other constraint registering a non-zero level of discontent (at 0.1256) is the example frame's peak absolute roof acceleration. Figures [6.5a],[6.6a] and [6.7a] graph the "frame section inertia" vs "iteration no" for the three design parameter distributions considered. In each case contours for the upper GOOD and BAD box constraints are also shown.

A significant increase in the frame member moments of inertia occurs for all three design parameter arrangements during the first iteration of optimization. The primary result is a stiffer structure that has all of its natural periods reduced, and an increased response sensitivity to the details of the ground motion accelerations. A small increase in the level of discontent for the peak roof acceleration is the consequence of the latter effect. However, the dissatisfaction registered for this constraint decreases with further increases in the frame element sizes during the second and third iterations; elastic frame responses are recorded for even the most severe ground input. Figures [6.5a] and [6.6a] show that during iterations two and three, the one and two design parameter distributions are bound by the GOOD value of the upper box constraint (recall that this constraint is HARD). Indeed, it is noted that these design modifications are physically attractive because each iteration is progressively closer to the global minimum for story drifts; ie, rigid body motion as the frame member sizes approach infinity. Unfortunately the behavior of the

three design parameter problem is different. After the first iteration the member sizes are redistributed in a manner that encourages a softening of the structure at the first floor level while retaining an increased structural stiffness in the upper levels. The story drifts design objective converges to a local minimum where the mean drift over the complete height of the structure is locally reduced due to increased displacements at the ground floor level. This behavior isolates the upper floors from the story forces necessary to impart high displacements. The additional protection given to the upper floors with this design is somewhat analogous to the behavior exhibited by base-isolated structures.

6.1.3 Maximum Dissipated Energy Designs

Figures [6.8a],[6.11a],[6.13a] and [6.15a] graph the "frame section inertia" vs "iteration no" for the three design parameter distributions considered. The corresponding plots of the "peak cost function dissatisfaction", "soft constraint group dissatisfaction", and "hard constraint group dissatisfaction" vs "iteration no" are shown in Figures [6.8b], [6.11b], [6.13b], and [6.15b].

The maximum level of dissatisfaction for the initial design is associated with the "mean dissipated energy" of the frame girders (ie, group 2 elements). It registers a value of 0.7531. The only constraint registering a non-zero level of discontent is the peak roof acceleration at 0.1256.

Figure [6.8a] shows the "section inertias" vs "iteration no" for the one design parameter problem, and Figure [6.8b] the corresponding levels of dissatisfaction for each of the iterations. One can easily see that the design has converged to a local design objective minimum because the peak soft constraint and design objective dissatisfactions do not converge. The local minimum is also shown in Figure[6.10]. Initially, the frame element sizes are decreased in

an effort to maximize the mean ratio "energy dissipated by each group 2 node" divided by the "corresponding node's dependable capacity for energy dissipation." Improved performance is due to an increase in this ratio. However, with further member size decreases the frame enters a region in which the gradient of the dissipated energy with respect to perturbations in the element sizes falls off faster than the corresponding member's dependable capacity for energy dissipation. The result is a local increase in the level of dissatisfaction. A reduction in the peak roof acceleration dissatisfaction also occurs with a decrease in the structure's stiffness.

The problem was rerun with the optimization parameter (α) controlling the slope of the Armijo step-length test line reduced[1] to 0.2. The revised results are shown in Figures [6.11] and [6.12]. Referring back to Figure [6.10] one can see that the Armijo step-length algorithm has missed the local minimum and converged to the global minimum. The primary result is a 26% reduction in the frame element inertias before the intersection of the cost and girder dissipated energy constraint is abruptly reached. The sensitivity of the peak dissipated energy constraint dissatisfaction to perturbations of the final design about the minimax point is clearly shown in Figure[6.10].

The lowest final design objective dissatisfaction is obtained for the two parameter layout. Figures[6.13a] and [6.13b] indicate that the algorithm initially gives emphasis on reducing the cost function. A 20% reduction in the girder moments of inertia with a small decrease in the column moments of inertia is the result at iteration one. The dissatisfaction for the peak roof acceleration constraint is lowered to a value just above zero. Further reductions in the column and girder moments of inertia occurs at iteration two with

[1] Reducing the Armijo slope increases the distance from the design vector coordinates to the intercept of the test line and the contour of peak performance dissatisfaction. The algorithm may now step further before the Armijo step length test fails [45]. A diagram of this test may be found in ref[9].

corresponding improvement in cost dissatisfaction. The first floor energy dissipation constraints become active during this iteration, and are consequently included in the direction vector calculation for iteration three. Nonetheless, because the cost has the greater dissatisfaction, a direction vector is chosen which emphasizes a reduction in the dissipated energy design objective, while also allowing for a possible improvement in the most active constraints. The result is an increase in the column moments of inertia with a continued reduction in the size of the girder inertias. The corresponding adjustment in the maximum soft constraint and design objective dissatisfactions is shown in Figure[6.13b]. It is worth noting that the design objective and soft constraint contours are allowed to cross because the Armijo stepsize rule only finds an approximate minimum (indeed, there is no guarantee that it will even converge to the closest minimum as demonstrated by the design process just described). If a fourth iteration were computed, emphasis would be given to lowering the dissatisfaction on the dissipated energy constraint. The design corresponding to the minimax of these conflicting design criteria would then be essentially determined.

Figures [6.15a] and [6.15b] show that the three parameter problem displays inferior performance. It converges to a local minimum with a final design objective dissatisfaction which exceeds the final values of the other two design parameter layouts.

The "total input energy" and "hysteretic dissipated energy" vs "iteration no" for each of the four ground motion inputs is graphed in Figures [6.9], [6.12], [6.14], and [6.16]. For some of the ground motion records the total input energy increases as the design changes, and in others it decreases[2]. These

[2] The individual records have not been labeled in these Figures so as to avoid overcrowding. If this information is required, then the reader can identify the appropriate contours from Table[5.15].

graphs also indicate that, in general, the mean ratio of "frame dissipated energy" divided by "total input energy" remains approximately constant for each ground motion. However, the overall level of the input energy can differ significantly among the ground motions, with levels of input energy being only slightly less sensitive to variations in the proportioning of the structure's elements. Moreover, the total input energies for the final one design variable minimum story drifts design were 31.1, 46.7, 29.7, and 78 $kip-in$, respectively. Because these values are significantly less than for the initial frame (see Table[6.16]), it is suggested that the average input energy locally increases for structures of increasing period. A corresponding increase in the variation of input and dissipated energies is similarly observed. Nonetheless, because very flexible structures are capable of moving through severe ground motion displacements without transferring large shear forces into their lower columns, a limit to the aforementioned trend must exist before the average input energy starts to decrease and approach zero for frames of very large fundamental period.

6.2 Multiple-Objective Design

Multiple objective problems arise in seismic design because an effective structure balances the attributes of cost, reliability and performance in some desirable way. The primary purpose of Section 6.1 was to investigate the optimal behavior of the "example" frame for each of the individual design criteria. It was shown that while the volume and dissipated energy objectives tend to be consistent in their notion of good performance, these criteria conflict with the story drifts objective. Also, the performance of an optimal design was shown to depend on the selection of a design parameter layout. Hence, instead of computing optimal designs for all the possible combinations and permuta-

tions of the design objective and parameter layouts, the scope of this section is reduced to finding a single combined volume, story drifts, and maximum dissipated energy design for the design parameter layout which potentially allows the best overall improvement in design performance. Section 6.2.1 discusses the criteria for selecting this layout. The results of the ensuing optimization problem are presented in Section 6.2.2.

6.2.1 Sensitivity of Design Performance to Design Parameter Layout

Sections 6.1.1 through 6.1.3 were designed to provide insight into the sensitivity of an optimal design to different design objectives and parameter layouts. The purpose of this section is to summarize the observations, and use the acquired information to select the design parameter layout which offers the best potential for performance improvement in a multi-objective design.

Design Objective	No of Design Parameters					
	1	2	3	1	2	3
Volume	0.2587	0.2701	0.1756	0.0831	0.0945	0.0000
Story Drifts	0.2211	0.2787	0.5846	0.0000	0.0576	0.3635
Dissipated Energy	0.5665	0.3167	0.6411	0.2498	0.0000	0.3244
Dissatisfaction Sum	1.0463	0.8655	1.4013	0.3329	0.1521	0.6879

Table[6.1] : Summary of Design Objective Dissatisfactions

Table [6.1] summarizes the final design dissatisfactions for the nine problems considered in Section 6.1. The results are assessed from two points of view. First, the left-hand block of Table [6.1] shows the final design objective dissatisfactions for each of the parameter layouts. The lowest average performance dissatisfaction summed over three cost functions occurs for the two parameter problem. However, because the average contribution of each row of the design objective dissatisfactions to the individual column sums may not be equal, overall frame performance is also viewed from the perspective of measur-

ing each cost function's dissatisfaction relative to the minimum among the three parameter layouts. These values are shown on the right-hand side of Table [6.1]. The right-hand side of Table [6.1] also shows that the final dissatisfactions for the volume, story drifts, and maximum dissipated energy design objectives are increasingly sensitive to the selection of design parameter layout. Thus, it is suggested that the success or failure of an energy based optimal design process (in particular) strongly depends on the spatial arrangement of the design parameters in relation to the beam and column design objective groups (see Section 4.5.3.3). Only the two parameter layout allows an independent adjustment of the design objective groups. Since it also has the lowest sum of relative dissatisfactions, the two parameter layout is selected for the multi-objective design. The poor performance of the single design parameter energy design is due to the design parameter layout over-constraining the design objectives. Additional difficulties are also caused by a non-convex design objective (see Figure[6.10]). Coupling of the energy groups and convergence to a local minimum in the three parameter layout leads to a poor level of design performance. Because the volume design objective includes all of the frame elements, any arrangement of design parameters always constitutes a subset of the total frame topology. This design objective also has the advantage of not depending on the dynamic response of the frame. Hence, it performs relatively well no matter what design parameter arrangement is chosen. By comparison, predicting the optimal performance of the story drifts design objective for perturbations in the different frame element groupings is often difficult because this design goal's behavior tends to be problem-dependent. Further difficulties may also arise if the design goal is non-convex.

6.2.2 A Combined Volume, Story Drifts and Energy Based Design

Figure [6.17] graphs the "frame section inertia" vs "iteration no" for the beam and column parameters. Plots of the "cost function dissatisfaction" for each objective, "peak soft constraint group dissatisfaction", and "hard constraint group dissatisfaction" vs "iteration no" are graphed in Figure [6.18].

The maximum level of dissatisfaction for the initial design (at 0.7185) is associated with the frame volume design objective. The "mean dissipated energy" of the frame girders (ie group 2 elements) registers a slightly smaller value of 0.6896. This is followed by the group 2 energy variation at 0.2561, and finally the story drifts design objective at 0.0069. The only constraint with a non-zero level of dissatisfaction is the peak roof acceleration at 0.1256.

Description	Response Dissatisfaction (p)	dp/dx1	dp/dx2
Frame volume design objective	0.7185	2.1367	1.1537
Group 2 energy obj (mean)	0.6896	-0.0078	0.7383
Group 2 energy obj (variation)	0.2561	6.3737	29.7295
3rd floor absolute floor acceleration	0.4000	3.0629	1.7158

Table [6.2] : Eps-active Design Objectives and Constraints

Table [6.2] summarizes the response dissatisfactions and the jacobian matrix of frame performance derivatives with respect to the design parameters **x1** and **x2** for the eps-active constraints and design objectives at the beginning of iteration one. This information is presented with the purpose of providing insight into how the interaction among performance attributes affects the choice of a direction vector during an iteration of optimization. The frame volume derivatives indicate that an increase in the designer dissatisfaction occurs with enlargements in both of the design parameters, and that 65% of the frame volume is located in the columns[3]. Element(2,1) in the jacobian matrix

[3] The proportion of the frame volume controlled by design parameter 1 is 2.1367 divided by (2.1367 + 1.1537).

indicates that an increase in the column moments of inertia decreases the level of dissatisfaction for the mean group 2 energy objective. Increasing the column sizes in the example frame results in higher lateral forces and increased level of hysteretic energy dissipation. The mean energy group 2 design objective is understandably more sensitive to perturbations in the beams than the columns. In a similar way, enlargement of the beam sizes increases the design objective's dissatisfaction due to an enhanced dependable capacity for energy dissipation. The third row in the jacobian matrix describes the changing dissatisfaction of the group 2 energy variation objectives with respect to perturbations in the design parameters. Recall that this objective's purpose is to quantify how effectively energy dissipation is shared among the nodes in an energy group. These derivatives indicate that a decrease in both the column and girder moments of inertia will improve the sharing of energy dissipation in the girders. Row four of the jacobian matrix shows that discontent with the peak roof acceleration constraint increases locally with increasing structural stiffness; it is more sensitive to perturbations in the column sizes than the beam moments of inertia.

Figure [6.17] shows that a small increase in the column moments of inertia and a significant decrease in the girder moments of inertia are the primary results of iteration one. Reductions in the levels of dissatisfaction for both the volume and energy group 2 design objectives are shown in Figure [6.18]. A small decrease in design objective 5 occurs with the reduction of the girder moments of inertia. This indicates that a slightly increased percentage of the hysteretic energy dissipation occurs in the frame's upper two floors. In addition, a minor increase in the story drifts design objective dissatisfaction accompanies a reduction of the frame stiffness. With respect to the constraints, this design modification decreases the level of discontent for the peak roof

acceleration constraint from 0.4 to 0.325. A minor level of dissatisfaction for the first floor dissipated energy constraint also occurs at iteration one.

A moderate decrease in the frame volume dissatisfaction and a significant improvement in the group 2 energy objective occurs with further reductions of the beam and column moments of inertia at iteration two. The design modification is accompanied by a substantial increase in the story drifts design objective. A reduction in the dissatisfaction level for design objective 5 occurs with the reduction in the girder moments of inertia. This improvement is primarily due to hysteretic energy dissipation now occurring at all three floor levels. Design objective 2 indicates that a small amount of energy is now dissipated at the column bases. Constraint dissatisfaction is recorded for the girder end moments under moderate lateral loads, story drifts at the second story level, and floor accelerations at the second and third floor levels. The minor level of dissatisfaction for the first floor energy dissipation constraints increases from 0.009 and 0.000 at iteration one, to 0.581 and 0.565 at iteration two. Figure [6.18] shows that this constraint group causes the largest level of dissatisfaction. Finally, moderate levels of dissatisfaction also occur for the second floor energy dissipation constraints.

Description	Response Dissatisfaction (p)	dp/dx1	dp/dx2
Frame volume design objective	0.523	2.1362	1.5710
1st floor energy dissipation constraint	0.581	-4.3078	-15.9302
1st floor energy dissipation constraint	0.565	-3.5259	-11.0553
1st floor girder bending moment constraint	0.332	-5.4302	-32.2927
2nd floor girder bending moment constraint	0.335	-5.0049	-34.5610
3rd floor absolute floor acceleration	0.437	-2.1888	-12.0608

Table [6.3] : Eps-active Design Objectives and Constraints

The purpose of Table [6.3] is to summarize the performance dissatisfaction and jacobian matrix of frame performance derivatives with respect to the design parameters **x1** and **x2** for the eps-active constraints and design

objectives at the beginning of iteration three. The description column indicates that the volume design objective and constraints from both the severe and moderate lateral loads limit states fall into the eps-active bandwidth. Moreover, the signs of the performance derivatives indicate that the most active constraints and design objectives controlling the design are conflicting in nature. While an increase in the frame element sizes leads to improvement in the constraint preformances, reduction of the frame element sizes decreases the volume design objective dissatisfaction. However, the relative magnitudes of the gradients suggest that enhanced preformance is most easily achieved by increasing the girder inertias. Improvement in the constraints might also be obtained to a lesser extent by increasing the column moments of inertia.

A redistribution of the frame element sizes due to an increase in the girder moments of inertia and a decrease the column moments of inertia is the main result at iteration three (see Figure[6.17]). Enlargement of the girders is accompanied by an increase in the dissatisfaction for the mean group 2 energy dissipation design objective. In addition, less significant improvements in the dissatisfactions for the design volume objective and the first floor energy dissipation constraint occur during this design iterate. Dissatisfactions for the three active limit state 2 constraints (rows 4 to 6 in the jacobian matrix) are also reduced. Figure [6.18] shows that intersection of the frame volume design objective, the mean group 2 energy dissipation objective and the first floor energy constraint dissatisfactions at iteration 3 corresponds to the solution of the *minimax* problem. It is called the ***final*** design.

The final design has a girder moment of inertia that is 65% of the column moment of inertia. The corresponding plastic moment capacities of the columns and girders are 3758 $kip-in$ and 2311 $kip-in$, respectively. The total element volume of the final design is $19110 in^3$. This is an 11% reduction of the

starting frame volume of $21470 in^3$.

6.2.3 A Comparison of Initial and Final Design Responses

Figure [6.18] shows that the final design (the result at iteration 3) has a lower peak dissatisfaction than the initial design (at iteration 0). It could be regarded as being a better design for this reason. However, a need exists to know precisely why it is better. A number of possibilities exist; better performance could be due to a lower overall mean frame response, decreased variation in the response parameters binding the design, changes in GOOD and BAD parameter values as the design is altered, or a combination of the aforementioned factors. The purpose of this section is to identify the contribution made by each of these options towards the overall design improvement.

6.2.3.1 Design Objectives

This section begins by recalling that dissatisfaction for the design objectives is only based on mean frame response and designer specified GOOD and BAD frame performance values. The GOOD and BAD design objective values are constants; they are not a function of an independent parameter such as a frame element size. In addition, variations in the frame response are not included in the calculations for the design objective dissatisfaction.

A summary of the design objective dissatisfactions for the initial and final designs is given in Table[6.4]. Design objective 1 is the total volume of the frame elements. This objective's GOOD and BAD parameter settings remain constant. The improved performance is due to a reduction in the frame volume; this reduces the frame's initial cost. Design goals 2 and 3 measure the mean and variation of energy dissipated for energy group 1. The columns remain elastic for the initial design, but dissipate a small quantity of energy in the final

OBJECTIVE	DESIGN	Dissatisfaction	MDO	GDO	BDO
OBJEC(1)	Initial	0.7185	21470	15000	24000
	Final	0.4566	19110	15000	24000
OBJEC(2)	Initial	0.0000	0.0000	0.000	0.150
	Final	0.0107	0.0107	0.000	0.150
OBJEC(3)	Initial	0.0000	0.0000	3.000	5.000
	Final	0.0000	0.0000	3.000	5.000
OBJEC(4)	Initial	0.6896	0.1552	0.500	0.000
	Final	0.4749	0.2626	0.500	0.000
OBJEC(5)	Initial	0.2565	1.513	1.000	3.000
	Final	0.1921	1.384	1.000	3.000
OBJEC(6)	Initial	0.0667	0.201%	0.2%	0.4%
	Final	0.1630	0.233%	0.2%	0.4%

Table [6.4] : Comparison of Design Objective Performances

design. In this respect, as the initial design was conservative, design objectives behave more like constraints than design objectives: the reasons for this are explained in Section 4.5.3.3. Accordingly, a minor level of dissatisfaction is noted. Objectives 4 and 5 measure the mean energy dissipation and the variation of energy dissipation for the frame's energy group 2 elements. Improvement in the dissatisfaction level for design objective 4 is due to both a 50% increase in the mean hysteretic dissipated energy (see Section 6.2.3.4), and a reduction in the beam's dependable capacity for energy dissipation. Relatively high values for the GOOD and BAD variation parameters were initially chosen in order to de-emphasize the importance of design objective 5. Nonetheless, a small quantity of dissatisfaction occurs for both the initial and final designs. As already mentioned, improved performance of the final design is due to energy dissipation being distributed to all three floor levels, whereas hysteretic energy dissipation for the initial design was primarily confined to the first floor, with a small quantity at the second floor level. Finally, objective 6 measures the mean frame story drift under combined gravity loads plus moderate earthquake load-

ing. A small increase in the level of discontent for this design objective is due to a more flexible final design. This modification is permissible because the magnitude of this design objective's dissatisfaction is less than levels of dissatisfaction for the frame performance attributes controlling the design.

6.2.3.2 Box Constraints

The box constraints are not active for the initial or final designs.

6.2.3.3 Limit State 1 : Gravity Loads Alone

As explained in Section 5.2.3 the standard deviation of the frame responses is assumed to equal zero for all frame response quantities in this limit state. Designer dissatisfaction for the maximum volume constraint is zero because the GOOD and BAD values were set to remove this constraint from influencing the design. Table [6.5] summarizes the column axial force constraints. Since the axial forces are independent of the member sizes, only modifications in the GOOD and BAD constraint values change the constraint's performance. Conventional constraint numbers 8 to 19 measure the column end moments under gravity loads alone; these are summarized in Table[6.6]. Notice that the GOOD and BAD constraint values remain constant over the height of the structure for both the initial and final designs. This indicates that the column axial loads are low; they do not exceed 0.15 of the force required to cause yielding in the columns of either the final or initial designs. In addition, the change in the GOOD and BAD values is much larger than changes in the moments between the initial and final designs. Conventional constraint numbers 20 to 25 (see the optimization problem description in Appendix 1) measure the girder end moments, and are shown in Table [6.7]. Once again, changes in the GOOD and BAD constraint values are larger than the differences between the initial and

final design girder bending moments. The girder midspan deflections under live loading are indicated in Table[6.8]. Even though the mean deflection increases slightly for decreased girder moment of inertia, neither the final nor initial design constraints is close to becoming active.

Hence, for the gravity loads alone limit state, alterations in the frame performance attributes are due more to modifications in the GOOD and BAD constraint values than changes in the frame response quantities.

6.2.3.4 Limit State 2 : Gravity Loads + Moderate Earthquake Loading

The frame's modal periods of vibration and eigenvectors are summarized in Table[6.9]. The initial frame's fundamental period increases from 0.343 seconds to 0.405 seconds for the final design. It is now recalled that a frame's response to moderate lateral loads should be essentially elastic with only a few minor excursions into the inelastic range. An elastic frame response is enforced by limiting the peak column and girder end moments. Table [6.10] summarizes the statistics of response for the peak column bending moments. This table shows that none of the constraints in this group is active, and that the c.o.v. generally decreases with increasing distance from the ground. Moreover, the response variation is slightly higher for the final design than for the initial design. A negligible difference in statistical response of the initial and final design's peak girder bending moments is shown in Table[6.11]. Rather, the main changes in constraint performance are due to modifications in the GOOD and BAD constraint values. The statistics of peak story drifts for the initial and final designs are summarized in Table[6.12]. This table shows that the final design has mean response and standard deviation values which are slightly larger than those for the initial design. Similarly, the statistics of peak absolute floor acceleration are shown in Table[6.13]. It is first noted that the aver-

age coefficients of variation for the floor acceleration are only a little less than the for the peak ground acceleration (0.494 : see Section 4.3.2). Mean response values and standard deviations increase with increasing distance from the ground. However, because the mean response values increase at a faster rate then the standard deviations, the coefficients of variation of this response quantity decrease with increasing height of the structure.

6.2.3.4 Limit State 3 : Gravity Loads + Severe Earthquake Loading

Table[6.14] indicates that the initial design's columns remain elastic for all 6 ground motion inputs. A small quantity of energy is dissipated in the columns of the final design. The statistics of hysteretic girder energy dissipation are summarized in Table[6.15]. Notice that the GOOD and BAD dissipated energy values are functions of the member size. Conventional constraints 45 and 46 indicate that while the roof girders remain elastic for the initial design, the final design dissipates a small quantity of hysteretic energy at the third floor level.

Terms from the energy balance equation of the global frame response are summarized in Table[5.15] for the initial design, and Table[6.16] for the final design. Similarly, Figures[5.2a] to [5.2d] graph the initial design input energy, total frame hysteretic dissipated energy, total element damped energy, and kinetic energy vs time for each of the records E1 - E6. The corresponding response quantities for the final design are shown in Figures[6.21a] to [6.21d]. The initial design has mean and standard deviation pairs for the input energy and hysteretic energy of [232.6,79.7] and [44.8,28.3] respectively. Similarly, the mean and standard deviation of total input energy and hysteretic energy for the final design is [240.5, 127.2] and [63.9, 67.2], respectively. The important points to note from these statistics are: (a) the c.o.v. for the input energy is

significantly less than for the hysteretic dissipated energy, and (b) the mean frame dissipated energy increases from 44.8 $kip-in$ to 63.9 $kip-in$ as the design is modified from the initial to final states. An increase in the uncertainty with which the response may be predicted is also captured by an enlargement of the c.o.v. for total frame dissipated energy from 0.632 to 1.05, and a corresponding increase in the average energy dissipation enhancement factors from 2.04 and 2.51. A slight increase from 19.2% to 26% in the ratio "total frame dissipated energy" divided by "total input energy" is also noted.

One therefore concludes that the increased dissatisfaction of the girder hysteretic energy constraint for the final design is due to a complex interaction of (a) a 50% increase in the mean dissipated energy (b) enhanced scatter in the statistical distribution of hysteretic energy dissipation and (c) decreased GOOD and BAD constraint values.

Figure [6.19] graphs the "total input energy" and "hysteretic dissipated energy" vs "iteration no" for each of 6 ground motions. It shows that in some instances an increase in the energy terms due to a particular ground motion input will occur with a design modification, yet reductions in the same energy terms will occur with other ground motion record inputs. The record E2 has the largest change. An examination of Table[6.16] shows that E2 is the only record to cause energy dissipation at the column bases. This suggests that input energy and hysteretically dissipated energy are sensitive to the spatial distribution of energy in the frame. In particular, the formation of column base hinges results in a significant increase in the structure's average resistance to movement through ground motion displacements. By comparing the responses shown in Figures(5.2a-b) and (6.21b-c), one can see that a significant increase in both the hysteretic energy dissipation and the input energy at the frame base occurs near the 10 second interval of the final design's response, whereas

it is absent from the response of the initial design.

It is concluded that the use of multiple ground motion inputs in an energy based design method of this type is essential because of our imperfect understanding of why the contribution made by the terms in the energy balance equation vary so significantly among members of a family of records, and with modifications in the proportioning of a frame's elements.

The frame sway constraint statistics shown in Table[6.17] indicate that a significant increase in the mean and standard deviation of the peak frame lateral displacements accompanies the modification of the initial design to the final design. For instance, the peak frame sway c.o.v. increases from 0.082 to 0.224. The latter value is significant because the c.o.v. for the peak accelerations (see Section 4.3.2) of the severe ground motions was only 0.122. It is suggested that enlargements in both the mean response and the standard deviation is caused by increased levels of inelastic deformation in the girders and the formation of column hinges at the frame base of the final design.

6.2.3 Sensitivity of Dissatisfactions to Limit State Reliability

In Section 4.5.2.3 the difficulties in choosing an appropriate level of reliability for each constraint and limit state were discussed. It was decided that since this was the first implementation of a design method of this type, constant values would be assumed for all constraints and limit states, and emphasis placed on demonstrating the design method. The purpose of this section is to briefly re-examine some of this assumption's consequences.

Figures[6.20a] and [6.20b] plot the initial and final design peak limit state dissatisfactions as a function of constraint reliability when the LOW exceedance probability is half the HIGH exceedance probability. Contours of the dissatisfaction for the design objectives are also shown. The gravity loads plus

moderate lateral loads limit state has the maximum dissatisfaction level for high values of allowable exceedance probability, and appears to be less sensitive to the level of frame reliability than the severe lateral loads limit state. By comparison, the peak dissatisfaction for the severe lateral loads limit state is more sensitive to the adopted level of reliability, and causes the maximum level of design dissatisfaction for small exceedance probabilities. Both of these observations occur because the variation in the statistical distributions of frame response for this limit state are higher than for either the gravity loads alone or the gravity loads plus moderate lateral loads limit state. Moreover, because the levels of dissatisfaction increase with decreasing exceedance probability, the proposed method suggests that a more conservative design can be obtained without adjustment of the ground motion loads. All that is required is a reduction of the acceptable levels of constraint failure probability.

6.3 A Summary and Assessment of the Optimal Design Problems

The limited number of examples given in this chapter clearly indicate that the proposed methodology does not lend itself to a "hands-off" approach to design. Rather, it demands a level of designer understanding and attention to detail that includes (a) how different parts of the structure are expected to behave under each of the limit state loading conditions, (b) how mathematical expressions can be written to impart these intents to a non-linear programming problem, and (c) what modifications to a frame's elements are necessary to maximize improvement in design performance. For the example problem, improvement in the minimum volume and maximum dissipated design objectives occurred with a reduction in the element sizes. By contrast, improvement in the story drifts objective occurred with an increase in the element sizes. This result indicates that simultaneous improvement in all of the objectives results

in design modifications that are conflicting in nature. A number of impractical designs were obtained with some of the problems cast with single design goals. It has also been demonstrated that inferior optimal performance may occur for design problems that are over-constrained by the design parameters, or spatially mis-constrained. Nonetheless, the design improvements encouraged by the Phase I-II-III Method of Feasible Directions algorithm for the simple 2 parameter multiple objective problem (see Section 6.2) resulted in a practical weak-beam strong-column design. Although this proportioning philosophy is well known, its benefits are not always appreciated by designers.

Another inherent feature of the design method demonstrated by these examples is its ability to increase the designer dissatisfaction for response variations of increasing magnitude. This means that a designer specified level of constraint reliability is assured because the method automatically adjusts the mean frame response enhancement factors to the changing conditions of structural performance as a design is modified over several iterations of optimization. The results indicate that the uncertainty in predicting the elastic frame response of the final frame is slightly more than for the initial frame. Under severe lateral loads the 50% increase in hysteretic energy dissipation during the design iterates is accompanied by a significant increase in the variability of the energy disspation response quantities. Hence, it is concluded that the final design is better than the initial design not because the response can be predicted with more accuracy, but because its initial cost is lower, and because the initial design was too conservative.

Constraint No	Initial Design				Final Design			
	MFR	STD	GFR	BFR	MFR	STD	GFR	BFR
SOFT_INEQ(2)	54.0	0.0	352.6	423.1	54.0	0.0	331.4	397.7
SOFT_INEQ(3)	54.0	0.0	352.6	423.1	54.0	0.0	331.4	397.7
SOFT_INEQ(4)	36.0	0.0	352.6	423.1	36.0	0.0	331.4	397.7
SOFT_INEQ(5)	36.0	0.0	352.6	423.1	36.0	0.0	331.4	397.7
SOFT_INEQ(6)	18.0	0.0	352.6	423.1	18.0	0.0	331.4	397.7
SOFT_INEQ(7)	18.0	0.0	352.6	423.1	18.0	0.0	331.4	397.7

Table [6.5] : Column Axial Force Constraints

Constraint No	Initial Design				Final Design			
	MFR	STD	GFR	BFR	MFR	STD	GFR	BFR
SOFT_INEQ(8)	105.5	0.0	2408	3210	111.4	0.0	2256	3008
SOFT_INEQ(9)	208.3	0.0	2408	3210	219.6	0.0	2256	3008
SOFT_INEQ(10)	105.5	0.0	2408	3210	111.4	0.0	2256	3008
SOFT_INEQ(11)	208.3	0.0	2408	3210	219.6	0.0	2256	3008
SOFT_INEQ(12)	263.2	0.0	2408	3210	272.9	0.0	2256	3008
SOFT_INEQ(13)	208.4	0.0	2408	3210	219.2	0.0	2256	3008
SOFT_INEQ(14)	263.2	0.0	2408	3210	272.9	0.0	2256	3008
SOFT_INEQ(15)	208.4	0.0	2408	3210	219.2	0.0	2256	3008
SOFT_INEQ(16)	285.1	0.0	2408	3210	296.8	0.0	2256	3008
SOFT_INEQ(17)	415.4	0.0	2408	3210	449.1	0.0	2256	3008
SOFT_INEQ(18)	285.1	0.0	2408	3210	296.8	0.0	2256	3008
SOFT_INEQ(19)	415.4	0.0	2408	3210	449.1	0.0	2256	3008

Table [6.6] : Column Bending Moment Constraints

Constraint No	Initial Design				Final Design			
	MFR	STD	GFR	BFR	MFR	STD	GFR	BFR
SOFT_INEQ(20)	471.5	0.0	1974	2632	492.5	0.0	1386	1849
SOFT_INEQ(21)	471.5	0.0	1974	2632	492.5	0.0	1386	1849
SOFT_INEQ(22)	502.2	0.0	1974	2632	516.0	0.0	1386	1849
SOFT_INEQ(23)	502.2	0.0	1974	2632	516.0	0.0	1386	1849
SOFT_INEQ(24)	415.4	0.0	1974	2632	449.1	0.0	1386	1849
SOFT_INEQ(25)	415.4	0.0	1974	2632	449.1	0.0	1386	1849

Table [6.7] : Girder Bending Moment Constraints

Constraint No	Initial Design				Final Design			
	MFR	STD	GFR	BFR	MFR	STD	GFR	BFR
SOFT_INEQ(26)	0.0133	0.0	.7506	.8226	0.0150	0.0	.7506	.8226
SOFT_INEQ(27)	0.0073	0.0	.7506	.8226	0.0075	0.0	.7506	.8226
SOFT_INEQ(28)	0.0242	0.0	.7506	.8226	0.0287	0.0	.7506	.8226

Table [6.8] : Maximum Girder Midspan Deflection Constraints

Period	Initial Design			Final Design		
mode 1	0.3437 sec			0.4015 sec		
mode 2	0.1022 sec			0.1142 sec		
mode 3	0.0561 sec			0.0592 sec		
Eigenvectors	**Initial Design**			**Final Design**		
dof/mode	1	2	3	1	2	3
1	0.3037	1.0000	1.0000	0.2805	1.0000	1.0000
4	0.7217	0.7633	-0.9127	0.6998	0.8328	-0.8645
7	1.0000	-0.8546	0.3549	1.0000	-0.8633	0.3244

Table [6.9] : Frame Eigenvalues and Modal Periods

Constraint No	Initial Design				Final Design			
	MFR	STD	HFR	LFR	MFR	STD	HFR	LFR
SOFT_FINEQ(1)	1287	529	1732	1965	1201	550	1664	1904
SOFT_FINEQ(2)	767	250	978	1088	602	202	772	861
SOFT_FINEQ(3)	1326	500	1747	1967	1203	432	1568	1758
SOFT_FINEQ(4)	791	243	996	1103	606	148	731	796
SOFT_FINEQ(5)	971	342	1258	1408	868	315	1133	1271
SOFT_FINEQ(6)	996	362	1301	1460	855	324	1128	1270
SOFT_FINEQ(7)	970	300	1223	1355	854	255	1069	1182
SOFT_FINEQ(8)	1012	333	1292	1439	854	259	1073	1187
SOFT_FINEQ(9)	614	165	753	826	566	141	686	748
SOFT_FINEQ(10)	989	249	1229	1355	965	277	1199	1321
SOFT_FINEQ(11)	600	132	711	769	566	140	684	746
SOFT_FINEQ(12)	979	237	1178	1283	965	247	1173	1282
	GFR = 3411 BFR = 4414				GFR = 3196 BFR = 4136			
c.o.v.	range = [0.22 - 0.41] average = 0.31				range = [0.25 - 0.46] average = 0.31			
E_1	range = [1.18 - 1.34] average = 1.26				range = [1.21 - 1.39] average = 1.27			
E_2	range = [1.28 - 1.57] average = 1.40				range = [1.31 - 1.59] average = 1.40			

Table [6.10] : Maximum Column Bending Moment Constraints

Constraint No	Initial Design				Final Design			
	MFR	STD	HFR	LFR	MFR	STD	HFR	LFR
SOFT_FINEQ(13)	1712	572	2194	2446	1416	477	1818	2027
SOFT_FINEQ(14)	1740	530	2186	2419	1416	382	1738	1907
SOFT_FINEQ(15)	1594	524	2034	2265	1381	464	1772	1976
SOFT_FINEQ(16)	1594	461	1982	2185	1377	388	1704	1875
SOFT_FINEQ(17)	990	285	1229	1355	965	277	1199	1321
SOFT_FINEQ(18)	979	237	1178	1283	965	247	1173	1282
	GDO = 2961 BDO = 3620				GDO = 2080 BDO = 2542			
c.o.v.	range = [0.24 - 0.33] average = 0.30				range = [0.26 - 0.34] average = 0.30			
E_1	range = [1.20 - 1.28] average = 1.25				range = [1.22 - 1.28] average = 1.25			
E_2	range = [1.31 - 1.43] average = 1.38				range = [1.33 - 1.43] average = 1.38			

Table [6.11] : Maximum Girder Bending Moment Constraints

Constraint No	Initial Design				Final Design			
	MFR	STD	HFR	LFR	MFR	STD	HFR	LFR
SOFT_FINEQ(19)	.2200	.0909	.2965	.3364	.2350	.1034	.3221	.3676
SOFT_FINEQ(20)	.3015	.1297	.4107	.4677	.3464	.1572	.4787	.5479
SOFT_FINEQ(21)	.2034	.0921	.2809	.3215	.2559	.1206	.3574	.4105
	GDO = 0.54 BDO = 0.96				GDO = 0.54 BDO = 0.96			
c.o.v.	range = [0.41 - 0.45] average = 0.43				range = [0.44 - 0.47] average = 0.46			
E_1	range = [1.34 - 1.38] average = 1.36				range = [1.37 - 1.40] average = 1.38			
E_2	range = [1.53 - 1.58] average = 1.55				range = [1.56 - 1.60] average = 1.58			

Table [6.12] : Statistics of Peak Story Drifts

Constraint No	Initial Design				Final Design			
	MFR	STD	HFR	LFR	MFR	STD	HFR	LFR
SOFT_FINEQ(22)	113	51	156	178	114	47	153	174
SOFT_FINEQ(23)	186	73	248	281	168	67	226	255
SOFT_FINEQ(24)	250	115	348	398	219	105	308	354
	GDO = 270 BDO = 540				GDO = 270 BDO = 540			
c.o.v.	range = [0.39 - 0.46] average = 0.43				range = [0.40 - 0.48] average = 0.43			
E_1	range = [1.33 - 1.39] average = 1.37				range = [1.34 - 1.41] average = 1.36			
E_2	range = [1.51 - 1.59] average = 1.56				range = [1.52 - 1.62] average = 1.55			

Table[6.13] : Statistics of Peak Absolute Floor Acceleration

Constraint No	Initial Design				Final Design			
	MFR	STD	HFR	LFR	MFR	STD	HFR	LFR
SOFT_INEQ(29)	0.000	0.000	0.000	0.000	1.879	4.202	6.600	10.09
SOFT_INEQ(31)	0.000	0.000	0.000	0.000	1.838	4.109	6.453	9.86
	GDO = 30.77 BDO = 47.25				GDO = 28.92 BDO = 44.41			

Table [6.14] : Hysteretic Energy Dissipation at the Column Bases

Constraint No	Initial Design				Final Design			
	MFR	STD	HFR	LFR	MFR	STD	HFR	LFR
SOFT_INEQ(41)	18.90	11.80	32.15	41.94	18.24	19.40	40.03	56.13
SOFT_INEQ(42)	19.17	11.45	32.03	41.52	20.78	18.96	42.08	57.81
SOFT_INEQ(43)	3.371	2.893	6.620	9.021	10.22	9.037	20.37	27.87
SOFT_INEQ(44)	2.935	1.705	4.850	6.265	10.58	6.840	18.26	23.94
SOFT_INEQ(45)	0.000	0.000	0.000	0.000	0.354	0.502	0.918	1.334
SOFT_INEQ(46)	0.000	0.000	0.000	0.000	0.000	0.000	0.000	0.000
	GDO = 47.66 BDO = 83.13				GDO = 38.20 BDO = 66.62			
c.o.v.	range = [0.58 - 0.85] average = 0.66				range = [0.65 - 1.41] average = 0.98			
E_1	range = [1.65 - 1.96] average = 1.76				range = [1.72 - 2.59] average = 2.10			
E_2	range = [2.13 - 2.67] average = 2.32				range = [2.26 - 3.76] average = 2.92			

Table [6.15] : Girder Hysteretic Energy Dissipation Constraints

Record Name	Input Energy	Hysteretic Energy	Work Done By Loads	Damped Energy
E1	0.203e+03	0.328e+02	0.614e+01	0.176e+03
E2	0.479e+03	0.195e+03	0.507e+01	0.289e+03
E3	0.136e+03	0.216e+02	0.284e+01	0.117e+03
E4	0.275e+03	0.736e+02	0.605e+01	0.207e+03
E5	0.206e+03	0.426e+02	0.462e+01	0.168e+03
E6	0.144e+03	0.180e+02	0.406e+01	0.130e+03

record name	E1	E2	E3	E4	E5	E6
energy group 1	0.0	22.3	.0.0	0.0	0.0	0.0
energy group 2	32.8	172.4	21.6	73.6	42.6	18.0

Table [6.16] : Energy Balance Equation for the Final Design

Constraint No	Initial Design				Final Design			
	MFR	STD	GFR	BFR	MFR	STD	GFR	BFR
SOFT_FINEQ(25)	2.070	.1694	2.212	2.267	2.609	.5844	3.101	3.356
	GDO = 5.04 BDO = 6.12				GDO = 5.04 BDO = 6.12			
c.o.v.	average = 0.082				average = 0.224			
E_1	average = 1.06				average = 1.188			
E_2	average = 1.10				average = 1.287			

Table[6.17] : Statistics of the Peak Frame Sway Constraint

CHAPTER 7

CONCLUSIONS AND FUTURE RESEARCH

7. Introduction

In Section 1.3 it was stated that the long term goal of this research program is to formulate a design methodology and develop computer-aided design software that will help engineers (a) achieve designs that are more consistent with the accepted design philosophy and (b) make rational decisions while designing seismic-resistant structures. This investigation has focussed on a subset of the defined goal; the formulation and preliminary testing of a methodology which allows the design of seismic-resistant structures to be completed in a rational manner. A procedure for explicitly including the effects of uncertainties and multiple objectives in the design process was proposed in Chapters 2 and 3. Chapter 4 dealt with the problem of describing the probabilistic limit states design of seismic-resistant steel frames in a nonlinear programming format. An assessment of the performance of the initial *example* frame was given in Chapter 5. Chapter 6 reported on the sensitivity and optimal behavior of the *example* frame designed according to a selection of single and multiple design criteria, and design parameter layouts. Now, it is appropriate to comment on the performance of the proposed method in terms of the defined research goal, and to identify areas for continued research.

The [GOOD,BAD] and [HIGH,LOW] performance pairs, and associated scaling procedures defined in Chapter 2 constitute a mechanism for combining into a single entity the consequences of structural response variations, and a designer's feelings on the relative performance of the design attributes. It has been demonstrated that the resulting dissatisfaction function models effectively the relationship between response scatter and the corresponding

level of frame response required to attain to a target level of reliability. The combined formulation has considerable versatility. For example, the preference pair parameters can be set to model situations in which the designer cannot define a problem with accuracy, as well as other instances where the designer's intents are sharply defined. Special performance criteria may be specified for structures that are constructed of non-conventional materials, or constitute an innovative structural system. Extra conservatism for important structures can be enforced without adjustment of the lateral loads. One simply decreases the values in the [HIGH,LOW] preference pair. Finally, the ability to designate HARD and SOFT constraint attributes is seen as a desirable feature because it allows the designer to impart a solution strategy to solving a problem in much the same way as would be done in a manual design procedure. First, design modifications are encouraged which will result in all of the HARD (important) constraints being satisfied, before attempts are made to minimize the maximum level of dissatisfation among the design objectives and the less important SOFT constraints.

A detailed performance assessment of the optimal design problems has already been documented in Section 6.3. This section of work demonstrated that due to the sensitivity of terms in the energy balance equation to the overall size and relative strengths of adjacent frame members, a set of ground motion inputs should be employed in a design process of this type. In addition, it has been shown that multiple criteria should be used because no single design objective by itself is capable of describing all of the attributes which characterize an effective design.

Although practical weak-beam strong-column designs were calculated when the design objectives and parameters were given sufficient freedom, less desirable designs were obtained for problems characterized by non-convex

design objectives, or over-constrained design parameters. This means that the design process cannot be regarded as a *black-box* operation with zero designer involvement. In the latter cases, designer intervention is necessary to modify the problem formulation before the design procedure can resume. Difficulties of this type are most effectively handled when the designer has (a) an understanding how the different parts of the structure are expected to behave under each of the limit state loadings, and (b) the ability to impart the desired attributes to the nonlinear programming problem. Because a significant proportion of designers may not have the required skills, a need exists to develop a user interface which allows graceful recovery from difficult situations, helps the designer see what needs to be done, and allows him or her to simply go and do it. Further, it should provide the inexperienced designer with the illusion that the details of the design method will be easy to learn, while making the experienced designer feel that his or her capabilities are not limited by the tools in the user interface. This aspect of the development is of primary importance because to novices and experts alike, what is presented to one's senses through the interface is one's computer, and in this case, an aid to the design method.

7.1 Recommendations for Further Work

The purpose of this section is to list some of the remaining avenues of research that should be pursued:

(a) The proposed design method places considerable emphasis on accounting for the consequences of response variation and uncertainties in seismic design. In this investigation the effects of material variations, dead and live gravity loads, and seismic lateral loads were considered. Uncertainties associated with ground motion duration were overlooked in order to simplify the computation. It has also been pointed out that uncertainties are

less desirable than response variations because the former cannot be described with statistical confidence. Consequently, further work must concentrate on improving our understanding of the various sources of uncertainty in the seismic environment. A need exists to examine the uncertainty in predicting (a) the intensity of a prescribed event and (b) the uncertainty in predicting an event of prescribed intensity over a structure's lifetime.

(b) The family of ground motion records used in this investigation consisted of three pairs of components recorded at the same site during three separate seismic events. This limited number of ground motions was assumed to be sufficient for demonstrating the design method. However, in other instances a sufficient number of ground motion records may not always be available, especially if high accuracy reliability estimates are required. A possible solution to this difficulty is to use data recorded from previous seismic events to construct an auto regressive moving average (ARMA) stochastic model.

Appendix 4 presents the results of a preliminary study in which the use of ARMA models in the proposed design method is investigated. It is shown that ARMA models are capable of reproducing the mean frame response for both the moderate and severe lateral load limit states. However, the variation in frame responses for the moderate lateral loads limit state was only about one half of that obtained with the family of recorded ground motions. It is suggested that this difference could be directly related to the variation in peak ground accelerations of the scaled records. Future research directions should attempt to determine a reliable means for scaling the ground motions. A strong need also exists to identify ground motion characteristics and structural response parameters which are sta-

tistically correlated to structural damage.

(c) The three design objectives developed and tested within this report are useful for the design of moment-resistant frames. Unfortunately this list is not complete, and further work should be directed towards the development of design criteria that are applicable to the design of less conventional structural systems. For example, minimum input energy at the frame base appears to be an important design objective for the design of base-isolated frames. There is little doubt that special design objectives and constraints will need to be formulated for the design of eccentrically-braced frames, and K-braced frames[57]. Another potential area for development occurs when the design problem is viewed as an optimal allocation of a fixed quantity of resources. In the context of seismic design, this problem could be interpreted as fixing the initial cost of the frame (possibly more than the minimum possible initial cost), and casting the design problem as one of determining the best proportioning of the frame's elements which maximizes the lifetime reliability of the structure.

(d) In this investigation, the statistical distribution types were assumed to be either extreme type I for hysteretic element dissipation, or normal for the remaining response quantities. Identification of the best statistical distributions for the ensuing frame response variations is an area requiring continued research. A need also exists to investigate more closely how the statistical distribution type and its parameters vary for (a) structures of different structural-system type and geometry and (b) earthquake loads of increasing intensity.

(e) Constant [HIGH,LOW] preference pair settings were assumed for both the moderate and severe lateral load limit states. Further work should be implemented to see if this assumption is reasonable, and to determine

preference pair settings implied by the design codes.

(f) The design method should be applied to a series of larger moment-resistant structures that have higher column axial forces. Objectives in a study of this type could include (a) investigating the sensitivity of frame response quantities to the magnitude and spatial arrangement hysteretic energy dissipation, and (b) evaluation of the best design parameter arrangements for a balance in "quality of the final design" vs "required computation."

(g) In general, the optimization algorithms used in DELIGHT require that the design objectives and constraints and their derivatives with respect to the design parameters be continuous. This requirement is usually satisfied, unless the constraints are composed of *abs*, max or min functions. Unfortunately, the derivatives of the maximum value of the time-dependent constraints (and story drifts design objective) with respect to the design parameters are not differentiable. Thus, problems arise when the derivatives of these constraints with respect to the design parameters are required for the direction vector calculation. For the case of a single ground motion input, this difficulty is overcome by including all of the locally eps-active maxima into the direction vector calculation. However, a procedure for including locally eps-active maxima from a number of time-dependent response quantities into the calculation of generalized gradients has yet to be worked out. Hence, a need exists to overcome this deficiency.

(h) The need for developing a flexible user interface has already been mentioned. In addition, development of a design method and associated software which provides a designer with computer assistance during the preliminary stages of the design process is needed. A related, but possibly

more fundamental problem is associated with the optimal selection of a structural system. In Chapter 1 it was noted that the choice of a structural system is usually left to the judgement of an experience designer. Yet, it seems plausible that if the resources were developed to enable the results from a series of preliminary design analyses to be presented to designers in a concise manner, selection of a structural system could be made efficiently, and with confidence that might otherwise be unobtainable.

REFERENCES

1. ANS58, "Building Code Requirements for Minimum Design Loads in Buildings and other Structures," National Bureau of Standards, Special Publication 577 1980.

2. ATC-10-1 "Seminar On Earthquake Ground Motion and Building Damage Potential," San Francisco Hilton, March 27, 1984.

3. American Institute of Steel Construction, **Manual of Steel Construction**, Seventh Edition, 1973.

4. American Petroleum Institute, "API Recommended Practice for Planning, Designing, and Constructing of Fixed Offshore Platforms," *Ninth Edition*, 1979.

5. Ang A.H.S., Tang W.H., **Probability Concepts in Engineering Planning and Design : Volume I - Basic Principles**, *John Wiley and Sons*, 1975.

6. Applied Technology Council, "Working Draft of Recommended Seismic Design Provisions for Buildings," January 1976.

7. Applied Technology Council, "Tentative Provisions for the Development of Seismic Regulations for Buildings," National Bureau of Standards, June 1978.

8. Arias A. "A Measure of Earthquake Intensity," Seismic Design for Nuclear Power Plants, *MIT Press*, Cambridge, Mass, 1970.

9. Austin M.A., Pister K.S., "A Guide to the Use of DELIGHT.STRUCT," *Report* No. UCB/SESM 83/07, Department of Civil Engineering, University of California, Berkeley, June 1983.

10. Austin M.A., Pister K.S., "Optimal Design of Friction-braced Frames under Seismic Loading," *Report* no UCB/EERC-83/10, Earthquake Engineering Research Center, Univ of Cal, Berkeley, June 1983.

11. Baber T.T., Wen Y.K, "Random Vibration of Hysteretic Degrading Systems," *Journal of the Engineering Mech Division*, ASCE, December 1981.

12. Balling R.J., Ciampi V., and Pister K.S., "Interactive Optimization-Based Design of Seismically Loaded Structures," *Proceedings*, 7th European Conference on Earthquake Engineering, Athens, Greece, September, 1982.

13. Balling R.J., Pister K.S., and Polak E., "DELIGHT.STRUCT: A Computer-Aided Design Environment for Structural Engineering," *Computer Methods in Applied Mechanics and Engineering*, (1983), pp 237-251, North-Holland Publishing Company.

14. Balling R.J., Ciampi V., Pister K.S., and Polak E., "Optimal Design of Seismic-Resistant planar Steel Frames," *Report No* EERC 81-20, Earthquake Engineering Research Center, Univ of Cal, Berkeley, December, 1981.

15. Bea R, Hong S.T., Mitchell J.S., "Decision Analysis Approach to Offshore Platform Design," *Journal of the Structural Engineering Division*, Vol. 110, No 1, January 1984.

16. Berg G.V., Thomides S., "Energy Consumption by Structures in Strong Ground Motion Earthquakes," *Proceedings of the 2nd World Conf on Earthquake Engineering*, Vol II, page 681, July 1960.

17. Bhatti M.A., Ciampi V., Kelly J.M. and Pister K.S., "An Earthquake Isolation System for Steam Generators in Nuclear Power Plants," *Nuclear Engineering and Design*, Vol 73, pp 229-252, 1982.

18. Blume J.A., "A Reserve Energy Technique for the Earthquake Design and Rating of Structures in the Inelastic Range," *Proceedings of 2nd WCEE*, page 1061, Vol II, July 1960.

19. Brayton R.K., Hachtel G.D., and Sangiovanni-Vincentelli A.L., " A Survey of Optimization Techniques for Intergrated Circuit Design," *Proceedings of*

the IEEE. Vol 69, No 10, October 1981.

20. Briseghella L. et al. "Optimum Elastoplastic Design under Stochastic Environment," *Fourth International Conference on Applications of Statistics and Probability in Soil and Structural Engineering*. Universita di Firenze (Italy) 1983.

21. Calahan D.A., **Computer-Aided Network Design**, McGraw-Hill Book Company, New York(1972).

22. Cornell A.C., "Engineering Seismic Risk Analysis," *Bulletin of the Seismological Society of America*, Vol 58, 1968, pp 1583-1600.

23. Der Kuireghian A., Ke J.B.,"Finite Element Based Reliability Analysis of Framed Structures," *4th International Conference on Structural Safety and Reliability*, 1984.

24. Dlesk D.C., Liebman J.S.,"Multi-Objective Engineering Design," *Engineering Optimization*, Vol 6, pp 161-175, 1983.

25. Ellingwood B., "Probability-Based Loading Criteria for Codified Design," *Fourth International Conference on Applications of Statistics and Probability in Soil and Structural Engineering*, Universita di Firenze (Italy) 1983.

26. Ferritto J.M., "Economics of Seismic Design for New Buildings," *Journal of the Structural Division*, ASCE, Vol 110, No ST12, December 1984.

27. Frangopol D.M., "A Reliability-based Optimization Technique for Automated Plastic Design," *Computer Methods in Applied Mechanics and Engineering*, Vol 44, 1984, pp 105-107.

28. Ghiocel D., Lungu D., **Wind, Snow and Temperature Effects on Structures Based on Probability**, Abacus Press, 1975.

29. Giannini R., Nuti C., Pinto P.E., "Seismic Reliability of Non-linear Structural Systems," *Fourth International Conference on Applications of Statistics and*

Probability in Soil and Structural Engineering, Italy, 1983.

30. Goicoechea A., Hansen D.R., Duckstein L., **Multi-Objective Analysis with Engineering and Business Applications**, *J. Wiley and Sons*, 1982.

31. Guangqian H. et al.,"A new procedure for Aseismic Design of Multi-story Shear Type Buildings based upon Deformation Checking," pp 483-490, Vol 5, *Proc.* 8th WCEE, San Francisco, 1984.

32. Gumbel E., **Statistics of Extremes**, *Columbia University Press*, 1958.

33. Housner G.W., "Limit Design of Structures to Resist Earthquakes," *Proceedings of Ist WCEE*, June 1956. Univ of Calif, 1975.

34. Kato B., Akiyama H., "Seismic Design of Steel Buildings," *Journal of the Engineering Structural Division*, No ST8, August 1982.

35. Kay A., "Computer Software; Presenting an Issue on the Concepts of Techniques that give Form to the Programmable Machine," *Scientific American*, Volume 251, No 3, September, 1984.

36. Kennedy R.P., "Peak Acceleration as a measure of Damage," Presented at the 4th International *Seminar on Extreme-Load Design of Nuclear Power* Facilities, Paris, France, 1981.

37. Lashkari B., Krawinkler H., "Damage Parameter for Bilinear Single Degree of Freedom Systems," *Proc 7th European Conference Earthquake Engineering*. Athens, September 1982.

38. Lin J., Mahin S.A., "Effect of Inelastic Behavior on the Analysis and Design of Earthquake Resistant Structures," *Report No* UCB/EERC-85/08, Earthquake Engineering Research Center, U. C. Berkeley, June 1985.

39. Mahin S.A., Bertero V.V., "An Evaluation of Some Methods for Predicting Seismic Behavior of Reinforced Concrete Buildings," EERC Report, No 75-5, Earthquake Engineering Research Center,

40. Mahin S.A., Bertero V.V., " Prediction of Nonlinear Seismic Building Behavior," *Journal of Technical Councils of ASCE*, TC1, November,1978.

41. Mondkar D.P., Powell G.H., "ANSR - 1 General Purpose program for Analysis of Nonlinear Structural Response," *Report No. EERC 75-37*, Earthquake Engineering Research Center, U. C. Berkeley, December 1975.

42. Murakami M., Penzien J., "Nonlinear Response Spectra for Probabilistic Seismic Design of Reinforced Concrete Structures," *Report No. EERC 75-38*, Earthquake Engineering Research Center, U. C. Berkeley, November 1975.

43. Newmark N.M., Hall W.J., **Earthquake Spectra and Design - A Primer**, Earthquake Research Institute, Berkeley, California 1982.

44. Nye W.T., " DELIGHT : An Interactive System for Optimization-Based Engineering Design," UCB/ERL M83/33 Univ of Cal, Berkeley, Ca, May, 1983.

45. Nye W.T., Tits A.L., "An Application-Oriented, Optimization-Based Methodology for Interactive Design of Engineering Systems," *Systems Research Report 84-4*, Dep't of Electrical Engineering, University of Maryland, 1984.

46. Ohi. K, Tanaka H. "Frequency Domain Analysis of Energy Input Made by Earthquakes," pp 67-74, Vol 4, Proc. 8th WCEE, San Francisco, 1984.

47. Pall A.S., Marsh C., "Response of Friction Damped Braced Frames," *Journal of the Structural Division*, ASCE, Vol(108), pp 1313-1323, No ST6, June 1982.

48. Paulay T.,"Capacity Design of Earthquake Resistant Ductile Multistory Reinforced Concrete Frames," *Proc of Third Canadian Conference Earthquake Engineering*. Montreal,Canada.

49. Penzien J., "Statistical Nature of Earthquake Ground Motions and Structural Response," *Proc. U.S.-Southeast Asia Symposium on Engineering for*

Natural Hazards Protection, Manila, Philippines, Sept 26-30, 1977.

50. Pierson B.L., "A Survey of Optimal Structural Design under Dynamic Constraints," *Int. J. Num. Method. Eng.*, No 4, 1974, pp 491-499.

51. Popov E.P., Bertero V.V., "Cyclic Loading of Steel Beams and Connections," ASCE, *Journal of the Structural Division*, Vol 99, No 6, 1973.

52. Rao S.S., **Optimization Theory and Applications**, *John Wiley and Sons*, New York, 1979, 711pp.

53. Ray D., Pister K.S., "Optimum Design of Earthquake-Resistant Shear Buildings," *Report No* EERC 74-3, Earthquake Engineering Research Center, January, 1974.

54. Recommended Lateral Force Requirements and Commentary, Seismology Committee, Structural Engineers Association of California, San Francisco, Calif, 1975.

55. Roeder C.W., Popov E.P., "Eccentrically Braced Steel Frames for Earthquakes," ASCE, pp 391-412, Vol 104, No ST3, March 1978.

56. Ruiz P., Penzien J., "Probabilistic Study of the Behavior of Structures during Earthquakes," Earthquake Engineering Research Center, *Report* No EERC 69-3, University of California, Berkeley, California, March 1969.

57. SEAONC Research Committee,"Earthquake Resistant Design of Concentric and K-Braced Frames," *Structural Engineers Association of Northern California*, July 1982.

58. Shah H.C., Dong W.M., "A Re-evaluation of the current Seismic Hazard Methodologies," *Proceedings of the 8th WCEE*. Vol 1, San Francisco, 1984.

59. Shah H.C., Dong W.M., "Reliability Assessment of Existing Buildings subject to Probabilistic Earthquake Loadings," *Journal of Engineering Structures*.

60. Singh J.P., "Characteristics of Near Field Ground Motions and their Importance in Building Design," *ATC-10 Seminar*, March 1984, San Francisco.

61. Sheu C.Y., Prager W., "Recent Developments in Optimal Structural Design," *Applied Mechanics Reviews*, No 21, 1968, pp 985-992.

62. Teal E.J. "Seismic Design Practice for Steel Buildings," *Engineering Journal of the American Institute of Steel Construction*, Vol (12), No 4, Fourth Quarter, 1975.

63. Uniform Building Code, International Conference of Building Officials, Whittier, Ca, 1979 Edition.

64. Veletos A.S., Vann W.P., "Response of Ground-Excited Elastoplastic Systems," *Journal of the Structural Division*, ASCE, pp 1257-1281, Vol 97, No ST4, April 1971.

65. Vitiello E., Pister K.S., "Optimal Earthquake-Resistant Design: A Reliability-Based, Global Cost Approach," Computer Methods in Applied Mechanics and Engineering, *North-Holland Publishing Company*, pp 277-299, No 8, 1976.

66. Walker N.D.,"Automated Design of Earthquake Resistant Multistory Steel Building Frames," *Report No* 77-12, Earthquake Engineering Research Center, University of California, Berkeley, Ca, May 1977.

67. Wen Y.K. "Method for Random Vibration of Hysteretic Systems," *Journal of the Engineering Mech Division*, ASCE, April 1976.

68. Zayas V.A., Shing P.S., Mahin S.A., Popov E.P.," Inelastic Structural Modeling of Braced Offshore Platforms for Seismic Loading," EERC Report, No 81/04, Earthquake Engineering Research Center, Univ of Calif, January 1981.

69. Zienkiewicz O.C., Taylor R.L., **The Finite Element Method - Chapter 24**, *3rd Edition*, Mc Graw-Hill, New York, 1977, 787pp.

APPENDIX 1

This appendix gives a description of the design objectives and constraints for the *example* frame discussed in Chapters 4-6.

```
*** DESCRIPTION OF THE DESIGN PROBLEM ***

The Problem:
   Design variable list: Xi (i = 1 to  1)
   Minimize the multiple objectives: O(X) (j = 1 to 6(max) )
   subject to :
   Conventional Constraints: Gj(X) < 0 (j = 1 to  64)
   Functional Constraints: max over t (Fk(X,t)) < 0 (k = 1 to  25)

*** DESIGN VARIABLES ***
    Leading Element No        Tracking Elements

   X( 1) =        1            2   3   4   5   6   7   8   9

*** DESIGN OBJECTIVES ***


   OBJEC( 1) : Volume of frame elements :
               1   2   3   4    5  6  7   8   9

===========
Limitstate 2 :
===========

   OBJEC( 2) : Sum of story drifts squared.
               top node  4 bottom node  2
               top node  6 bottom node  4
               top node  8 bottom node  6

===========
Limitstate 3 : Input energy and Dissipated energy
===========   for the frame and element groups.

    OBJEC( 3) = Input energy at the frame base

  FRAME GROUP(1) :   1   2   3   4   5   8

    SUB_OBJEC( 4) = Dissipated Energy
    SUB_OBJEC( 5) = Variation of Dissipated Energy

  FRAME GROUP(2) :   7   8   9

    SUB_OBJEC( 6) = Dissipated Energy
    SUB_OBJEC( 7) = Variation of Dissipated Energy

=========================
```

```
Element Size Box Constraint : Conventional
==========================
   element size > min size [ bad , good ]
      B  1:     element  1
      B  2:     element  2
      B  3:     element  3
      B  4:     element  4
      B  5:     element  5
      B  6:     element  6
      B  7:     element  7
      B  8:     element  8
      B  9:     element  9

==========================
Element Size Box Constraint : Conventional
==========================
   element size < max size [ good , bad ]
      B 10:     element  1
      B 11:     element  2
      B 12:     element  3
      B 13:     element  4
      B 14:     element  5
      B 15:     element  6
      B 16:     element  7
      B 17:     element  8
      B 18:     element  9

*** CONVENTIONAL CONSTRAINTS ***

================
Volume Constraint : Conventional
================
   volume of designed elements < Volmax
      G  1

===========
Limitstate 1 : Gravity Load Conventional Constraints:
===========
   |column axial force| < column yield or buckling force*Colax
      G  2:     element  1
      G  3:     element  2
      G  4:     element  3
      G  5:     element  4
      G  6:     element  5
      G  7:     element  6
   |column end moment| < column yield moment*Colgra
      G  8:     element  1  node  1
      G  9:     element  1  node  3
      G 10:     element  2  node  2
      G 11:     element  2  node  4
      G 12:     element  3  node  3
      G 13:     element  3  node  5
      G 14:     element  4  node  4
      G 15:     element  4  node  6
```

```
      G 16:    element  5  node  5
      G 17:    element  5  node  7
      G 18:    element  8  node  6
      G 19:    element  8  node  8
   |girder end moment| < girder yield moment*Girgra
      G 20:    element  7  node  3
      G 21:    element  7  node  4
      G 22:    element  8  node  5
      G 23:    element  8  node  6
      G 24:    element  9  node  7
      G 25:    element  9  node  8
   |girder live-load midspan deflection| < span*Girdef
      G 26:    element  7
      G 27:    element  8
      G 28:    element  9

============
Limitstate 2 : There are no conventional constraints
============   for limitstate 2

============
Limitstate 3 : Severe Quake Conventional Constraints:
============
   column end energy < column failure energy (Colduc)
      G 29:    element  1  node  1
      G 30:    element  1  node  3
      G 31:    element  2  node  2
      G 32:    element  2  node  4
      G 33:    element  3  node  3
      G 34:    element  3  node  5
      G 35:    element  4  node  4
      G 36:    element  4  node  6
      G 37:    element  5  node  5
      G 38:    element  5  node  7
      G 39:    element  6  node  6
      G 40:    element  6  node  8
   girder end energy < girder failure energy (Girduc)
      G 41:    element  7  node  3
      G 42:    element  7  node  4
      G 43:    element  8  node  5
      G 44:    element  8  node  6
      G 45:    element  9  node  7
      G 46:    element  9  node  8

*** FUNCTIONAL CONSTRAINTS ***

============
Limitstate 1 : There are no functional constraints
============   for limitstate 1

============
Limitstate 2 : Moderate Quake Functional Constraints:
============
   |column end moment| < column yield moment*Colyld
```

```
   F  1:    element  1  node  1
   F  2:    element  1  node  3
   F  3:    element  2  node  2
   F  4:    element  2  node  4
   F  5:    element  3  node  3
   F  6:    element  3  node  5
   F  7:    element  4  node  4
   F  8:    element  4  node  6
   F  9:    element  5  node  5
   F 10:    element  5  node  7
   F 11:    element  6  node  6
   F 12:    element  6  node  8
|girder end moment| < girder yield moment*Giryld
   F 13:    element  7  node  3
   F 14:    element  7  node  4
   F 15:    element  8  node  5
   F 16:    element  8  node  6
   F 17:    element  9  node  7
   F 18:    element  9  node  8
|story drift| < Drift
   F 19:    top node  4  bottom node  2
   F 20:    top node  6  bottom node  4
   F 21:    top node  8  bottom node  6
|floor acceleraction| < Accel*g
   F 22:    floor node  4
   F 23:    floor node  6
   F 24:    floor node  8

==========
Limitstate 3 : Severe Quake Functional Constraints:
==========
   |structure sway| < Sway
   F 25:    top node  8  bottom node  2
```

APPENDIX 2

This appendix summarizes the assumption files used in the evaluation of a frame's performance.

(1) The file named *assum_elmt* contains the material values and the assumptions for reducing each element to a single degree of freedom.

```
*** ASSUMED MATERIAL VALUES AND SECTION RELATIONSHIPS ***

BEAMS AND COLUMN ELEMENTS.

   Young's modulus for steel = 29000.
   Yield stress for steel = 36.
   Strain hardening ratio for steel = 0.05

   For columns:
   min = [ bad,good ]  <  inertia  <  max = [ good,bad ]
   [ 50.00, 100.00 ]   <  inertia  <  [ 2500.00 , 3000.00 ]
      moment yield coordinate fraction = 1.
      axial yield coordinate fraction = 0.15
      radius of gyration =  0.39      * depth    ** 1.04
      for inertia <= 429.
      depth              =  1.47      * inertia ** 0.368
      otherwise
      depth              = 10.5       * inertia ** 0.0436

   For rubber bearings:
   min = [ bad,good ] < edge length < max = [ good,bad ]
   [  5.00,  10.00 ]  < edge length < [  100.00 ,  120.00 ]
      shear modulus of rubber = 0.0984
      bearing height = 25.

   For girders:
   min = [ bad,good ]  <  inertia  <  max = [ good,bad ]
   [ 50.00, 100.00 ]   <  inertia  <  [ 2500.00 , 3000.00 ]
      steel poisson ratio = 0.3
      radius of gyration =  0.52      * depth    ** 0.92
      depth              =  2.66      * inertia ** 0.287

   For dissipators:
   min = [ bad,good ]  < thickness <  max = [ good,bad ]
   [  0.25,   0.30 ]   < thickness <  [   10.00 ,   12.00 ]
      height of dissipator = 75.
      width of dissipator = 36.
```

(2) A file named *assume_frame* contains information on the live to dead load ratio, live load reduction factors, and percentage of critical Rayleigh damping.

```
*** ASSUMED FRAME MODELING PARAMETER VALUES ***

Frame assumptions.
   Ratio of live uniform load to total uniform load = 0.33333
   Live load reduction factor                       = 0.88000
   Global damping ratio = 0.030
```

(3) The file named *assume_sim* specifies the number of time-history simulations required for each limit state. Under the present setup the maximum number of ground motion records that can be used within a limitstate is 6. The minimum number is zero; if a limitstate is to be omitted from the design check.

```
*** FRAME SIMULATION ASSUMPTIONS ***

Modelling assumptions.

   Number of load cases for limit state 1      = 1
   Number of load cases for limit state 2      = 4
   Number of load cases for limit state 3      = 4
   Number of earthquake records utilized       = 4
```

APPENDIX 3

This appendix contains a script of the input and output for the two iterations of the combined minimum volume, minimum story drifts and maximum dissipated energy optimal design problem. Extra comments have been added to clarify the purpose of each section. The commands that should be typed from the screen or accepted from a file during a batch-mode run of DELIGHT.STRUCT are shown in **boldface**.

```
1> # ═══════════════════════════════════════════
1> # optimization test run with records E1-E8 for a
1> # combined volume, story drifts and energy design.
1> #
1> # starting column inertia = 720
1> # starting girder inertia = 720
1> #
1> # Variable X(1) is elements 1,2,3,4,5 and 6
1> # Variable X(2) is elements 7,8 and 9
1> #
1> # ═══════════════════════════════════════════
1> #
1> # reset variables
1> #
1> Group1_gmean_dis = 0.000
1> Group1_bmean_dis = 0.150
1> Group1_gvar_dis =  3.000
1> Group1_bvar_dis =  5.000
1> Group2_gmean_dis = 0.500
1> Group2_bmean_dis = 0.000
1> Group2_gvar_dis =  1.000
1> Group2_bvar_dis =  3.000
1> Good_Costvol = 15000
1> Bad_Costvol  = 24000
1> Good_Costdri = 0.002
1> Bad_Costdri  = 0.004
1> date
Date: 07/02/85  Time: 20:23:03
1> printv X
Column X(2):
  .66670
  .33330
1> simulate -no -verbose
*** state_no
*** ansrsim
*** Limit state number 1
```

```
*** Limit state number 2
*** Limit state number 3
--- start evaluation of design objectives
--- start conventional constraints
--- start functional constraints
1> date
Date: 07/02/85  Time: 22:37:25
1> sprint -mo -files -all -active
1> cprint -files
1> list print_statemo
------------------- Begin print_statemo --------------------

** DESIGN OBJECTIVES **

   OBJEC(   1) : Disatisfied = 0.7185e+00
   MDO = 0.2147e+05  STD = 0.     e+00   HPE = 0.     e+00  LPE = 0.     e+00
   HFR = 0.2147e+05  LFR = 0.2147e+05   GDO = 0.1500e+05  BDO = 0.2400e+05

   OBJEC(   4) : Disatisfied = 0.6896e+00
   MDO = 0.1552e+00  STD = 0.     e+00   HPE = 0.     e+00  LPE = 0.     e+00
   HFR = 0.1552e+00  LFR = 0.1552e+00   GDO = 0.5000e+00  BDO = 0.     e+00

   OBJEC(   5) : Disatisfied = 0.2561e+00
   MDO = 0.1512e+01  STD = 0.     e+00   HPE = 0.     e+00  LPE = 0.     e+00
   HFR = 0.1512e+01  LFR = 0.1512e+01   GDO = 0.1000e+01  BDO = 0.3000e+01

   OBJEC(   6) : Disatisfied = 0.6880e-02
   MDO = 0.2014e-02  STD = 0.8685e-03   HPE = 0.2000e+00  LPE = 0.1000e+00
   HFR = 0.2745e-02  LFR = 0.3127e-02   GDO = 0.2000e-02  BDO = 0.4000e-02

** CONSTRAINT SUMMARY **

** BOX CONSTRAINTS ***

** CONVENTIONAL CONSTRAINTS **

** FUNCTIONAL CONSTRAINTS **

   SOFT_FINEQ( 23  82 900 507 119 782 538) : Disatisfied     = 0.358e-01
   MDO = 0.1867e+03  STD = 0.7369e+02   HPE = 0.2000e+00  LPE = 0.1000e+00
   HFR = 0.2487e+03  LFR = 0.2611e+03   GDO = 0.2703e+03  BDO = 0.5405e+03

   SOFT_FINEQ( 24  80 848 545  83 782 535) : Disatisfied     = 0.400e+00
   MDO = 0.2507e+03  STD = 0.1153e+03   HPE = 0.2000e+00  LPE = 0.1000e+00
   HFR = 0.3478e+03  LFR = 0.3985e+03   GDO = 0.2703e+03  BDO = 0.5405e+03

-------------------- End print_statemo --------------------
1> list print_objectives
------------------- Begin print_objectives --------------------

ENERGY OBJECTIVES FOR GROUND MOTION INPUTS


Record No          Input     Dissipated  Work Done By Loads
```

```
-----------------------------------------------------------

        1     0.145e+03     0.202e+02          0.819e+01
        2     0.261e+03     0.385e+02          0.164e+01
        3     0.225e+03     0.748e+02          0.364e+01
        4     0.174e+03     0.767e+01          0.384e+00
        5     0.870e+03     0.774e+02          0.336e+01
        6     0.209e+03     0.478e+02          0.336e+01

record no                 1            2            3            4

energy group 1    0.    e+00    0.    e+00    0.    e+00    0.    e+00
energy group 2    0.2024e+02    0.3851e+02    0.7481e+02    0.7673e+01
-------------------- End print_objectives --------------------
1> list modal_results
------------------- Begin modal_results -------------------
EIGENVALUE ANALYSIS.

FRAME EIGENVALUES and modal periods.

mode 1  w**2 =  0.33417534e+03  T =  0.34371040e+00 sec
mode 2  w**2 =  0.37764374e+04  T =  0.10224421e+00 sec
mode 3  w**2 =  0.12542520e+05  T =  0.56103179e-01 sec

  dampm =   0.8454e+00  dampkt =   0.    e+00
 dampko =   0.7525e-03

FRAME EIGENVECTORS : these are orthogonal wrt to the mass matrix

    matrix  egvector

   row/col       1          2          3
     1      0.3037e+00  0.1000e+01  0.1000e+01
     4      0.7217e+00  0.7633e+00 -0.9127e+00
     7      0.1000e+01 -0.8546e+00  0.3549e+00
-------------------- End modal_results --------------------
1>
1> Alpha   = 0.3     # adjust optimization algorithm parameters
1> Fd_rel_ = 0.005
1>
1> run ~verbose 1
PARAMETER           VALUE       DESCRIPTION
Good_Costvol        1.500e+4    good volume objective
Bad_Costvol         2.400e+4    bad volume objective
Good_Costdri        2.000e-3    good drift objective
Bad_Costdri         4.000e-3     bad drift objective
Group1_gmean_dis    0.000       Group1 : mean dissipated energy
Group1_bmean_dis    .1500
Group1_gvar_dis     3.000       Group1 : energy variation
Group1_bvar_dis     5.000
Group2_gmean_dis    .5000       Group2 : mean dissipated energy
Group2_bmean_dis    0.000
Group2_gvar_dis     1.000       Group2 : energy variation
Group2_bvar_dis     3.000
```

Good_Volmax	1.000e+5	good volume maximum
Bad_Volmax	1.200e+5	bad volume maximum
Good_Colax	.5000	good gravity column axial force factor
Bad_Colax	.6000	bad gravity column axial force factor
Good_Colgra	.6000	good gravity column yield factor
Bad_Colgra	.8000	bad gravity column yield factor
Good_Girgra	.6000	good gravity girder yield factor
Bad_Girgra	.8000	bad gravity girder yield factor
Good_Girdef	4.170e-3	good girder midspan deflection
Bad_Girdef	4.570e-3	bad girder midspan deflection
Good_Drift	4.500e-3	good max moderate story drift
Bad_Drift	8.000e-3	bad max moderate story drift
Good_Accel	.7000	good max moderate floor accel in gs
Bad_Accel	1.400	bad max moderate floor accel in gs
Good_Colyld	.8500	good moderate column yield factor
Bad_Colyld	1.100	bad moderate column yield factor
Good_Giryld	.9000	good girder yield factor
Bad_Giryld	1.100	bad girder yield factor
Good_Sway	1.400e-2	good structure sway max
Bad_Sway	2.000e-2	bad structure sway max
Good_Colduc	3.000	good column ductility
Bad_Colduc	4.000	bad column ductility
Good_Girduc	4.000	good girder ductility
Bad_Girduc	6.000	bad girder ductility
High_Volmax_prob	.2000	high volmax probability
Low_Volmax_prob	.1000	low volmax probability
High_Colax_prob	.2000	high gravity column axial force factor
Low_Colax_prob	.1000	low gravity column axial force factor
High_Colgra_prob	.2000	high gravity column yield factor
Low_Colgra_prob	.1000	low gravity column yield factor
High_Girgra_prob	.2000	high gravity girder yield factor
Low_Girgra_prob	.1000	low gravity girder yield factor
High_Girdef_prob	.2000	high girder midspan deflection
Low_Girdef_prob	.1000	low girder midspan deflection
High_Drift_prob	.2000	high max moderate story drift
Low_Drift_prob	.1000	low max moderate story drift
High_Accel_prob	.2000	high max moderate floor accel in gs
Low_Accel_prob	.1000	low max moderate floor accel in gs
High_Colyld_prob	.2000	high moderate column yield factor
Low_Colyld_prob	.1000	low moderate column yield factor
High_Giryld_prob	.2000	high girder yield factor
Low_Giryld_prob	.1000	low girder yield factor
High_Sway_prob	.2000	high structure sway max
Low_Sway_prob	.1000	low structure sway max
High_Colduc_prob	.2000	high column ductility
Low_Colduc_prob	.1000	low column ductility
High_Girduc_prob	.2000	high girder ductility
Low_Girduc_prob	.1000	low girder ductility
Const_type_Volmax	2.000	volume maximum
Const_type_Lowbox	1.000	Low box constraint
Const_type_Upbox	1.000	Upper box constraint
Const_type_Colax	2.000	gravity column axial force factor
Const_type_Colgra	2.000	gravity column yield factor
Const_type_Girgra	2.000	gravity girder yield factor

```
 Const_type_Girdef   2.000       girder midspan deflection
 Const_type_Drift    2.000       max moderate story drift
 Const_type_Accel    2.000       max moderate floor accel in gs
 Const_type_Colyld   2.000       moderate column yield factor
 Const_type_Giryld   2.000       girder yield factor
 Const_type_Sway     2.000       structure sway max
 Const_type_Colduc   2.000       column ductility
 Const_type_Girduc   2.000       girder ductility
 Tolx                5.000e-4    tolerance for resimulating
 Numsim              1.300e+1    number of simulations
 Numsteps            1.321e+4    number of simulation time steps
 Numref              6.807e+3    number stiffness reformulations
 Maxerr              1.051e-5    maximum energy error ratio
 Print               1.000       simulation printout code
 Eps0                .1000       initial value of eps(ilon) for eps-active sch
                                 eme
 Q0                  1.000e+1    initial number of discretization points for f
                                 unc constr
 Mu1                 1.000       q increased if eps < Eps0*Mu1/q
 Mu2                 1.000       q increased if eps decreased and psiplus < Mu
                                 2/q
 Pushcost_1          1.000       Importance of cost in phase 1 (0=no cost)
 Pushcost_23         1.000e+1    Pushes cost-soft in phase 2-3:1=same as constr
 Epsscale            5.000       Used in phase-2 eps-active scheme
 Eps                 2.000       Epscost-active cost and soft constr. are cons
                                 idered
 Tradeoff            .5000       With high value, aims at tradeoff curve
 Alpha               .3000       Slope of Armijo test line
 Beta                .5000       Trial stepsize along h is Beta**k
 Kmin               -1.000e+1    Smallest k tried for stepsize in Beta**k:>= 0
 Mu                  5.000e-3    Number of samples doubled if eps < Mu/q
 Hcuteps             .9000       eps is cut if ||h|| < Hcuteps*eps
 NewQuadprog         1.000       =0 for old Harwell QP, =1 for new Mesoud QP
 Fd_abs_             1.000e-7    Perturbation variable
 Fd_rel_             5.000e-3    Perturbation variable
*** algo
*** mo_interact
*** state_mo
*** ansrsim
*** anskip = 1 => no simulation
--- constraint and objective evaluation
maxval [ hard_ineq ] =  0.000
maxval [ cost ] =  .7185 [ soft_ineq ] =  .3995

finding the descent direction

eps =  .1000

*** starting direction

maxval [ hard_ineq ] =  0.000
maxval [ cost ] =  .7185 [ soft_ineq ] =  .3995

phaseno  =  2.000     psiplus =  .7185
```

```
Epsscale =  5.000         eps =  .1000

starting LFD loop
Column xnewraw(2):
  7.20036e+2
  7.19928e+2

partial derivatives : column 1
Column xnewraw(2):
  7.25436e+2
  7.19928e+2
*** state_mo
*** ansrsim
*** Limit state number 1
*** Limit state number 2
*** Limit state number 3
--- constraint and objective evaluation

partial derivatives : column 2
Column xnewraw(2):
  7.20036e+2
  7.30728e+2
*** state_mo
*** ansrsim
*** Limit state number 1
*** Limit state number 2
*** Limit state number 3
--- constraint and objective evaluation

Matrix jacobian(99,2):
  2.136725       1.153710
 -7.829369e-2    .7382936
  6.373683       2.972947e+1
  3.062851       1.715811
  0.000000       0.000000

  --- lines deleted ---

  0.000000       0.000000
  0.000000       0.000000

Matrix e_jacobian(4,2):
  2.136725       1.153710
 -7.829369e-2    .7382936
  6.373683       2.972947e+1
  3.062851       1.715811

Matrix qq(4,4):
  5.898641       .6844848       4.791800e+1    8.524019
   .6844848      .5512073       2.145006e+1    1.026971
  4.791800e+1    2.145006e+1    9.244653e+2    7.053180e+1
  8.524019       1.026971       7.053180e+1    1.232508e+1

direction vector
```

```
Column h(2):
  7.829368e-2
 -.7382936

*** armijo

Column x(2):
   .66670
   .33330
maxval [ hard_ineq ] =  0.000
maxval [ cost ] =  .7185 [ soft_ineq ] =  .3995

starting loop to decrease steplength

k =  0.000
Column xnew(2):
   .6772455
   .2338576
maxval [ hard_ineq ] =  0.000
maxval [ cost ] =  .6151 [ soft_ineq ] =  .3254

starting loop to increase steplength

k = -1.000
Column xnew(2):
   .6877911
   .1344152
maxval [ hard_ineq ] =  0.000
maxval [ cost ] =  .5704 [ soft_ineq ] =  .8299

*** mo_interact
--------- ITERATION 1 ---------

direction finding phase:
phaseno = 2           psiplus =  .7185
eps     =  1.000     Epsscale =  5.000

active costs and constraints
Column act_ind(4):
  1.0
  4.0
  5.0
  8.8e+1

clipped jacobian matrix
Matrix e_jacobian(4,2):
  2.136725       1.158710
 -7.829368e-2    .7382936
  6.373688       2.972947e+1
  3.062851       1.715811

direction vector.
Column h(2):
  7.829368e-2
```

```
 -.7382936

armijo steplength :
Beta         =  .5000     bestk        =  0.000

scaled design vector  raw design vector
X(1 ) =  .6772        X_raw(1 ) =  7.314e+2
X(2 ) =  .2339        X_raw(2 ) =  5.051e+2
--------simulation output-------
number of simulations = 65
number of time steps = 66065
number of stiffness reformulations = 34315
maximum energy error ratio =  1.052e-5
--------------------------------

Interrupt...
2> date
Date: 07/03/85  Time: 03:47:37
2> ## calculate constraints for iteration 1
2> simulate -mo -verbose
*** state_mo
*** ansrsim
*** anskip = 1 => no simulation
--- finished ansrsim !!
--- start evaluation of design objectives
--- start conventional constraints
--- start functional constraints
2> sprint -mo -all -files -active -concise
2> cprint -files
2> list print_statemo
------------------- Begin print_statemo --------------------

** DESIGN OBJECTIVES **

   OBJEC(   1) : Disatisfied = 0.6151e+00
   OBJEC(   4) : Disatisfied = 0.6147e+00
   OBJEC(   5) : Disatisfied = 0.2254e+00
   OBJEC(   6) : Disatisfied = 0.4259e-01

** CONSTRAINT SUMMARY **

** BOX CONSTRAINTS ***

** CONVENTIONAL CONSTRAINTS **

   SOFT_INEQ( 42) : Disatisfied =  0.999e-02

** FUNCTIONAL CONSTRAINTS **

   SOFT_FINEQ( 24 314  41 395 3781004 408) : Disatisfied     = 0.325e+00

-------------------- End print_statemo --------------------
2> list print_objectives
------------------- Begin print_objectives -------------------
```

```
ENERGY OBJECTIVES FOR GROUND MOTION INPUTS

Record No          Input    Dissipated  Work Done By Loads
-----------------------------------------------------------

        1     0.265e+03     0.882e+02          0.590e+01
        2     0.906e+02     0.584e+01          0.447e+00
        3     0.194e+03     0.221e+02          0.151e+01
        4     0.248e+03     0.475e+02          0.321e+01
        5     0.298e+03     0.101e+03          0.593e+01
        6     0.133e+03     0.169e+02          0.328e+01

record no                 1            2            3            4

energy group 1    0.    e+00    0.    e+00    0.    e+00    0.    e+00    0.
energy group 2    0.8816e+02    0.5837e+01    0.2205e+02    0.4747e+02    0.1008
-------------------- End print_objectives --------------------
2>
2> cont 1
maxval [ hard_ineq ] =  0.000
maxval [ cost ] =  .6151 [ soft_ineq ] =  .3254

finding the descent direction

eps =  .1000

*** starting direction

maxval [ hard_ineq ] =  0.000
maxval [ cost ] =  .6151 [ soft_ineq ] =  .3254

starting LFD loop
Column xnewraw(2):
  7.31425e+2
  5.05132e+2

partial derivatives : column 1
Column xnewraw(2):
  7.36826e+2
  5.05132e+2

partial derivatives : column 2
Column xnewraw(2):
  7.31425e+2
  5.15932e+2

Matrix jacobian(99,2):
  2.133697       1.388795
  4.172840e-2    1.765627
  .4780576       1.412215e+1
 -1.071588      -2.376815
  0.000000       0.000000
```

```
   --- lines deleted ---

   0.000000       0.000000
   0.000000       0.000000

Matrix e_jacobian(3,2):
   2.133697       1.388795
   4.172840e-2    1.765627
   .4780576       1.412215e+1

Matrix qq(3,3):
   6.48142        2.54113        2.06328e+1
   2.54113        3.11918        2.49544e+1
   2.06328e+1     2.49544e+1     1.99664e+2

direction vector
Column h(2):
 -.3093631
 -1.717417

*** armijo

Column x(2):
   .6772455
   .2338578
maxval [ hard_ineq ] =  0.000
maxval [ cost ] =  .6151 [ soft_ineq ] =  .3254

starting loop to decrease steplength

k =  0.000
Column xnew(2):
   .6595176
   .1354415
maxval [ hard_ineq ] =  0.000
maxval [ cost ] =  .5813 [ soft_ineq ] =  .8458

k =  1.000
Column xnew(2):
   .6683816
   .1846496
maxval [ hard_ineq ] =  0.000
maxval [ cost ] =  .5231 [ soft_ineq ] =  .5810
*** no_interact
--------- ITERATION 2 ---------

direction finding phase:
phaseno = 2            psiplus =  .6151
eps     =  1.000     Epsscale =  5.000

active costs and constraints
Column act_ind(3):
  1
  4
```

```
  5

clipped jacobian matrix
Matrix e_jacobian(3,2):
  2.133697       1.388795
  4.172840e-2    1.766627
  .4780576       1.412215e+1

direction vector.
Column h(2):
 -.3093831
 -1.717417

armijo steplength :
Beta          =  .5000      bestk         =  1.000

scaled design vector  raw design vector
X(1 ) =  .6684          X_raw(1 ) =  7.219e+2
X(2 ) =  .1848          X_raw(2 ) =  3.988e+2
--------simulation output-------
number of simulations = 117
number of time steps = 118917
number of stiffness reformulations = 62013
maximum energy error ratio =  1.052e-5
--------------------------------


Interrupt...
3> date
Date: 07/03/85  Time: 08:20:22
3> sprint ~no ~all ~files ~active ~concise
3> eprint ~files
3> list print_statemo
------------------- Begin print_statemo --------------------

** DESIGN OBJECTIVES **

   OBJEC(   1) : Disatisfied = 0.5231e+00
   OBJEC(   2) : Disatisfied = 0.2366e-01
   OBJEC(   4) : Disatisfied = 0.2530e+00
   OBJEC(   5) : Disatisfied = 0.7646e-01
   OBJEC(   6) : Disatisfied = 0.3176e+00

** CONSTRAINT SUMMARY **

** BOX CONSTRAINTS ***

** CONVENTIONAL CONSTRAINTS **

   SOFT_INEQ( 41) : Disatisfied =  0.581e+00
   SOFT_INEQ( 42) : Disatisfied =  0.585e+00
   SOFT_INEQ( 43) : Disatisfied =  0.151e+00
   SOFT_INEQ( 44) : Disatisfied =  0.109e+00
```

```
** FUNCTIONAL CONSTRAINTS **

   SOFT_FINEQ( 13 194 502 633 9811004 971) : Disatisfied     = 0.332e+00
   SOFT_FINEQ( 14  89 521 61310031025 258) : Disatisfied     = 0.265e+00
   SOFT_FINEQ( 15 192 717 633 9811004 970) : Disatisfied     = 0.335e+00
   SOFT_FINEQ( 16 172 523 61310031024 257) : Disatisfied     = 0.220e+00
   SOFT_FINEQ( 20 172 522 613 9811004 257) : Disatisfied     = 0.233e+00
   SOFT_FINEQ( 23 167 520 55110031064 261) : Disatisfied     = 0.571e-01
   SOFT_FINEQ( 24  92 524 612 9801005 256) : Disatisfied     = 0.437e+00

-------------------- End print_statemo --------------------
3> list print_objectives
------------------- Begin print_objectives -------------------

ENERGY OBJECTIVES FOR GROUND MOTION INPUTS


Record No          Input     Dissipated  Work Done By Loads
-----------------------------------------------------------


        1      0.197e+03      0.325e+02          0.747e+01
        2      0.185e+03      0.430e+02          0.535e+01
        3      0.259e+03      0.602e+02          0.482e+01
        4      0.512e+03      0.223e+03          0.721e+01
        5      0.309e+03      0.117e+03          0.850e+01
        6      0.148e+03      0.220e+02          0.537e+01

record no                  1             2             3             4

energy group 1     0.     e+00     0.     e+00     0.     e+00     0.7879e+01
energy group 2     0.3254e+02     0.4295e+02     0.6021e+02     0.2153e+03
-------------------- End print_objectives --------------------
3>
3> ## ... store results into a memfile ...
3>
3> saveall
Writing over existing file "xfile"
Output is in file "xfile".
Storing into memprob ...
CRUNCH
3> quit
```

APPENDIX 4 - ARMA SIMULATIONS

Introduction

The main body of this report has focussed on the development of a methodology for customizing a seismic design process to the overall level and variation of peak structural response quantities caused by a family of ground motion record inputs. The results indicate that when the statistical distribution of peak response quantities is characterized by large variations, mean extreme frame response values may need to be significantly enhanced in order to achieve a desirable level of reliability. Thus, the reliable reproduction of the mean extreme frame response levels and their variations is essential to the effective implementation of the proposed design method.

The family of ground motion records used in this investigation consisted of three pairs of components recorded at the same site during three separate seismic events. This small number of ground motions was assumed to be sufficient for demonstrating the design method. However, in other instances a sufficient number of ground motion records may not always be available, especially when high accuracy reliability estimates are required. A possible solution to this difficulty is to use data recorded from previous seismic events to construct an auto regressive moving average (ARMA) stochastic model. ARMA models have not yet been used in a design study of the type proposed here. Nonetheless, they are attractive because they are characterized by a small number of parameters, lend themselves to digital simulation in the time domain and can be easily adapted to include changes in frequency contents of correlated random processes that characterize the ground motion. While the coefficients of the ARMA model can be set to account for the filtering of ground motion due to transmission path and local site condition effects, the variance

envelopes of the model can account for the overall intensity and energy distribution of ground motion with time. Hence, as a complete unit, the ARMA formulation has a rational basis for the modeling of ground motion with considerable flexibility.

This Appendix reports on a preliminary investigation which was carried out to establish the potential of using ARMA ground motions in a design method of this type. The next section explains how ARMA models can be used to generate a family of artificial earthquake ground motions. An ensemble of 6 ground motions is produced. This family of ground motions is then used as input for simulations of the initial and final designs. Principal results of the frame simulations and comparisons of the frame response statistics with those caused by the recorded[1] family of ground motions are given in the final section of the appendix.

Simulation of the Earthquake Acceleration Records.

An ARMA(2,1) model was adopted for this study. For a stationary correlated process the ground acceleration at time t is denoted by a_t, and is defined by the second order autoregressive - first order moving average difference equation:

$$a_t - \varphi_1 a_{[t-1]} - \varphi_2 a_{[t-2]} = e_t - \vartheta_1 e_{[t-1]} \qquad (1)$$

in which e_t is independently and identically distributed white noise. The parameters φ_1 and φ_2 are known as the autoregressive parameters, and ϑ_1 is called the moving average parameter. Although it is conceivable that each of these parameters could be varied continuously as a function of time, simplicity is usually preferred; previous studies have assumed that the parameters remain

[1] A nomenclature convenience is now introduced. The family of artificial ground motions is referred to as the ARMA set and the ensemble of scaled ground motions discussed in Section 4.2.3 is called the *recorded* set.

constant for the entire duration of the ground motion, or at most, take different constant values over short intervals of time (see refs[A1],[A2] and [A3]). The second assumption was used in this study. Filter parameters for the ARMA model were taken from two five second segments covering the the 5-15 second interval of the S90W Component of the 1940 Imperial Valley earthquake[A2]. They are summarized in Table [A1].

Time interval	φ_1	φ_2	ϑ_1
5 - 10 sec	1.35	-0.54	0.01
10 - 15 sec	1.43	-0.58	0.06

Table [A1]: ARMA Ground Motion Parameters

In the same report, Chang et al.[A2] showed that for the ARMA(2,1) model the ratio of the standard deviation of the filtered output process σ_a, to the standard deviation of the input process σ_e, is given by the expression:

$$\left[\frac{\sigma_a}{\sigma_e}\right] = \left[\frac{1-\varphi_2}{1+\varphi_2}\ \frac{1+\vartheta_1^2}{\left[1-\varphi_2\right]^2-\varphi_1^2}\right]^{\frac{1}{2}} \qquad (2)$$

Thus, for a stationary white noise input, the limiting standard deviation of the filtered output is 2.468 and 2.891 times the unit input standard deviation for the 0-5 and 5-10 second intervals of the ARMA ground motions.

The non-stationary characteristics of ground motion are modeled by adding a time-dependent variance envelope in the model. This can be achieved by either multiplying the filtered noise or the white noise by a non-negative time varying function. The first case is very amenable to analytical studies because the instantaneous amplitude of the of the final time-dependent output is simply the amplitude of the filtered output multiplied by the time-dependent function. Nau et al.[A3] report, however, that the latter arrangement is more plausible physically because it allows the transient response of the filter to be

reflected in the output. Consequently, a time-dependent envelope, f(t), of the form:

$$f(t) = C_0 \alpha \left[\frac{t}{\tau} \right]^3 e^{\left\{ -C_1 \left[\frac{t}{\tau} \right] \right\}} \tag{3}$$

where $C_0 = \left\{ \frac{8e^3}{3\sqrt{3}} \right\}$

$C_1 = 2\sqrt{3}$

t = *time (seconds)*

α = *max amplitude of f(t)*

τ = *duration of shaking*

assumed by Cakmak et al.[A1] was introduced immediately after the generation of the white noise. Cakmak et al.[A1] also derived empirical relations for the parameters in this model as a function of earthquake magnitude and epicentral distance. Parameter values for a typical shape of the time dependent function were obtained by substituting an epicentral distance of 32 km and an earthquake magnitude of 7.3 into their expressions. Values of 73.1cm (28.77 in) and 5.00 (seconds) were obtained for α and τ, respectively. In addition, a minimum threshold multiplier of 4cm (1.57 in) was placed in the time-dependent function. The combined function is plotted in Figure [A4.1].

Figures [A4.2] and [A4.3] graph the "Spectral Velocity vs Period" and "Husid Ratio vs Time" for the ARMA generated family of severe ground motions. The statistics of these records is summarized in Table[A2]. First, it is noted that the variation in Husid Ratio for the ARMA generated family is much more regular than for the *recorded* set of ground motions(see Figure[4.6b]). This suggests that the time-dependent intensity of ground motion for the *recorded* set is more irregular than for the ARMA set. Additionally, the c.o.v. of the peak ground acceleration equals 0.212. This compares to coefficients of variation

Record No	Peak ground acc'n (g)	Arias Intensity (in / sec)	Spectral Intensity (in / sec)
1	0.493g	104.77	124.90
2	0.798g	126.76	128.37
3	0.543g	123.32	111.48
4	0.549g	100.53	102.87
5	0.577g	120.83	94.78
6	0.453g	87.03	84.95
mean	0.568g	112.17	107.89
std	0.120g	17.62	16.99
c.o.v.	0.212	0.157	0.157

Table [A2]: Statistics of Severe Ground Motion Records

obtained in Section 4.2.3 for the moderate and severe scaled ground motions of 0.494 and 0.122, respectively. The ARMA model peak ground acceleration c.o.v. seems reasonable, and is in fact, close to the variation in peak ground accelerations obtained by Nau et al.[A3]. The most important feature to note from Table [A2] is that the c.o.v. for the Arias intensity is smaller than for the peak ground accelerations. Since each ground motion record has the same duration, this observation implies that the α_{rms} is a more reliable statistic than peak ground acceleration, as noted in [3]. A family of moderate ground motions was obtained by simply multiplying the intensity of each severe ground motion by 0.264. This gave an average peak ground acceleration of 0.15g in the family[2] of moderate ground motions.

Simulation Results

Table[A3] summarizes the design objective dissatisfactions for both the initial and final designs. By comparing the values in this table to those presented in Table[6.4] one can see that the frame performances for each of the ground motion inputs is about the same.

[2] Strictly speaking, each level of earthquake loading should also have its own set of parameter settings. This technicality was overlooked in this study.

OBJECTIVE	DISSATISFACTION	
	Initial Design	Final Design
OBJEC(1)	0.7185	0.4568
OBJEC(2)	0.0698	0.0851
OBJEC(3)	0.0000	0.0000
OBJEC(4)	0.6863	0.1946
OBJEC(5)	0.1625	0.0543
OBJEC(6)	0.0000	0.1724

Table [A3]: Design Objective Dissatisfactions

It is now recalled that the frame response variation for the gravity loads only limit state is assumed to equal zero. Hence, the statistics of frame response for the gravity loads alone limit state are not discussed here. Summaries of the floor acceleration and story drift frame dissatisfactions occurring for the moderate lateral loads limit state are shown in Tables [A4] and [A5]. Whereas the mean story drift and floor acceleration frame response quantities of the ARMA generated frame responses are a only little less than for the recorded set (see Tables[6.12] and [6.13]), the average coefficients of variation for the same response quantities are barely more than half of those obtained with the *recorded set*. Similarly, the ARMA and recorded ground motion sets produced almost identical mean peak column and girder bending moments, but the coefficients of variation for the ARMA generated responses were less than one half of those obtained with the *recorded* family of scaled ground motions. It is concluded that the variation in these peak frame response quantities is related to the variation in peak ground accelerations.

Tables[A6] and [A7] summarize terms from the energy balance equation for the initial and final designs, respectively, and Figure [A4.4] the corresponding time history responses for the final design only. By comparing Figures [A4.4a-d] and [6.21a-d], and the corresponding values in Tables[A7] and [6.16], it is evident that the final statistics of mean hysteretic energy dissipation are similar

Constraint No	Initial Design				Final Design			
	MFR	STD	HFR	LFR	MFR	STD	HFR	LFR
SOFT_FINEQ(19)	.1817	.0391	.2146	.2318	.2383	.0411	.2729	.2910
SOFT_FINEQ(20)	.2442	.0537	.2894	.3130	.3513	.0571	.3993	.4244
SOFT_FINEQ(21)	.1646	.0359	.1949	.2107	.2546	.0403	.2885	.3063
c.o.v.	GDO = 0.54 BDO = 0.96 range = [0.26 - 0.27] average = 0.226				GDO = 0.54 BDO = 0.96 range = [0.27 - 0.28] average = 0.277			

Table [A4] : Statistics of Peak Story Drifts

Constraint No	Initial Design				Final Design			
	MFR	STD	HFR	LFR	MFR	STD	HFR	LFR
SOFT_FINEQ(22)	89.4	21.4	107.3	116.7	96.2	15.5	109.3	116.1
SOFT_FINEQ(23)	154.5	36.2	184.9	200.8	156.8	27.2	179.6	191.6
SOFT_FINEQ(24)	200.0	44.9	237.1	256.5	213.8	34.6	242.9	258.1
c.o.v.	GDO = 270 BDO = 540 range = [0.23 - 0.27] average = 0.253				GDO = 270 BDO = 540 range = [0.25 - 0.28] average = 0.256			

Table [A5] : Statistics of Peak Absolute Floor Acceleration

for both sets of ground motion inputs. For example, the initial design has mean and standard deviation pairs for the Input energy and Hysteretic energy of [367.6,254.2] and [45.2,52.5]. The corresponding pairs in the energy balance equation for the initial design's response to the recorded set of ground motions are [232.6,79.7] and [44.8,28.3], respectively (see Table[5.15]). Similarly, the mean and standard deviation pairs of total input energy and hysteretic energy for the final design are [434.6, 259.4] and [80.8, 60.0], respectively. Table [6.16] shows the corresponding pairs ([240.5, 127.2] and [63.9, 67.2]) for the final design loaded with the family of *recorded* ground motions.

Yet, it is also clear that the point of incipient hysteretic energy dissipation and the ensuing inelastic deformations as a function of time strongly depends on the time varying intensity of ground shaking. Figure[A4.4] shows a well defined point of incipient plastic deformation followed immediately a significant

Record No	Input Energy	Hysteretic Energy	Work Done By Loads	Damped Energy
1	0.535e+03	0.147e+03	-0.106e+02	0.377e+03
2	0.716e+03	0.371e+02	0.186e+02	0.363e+03
3	0.142e+03	0.288e+02	0.461e+01	0.117e+03
4	0.216e+02	0.132e+02	0.406e+01	0.124e+02
5	0.423e+03	0.451e+02	0.343e+01	0.381e+03
6	0.368e+03	0.000e+02	-0.169e+01	0.366e+03

record no	1.0	2.0	3.0	4.0	5.0	6.0
energy group 1	2.3	0.0	0.0	0.0	0.0	0.0
energy group 2	144.9	37.1	28.8	13.2	45.1	0.0

Table [A6] : Energy Balance for the Initial Design

Record No	Input Energy	Hysteretic Energy	Work Done By Loads	Damped Energy
1	0.278e+03	0.924e+02	0.215e+02	0.164e+03
2	0.954e+03	0.115e+02	-0.215e+03	0.727e+03
3	0.268e+03	0.104e+03	0.505e+01	0.169e+03
4	0.394e+03	0.163e+02	0.492e+01	0.382e+03
5	0.369e+03	0.889e+02	0.745e+01	0.287e+03
6	0.345e+03	0.172e+03	0.796e+01	0.181e+03

record no	1.0	2.0	3.0	4.0	5.0	6.0
energy group 1	0.0	26.3	0.0	0.0	0.0	26.4
energy group 2	92.4	87.9	103.9	16.3	88.9	145.6

Table [A7] : Energy Balance for the Final Design

proportion of the total hysteretic energy dissipation. This compares to a more uniform rate of hysteretic dissipation as a function of time, with less well defined points of incipient hysteretic energy dissipation for the *recorded* set of ground motions. Tables [A6] and [A7] indicate that both designs dissipate a small quantity of energy at the column bases.

The above mentioned statistics indicate that the average total frame dissipated energy increases from 45.2 $kip-in$ to 80.8 $kip-in$, and that the ratio "total frame dissipated energy" divided by "total input energy" increases from 12.3% to 18% as the design is modified from its initial to final states. A less significant increase in the standard deviation of the dissipated energy also

occurs during the design iterates. Consequently, the coefficient of variation for total frame dissipated energy decreases from 1.161 to 0.742.

Constraint No	Initial Design				Final Design			
	MFR	STD	HFR	LFR	MFR	STD	HFR	LFR
SOFT_INEQ(41)	19.26	19.31	40.94	56.96	32.06	17.29	51.48	65.82
SOFT_INEQ(42)	19.44	21.61	43.71	61.64	32.27	14.43	46.48	58.45
SOFT_INEQ(43)	2.49	2.03	4.77	6.46	15.12	8.51	24.68	31.74
SOFT_INEQ(44)	3.66	4.59	8.82	12.63	14.49	5.90	21.12	26.02
SOFT_INEQ(45)	0.00	0.00	0.00	00.00	0.00	0.00	0.00	0.00
SOFT_INEQ(46)	0.00	0.00	0.00	00.00	0.34	0.76	1.21	1.85
c.o.v.	GDO = 47.66 BDO = 83.13 range = [0.78 - 1.68] average = 1.18				GDO = 38.20 BDO = 66.62 range = [0.39 - 2.45] average = 0.93			

Table [A8] : Girder Hysteretic Energy Dissipation

The statistics of hysteretic girder energy dissipation are summarized in Table[A8]. First, it is recalled that the girders dissipate most of the frame hysteretic energy. Hence by comparing the values in this table to those in Table[5.15] and the aforementioned total frame dissipated energy statistics, one can see that the initial design dissipates approximately the same mean value of hysteretic energy for both sets of ground motions. However, the final frame dissipates more hysteretic energy with the *ARMA* set than with the ***recorded*** ground motion set. Both families of ground motion produce statistical distributions of hysteretic energy dissipation which are characterized by large coefficients of variation (0.93 and 0.98, respectively). This means that enhancement factors of about 2 are required to achieve the specified level of reliability.

The frame sway under severe quake loading is shown in Table[A9]. Even though the c.o.v. remains approximately constant, increases in both the mean frame sway and its standard deviation result when the initial design is modified to the final design. This trend in behavior is similar to that obtained with the

Constraint No	Initial Design				Final Design			
	MFR	STD	HFR	LFR	MFR	STD	HFR	LFR
SOFT_FINEQ(25)	1.962	.3377	2.246	2.394	2.782	.5452	3.241	3.481
c.o.v.	GDO = 5.04 BDO = 6.12 average = 0.172				GDO = 5.04 BDO = 6.12 average = 0.164			

Table [A9] : Statistics of Peak Frame Sway

recorded set of ground motions.

Summary

It has been shown that the ARMA model is capable of reproducing mean extreme frame response quantities for both the moderate and severe lateral loads limit states. The variation in frame responses for the moderate loads limit state, however, appears to be associated with the variation of peak ground accelerations. Behavior of the frame under severe lateral loads depends on a ground motions intensity, duration and distribution on energy content. The preliminary results of this study suggest that ARMA models can produce an equivalent variation in frame response quantities resulting from these features of ground motion. Nonetheless, our understanding of this process is inadequate. A study should be carried out to systematically investigate the sensitivity of frame response quantities to the setting of ARMA model parameters, the duration of shaking, and the overall shape and intensity of the variance envelope.

References

A1. Cakmak A.S., Sherif R.L. and Ellis G., "Modelling Earthquake Ground Motions in California using Parametric Time Series Methods," *Soil Dynamics and Earthquake Engineering*, Vol 4, No 3, 1985.

A2. Chang M.K., Kwiakowski J.W., Nau R.F., Oliver R.M. and Pister K.S. "ARMA Models for Earthquake Ground Motions," *Earthquake Engineering and Structural Dynamics*, Vol 10, pp 651-662, 1982.

A3. Nau R.F., Oliver R.M. and Pister K.S., "Simulating and analyzing artificial non-stationary earthquake ground motions." University of California, *Technical Report* ORC 80-16, Operations Research Center, Berkeley, California (1980).

A4. Poliemus N.W., Cakmak A.S., "Simulation of Earthquake Ground Motions Using Autoregressive Moving Average (ARMA) Models, *Earthquake Engineering and Structural Dynamics*, Vol 9, pp 343-354, 1981.

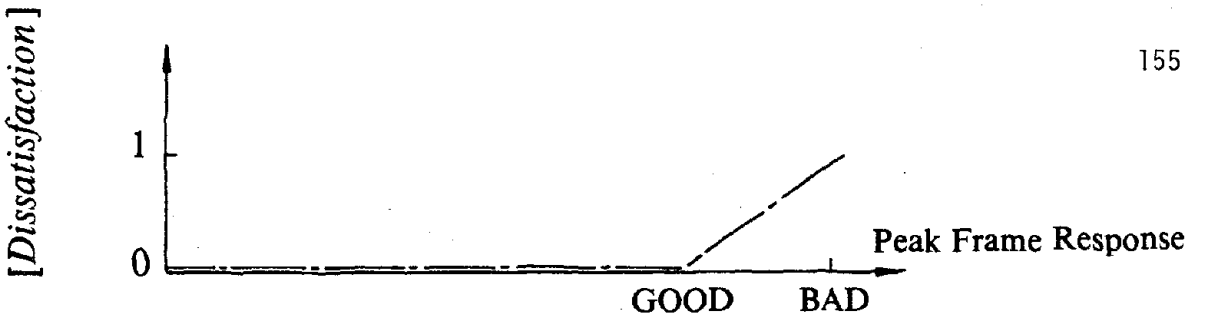

FIG 3.1 Performance Dissatisfaction vs Peak Frame Response for *Conventional Constraints.*

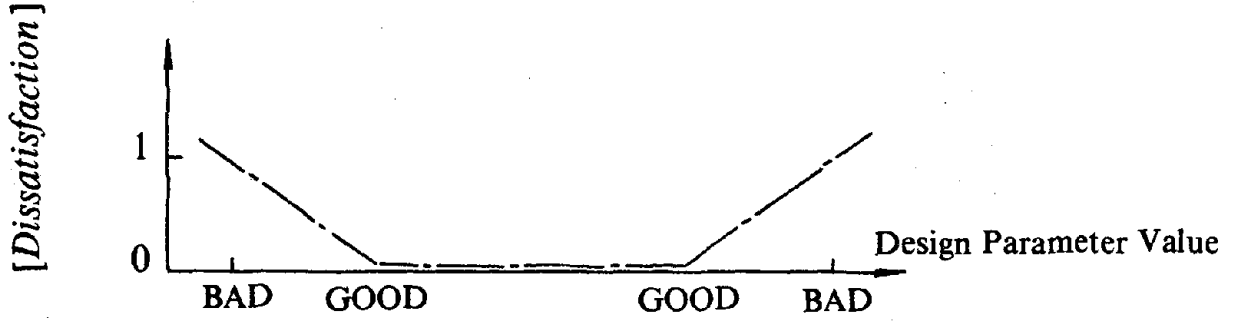

FIG 3.2 Performance Dissatisfaction vs Design Parameter Value for *Box Constraints.*

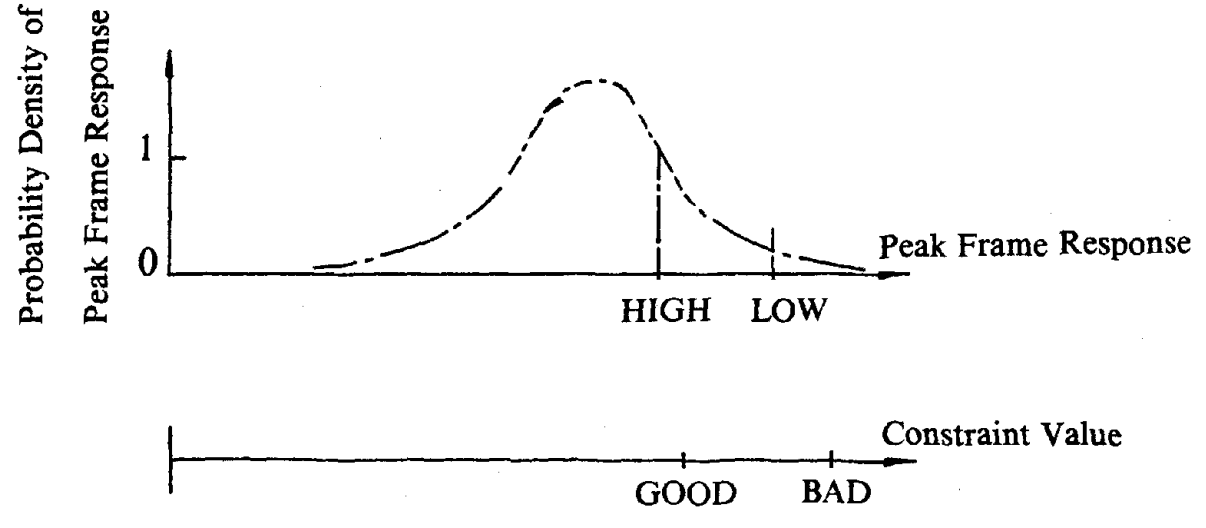

FIG 3.3 Relationship of the Distribution of Peak Frame Response Quantities to the [GOOD,BAD] Response Values.

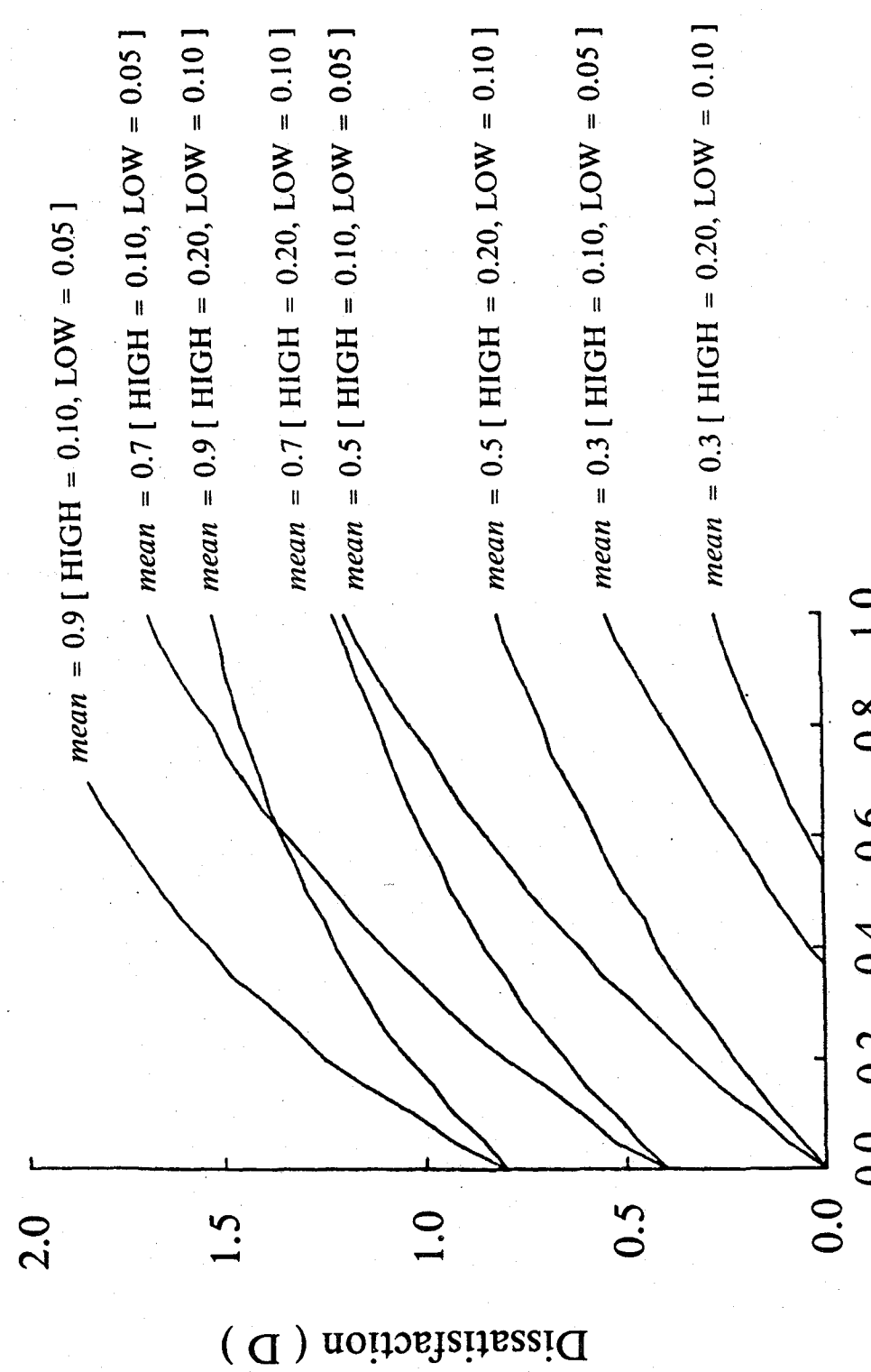

FIG 3.4 Dissatisfaction function vs c.o.v. for the Extreme Type 1 distribution and *ramp* = 0.5.

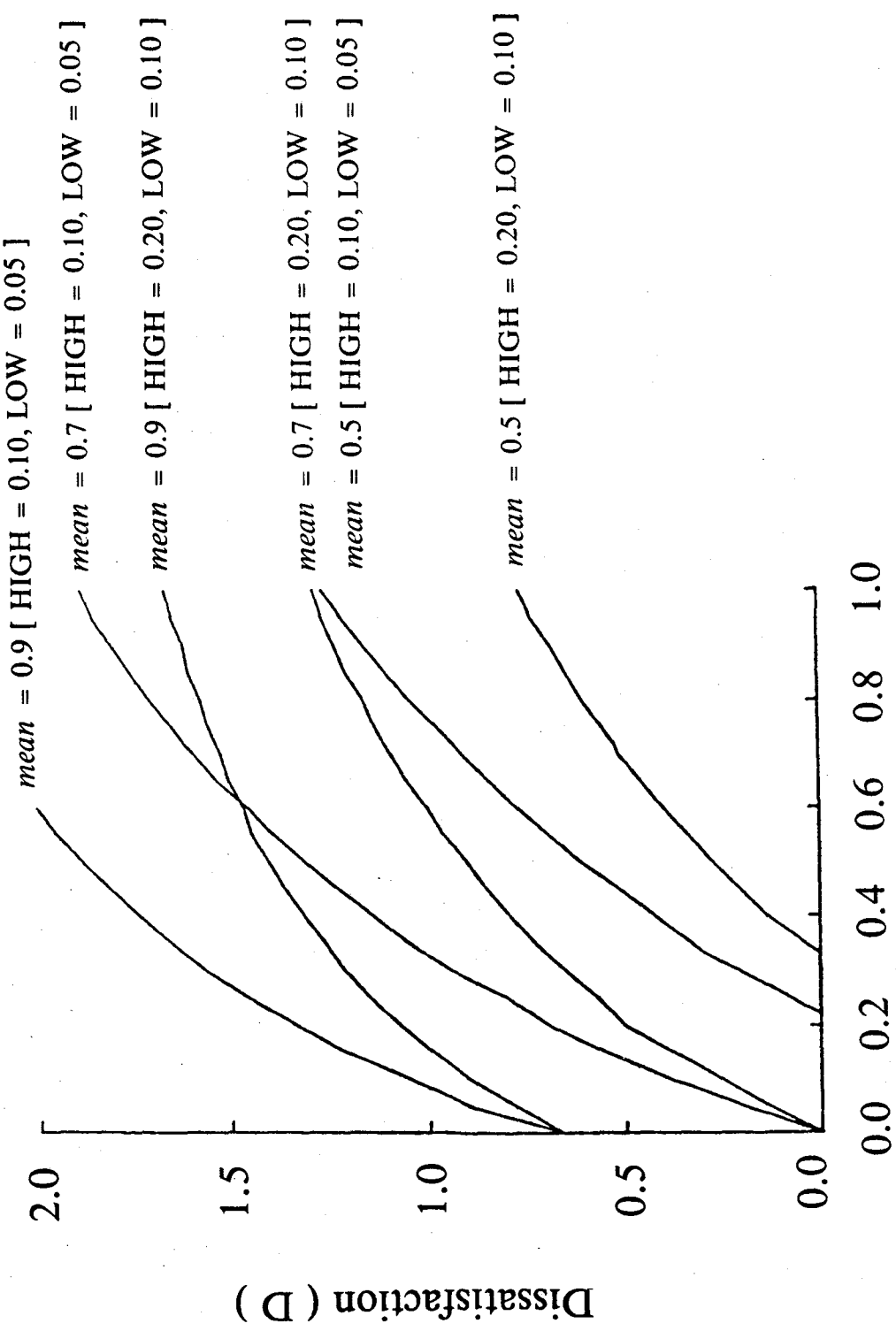

FIG 3.5 Dissatisfaction function vs c.o.v. for the Extreme Type 1 distribution and *ramp* = 0.7.

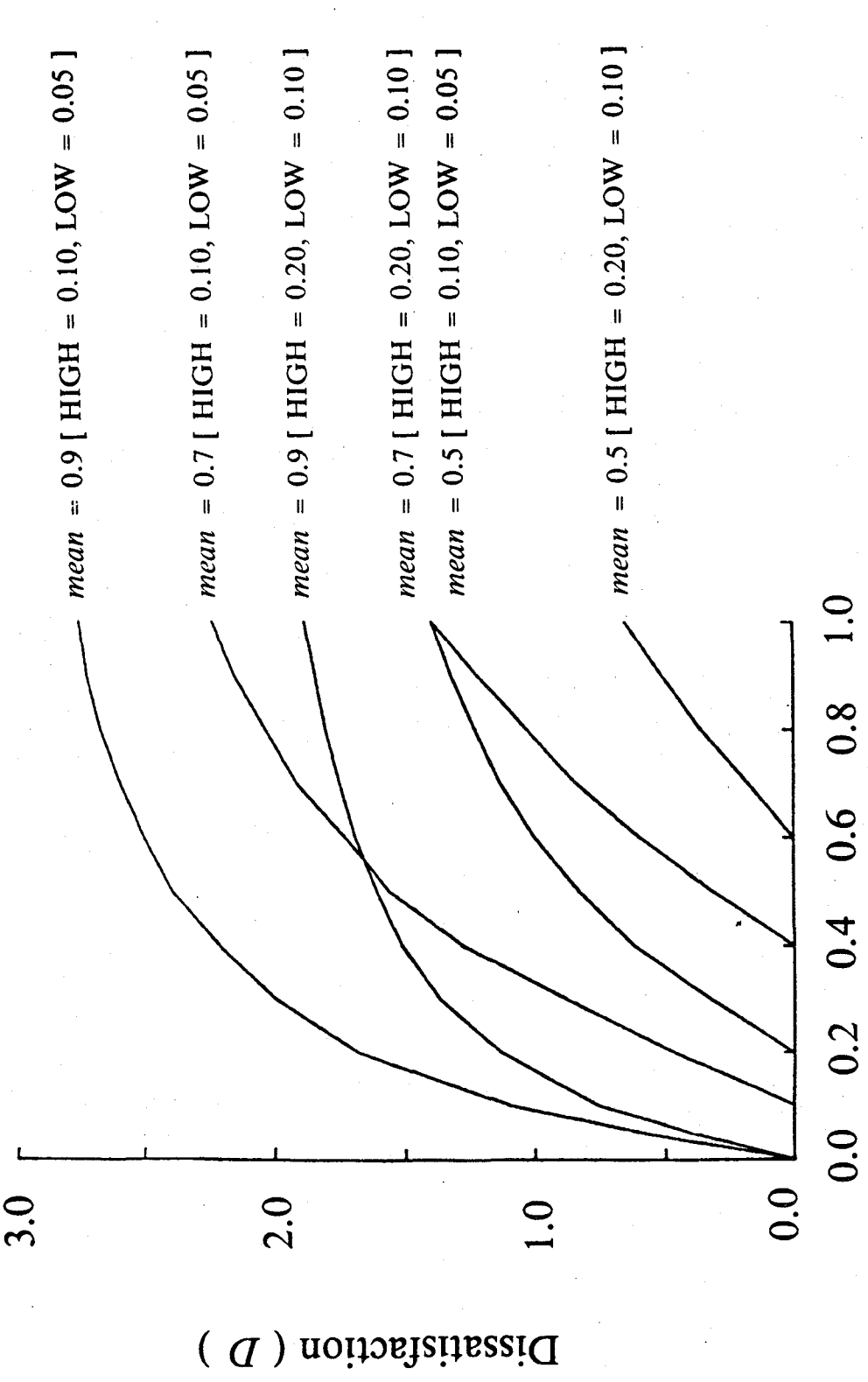

FIG 3.6 Dissatisfaction function vs c.o.v. for the Extreme Type 1 distribution and *ramp* = 0.9.

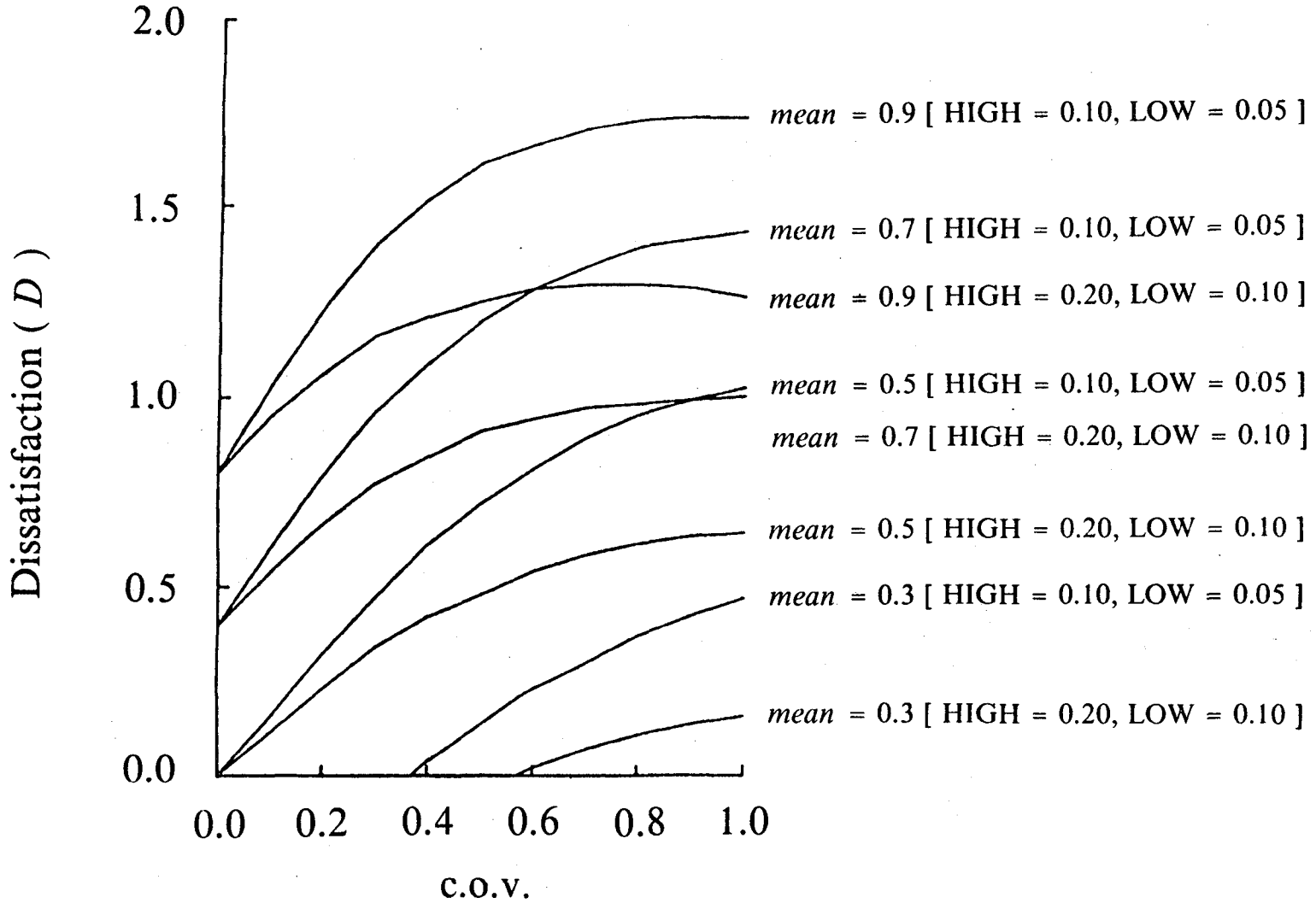

FIG 3.7 Dissatisfaction function vs c.o.v. for the Lognormal distribution and *ramp* = 0.5.

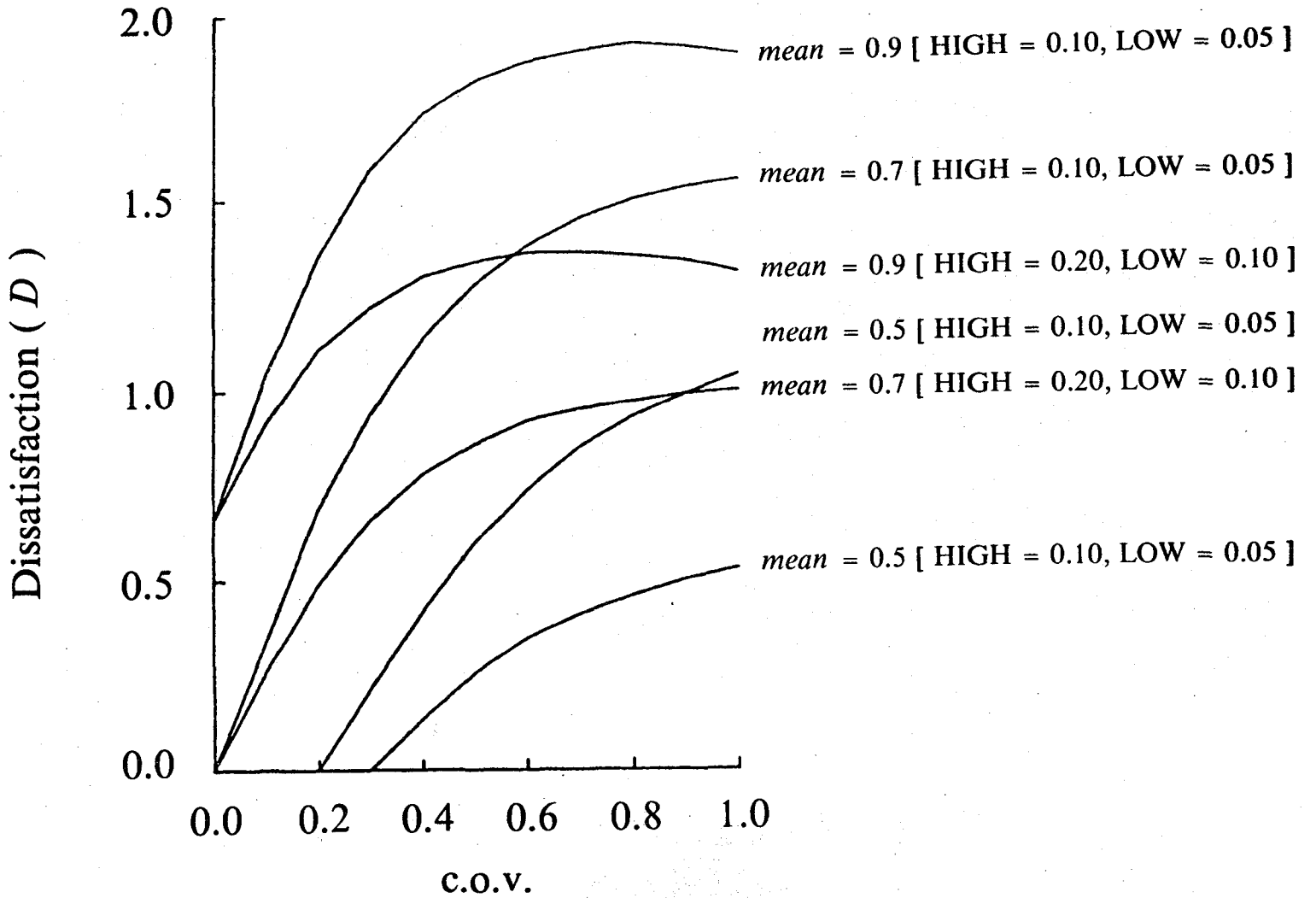

FIG 3.8 Dissatisfaction function vs c.o.v. for the Lognormal distribution and *ramp* = 0.7.

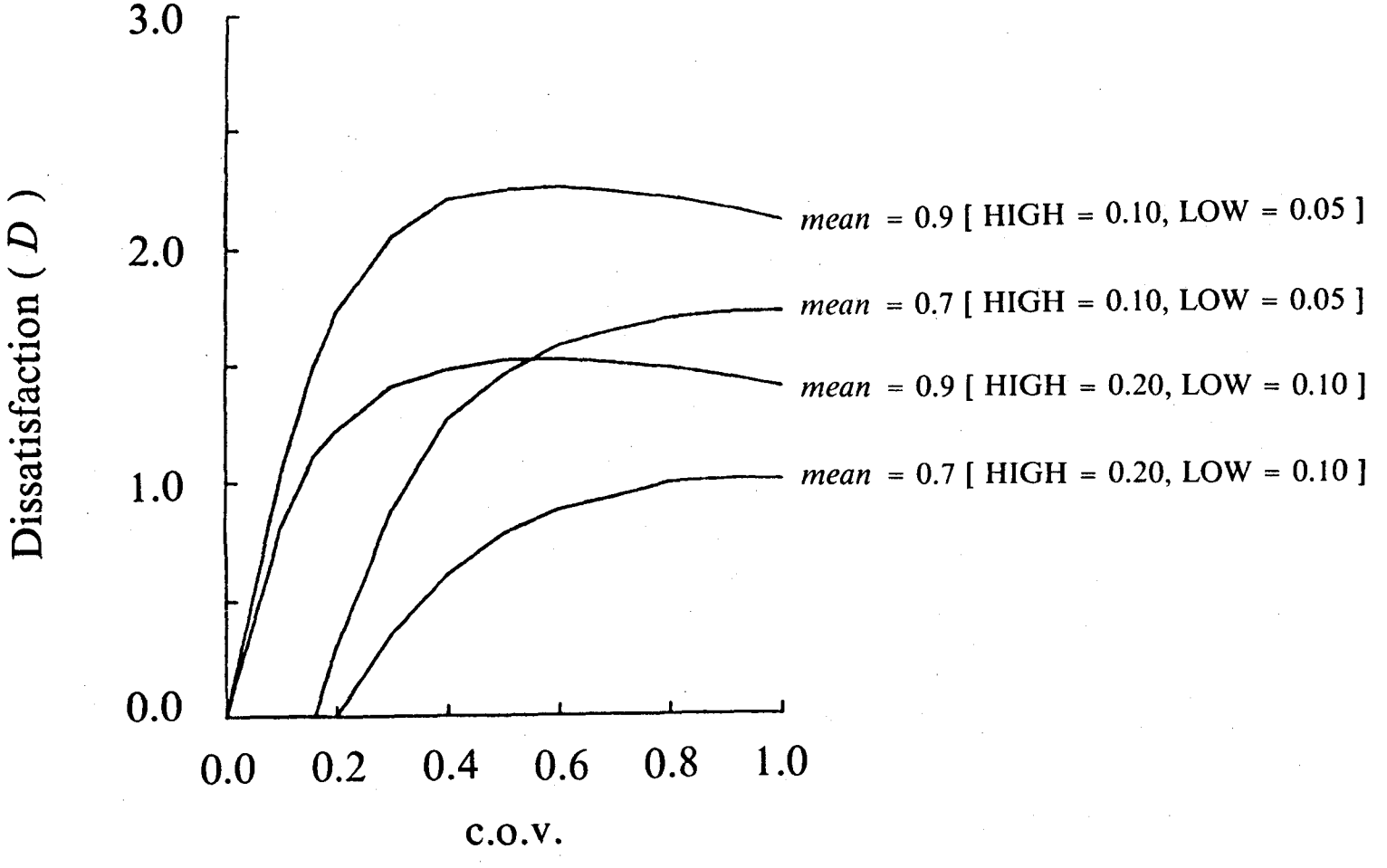

FIG 3.9 Dissatisfaction function vs c.o.v. for the Lognormal distribution and *ramp* = 0.9.

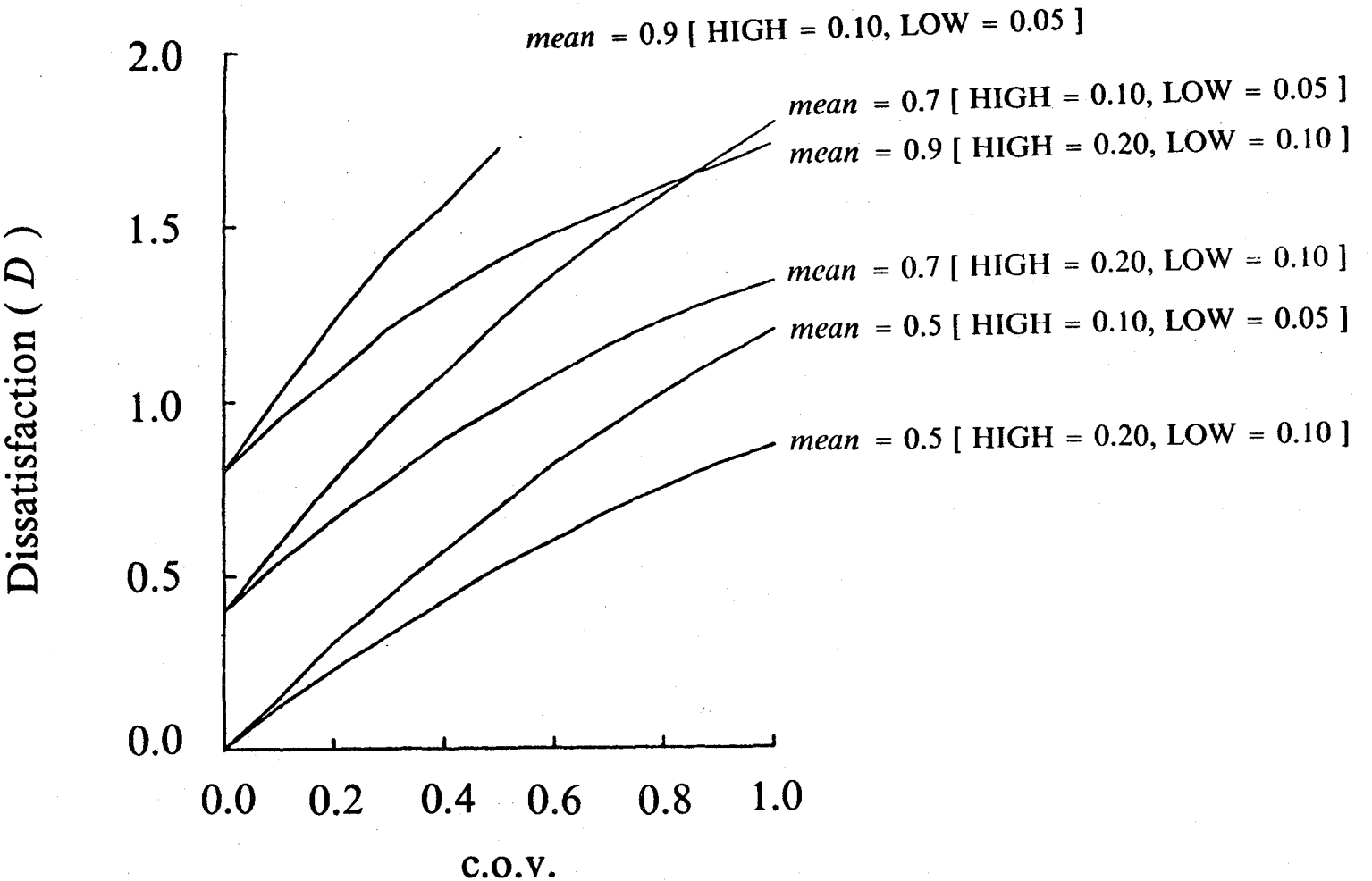

FIG 3.10 Dissatisfaction function vs c.o.v. for the Normal distribution and *ramp* = 0.5.

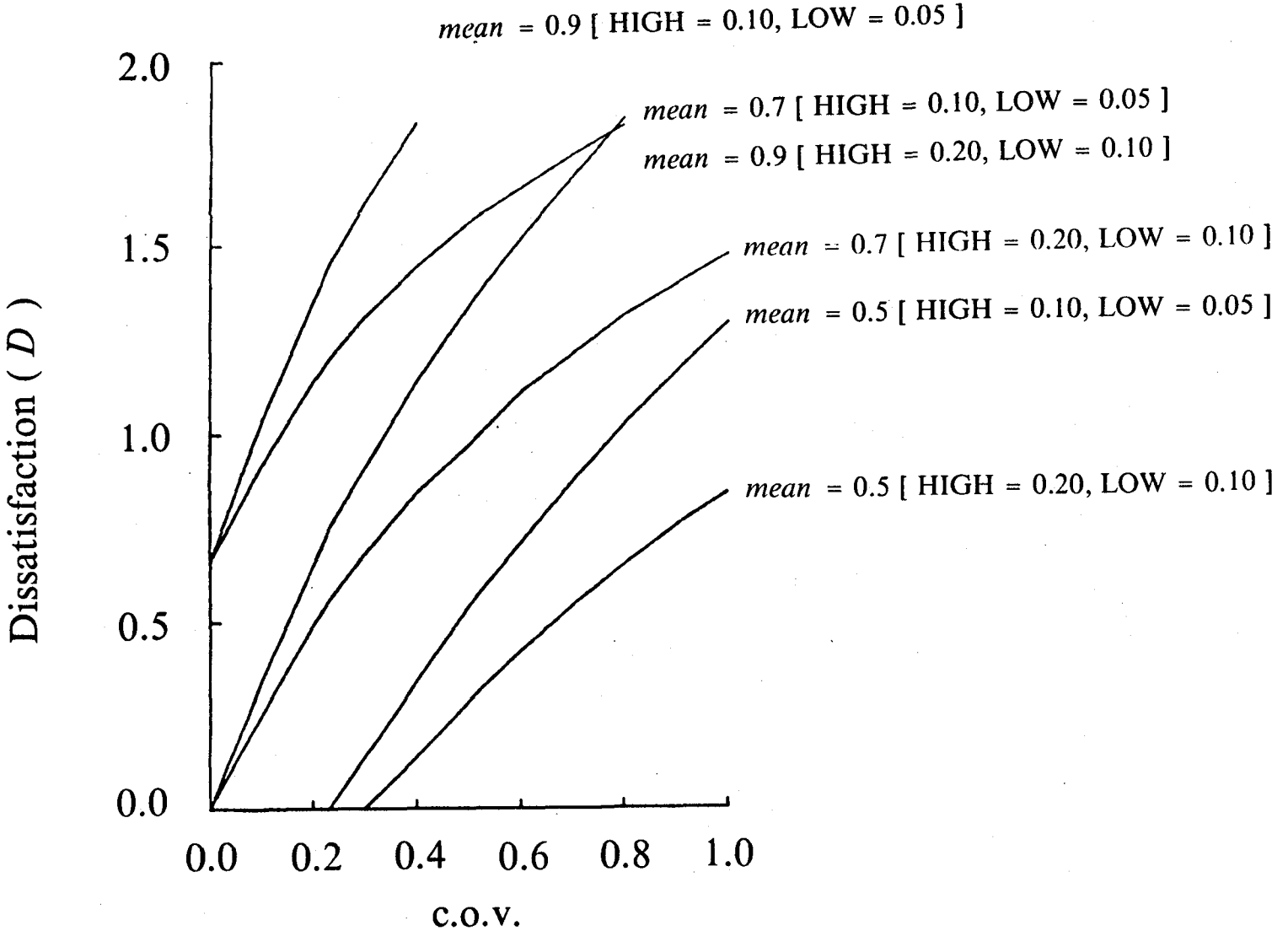

FIG 3.11 Dissatisfaction function vs c.o.v. for the Normal distribution and *ramp* = 0.7.

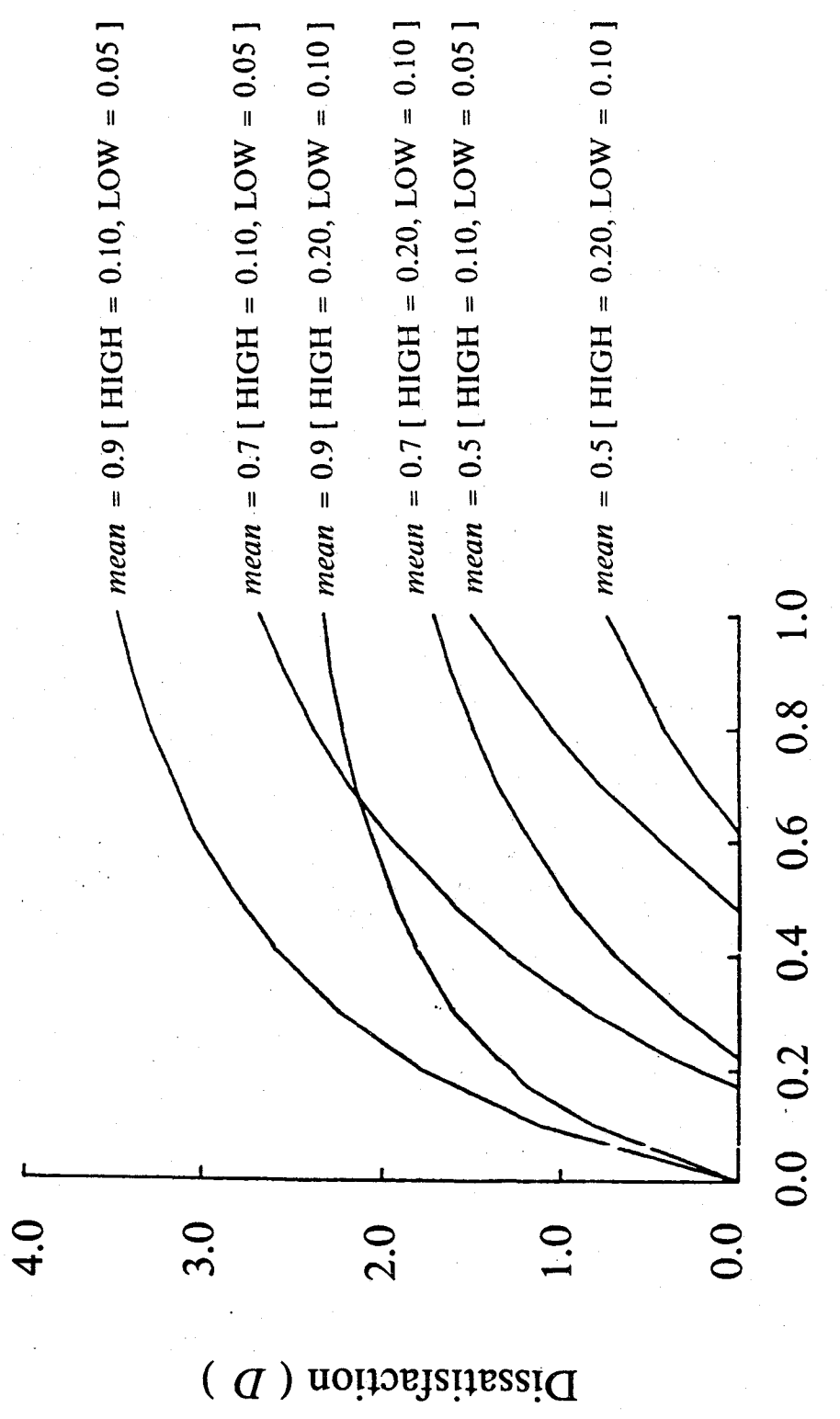

FIG 3.12 Dissatisfaction function vs c.o.v. for the Normal distribution and *ramp* = 0.9.

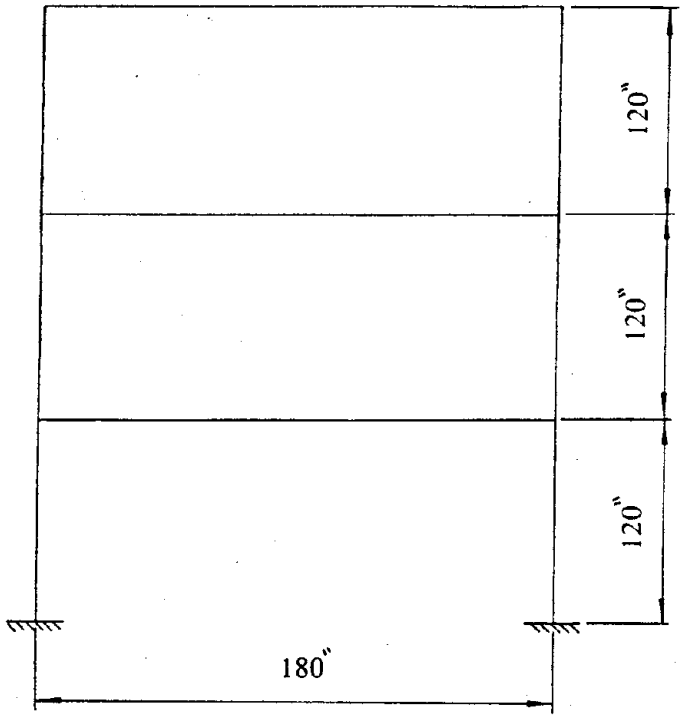

FIG 4.1 Geometry of the Example Frame.

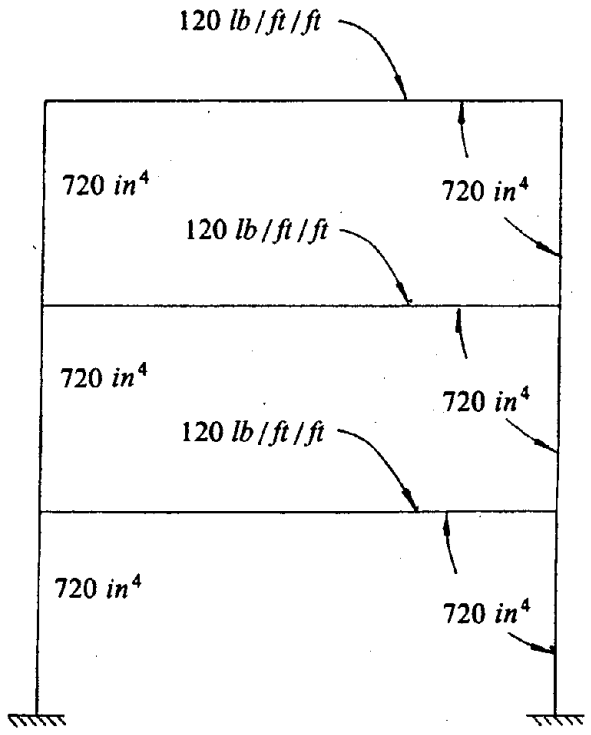

FIG 4.2 Gravity Loads and Initial Moments of Inertia.

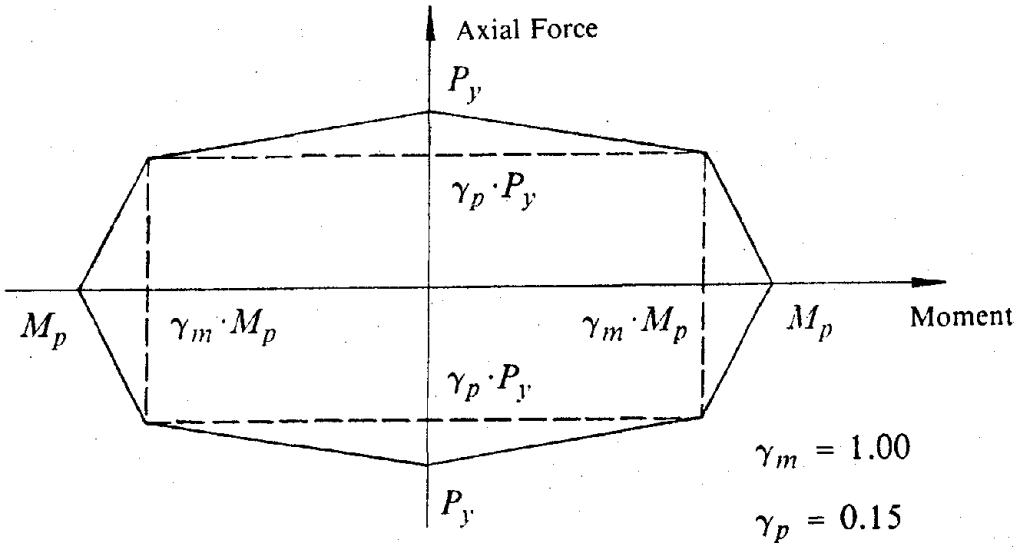

Columns

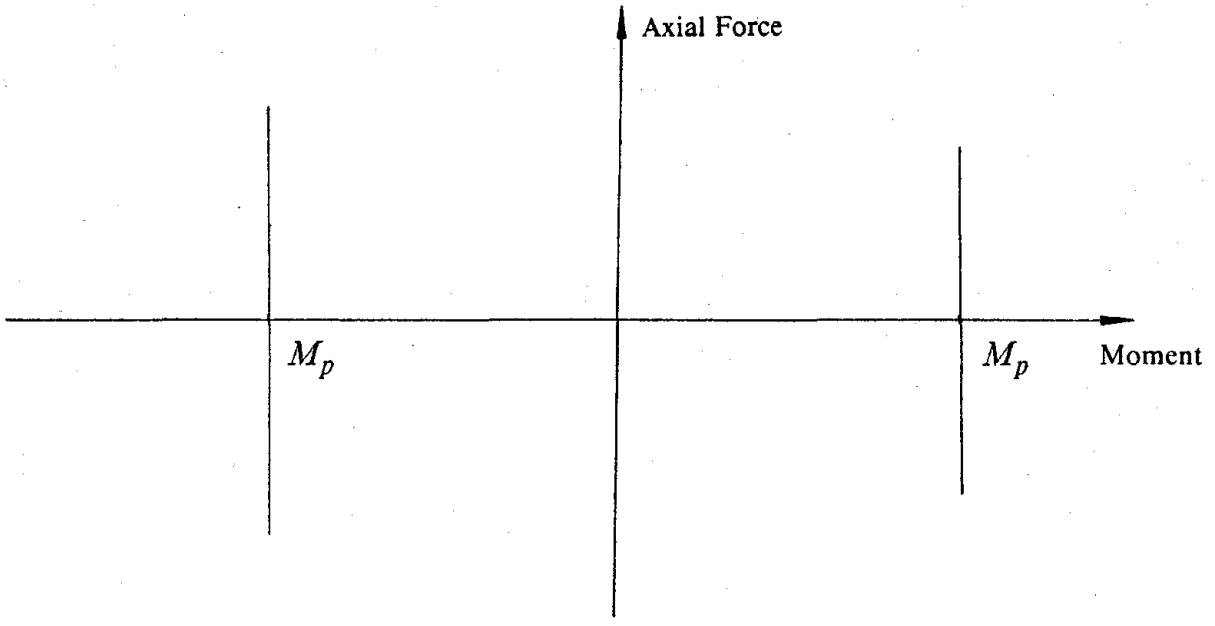

Girders

FIG 4.3 Column and Girder Yield Interaction Diagrams.

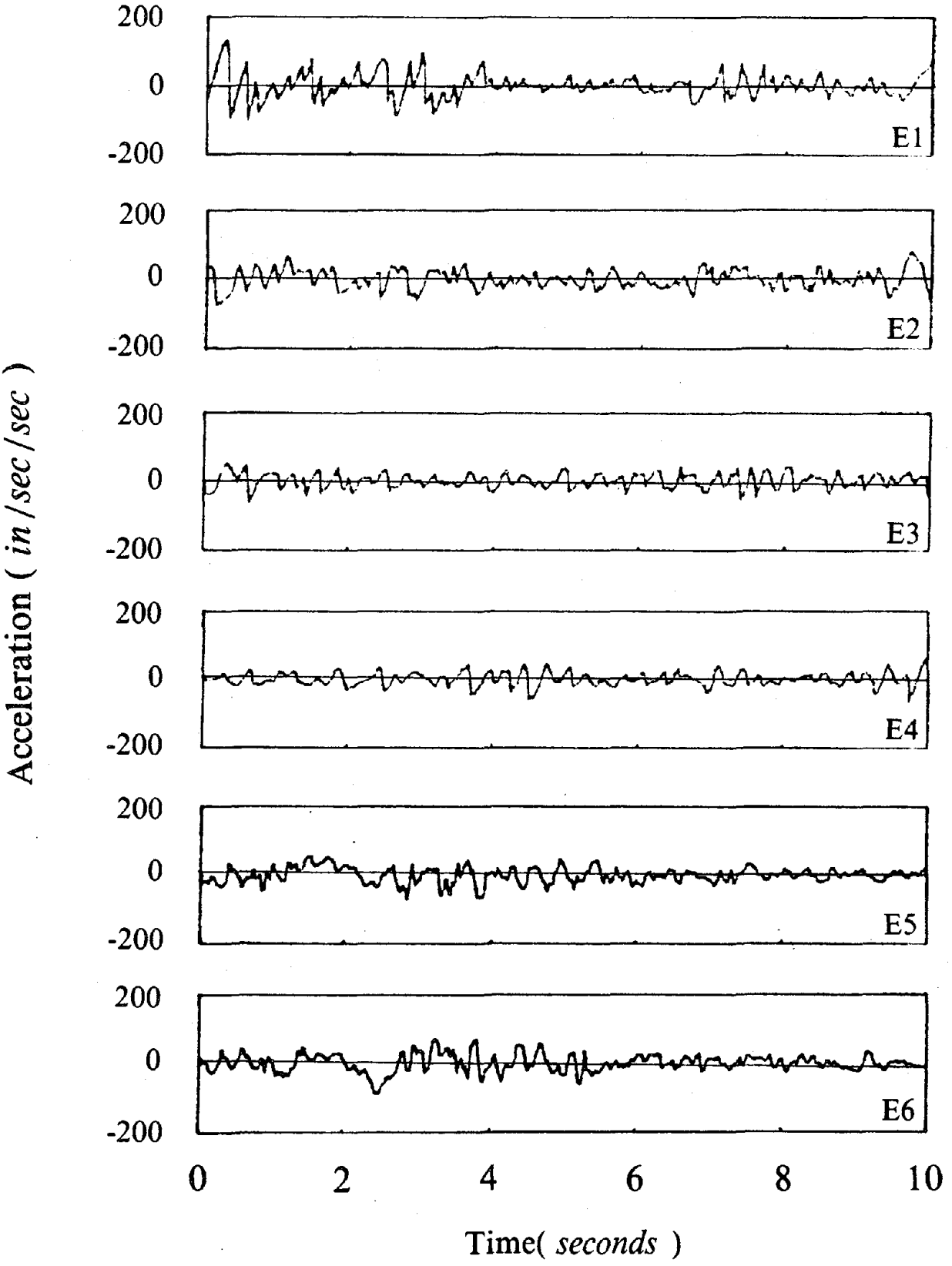

FIG 4.4 Ground Motion Records E1-E6.

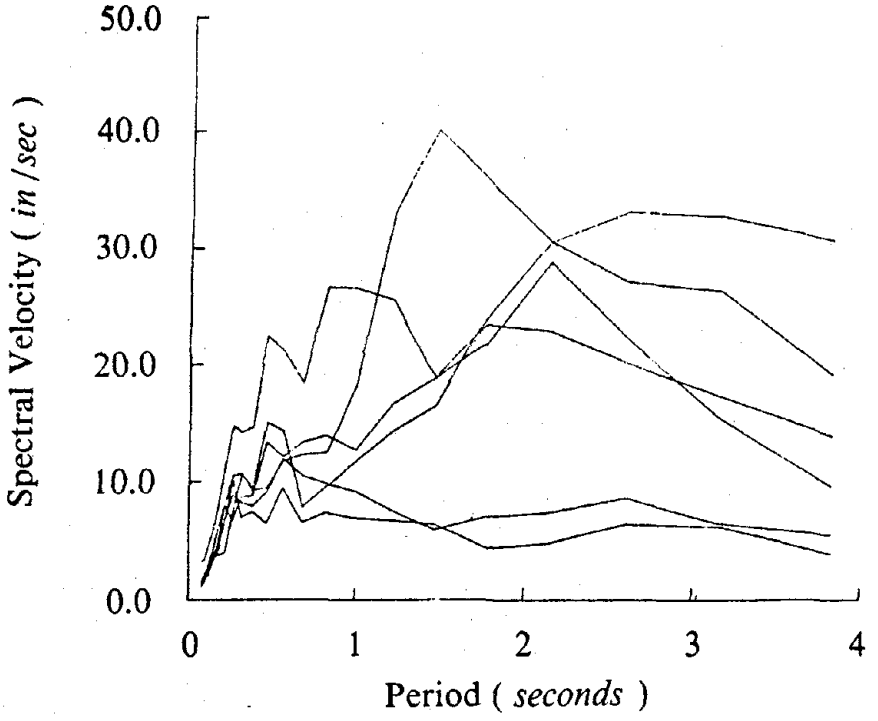

(a)

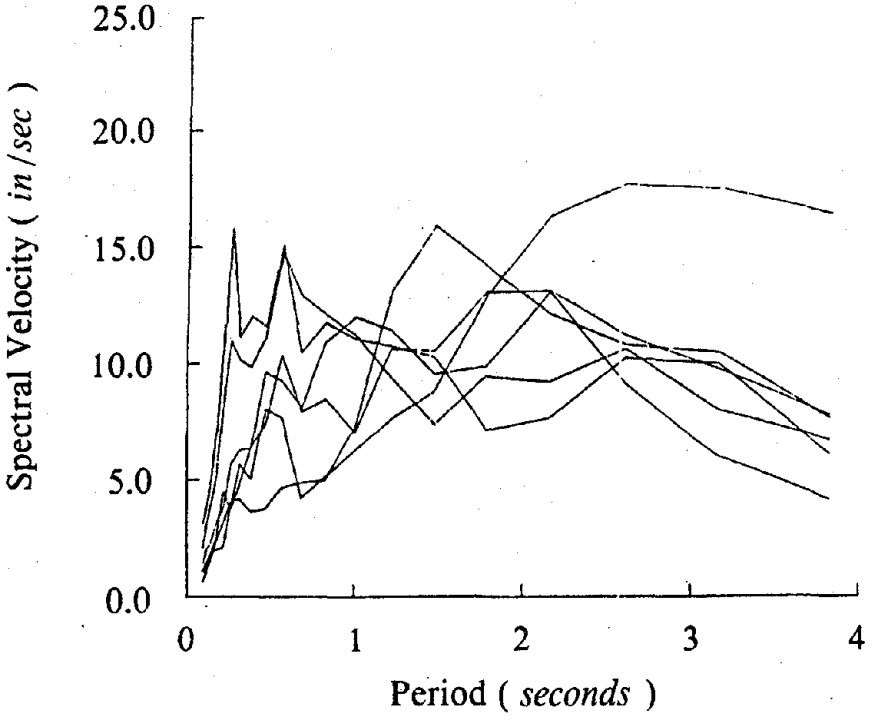

(b)

FIG 4.5 Spectral Velocity(*in /sec*) vs Period(*seconds*)
a) Before Scaling b) After Scaling.

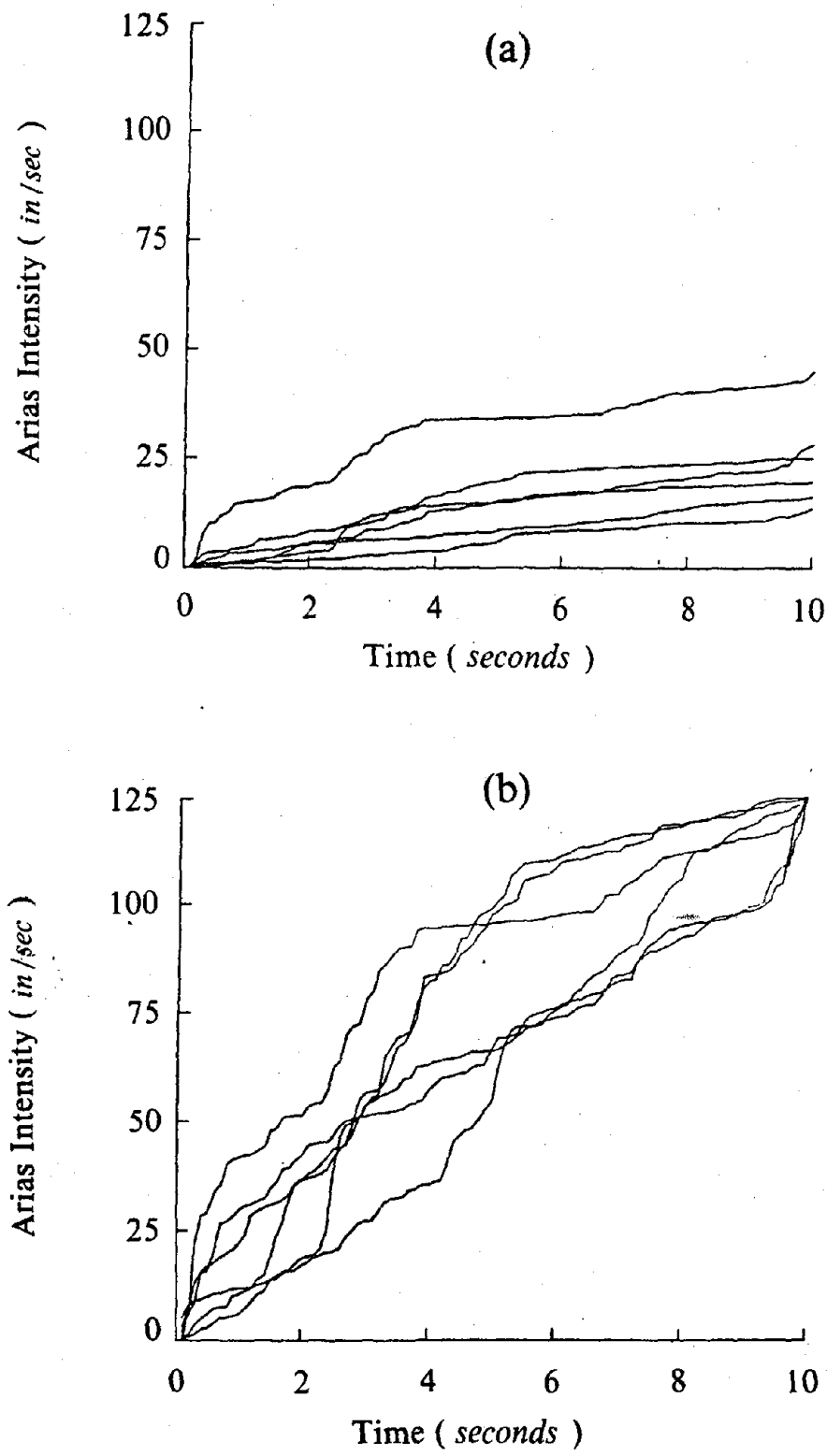

FIG 4.6 Arias Intensity(*in /sec*) vs Time(*seconds*)
a) Before Scaling b) After Scaling.

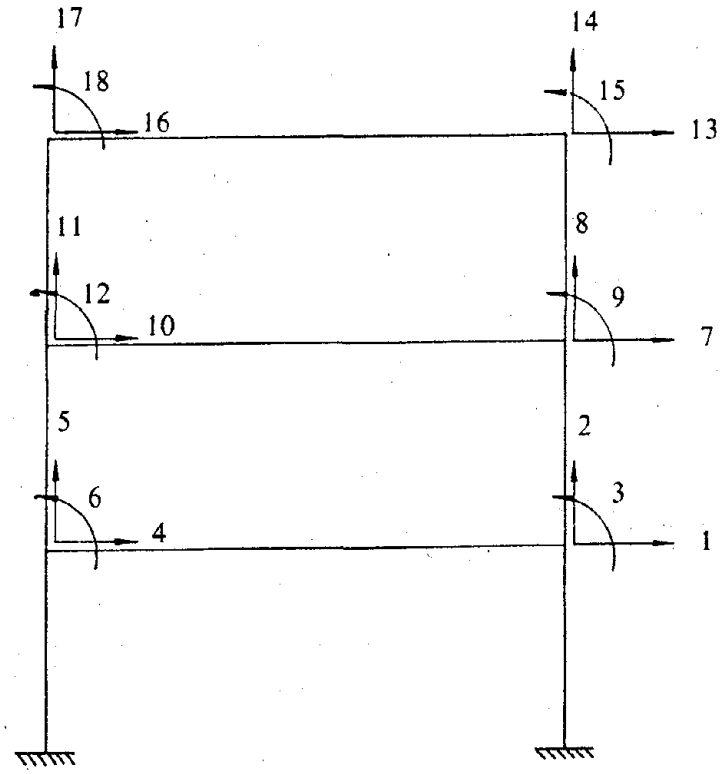

FIG 4.7 Frame d.o.f. for the Gravity Loads Alone Limit State.

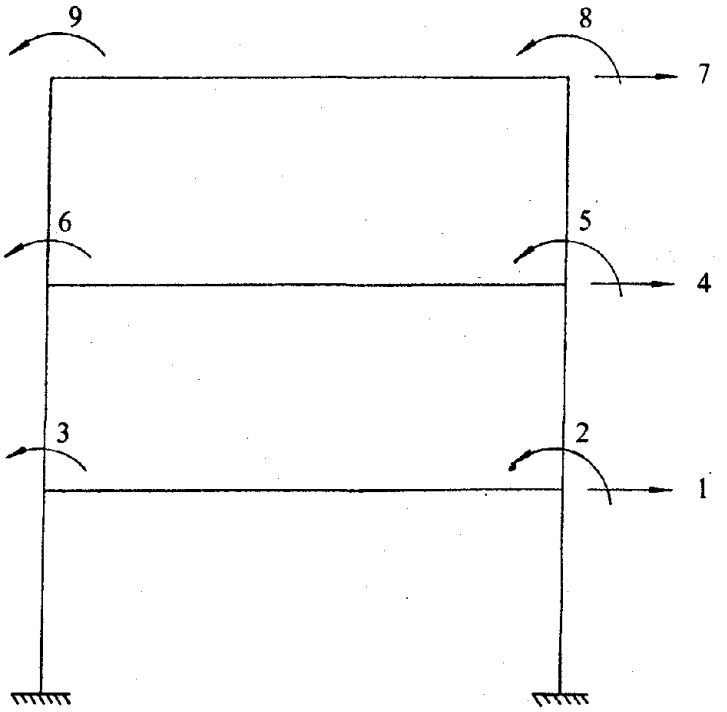

FIG 4.8 Frame d.o.f. for the Moderate and Severe Lateral Loads Limit States.

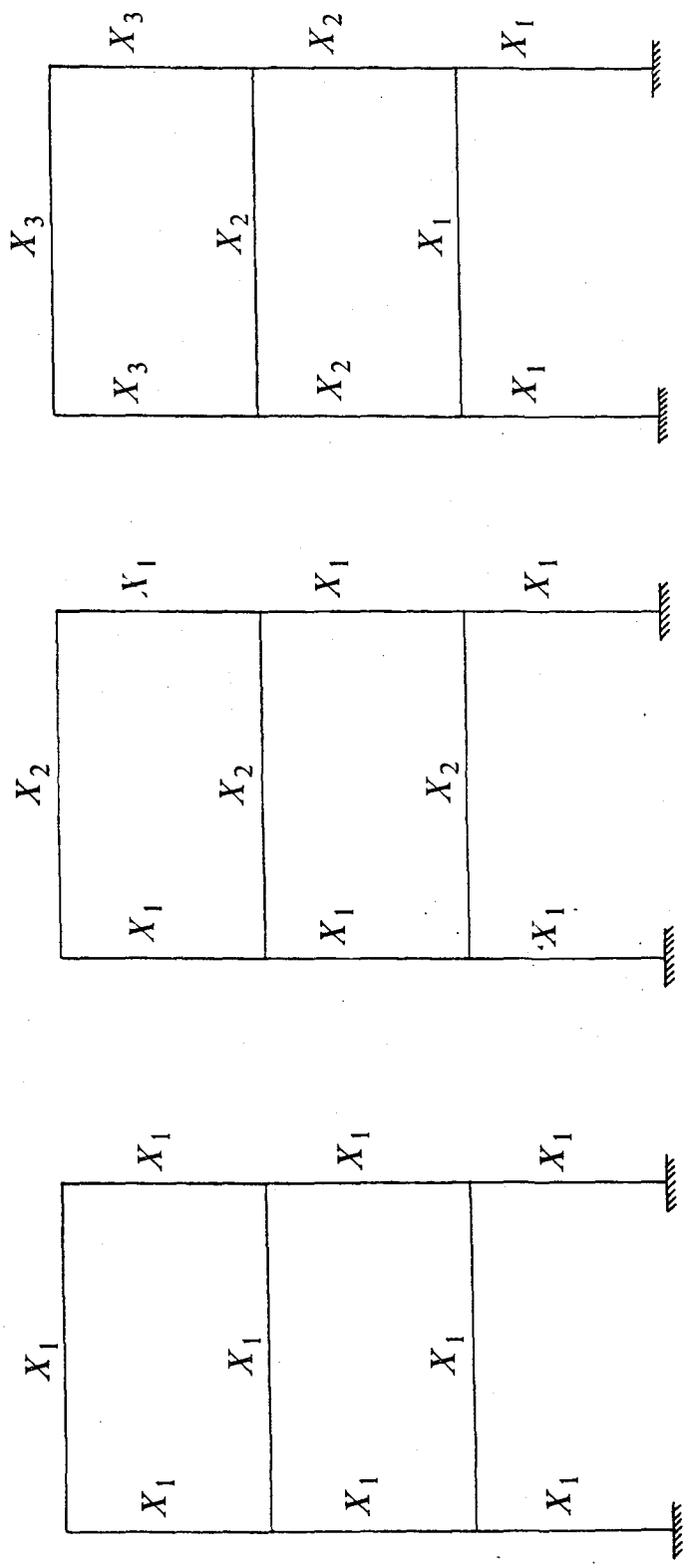

FIG 4.9 Design Parameter Groupings for the Optimization

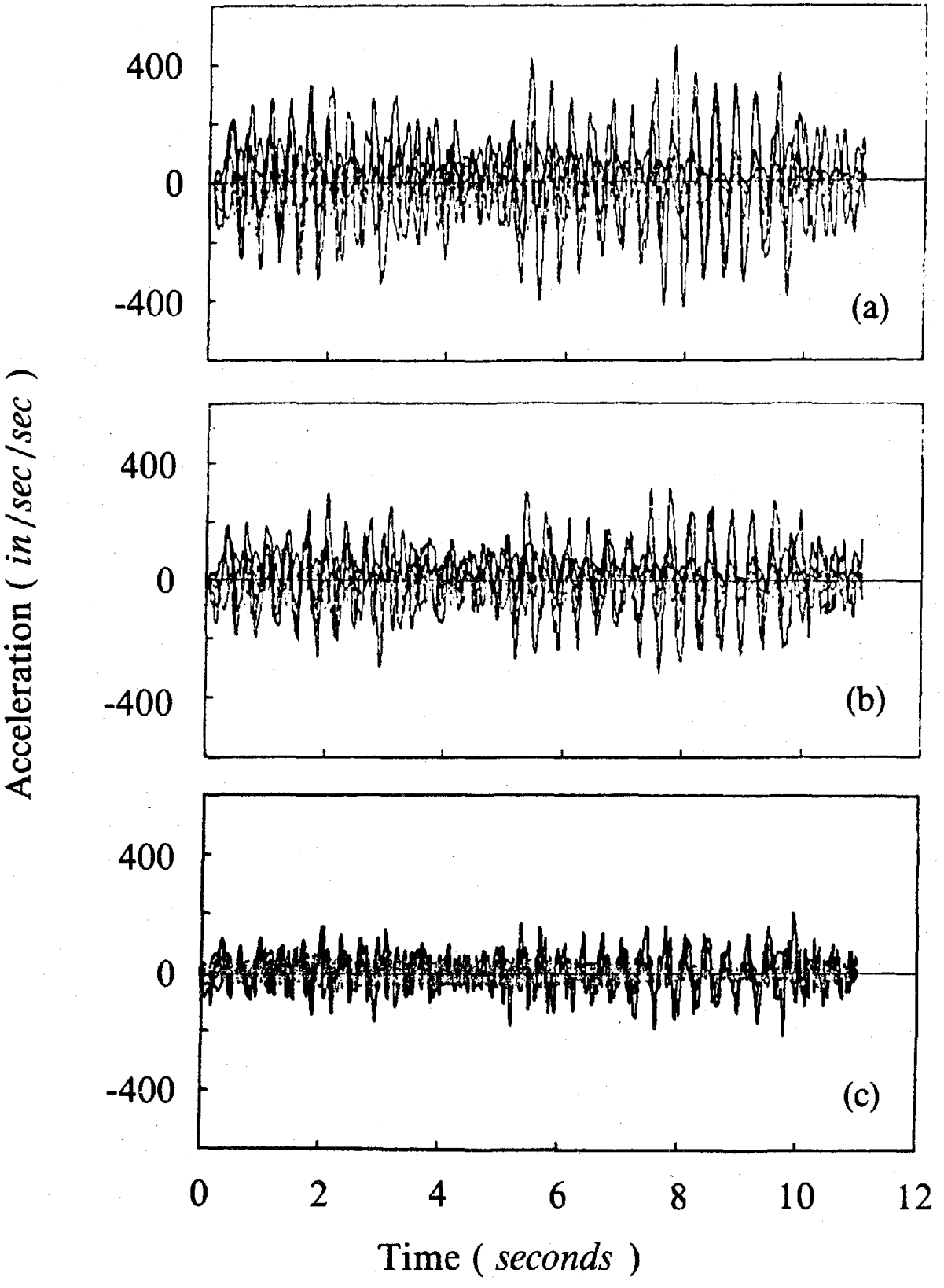

FIG 5.1 Floor Accelerations(*in /sec /sec*) vs Time(*seconds*)
a) 3rd Floor b) 2nd Floor c) 1st Floor.

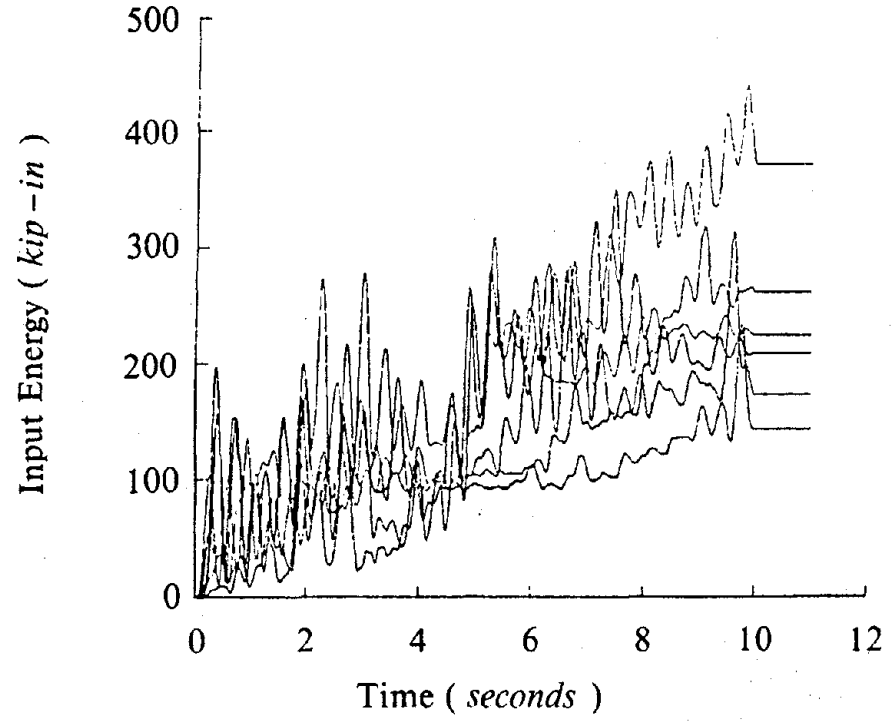

(a)

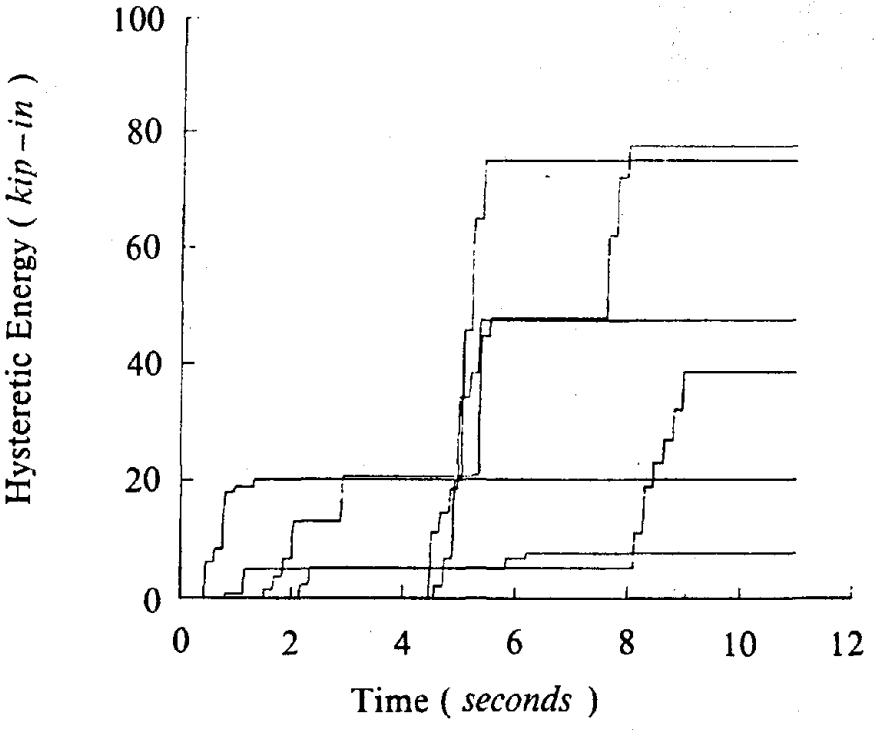

(b)

FIG 5.2 Initial Design
a) Input Energy(*kip - in*) vs Time(*seconds*)
b) Hysteretic Damped Energy(*kip - in*) vs Time(*seconds*)

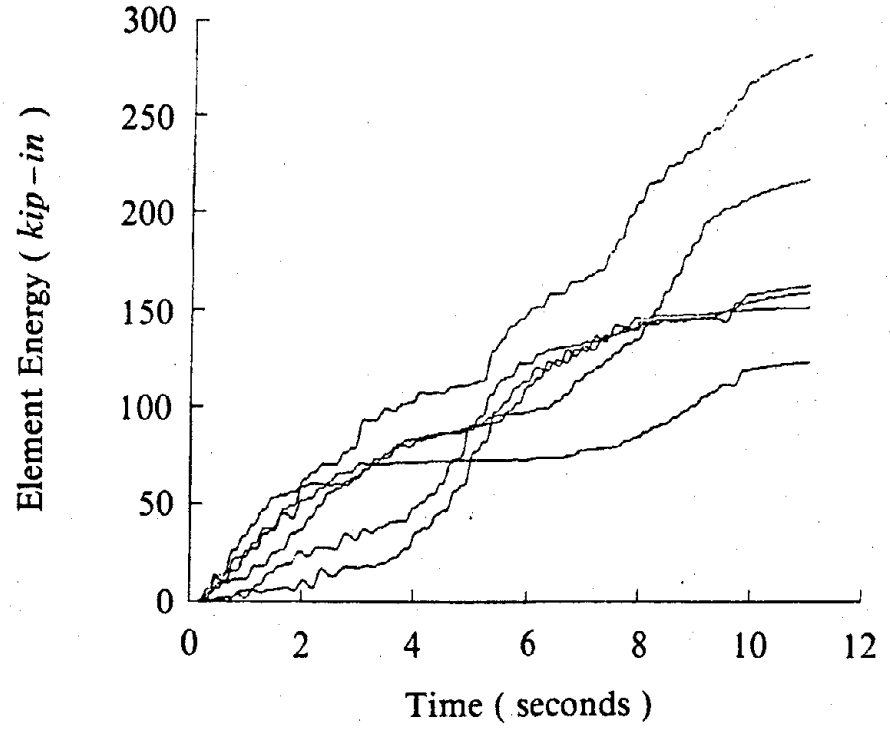

(c)

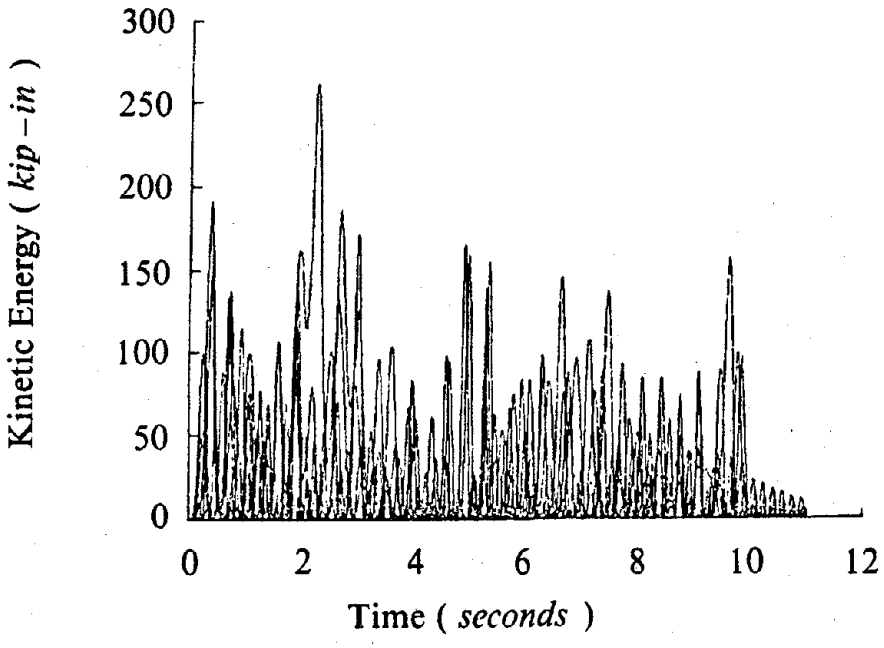

(d)

FIG 5.2 Initial Design
c) Element Damped Energy(*kip – in*) vs Time(*seconds*)
d) Kinetic Energy(*kip – in*) vs Time(*seconds*)

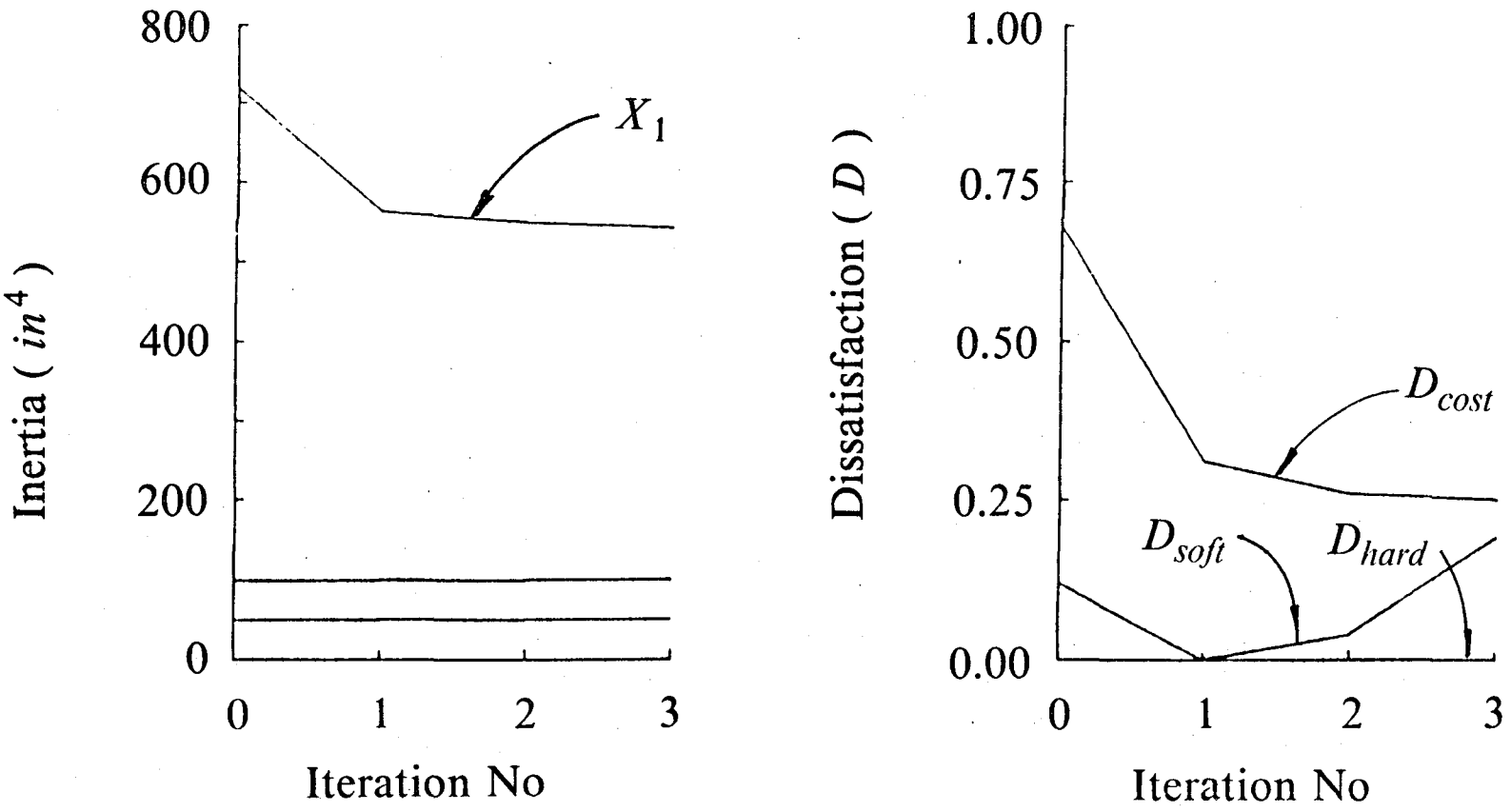

FIG 6.1 Minimum Volume Design [1 Design Variable]
a) Section Moment of Inertia (in^4) vs Iteration No
b) Dissatisfaction vs Iteration No.

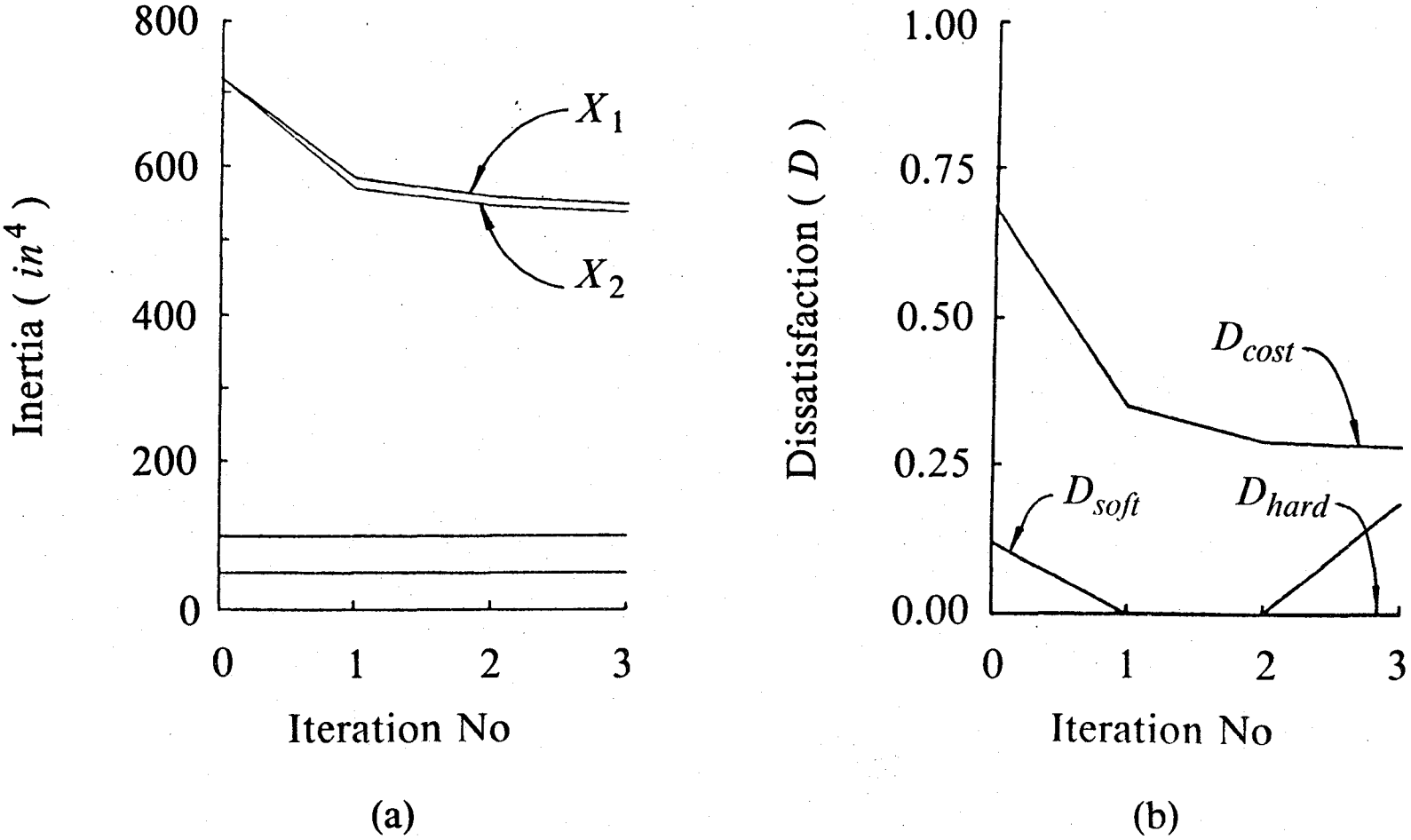

FIG 6.2 Minimum Volume Design [2 Design Variables]
a) Section Moment of Inertia (in^4) vs Iteration No
b) Dissatisfaction vs Iteration No.

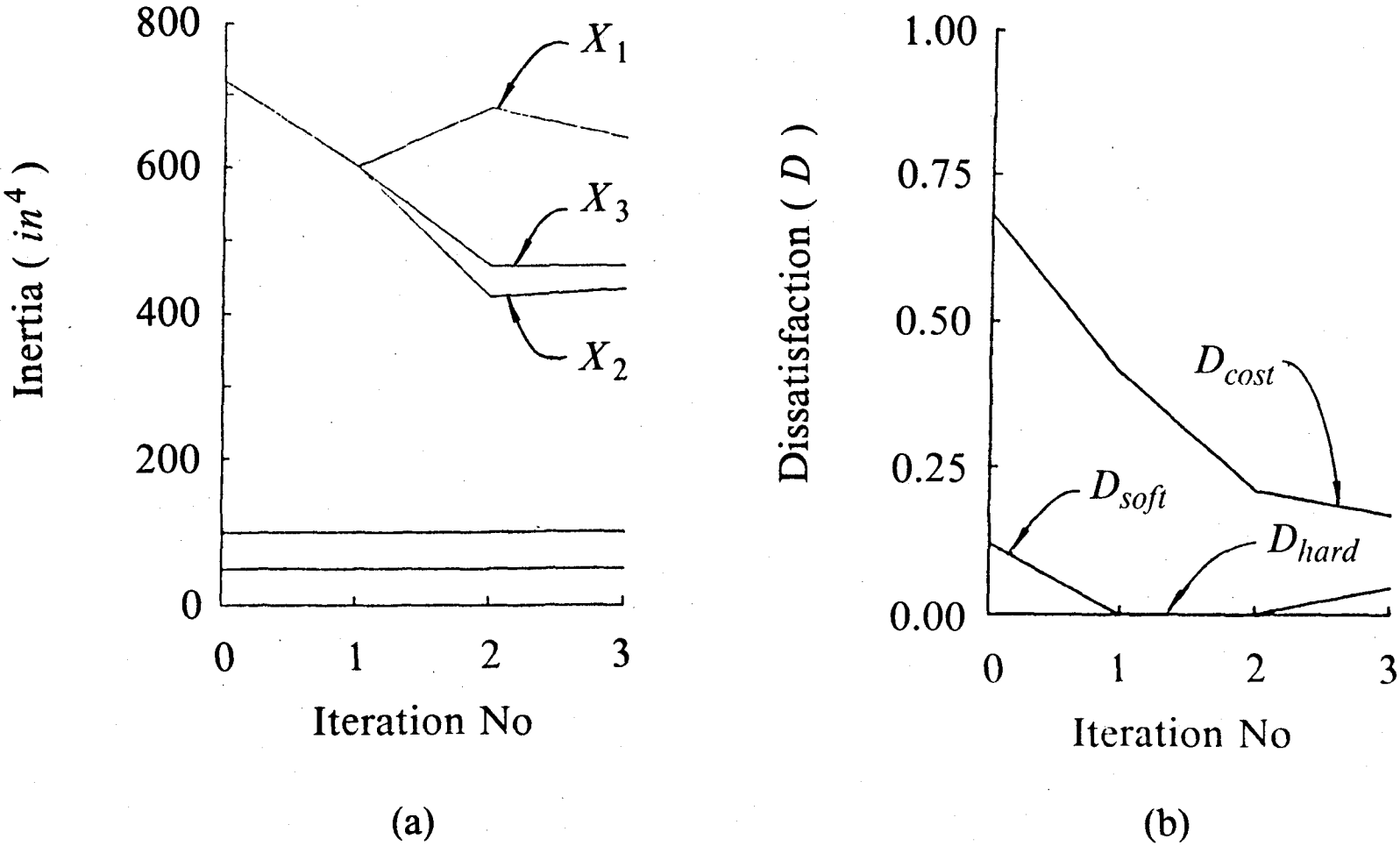

FIG 6.3 Minimum Volume Design [3 Design Variables]
a) Section Moment of Inertia (in^4) vs Iteration No
b) Dissatisfaction vs Iteration No.

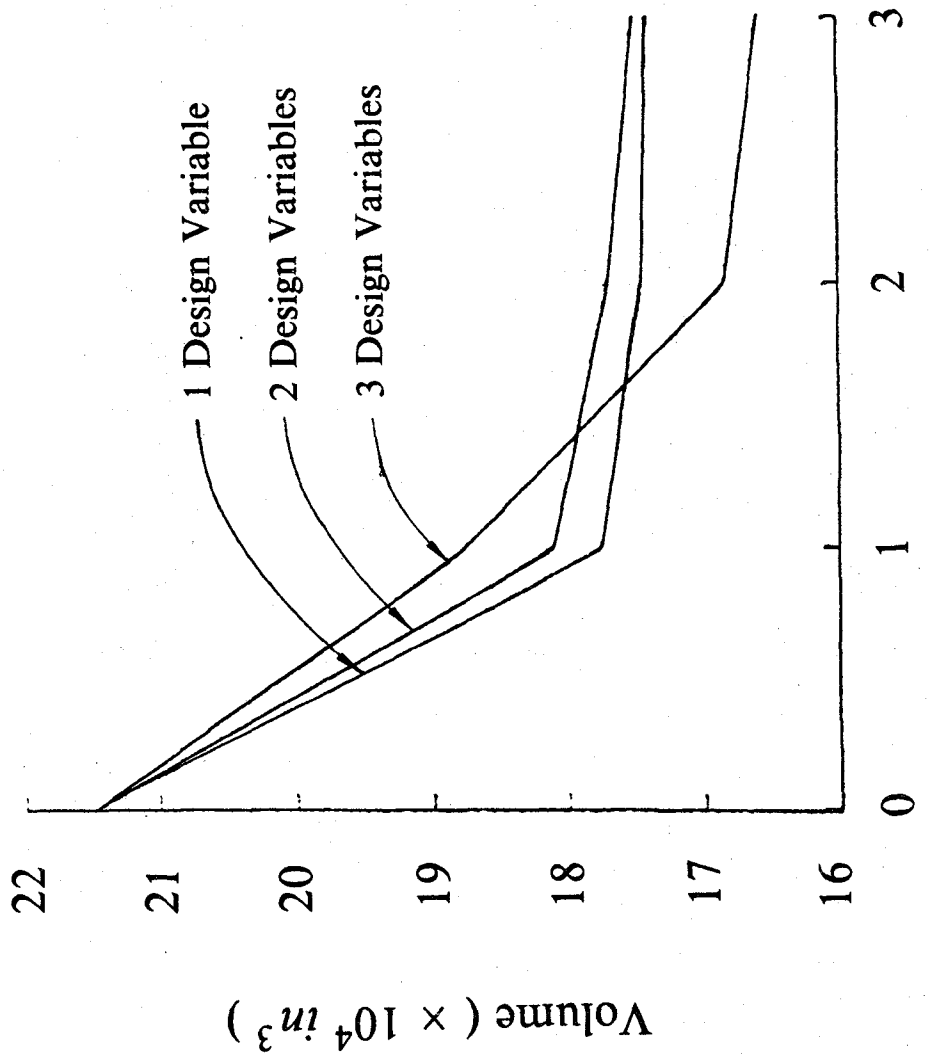

FIG 6.4 Minimum Volume Design - Frame Volume (in^3) vs Iteration No for 1,2 and 3 Design Variables.

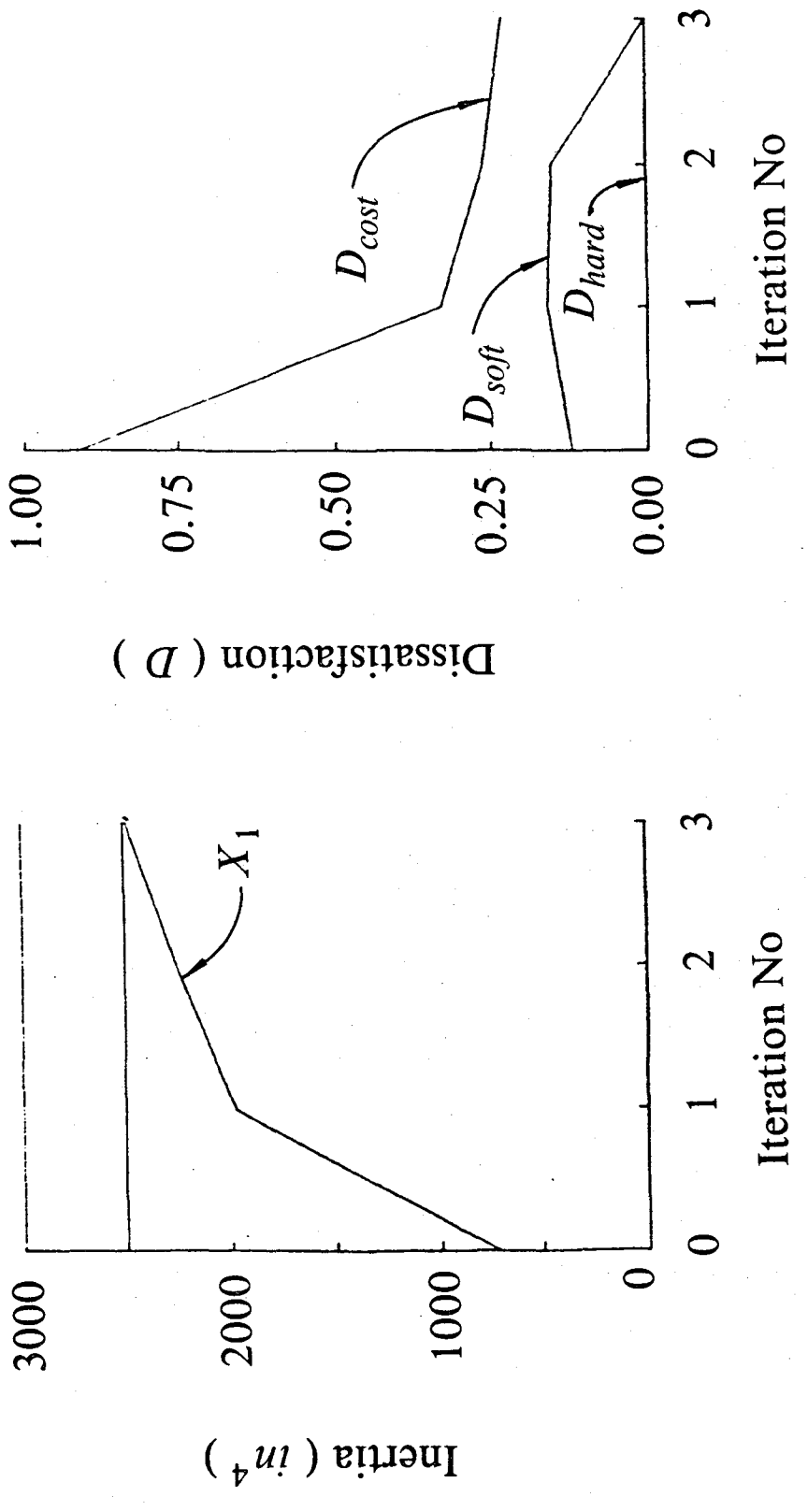

FIG 6.5 Minimum Story Drifts Design [1 Design Variable]
a) Section Moment of Inertia (in^4) vs Iteration No
b) Dissatisfaction vs Iteration No.

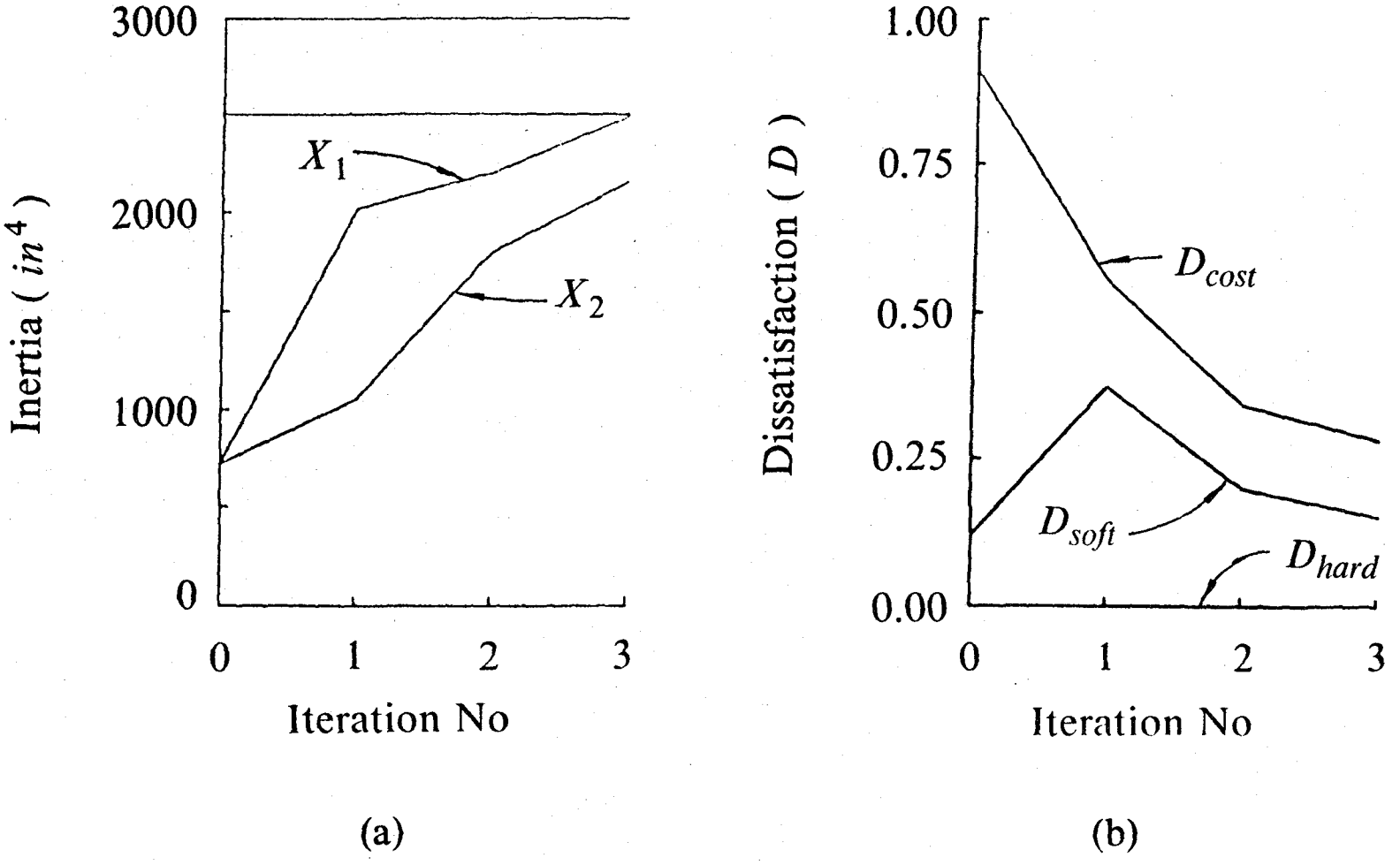

FIG 6.6 Minimum Story Drifts Design [2 Design Variables]
a) Section Moment of Inertia (in^4) vs Iteration No
b) Dissatisfaction vs Iteration No.

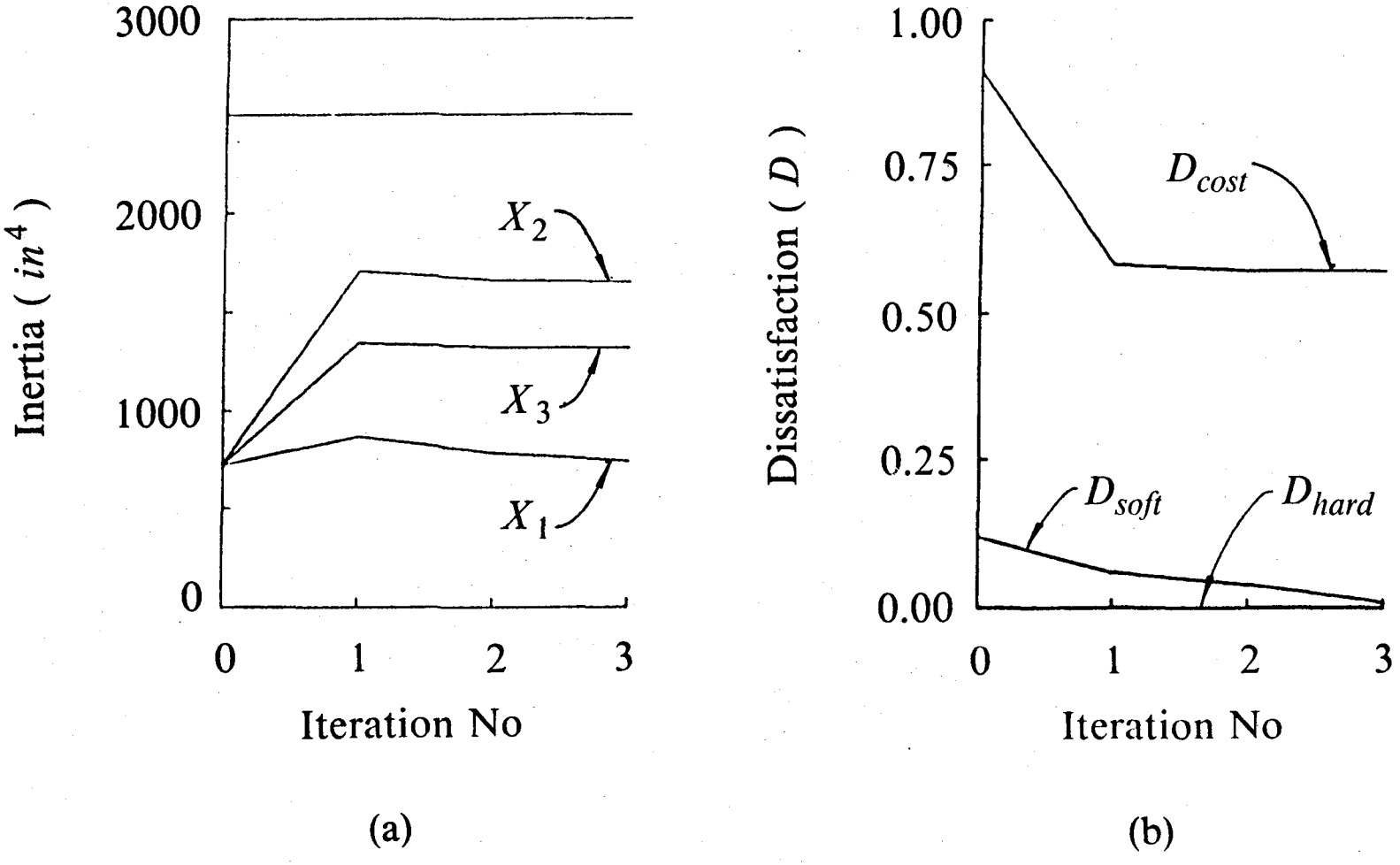

FIG 6.7 Minimum Story Drifts Design [3 Design Variables]
a) Section Moment of Inertia (in^4) vs Iteration No
b) Dissatisfaction vs Iteration No.

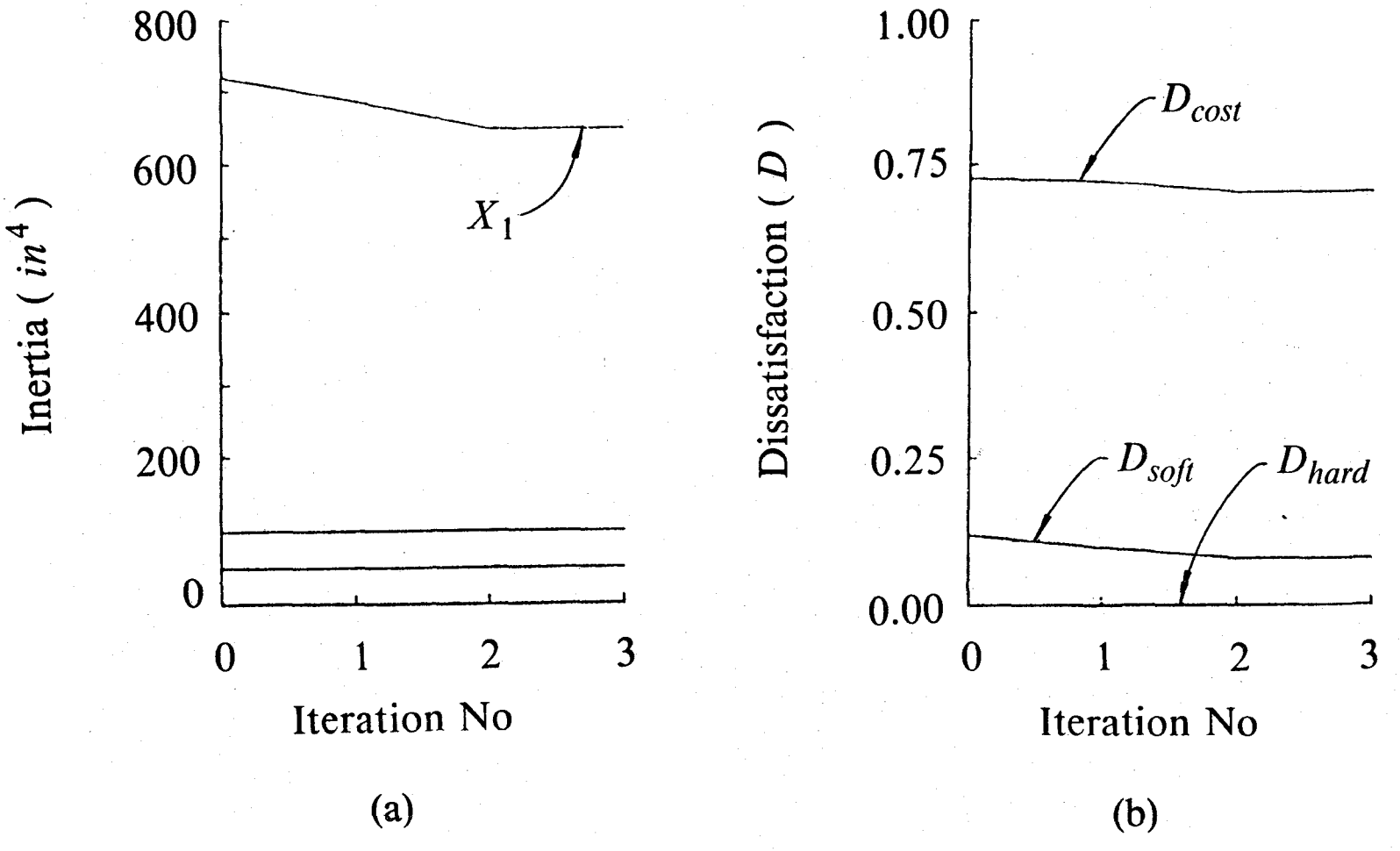

FIG 6.8 Maximum Dissipated Energy Design [1 Design Variable]
a) Section Moment of Inertia (in^4) vs Iteration No
b) Dissatisfaction vs Iteration No.

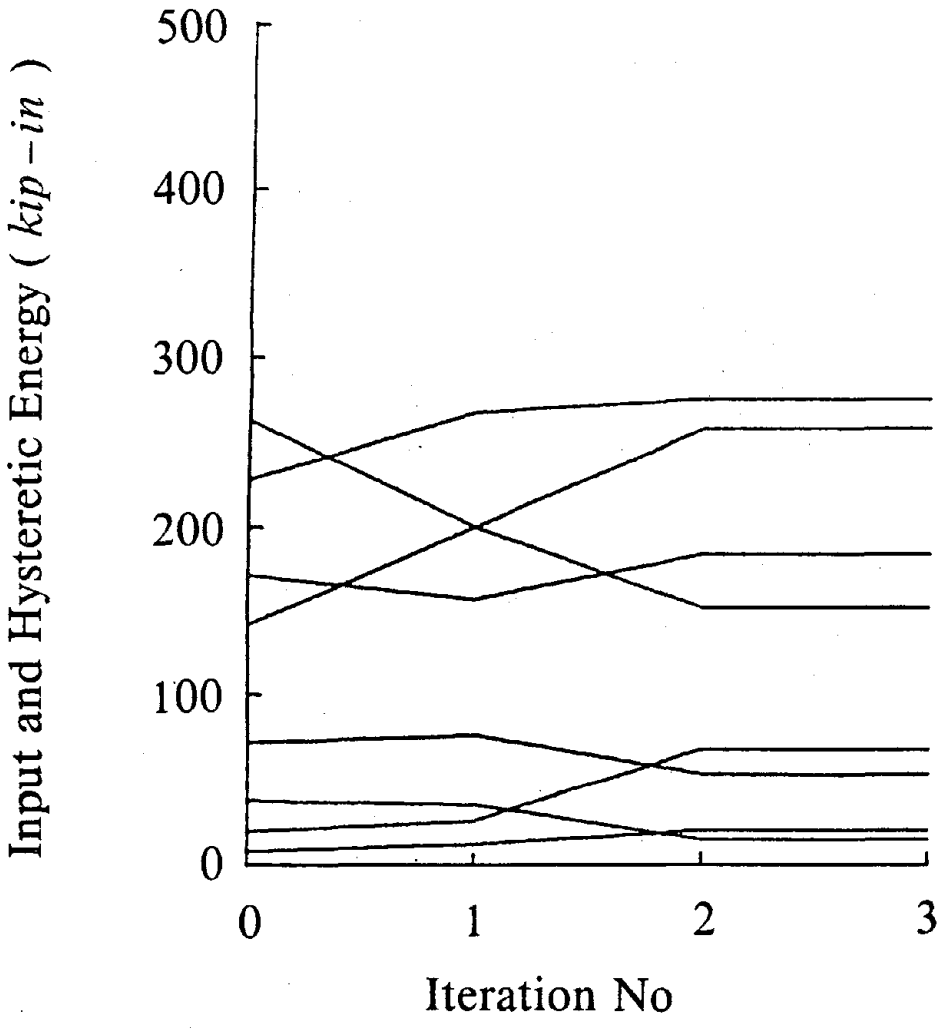

FIG 6.9 Maximum Dissipated Energy Design [1 Design Variable] Input and Hysteretic Energy vs Iteration No.

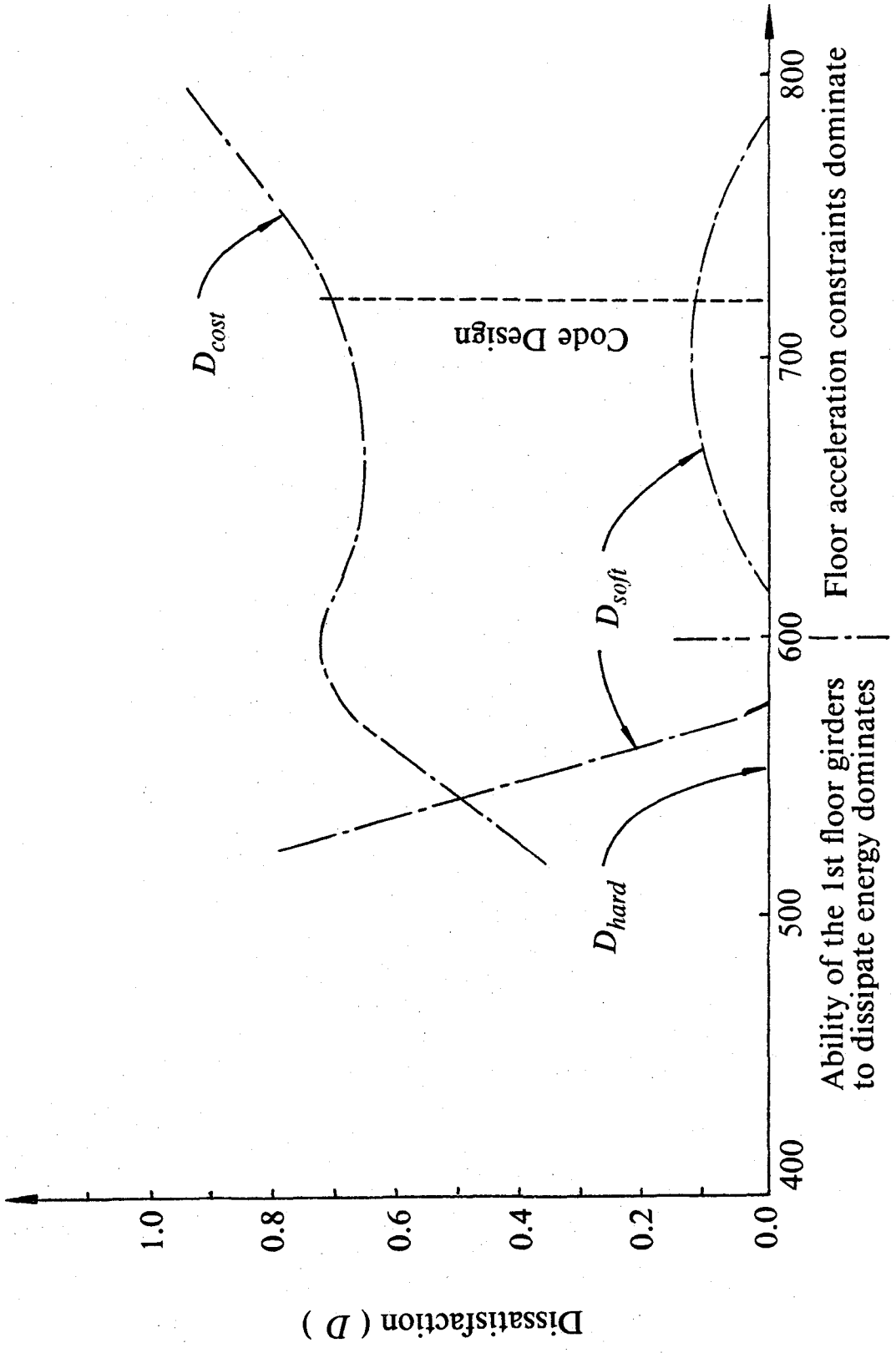

FIG 6.10 Maximum Dissipated Energy Design [1 Design Variable]
Frame Performance vs Frame Member Size.

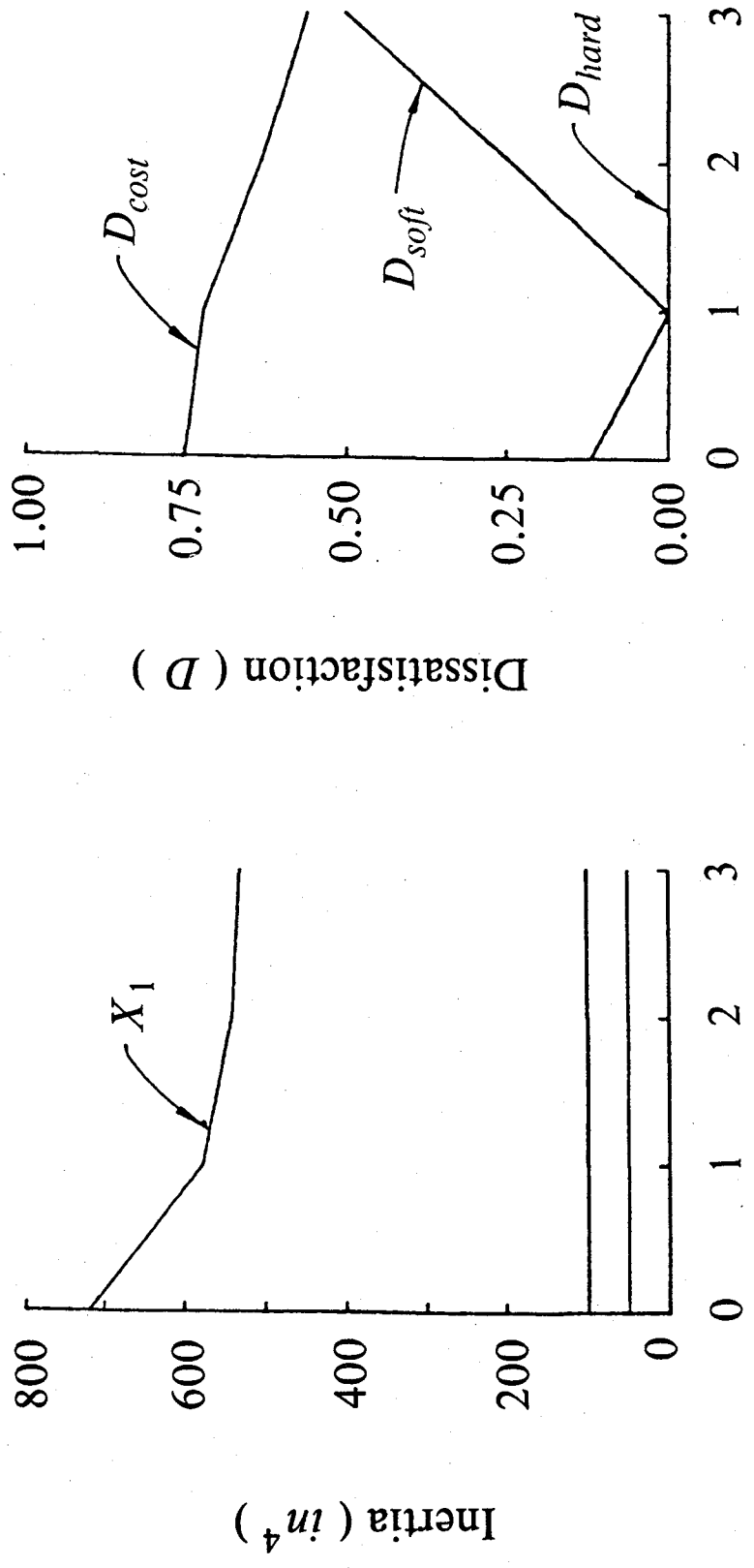

FIG 6.11 Maximum Dissipated Energy Design [1 Design Variable]
a) Section Moment of Inertia (in^4) vs Iteration No
b) Dissatisfaction vs Iteration No.

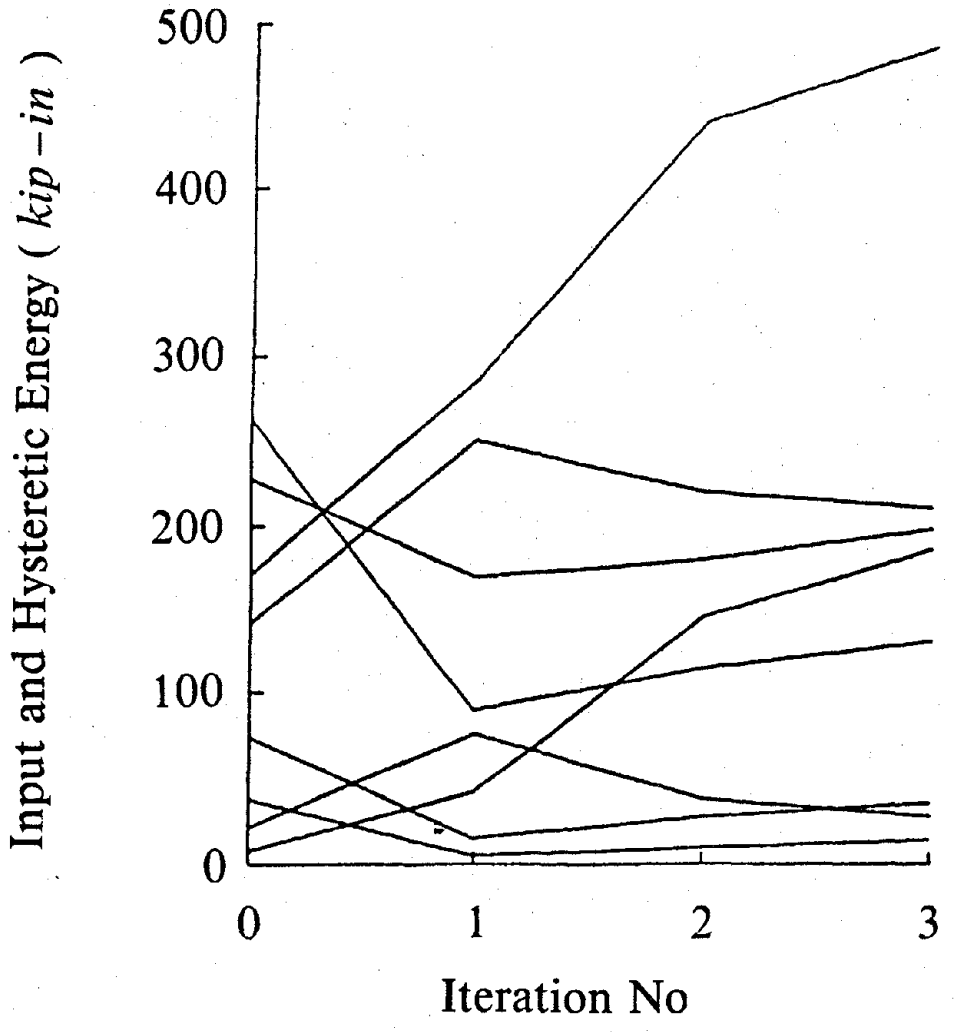

FIG 6.12 Maximum Dissipated Energy [1 Design Variable]
Input and Hysteretic Energy (*kip – in*) vs Iteration No

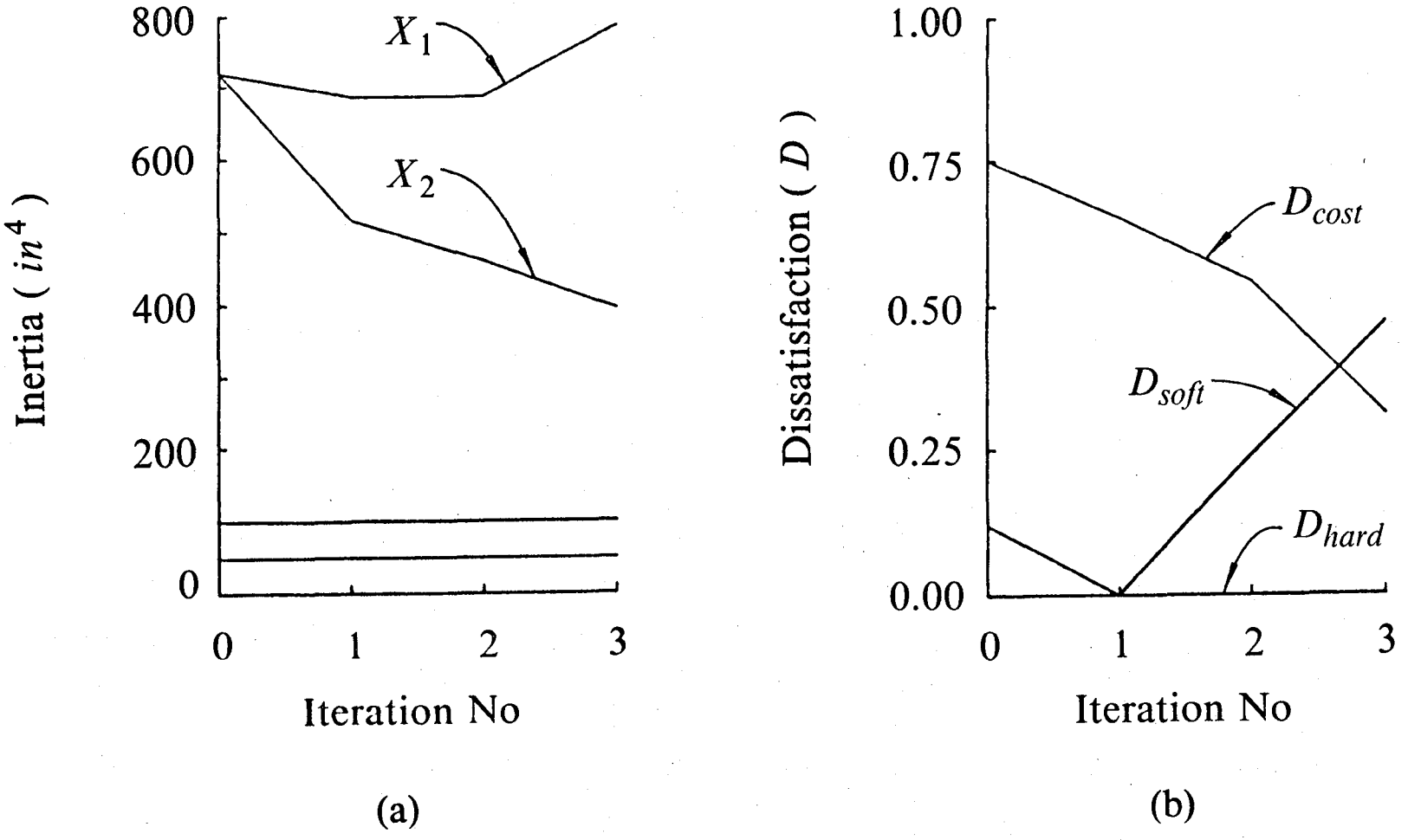

FIG 6.13 Maximum Dissipated Energy Design [2 Design Variables]
a) Section Moment of Inertia (in^4) vs Iteration No
b) Dissatisfaction vs Iteration No.

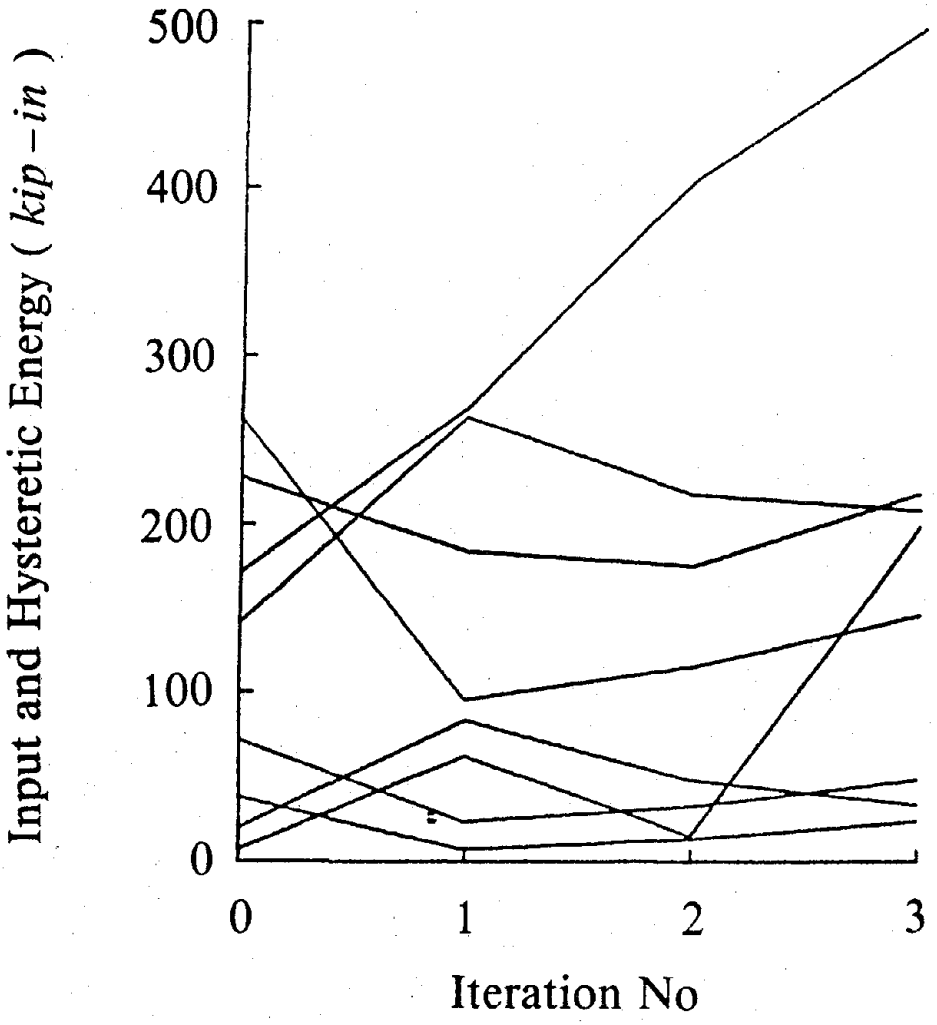

FIG 6.14 Maximum Dissipated Energy [2 Design Variables]
Input and Hysteretic Energy (*kip – in*) vs Iteration No

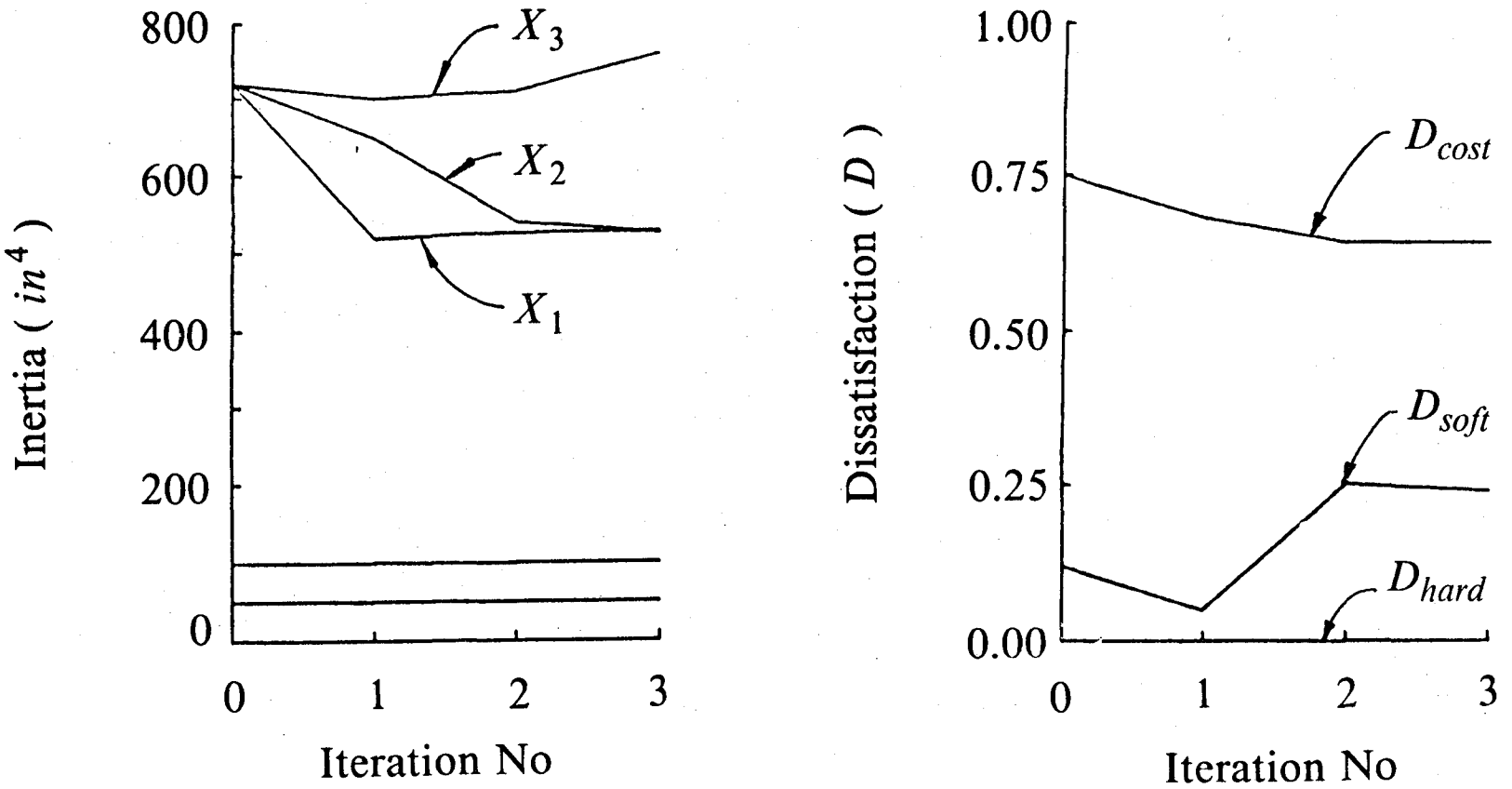

FIG 6.15 Maximum Dissipated Energy Design [3 Design Variables]
a) Section Moment of Inertia (in^4) vs Iteration No
b) Dissatisfaction vs Iteration No.

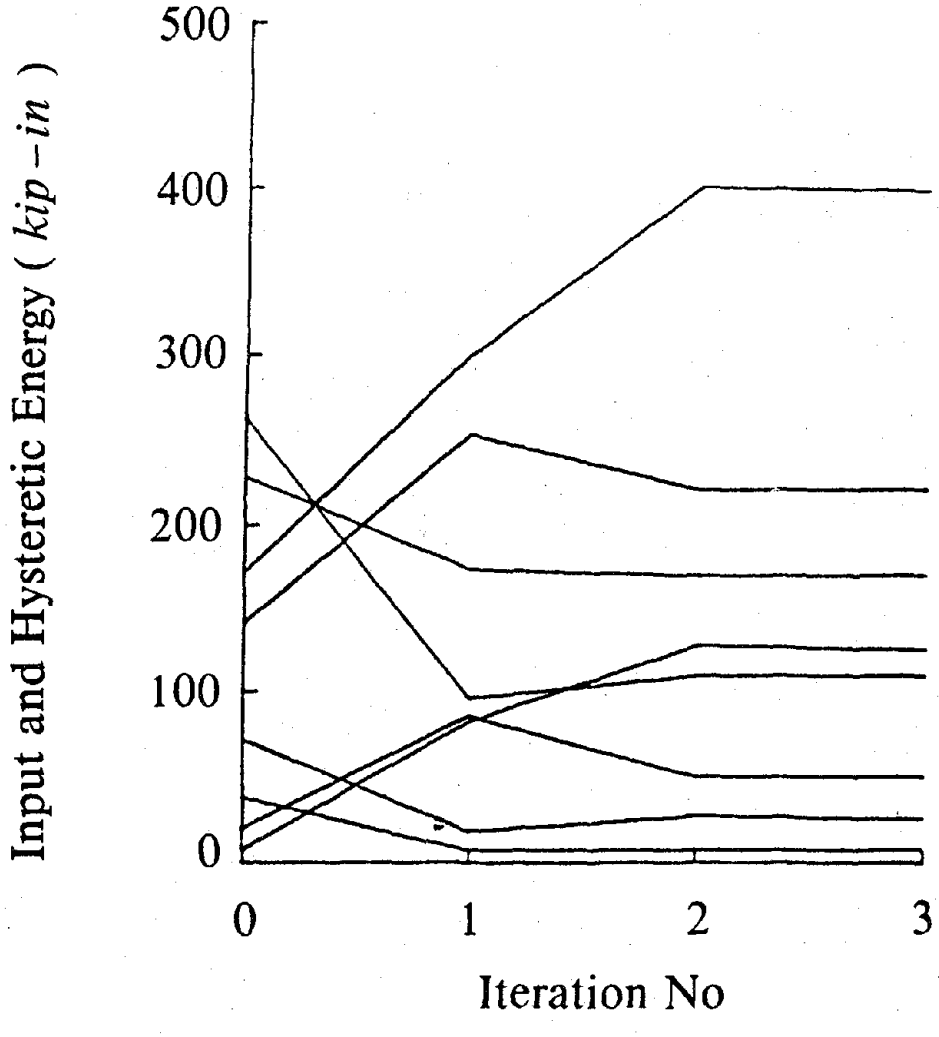

FIG 6.16 Maximum Dissipated Energy Design [3 Design Variables] Input and Hysteretic Energy (*kip – in*) vs Iteration No.

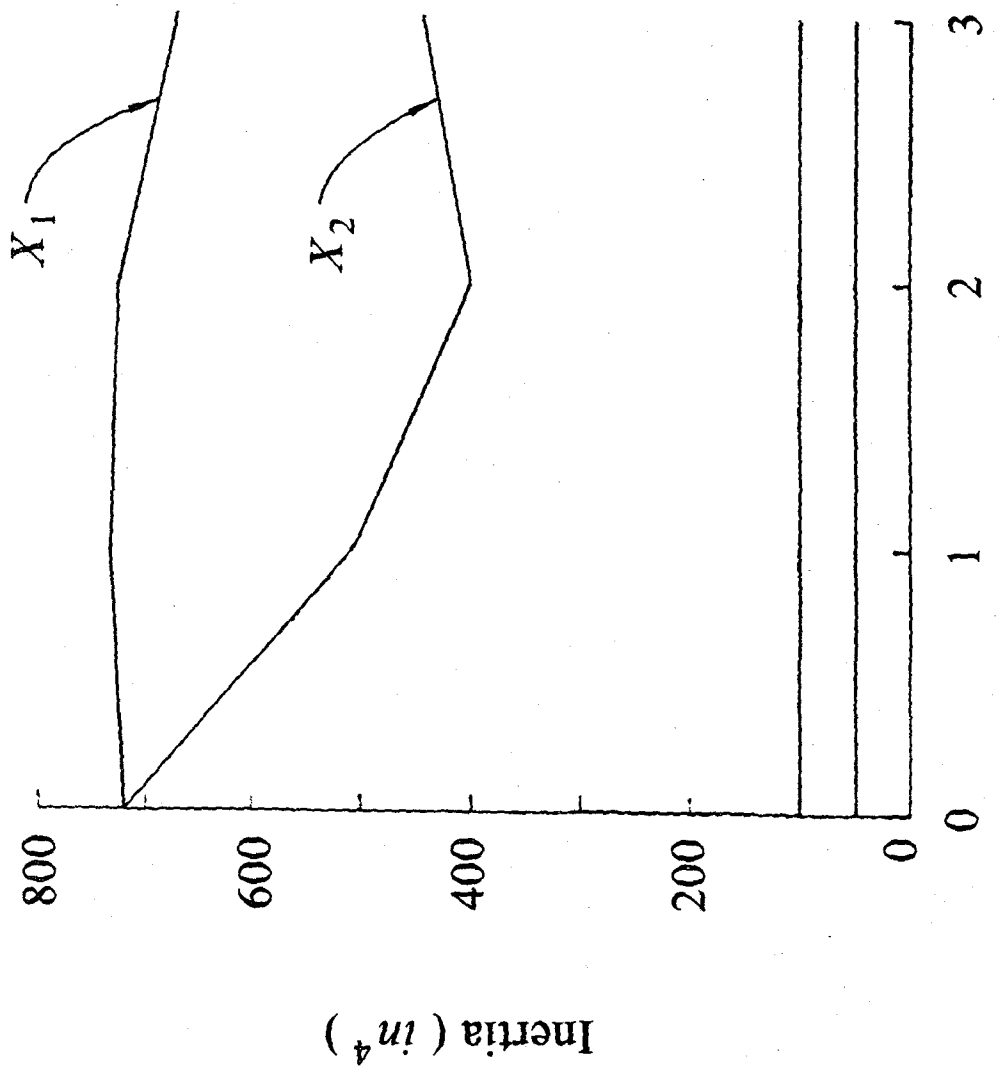

FIG 6.17 Multiple Objective Design
Section Moment of Inertia (in^4) vs Iteration No.

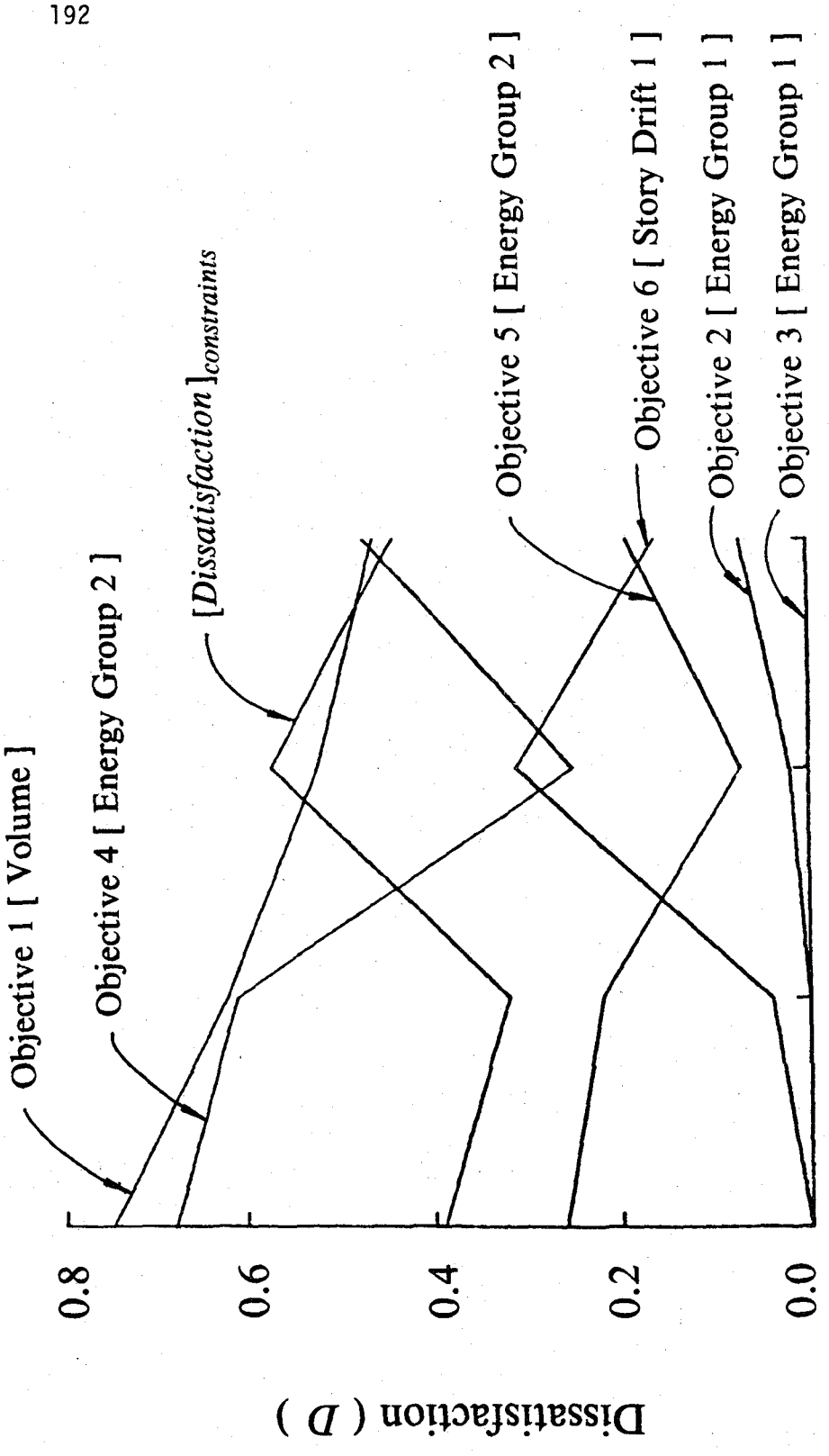

FIG 6.18 Multiple Objective Design - Dissatisfaction vs Iteration No.

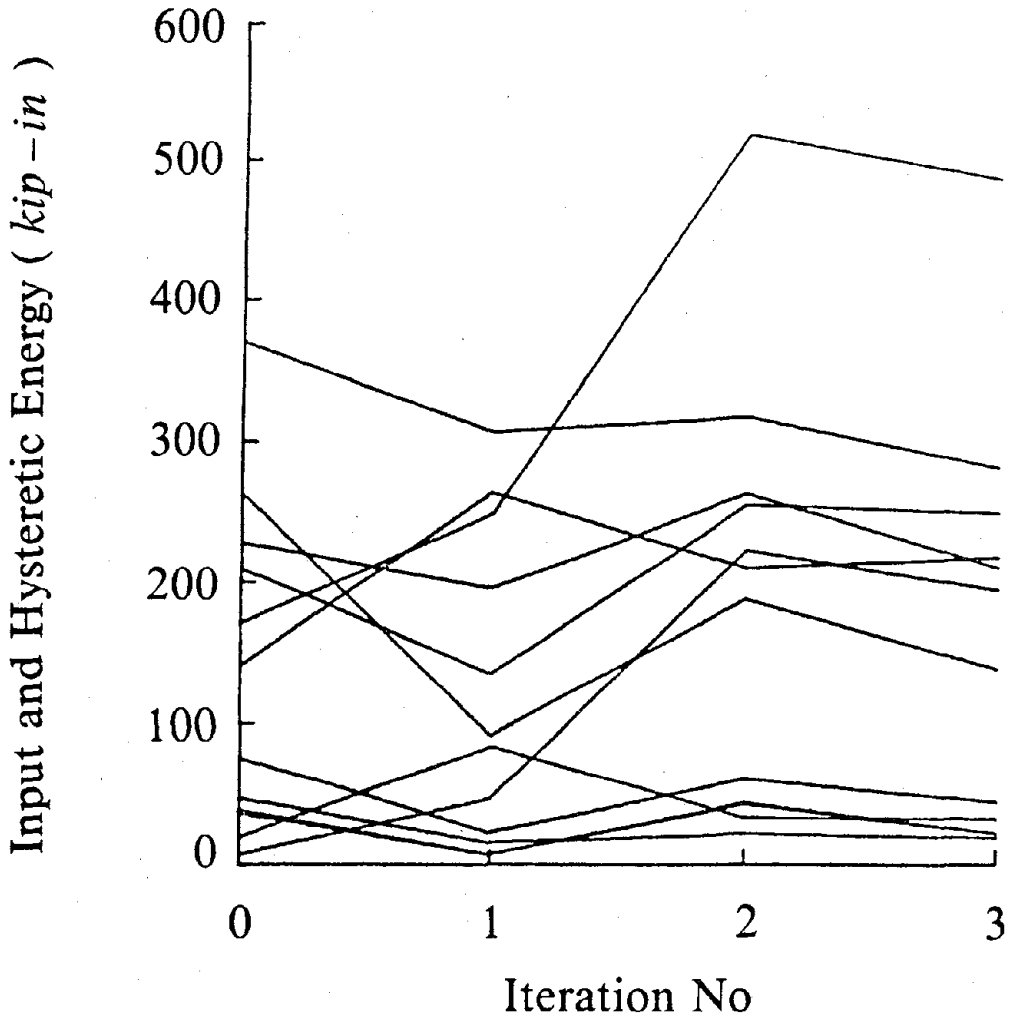

FIG 6.19 Multiple Objective Design - Input and Hysteretic Energy (*kip – in*) vs Iteration No.

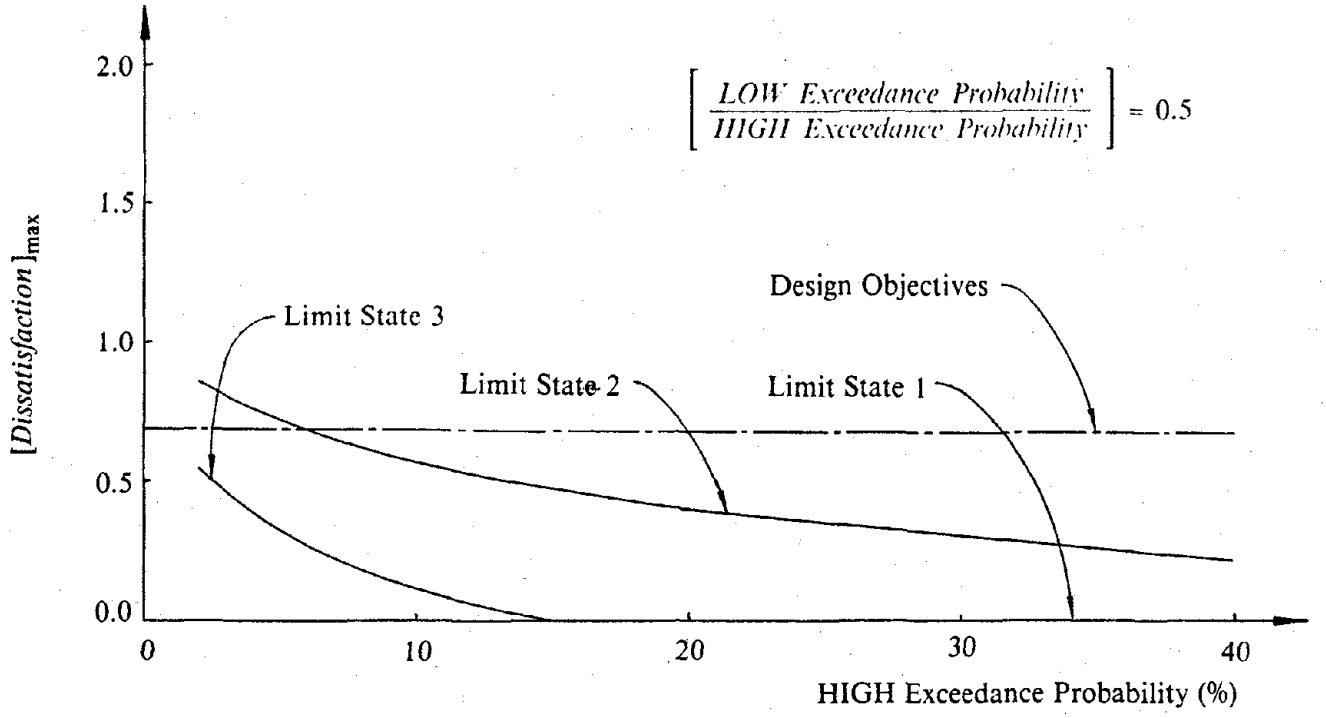

(a)

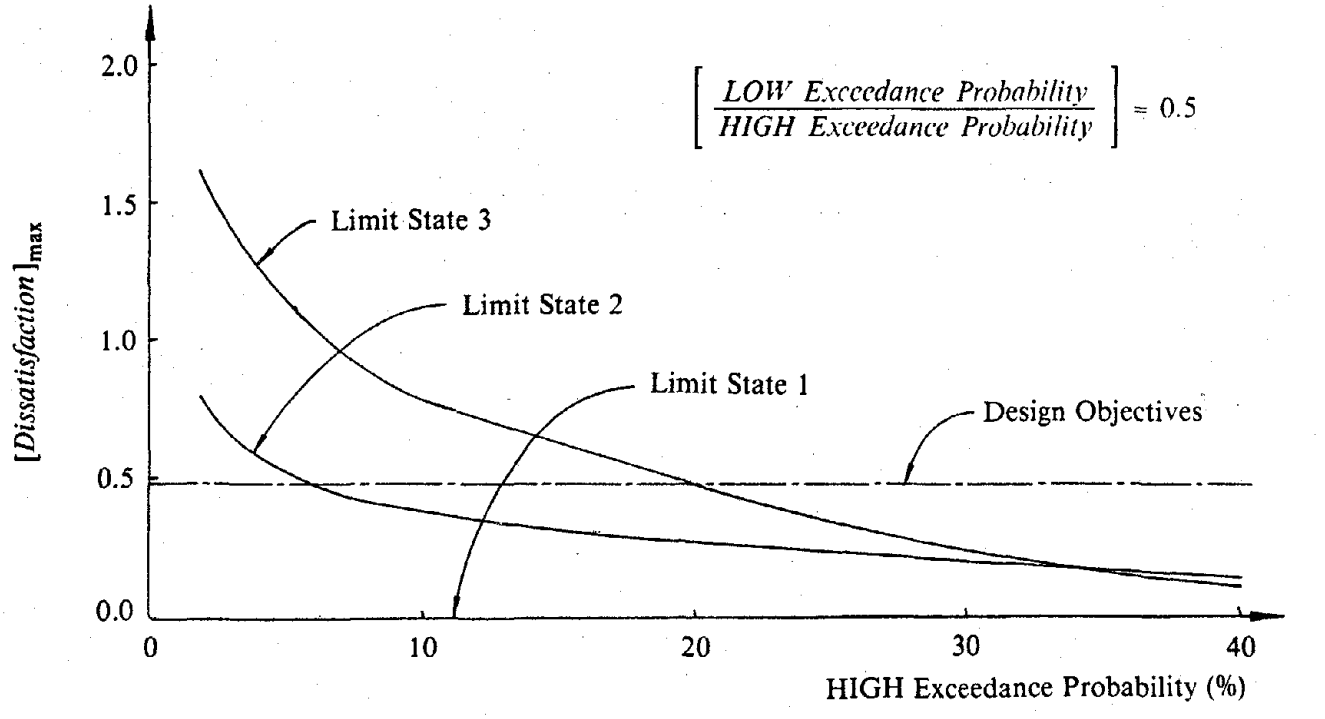

(b)

FIG 6.20 Dissatisfaction vs HIGH Exceedance Probability
a) Initial Design b) Final Design.

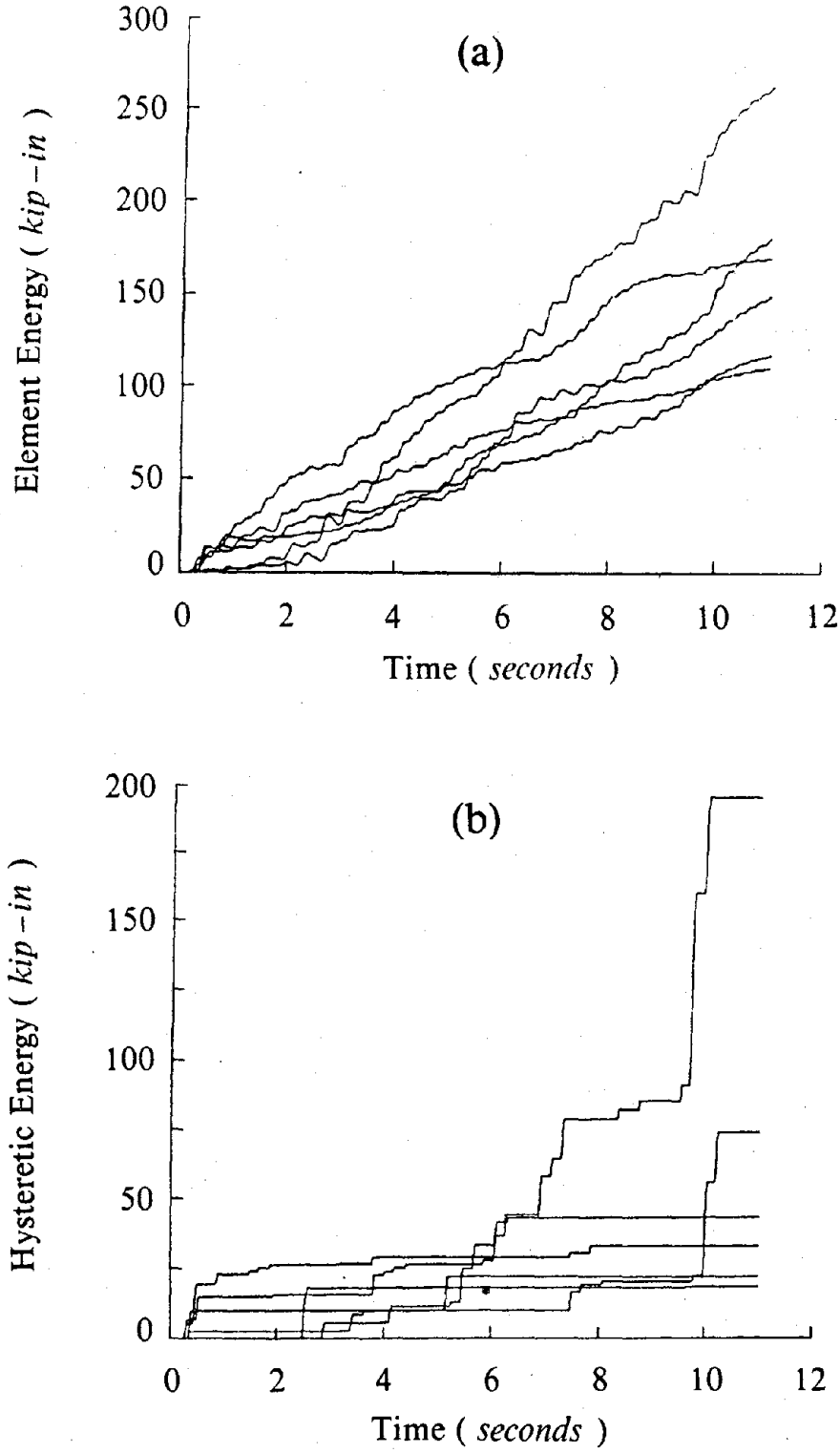

FIG 6.21 Final Design
a) Element Damped Energy(*kip – in*) vs Time(*seconds*)
b) Hysteretic Damped Energy(*kip – in*) vs Time(*seconds*)

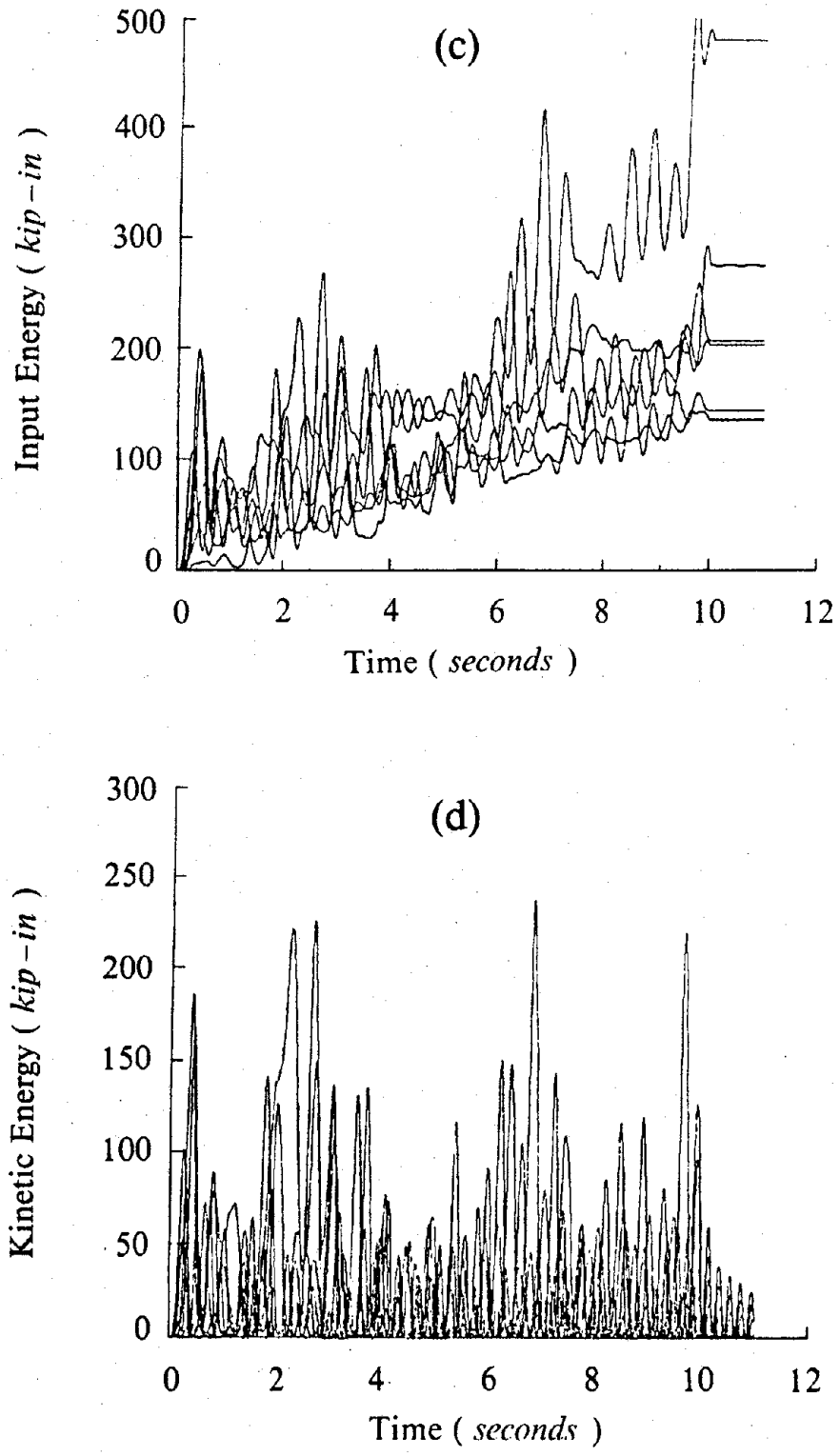

FIG 6.21 Final Design
c) Input Energy(*kip – in*) vs Time(*seconds*)
d) Kinetic Energy(*kip – in*) vs Time(*seconds*).

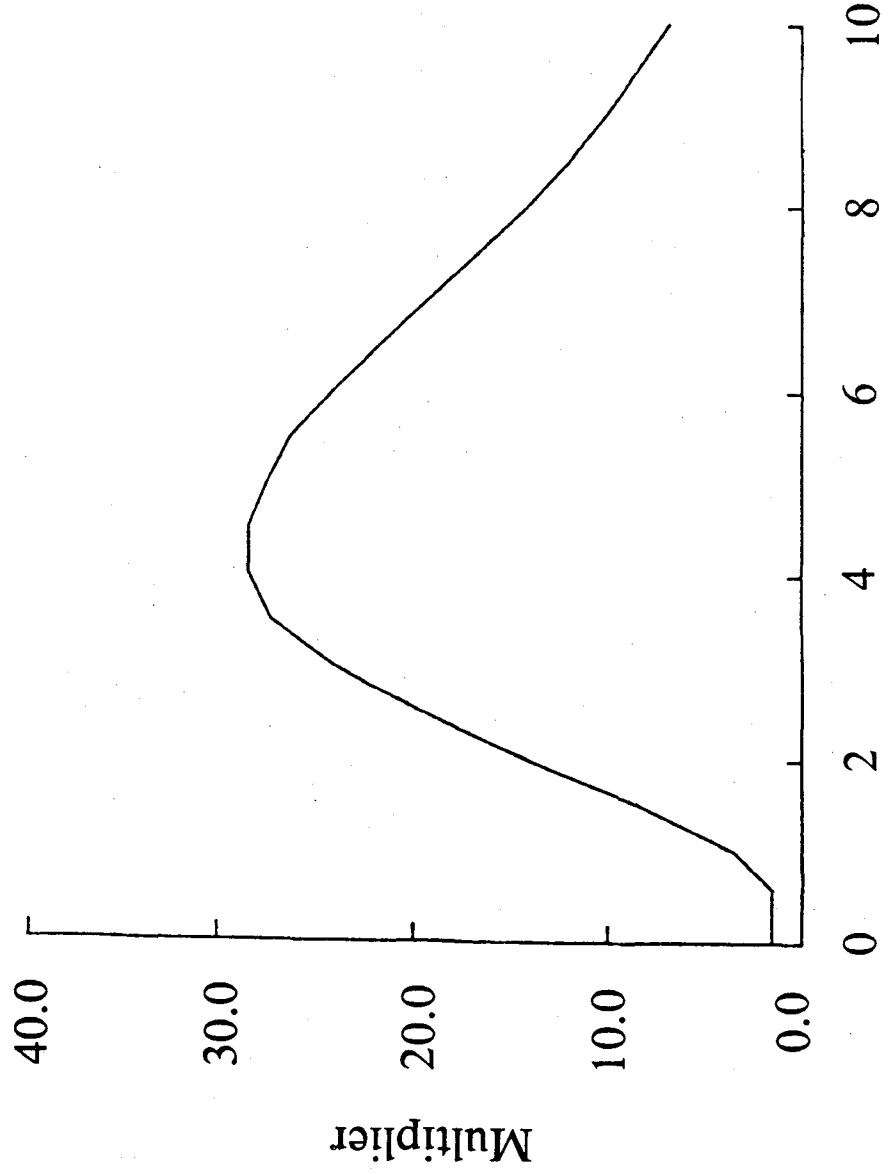

FIG A4.1 ARMA Variance Multiplier vs Time(*seconds*).

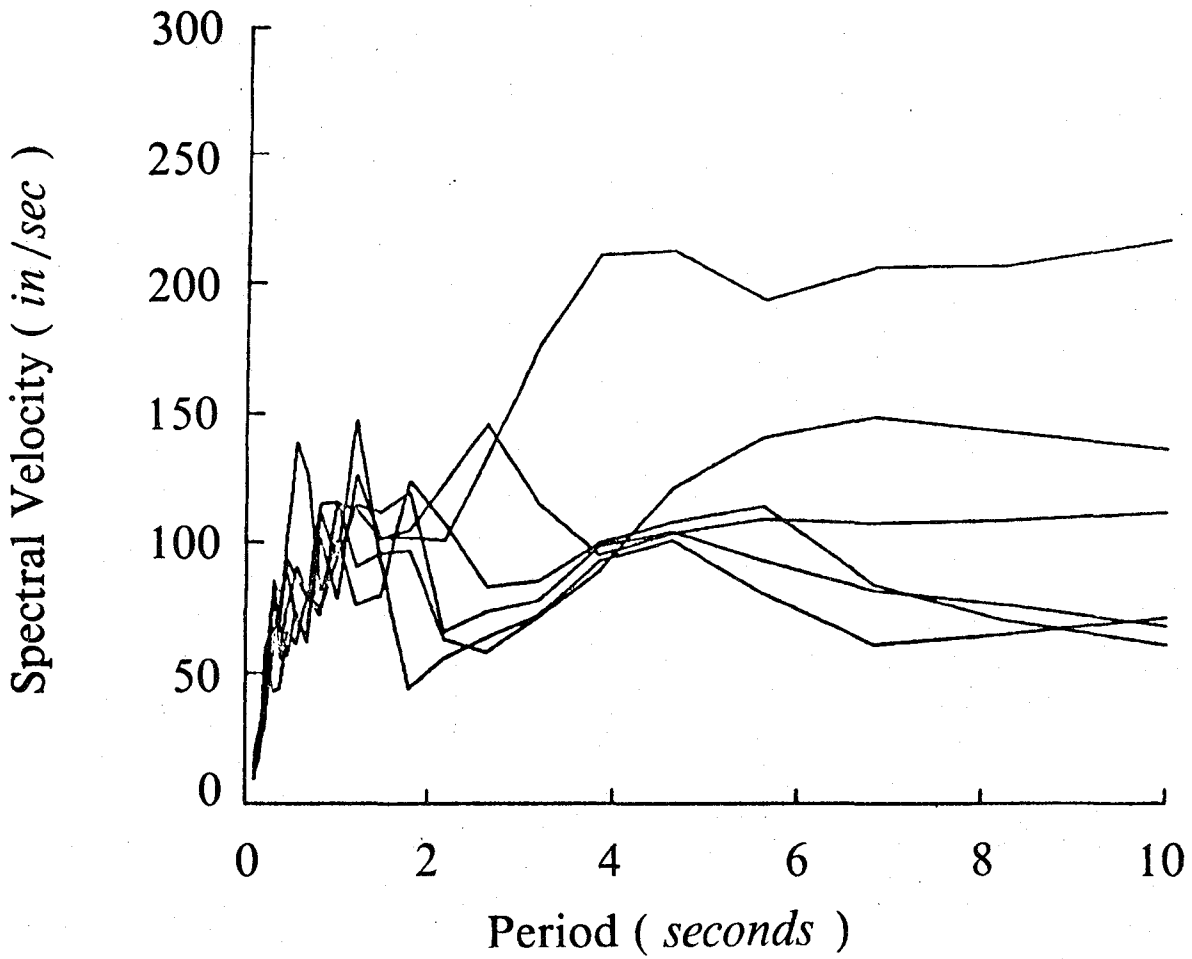

FIG A4.2 ARMA Spectral Velocity(*in /sec*) vs Period(*seconds*).

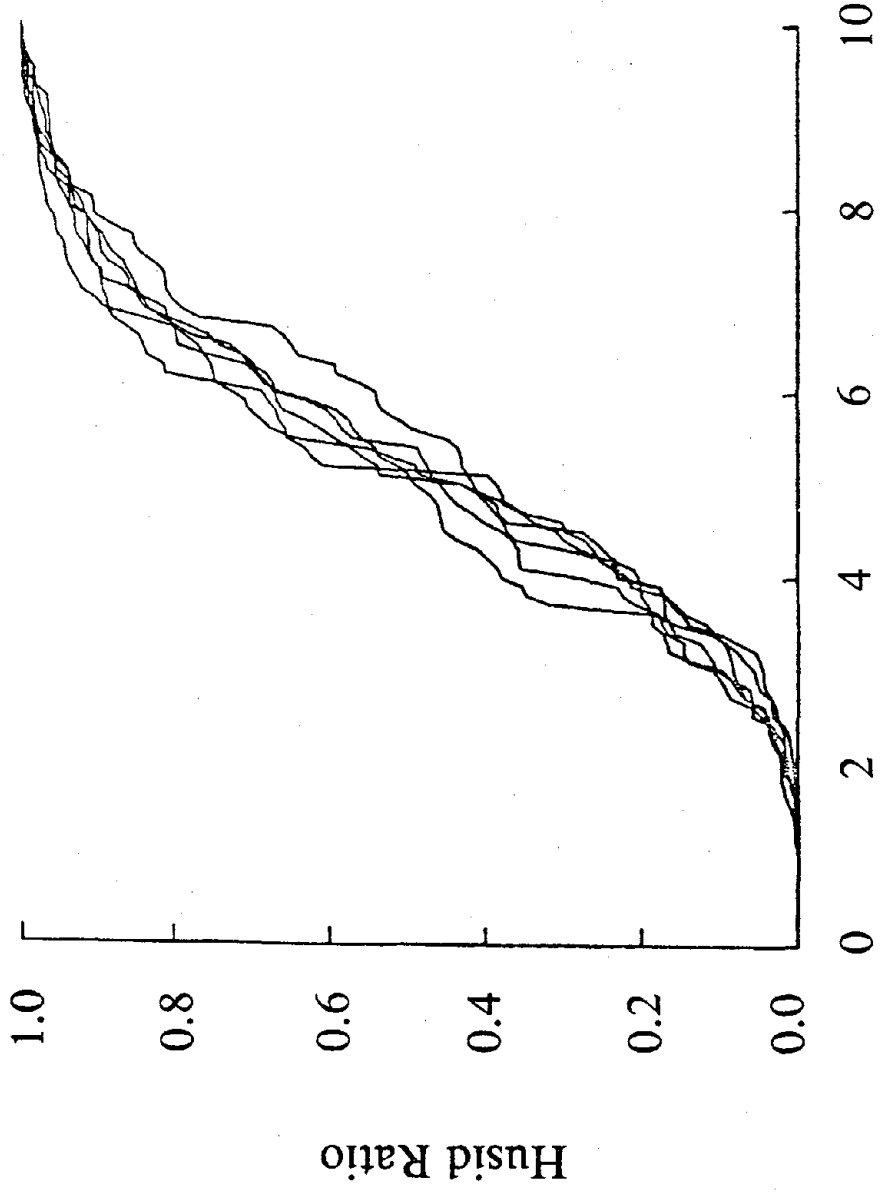

FIG A4.3 ARMA Husid Ratio vs Time(*seconds*)

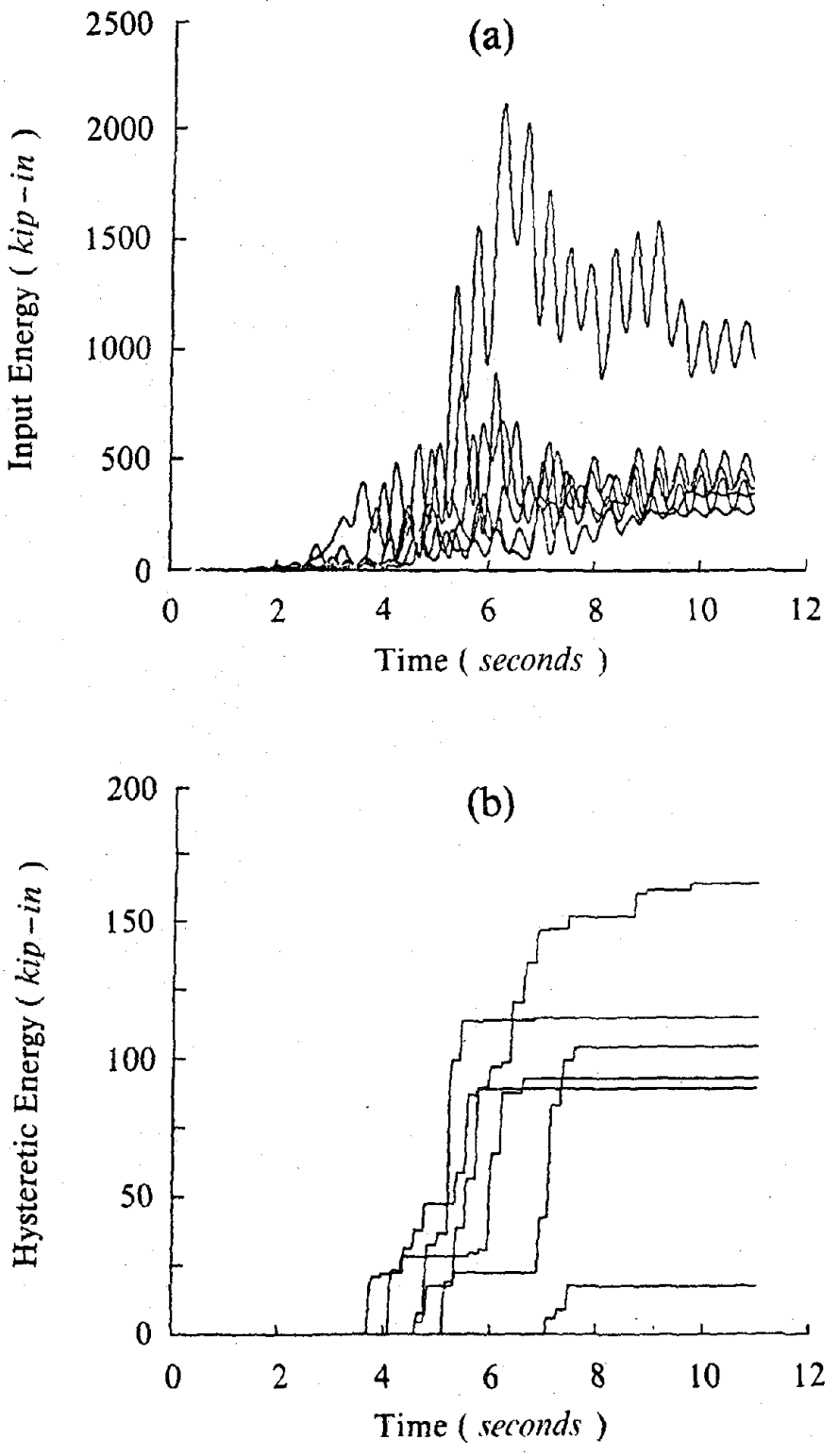

FIG A4.4 Final Design
a) Input Energy(*kip-in*) vs Time(*seconds*)
b) Hysteretic Damped Energy(*kip-in*) vs Time(*seconds*).

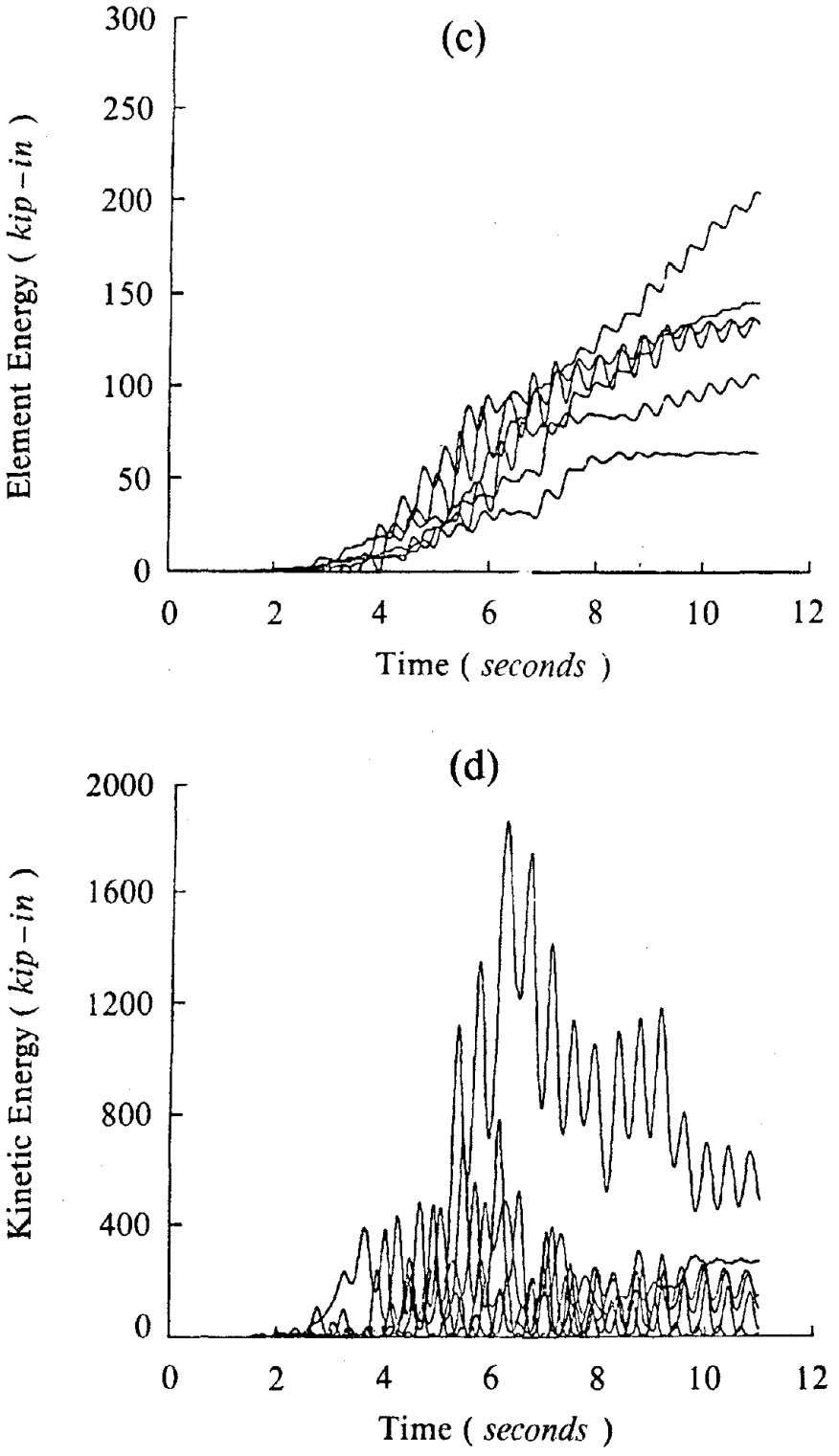

FIG A4.4 Final Design
c) Element Damped Energy(*kip – in*) vs Time(*seconds*)
d) Kinetic Energy(*kip – in*) vs Time(*seconds*).

EARTHQUAKE ENGINEERING RESEARCH CENTER REPORTS

NOTE: Numbers in parentheses are Accession Numbers assigned by the National Technical Information Service: these are followed by a price code. Copies of the reports may be ordered from the National Technical Information Service, 5285 Port Royal Road, Springfield, Virginia, 22161. Accession Numbers should be quoted on orders for reports (PB --- ---) and remittance must accompany each order. Reports without this information were not available at time of printing. The complete list of EERC reports (from EERC 67-1) is available upon request from the Earthquake Engineering Research Center, University of California, Berkeley, 47th Street and Hoffman Boulevard, Richmond, California 94804.

UCB/EERC-79/01 "Hysteretic Behavior of Lightweight Reinforced Concrete Beam-Column Subassemblages," by B. Forzani, E.P. Popov and V.V. Bertero - April 1979(PB 298 267)A06

UCB/EERC-79/02 "The Development of a Mathematical Model to Predict the Flexural Response of Reinforced Concrete Beams to Cyclic Loads, Using System Identification," by J. Stanton & H. McNiven - Jan. 1979(PB 295 875)A10

UCB/EERC-79/03 "Linear and Nonlinear Earthquake Response of Simple Torsionally Coupled Systems," by C.L. Kan and A.K. Chopra - Feb. 1979(PB 298 262)A06

UCB/EERC-79/04 "A Mathematical Model of Masonry for Predicting its Linear Seismic Response Characteristics," by Y. Mengi and H.D. McNiven - Feb. 1979(PB 298 266)A06

UCB/EERC-79/05 "Mechanical Behavior of Lightweight Concrete Confined by Different Types of Lateral Reinforcement," by M.A. Manrique, V.V. Bertero and E.P. Popov - May 1979(PB 301 114)A06

UCB/EERC-79/06 "Static Tilt Tests of a Tall Cylindrical Liquid Storage Tank," by R.W. Clough and A. Niwa - Feb. 1979 (PB 301 167)A06

UCB/EERC-79/07 "The Design of Steel Energy Absorbing Restrainers and Their Incorporation into Nuclear Power Plants for Enhanced Safety: Volume 1 - Summary Report," by P.N. Spencer, V.F. Zackay, and E.R. Parker - Feb. 1979(UCB/EERC-79/07)A09

UCB/EERC-79/08 "The Design of Steel Energy Absorbing Restrainers and Their Incorporation into Nuclear Power Plants for Enhanced Safety: Volume 2 - The Development of Analyses for Reactor System Piping,""Simple Systems" by M.C. Lee, J. Penzien, A.K. Chopra and K, Suzuki "Complex Systems" by G.H. Powell, E.L. Wilson, R.W. Clough and D.G. Row - Feb. 1979(UCB/EERC-79/08)A10

UCB/EERC-79/09 "The Design of Steel Energy Absorbing Restrainers and Their Incorporation into Nuclear Power Plants for Enhanced Safety: Volume 3 - Evaluation of Commercial Steels," by W.S. Owen, R.M.N. Pelloux, R.O. Ritchie, M. Faral, T. Ohhashi, J. Toplosky, S.J. Hartman, V.F. Zackay and E.R. Parker - Feb. 1979(UCB/EERC-79/09)A04

UCB/EERC-79/10 "The Design of Steel Energy Absorbing Restrainers and Their Incorporation into Nuclear Power Plants for Enhanced Safety: Volume 4 - A Review of Energy-Absorbing Devices," by J.M. Kelly and M.S. Skinner - Feb. 1979(UCB/EERC-79/10)A04

UCB/EERC-79/11 "Conservatism In Summation Rules for Closely Spaced Modes," by J.M. Kelly and J.L. Sackman - May 1979(PB 301 328)A03

UCB/EERC-79/12 "Cyclic Loading Tests of Masonry Single Piers; Volume 3 - Height to Width Ratio of 0.5," by P.A. Hidalgo, R.L. Mayes, H.D. McNiven and R.W. Clough - May 1979(PB 301 321)A08

UCB/EERC-79/13 "Cyclic Behavior of Dense Course-Grained Materials in Relation to the Seismic Stability of Dams," by N.G. Banerjee, H.B. Seed and C.K. Chan - June 1979(PB 301 373)A13

UCB/EERC-79/14 "Seismic Behavior of Reinforced Concrete Interior Beam-Column Subassemblages," by S. Viwathanatepa, E.P. Popov and V.V. Bertero - June 1979(PB 301 326)A10

UCB/EERC-79/15 "Optimal Design of Localized Nonlinear Systems with Dual Performance Criteria Under Earthquake Excitations," by M.A. Bhatti - July 1979(PB 80 167 109)A06

UCB/EERC-79/16 "OPTDYN - A General Purpose Optimization Program for Problems with or without Dynamic Constraints," by M.A. Bhatti, E. Polak and K.S. Pister - July 1979(PB 80 167 091)A05

UCB/EERC-79/17 "ANSR-II, Analysis of Nonlinear Structural Response, Users Manual," by D.P. Mondkar and G.H. Powell July 1979(PB 80 113 301)A05

UCB/EERC-79/18 "Soil Structure Interaction in Different Seismic Environments," A. Gomez-Masso, J. Lysmer, J.-C. Chen and H.B. Seed - August 1979(PB 80 101 520)A04

UCB/EERC-79/19 "ARMA Models for Earthquake Ground Motions," by M.K. Chang, J.W. Kwiatkowski, R.F. Nau, R.M. Oliver and K.S. Pister - July 1979(PB 301 166)A05

UCB/EERC-79/20 "Hysteretic Behavior of Reinforced Concrete Structural Walls," by J.M. Vallenas, V.V. Bertero and E.P. Popov - August 1979(PB 80 165 905)A12

UCB/EERC-79/21 "Studies on High-Frequency Vibrations of Buildings - 1: The Column Effect," by J. Lubliner - August 1979 (PB 80 158 553)A03

UCB/EERC-79/22 "Effects of Generalized Loadings on Bond Reinforcing Bars Embedded in Confined Concrete Blocks," by S. Viwathanatepa, E.P. Popov and V.V. Bertero - August 1979(PB 81 124 018)A14

UCB/EERC-79/23 "Shaking Table Study of Single-Story Masonry Houses, Volume 1: Test Structures 1 and 2," by P. Gülkan, R.L. Mayes and R.W. Clough - Sept. 1979 (HUD-000 1763)A12

UCB/EERC-79/24 "Shaking Table Study of Single-Story Masonry Houses, Volume 2: Test Structures 3 and 4," by P. Gülkan, R.L. Mayes and R.W. Clough - Sept. 1979 (HUD-000 1836)A12

UCB/EERC-79/25 "Shaking Table Study of Single-Story Masonry Houses, Volume 3: Summary, Conclusions and Recommendations," by R.W. Clough, R.L. Mayes and P. Gülkan - Sept. 1979 (HUD-000 1837)A06

UCB/EERC-79/26 "Recommendations for a U.S.-Japan Cooperative Research Program Utilizing Large-Scale Testing Facilities," by U.S.-Japan Planning Group - Sept. 1979(PB 301 407)A06

UCB/EERC-79/27 "Earthquake-Induced Liquefaction Near Lake Amatitlan, Guatemala," by H.B. Seed, I. Arango, C.K. Chan, A. Gomez-Masso and R. Grant de Ascoli - Sept. 1979(NUREG-CR1341)A03

UCB/EERC-79/28 "Infill Panels: Their Influence on Seismic Response of Buildings," by J.W. Axley and V.V. Bertero Sept. 1979(PB 80 163 371)A10

UCB/EERC-79/29 "3D Truss Bar Element (Type 1) for the ANSR-II Program," by D.P. Mondkar and G.H. Powell - Nov. 1979 (PB 80 169 709)A02

UCB/EERC-79/30 "2D Beam-Column Element (Type 5 - Parallel Element Theory) for the ANSR-II Program," by D.G. Row, G.H. Powell and D.P. Mondkar - Dec. 1979(PB 80 167 224)A03

UCB/EERC-79/31 "3D Beam-Column Element (Type 2 - Parallel Element Theory) for the ANSR-II Program," by A. Riahi, G.H. Powell and D.P. Mondkar - Dec. 1979(PB 80 167 216)A03

UCB/EERC-79/32 "On Response of Structures to Stationary Excitation," by A. Der Kiureghian - Dec. 1979(PB 80166 929)A03

UCB/EERC-79/33 "Undisturbed Sampling and Cyclic Load Testing of Sands," by S. Singh, H.B. Seed and C.K. Chan Dec. 1979(ADA 087 298)A07

UCB/EERC-79/34 "Interaction Effects of Simultaneous Torsional and Compressional Cyclic Loading of Sand," by P.M. Griffin and W.N. Houston - Dec. 1979(ADA 092 352)A15

UCB/EERC-80/01 "Earthquake Response of Concrete Gravity Dams Including Hydrodynamic and Foundation Interaction Effects," by A.K. Chopra, P. Chakrabarti and S. Gupta - Jan. 1980(AD-A087297)A10

UCB/EERC-80/02 "Rocking Response of Rigid Blocks to Earthquakes," by C.S. Yim, A.K. Chopra and J. Penzien - Jan. 1980 (PB80 166 002)A04

UCB/EERC-80/03 "Optimum Inelastic Design of Seismic-Resistant Reinforced Concrete Frame Structures," by S.W. Zagajeski and V.V. Bertero - Jan. 1980(PB80 164 635)A06

UCB/EERC-80/04 "Effects of Amount and Arrangement of Wall-Panel Reinforcement on Hysteretic Behavior of Reinforced Concrete Walls," by R. Iliya and V.V. Bertero - Feb. 1980(PB81 122 525)A09

UCB/EERC-80/05 "Shaking Table Research on Concrete Dam Models," by A. Niwa and R.W. Clough - Sept. 1980(PB81 122 368)A06

UCB/EERC-80/06 "The Design of Steel Energy-Absorbing Restrainers and their Incorporation into Nuclear Power Plants for Enhanced Safety (Vol 1A): Piping with Energy Absorbing Restrainers: Parameter Study on Small Systems," by G.H. Powell, C. Oughourlian and J. Simons - June 1980

UCB/EERC-80/07 "Inelastic Torsional Response of Structures Subjected to Earthquake Ground Motions," by Y. Yamazaki April 1980(PB81 122 327)A08

UCB/EERC-80/08 "Study of X-Braced Steel Frame Structures Under Earthquake Simulation," by Y. Ghanaat - April 1980 (PB81 122 335)A11

UCB/EERC-80/09 "Hybrid Modelling of Soil-Structure Interaction," by S. Gupta, T.W. Lin, J. Penzien and C.S. Yeh May 1980(PB81 122 319)A07

UCB/EERC-80/10 "General Applicability of a Nonlinear Model of a One Story Steel Frame," by B.I. Sveinsson and H.D. McNiven - May 1980(PB81 124 877)A06

UCB/EERC-80/11 "A Green-Function Method for Wave Interaction with a Submerged Body," by W. Kioka - April 1980 (PB81 122 269)A07

UCB/EERC-80/12 "Hydrodynamic Pressure and Added Mass for Axisymmetric Bodies," by F. Nilrat - May 1980(PB81 122 343)A08

UCB/EERC-80/13 "Treatment of Non-Linear Drag Forces Acting on Offshore Platforms," by B.V. Dao and J. Penzien May 1980(PB81 153 413)A07

UCB/EERC-80/14 "2D Plane/Axisymmetric Solid Element (Type 3 - Elastic or Elastic-Perfectly Plastic) for the ANSR-II Program," by D.P. Mondkar and G.H. Powell - July 1980(PB81 122 350)A03

UCB/EERC-80/15 "A Response Spectrum Method for Random Vibrations," by A. Der Kiureghian - June 1980(PB81 122 301)A03

UCB/EERC-80/16 "Cyclic Inelastic Buckling of Tubular Steel Braces," by V.A. Zayas, E.P. Popov and S.A. Mahin June 1980(PB81 124 885)A10

UCB/EERC-80/17 "Dynamic Response of Simple Arch Dams Including Hydrodynamic Interaction," by C.S. Porter and A.K. Chopra - July 1980(PB81 124 000)A13

UCB/EERC-80/18 "Experimental Testing of a Friction Damped Aseismic Base Isolation System with Fail-Safe Characteristics," by J.M. Kelly, K.E. Beucke and M.S. Skinner - July 1980(PB81 148 595)A04

UCB/EERC-80/19 "The Design of Steel Energy-Absorbing Restrainers and their Incorporation into Nuclear Power Plants for Enhanced Safety (Vol 1B): Stochastic Seismic Analyses of Nuclear Power Plant Structures and Piping Systems Subjected to Multiple Support Excitations," by M.C. Lee and J. Penzien - June 1980

UCB/EERC-80/20 "The Design of Steel Energy-Absorbing Restrainers and their Incorporation into Nuclear Power Plants for Enhanced Safety (Vol 1C): Numerical Method for Dynamic Substructure Analysis," by J.M. Dickens and E.L. Wilson - June 1980

UCB/EERC-80/21 "The Design of Steel Energy-Absorbing Restrainers and their Incorporation into Nuclear Power Plants for Enhanced Safety (Vol 2): Development and Testing of Restraints for Nuclear Piping Systems," by J.M. Kelly and M.S. Skinner - June 1980

UCB/EERC-80/22 "3D Solid Element (Type 4-Elastic or Elastic-Perfectly-Plastic) for the ANSR-II Program," by D.P. Mondkar and G.H. Powell - July 1980(PB81 123 242)A03

UCB/EERC-80/23 "Gap-Friction Element (Type 5) for the ANSR-II Program," by D.P. Mondkar and G.H. Powell - July 1980 (PB81 122 285)A03

UCB/EERC-80/24 "U-Bar Restraint Element (Type 11) for the ANSR-II Program," by C. Oughourlian and G.H. Powell July 1980(PB81 122 293)A03

UCB/EERC-80/25 "Testing of a Natural Rubber Base Isolation System by an Explosively Simulated Earthquake," by J.M. Kelly - August 1980(PB81 201 360)A04

UCB/EERC-80/26 "Input Identification from Structural Vibrational Response," by Y. Hu - August 1980(PB81 152 308)A05

UCB/EERC-80/27 "Cyclic Inelastic Behavior of Steel Offshore Structures," by V.A. Zayas, S.A. Mahin and E.P. Popov August 1980(PB81 196 180)A15

UCB/EERC-80/28 "Shaking Table Testing of a Reinforced Concrete Frame with Biaxial Response," by M.G. Oliva October 1980(PB81 154 304)A10

UCB/EERC-80/29 "Dynamic Properties of a Twelve-Story Prefabricated Panel Building," by J.G. Bouwkamp, J.P. Kollegger and R.M. Stephen - October 1980(PB82 117 128)A06

UCB/EERC-80/30 "Dynamic Properties of an Eight-Story Prefabricated Panel Building," by J.G. Bouwkamp, J.P. Kollegger and R.M. Stephen - October 1980(PB81 200 313)A05

UCB/EERC-80/31 "Predictive Dynamic Response of Panel Type Structures Under Earthquakes," by J.P. Kollegger and J.G. Bouwkamp - October 1980(PB81 152 316)A04

UCB/EERC-80/32 "The Design of Steel Energy-Absorbing Restrainers and their Incorporation into Nuclear Power Plants for Enhanced Safety (Vol 3): Testing of Commercial Steels in Low-Cycle Torsional Fatigue," by P. Spencer, E.R. Parker, E. Jongewaard and M. Drory

UCB/EERC-80/33 "The Design of Steel Energy-Absorbing Restrainers and their Incorporation into Nuclear Power Plants for Enhanced Safety (Vol 4): Shaking Table Tests of Piping Systems with Energy-Absorbing Restrainers," by S.F. Stiemer and W.G. Godden - Sept. 1980

UCB/EERC-80/34 "The Design of Steel Energy-Absorbing Restrainers and their Incorporation into Nuclear Power Plants for Enhanced Safety (Vol 5): Summary Report," by P. Spencer

UCB/EERC-80/35 "Experimental Testing of an Energy-Absorbing Base Isolation System," by J.M. Kelly, M.S. Skinner and K.E. Beucke - October 1980(PB81 154 072)A04

UCB/EERC-80/36 "Simulating and Analyzing Artificial Non-Stationary Earthquake Ground Motions," by R.F. Nau, R.M. Oliver and K.S. Pister - October 1980(PB81 153 397)A04

UCB/EERC-80/37 "Earthquake Engineering at Berkeley - 1980," - Sept. 1980(PB81 205 874)A09

UCB/EERC-80/38 "Inelastic Seismic Analysis of Large Panel Buildings," by V. Schricker and G.H. Powell - Sept. 1980 (PB81 154 338)A13

UCB/EERC-80/39 "Dynamic Response of Embankment, Concrete-Gravity and Arch Dams Including Hydrodynamic Interaction," by J.F. Hall and A.K. Chopra - October 1980(PB81 152 324)A11

UCB/EERC-80/40 "Inelastic Buckling of Steel Struts Under Cyclic Load Reversal," by R.G. Black, W.A. Wenger and E.P. Popov - October 1980(PB81 154 312)A08

UCB/EERC-80/41 "Influence of Site Characteristics on Building Damage During the October 3, 1974 Lima Earthquake," by P. Repetto, I. Arango and H.B. Seed - Sept. 1980(PB81 161 739)A05

UCB/EERC-80/42 "Evaluation of a Shaking Table Test Program on Response Behavior of a Two Story Reinforced Concrete Frame," by J.M. Blondet, R.W. Clough and S.A. Mahin

UCB/EERC-80/43 "Modelling of Soil-Structure Interaction by Finite and Infinite Elements," by F. Medina - December 1980(PB81 229 270)A04

UCB/EERC-81/01 "Control of Seismic Response of Piping Systems and Other Structures by Base Isolation," edited by J.M. Kelly - January 1981 (PB81 200 735)A05

UCB/EERC-81/02 "OPTNSR - An Interactive Software System for Optimal Design of Statically and Dynamically Loaded Structures with Nonlinear Response," by M.A. Bhatti, V. Ciampi and K.S. Pister - January 1981 (PB81 218 851)A09

UCB/EERC-81/03 "Analysis of Local Variations in Free Field Seismic Ground Motions," by J.-C. Chen, J. Lysmer and H.B. Seed - January 1981 (AD-A099508)A13

UCB/EERC-81/04 "Inelastic Structural Modeling of Braced Offshore Platforms for Seismic Loading," by V.A. Zayas, P.-S.B. Shing, S.A. Mahin and E.P. Popov - January 1981(PB82 138 777)A07

UCB/EERC-81/05 "Dynamic Response of Light Equipment in Structures," by A. Der Kiureghian, J.L. Sackman and B. Nour-Omid - April 1981 (PB81 218 497)A04

UCB/EERC-81/06 "Preliminary Experimental Investigation of a Broad Base Liquid Storage Tank," by J.G. Bouwkamp, J.P. Kollegger and R.M. Stephen - May 1981(PB82 140 385)A03

UCB/EERC-81/07 "The Seismic Resistant Design of Reinforced Concrete Coupled Structural Walls," by A.E. Aktan and V.V. Bertero - June 1981(PB82 113 358)A11

UCB/EERC-81/08 "The Undrained Shearing Resistance of Cohesive Soils at Large Deformations," by M.R. Pyles and H.B. Seed - August 1981

UCB/EERC-81/09 "Experimental Behavior of a Spatial Piping System with Steel Energy Absorbers Subjected to a Simulated Differential Seismic Input," by S.F. Stiemer, W.G. Godden and J.M. Kelly - July 1981

UCB/EERC-81/10 "Evaluation of Seismic Design Provisions for Masonry in the United States," by B.I. Sveinsson, R.L. Mayes and H.D. McNiven - August 1981 (PB82 166 075)A08

UCB/EERC-81/11 "Two-Dimensional Hybrid Modelling of Soil-Structure Interaction," by T.-J. Tzong, S. Gupta and J. Penzien - August 1981(PB82 142 118)A04

UCB/EERC-81/12 "Studies on Effects of Infills in Seismic Resistant R/C Construction," by S. Brokken and V.V. Bertero - September 1981 (PB82 166 190)A09

UCB/EERC-81/13 "Linear Models to Predict the Nonlinear Seismic Behavior of a One-Story Steel Frame," by H. Valdimarsson, A.H. Shah and H.D. McNiven - September 1981(PB82 138 793)A07

UCB/EERC-81/14 "TLUSH: A Computer Program for the Three-Dimensional Dynamic Analysis of Earth Dams," by T. Kagawa, L.H. Mejia, H.B. Seed and J. Lysmer - September 1981(PB82 139 940)A06

UCB/EERC-81/15 "Three Dimensional Dynamic Response Analysis of Earth Dams," by L.H. Mejia and H.B. Seed - September 1981 (PB82 137 274)A12

UCB/EERC-81/16 "Experimental Study of Lead and Elastomeric Dampers for Base Isolation Systems," by J.M. Kelly and S.B. Hodder - October 1981 (PB82 166 182)A05

UCB/EERC-81/17 "The Influence of Base Isolation on the Seismic Response of Light Secondary Equipment," by J.M. Kelly - April 1981 (PB82 255 266)A04

UCB/EERC-81/18 "Studies on Evaluation of Shaking Table Response Analysis Procedures," by J. Marcial Blondet - November 1981 (PB82 197 278)A10

UCB/EERC-81/19 "DELIGHT.STRUCT: A Computer-Aided Design Environment for Structural Engineering," by R.J. Balling, K.S. Pister and E. Polak - December 1981 (PB82 218 496)A07

UCB/EERC-81/20 "Optimal Design of Seismic-Resistant Planar Steel Frames," by R.J. Balling, V. Ciampi, K.S. Pister and E. Polak - December 1981 (PB82 220 179)A07

UCB/EERC-82/01 "Dynamic Behavior of Ground for Seismic Analysis of Lifeline Systems," by T. Sato and A. Der Kiureghian - January 1982 (PB82 218 926)A05

UCB/EERC-82/02 "Shaking Table Tests of a Tubular Steel Frame Model," by Y. Ghanaat and R. W. Clough - January 1982 (PB82 220 161)A07

UCB/EERC-82/03 "Behavior of a Piping System under Seismic Excitation: Experimental Investigations of a Spatial Piping System supported by Mechanical Shock Arrestors and Steel Energy Absorbing Devices under Seismic Excitation," by S. Schneider, H.-M. Lee and W. G. Godden - May 1982 (PB83 172 544)A09

UCB/EERC-82/04 "New Approaches for the Dynamic Analysis of Large Structural Systems," by E. L. Wilson - June 1982 (PB83 148 080)A05

UCB/EERC-82/05 "Model Study of Effects of Damage on the Vibration Properties of Steel Offshore Platforms," by F. Shahrivar and J. G. Bouwkamp - June 1982 (PB83 148 742)A10

UCB/EERC-82/06 "States of the Art and Practice in the Optimum Seismic Design and Analytical Response Prediction of R/C Frame-Wall Structures," by A. E. Aktan and V. V. Bertero - July 1982 (PB83 147 736)A05

UCB/EERC-82/07 "Further Study of the Earthquake Response of a Broad Cylindrical Liquid-Storage Tank Model," by G. C. Manos and R. W. Clough - July 1982 (PB83 147 744)A11

UCB/EERC-82/08 "An Evaluation of the Design and Analytical Seismic Response of a Seven Story Reinforced Concrete Frame - Wall Structure," by F. A. Charney and V. V. Bertero - July 1982(PB83 157 628)A09

UCB/EERC-82/09 "Fluid-Structure Interactions: Added Mass Computations for Incompressible Fluid," by J. S.-H. Kuo - August 1982 (PB83 156 281)A07

UCB/EERC-82/10 "Joint-Opening Nonlinear Mechanism: Interface Smeared Crack Model," by J. S.-H. Kuo - August 1982 (PB83 149 195)A05

UCB/EERC-82/11 "Dynamic Response Analysis of Techi Dam," by R. W. Clough, R. M. Stephen and J. S.-H. Kuo - August 1982 (PB83 147 496)A06

UCB/EERC-82/12 "Prediction of the Seismic Responses of R/C Frame-Coupled Wall Structures," by A. E. Aktan, V. V. Bertero and M. Piazza - August 1982 (PB83 149 203)A09

UCB/EERC-82/13 "Preliminary Report on the SMART 1 Strong Motion Array in Taiwan," by B. A. Bolt, C. H. Loh, J. Penzien, Y. B. Tsai and Y. T. Yeh - August 1982 (PB83 159 400)A10

UCB/EERC-82/14 "Shaking-Table Studies of an Eccentrically X-Braced Steel Structure," by M. S. Yang - September 1982 (PB83 260 778)A12

UCB/EERC-82/15 "The Performance of Stairways in Earthquakes," by C. Roha, J. W. Axley and V. V. Bertero - September 1982 (PB83 157 693)A07

UCB/EERC-82/16 "The Behavior of Submerged Multiple Bodies in Earthquakes," by W.-G. Liao - Sept. 1982 (PB83 158 709)A07

UCB/EERC-82/17 "Effects of Concrete Types and Loading Conditions on Local Bond-Slip Relationships," by A. D. Cowell, E. P. Popov and V. V. Bertero - September 1982 (PB83 153 577)A04

UCB/EERC-82/18 "Mechanical Behavior of Shear Wall Vertical Boundary Members: An Experimental Investigation," by M. T. Wagner and V. V. Bertero - October 1982 (PB83 159 764)A05

UCB/EERC-82/19 "Experimental Studies of Multi-support Seismic Loading on Piping Systems," by J. M. Kelly and A. D. Cowell - November 1982

UCB/EERC-82/20 "Generalized Plastic Hinge Concepts for 3D Beam-Column Elements," by P. F.-S. Chen and G. H. Powell - November 1982 (PB03 247 981)A13

UCB/EERC-82/21 "ANSR-III: General Purpose Computer Program for Nonlinear Structural Analysis," by C. V. Oughourlian and G. H. Powell - November 1982 (PB83 251 330)A12

UCB/EERC-82/22 "Solution Strategies for Statically Loaded Nonlinear Structures," by J. W. Simons and G. H. Powell - November 1982 (PB83 197 970)A06

UCB/EERC-82/23 "Analytical Model of Deformed Bar Anchorages under Generalized Excitations," by V. Ciampi, R. Eligehausen, V. V. Bertero and E. P. Popov - November 1982 (PB83 169 532)A06

UCB/EERC-82/24 "A Mathematical Model for the Response of Masonry Walls to Dynamic Excitations," by H. Sucuoğlu, Y. Mengi and H. D. McNiven - November 1982 (PB83 169 011)A07

UCB/EERC-82/25 "Earthquake Response Considerations of Broad Liquid Storage Tanks," by F. J. Cambra - November 1982 (PB83 251 215)A09

UCB/EERC-82/26 "Computational Models for Cyclic Plasticity, Rate Dependence and Creep," by B. Mosaddad and G. H. Powell - November 1982 (PB83 245 829)A08

UCB/EERC-82/27 "Inelastic Analysis of Piping and Tubular Structures," by M. Mahasuverachai and G. H. Powell - November 1982 (PB83 249 987)A07

UCB/EERC-83/01 "The Economic Feasibility of Seismic Rehabilitation of Buildings by Base Isolation," by J. M. Kelly - January 1983 (PB83 197 988)A05

UCB/EERC-83/02 "Seismic Moment Connections for Moment-Resisting Steel Frames," by E. P. Popov - January 1983 (PB83 195 412)A04

UCB/EERC-83/03 "Design of Links and Beam-to-Column Connections for Eccentrically Braced Steel Frames," by E. P. Popov and J. O. Malley - January 1983 (PB83 194 811)A04

UCB/EERC-83/04 "Numerical Techniques for the Evaluation of Soil-Structure Interaction Effects in the Time Domain," by E. Bayo and E. L. Wilson - February 1983 (PB83 245 605)A09

UCB/EERC-83/05 "A Transducer for Measuring the Internal Forces in the Columns of a Frame-Wall Reinforced Concrete Structure," by R. Sause and V. V. Bertero - May 1983 (PB84 119 494)A06

UCB/EERC-83/06 "Dynamic Interactions between Floating Ice and Offshore Structures," by P. Croteau - May 1983 (PB84 119 486)A16

UCB/EERC-83/07 "Dynamic Analysis of Multiply Tuned and Arbitrarily Supported Secondary Systems," by T. Igusa and A. Der Kiureghian - June 1983 (PB84 118 272)A11

UCB/EERC-83/08 "A Laboratory Study of Submerged Multi-body Systems in Earthquakes," by G. R. Ansari - June 1983 (PB83 261 842)A17

UCB/EERC-83/09 "Effects of Transient Foundation Uplift on Earthquake Response of Structures," by C.-S. Yim and A. K. Chopra - June 1983 (PB83 261 396)A07

UCB/EERC-83/10 "Optimal Design of Friction-Braced Frames under Seismic Loading," by M. A. Austin and K. S. Pister - June 1983 (PB84 119 288)A06

UCB/EERC-83/11 "Shaking Table Study of Single-Story Masonry Houses: Dynamic Performance under Three Component Seismic Input and Recommendations," by G. C. Manos, R. W. Clough and R. L. Mayes - June 1983

UCB/EERC-83/12 "Experimental Error Propagation in Pseudodynamic Testing," by P. B. Shing and S. A. Mahin - June 1983 (PB84 119 270)A09

UCB/EERC-83/13 "Experimental and Analytical Predictions of the Mechanical Characteristics of a 1/5-scale Model of a 7-story R/C Frame-Wall Building Structure," by A. E. Aktan, V. V. Bertero, A. A. Chowdhury and T. Nagashima - August 1983 (PB84 119 213)A07

UCB/EERC-83/14 "Shaking Table Tests of Large-Panel Precast Concrete Building System Assemblages," by M. G. Oliva and R. W. Clough - August 1983

UCB/EERC-83/15 "Seismic Behavior of Active Beam Links in Eccentrically Braced Frames," by K. D. Hjelmstad and E. P. Popov - July 1983 (PB84 119 676)A09

UCB/EERC-83/16 "System Identification of Structures with Joint Rotation," by J. S. Dimsdale and H. D. McNiven - July 1983

UCB/EERC-83/17 "Construction of Inelastic Response Spectra for Single-Degree-of-Freedom Systems," by S. Mahin and J. Lin - July 1983

UCB/EERC-83/18 "Interactive Computer Analysis Methods for Predicting the Inelastic Cyclic Behaviour of Structural Sections," by S. Kaba and S. Mahin - July 1983 (PB84 192 012) A06

UCB/EERC-83/19 "Effects of Bond Deterioration on Hysteretic Behavior of Reinforced Concrete Joints," by F.C. Filippou, E.P. Popov and V.V. Bertero - August 1983 (PB84 192 020) A10

UCB/EERC-83/20 "Analytical and Experimental Correlation of Large-Panel Precast Building System Performance," by M.G. Oliva, R.W. Clough, M. Velkov, P. Gavrilovic and J. Petrovski - November 1983

UCB/EERC-83/21 "Mechanical Characteristics of Materials Used in a 1/5 Scale Model of a 7-Story Reinforced Concrete Test Structure," by V.V. Bertero, A.E. Aktan, H.G. Harris and A.A. Chowdhury - September 1983 (PB84 193 697) A05

UCB/EERC-83/22 "Hybrid Modelling of Soil-Structure Interaction in Layered Media," by T.-J. Tzong and J. Penzien - October 1983 (PB84 192 178) A08

UCB/EERC-83/23 "Local Bond Stress-Slip Relationships of Deformed Bars under Generalized Excitations," by R. Eligehausen, E.P. Popov and V.V. Bertero - October 1983 (PB84 192 848) A09

UCB/EERC-83/24 "Design Considerations for Shear Links in Eccentrically Braced Frames," by J.O. Malley and E.P. Popov - November 1983 (PB84 192 186) A07

UCB/EERC-84/01 "Pseudodynamic Test Method for Seismic Performance Evaluation: Theory and Implementation," by P.-S. B. Shing and S. A. Mahin - January 1984 (PB84 190 644) A08

UCB/EERC-84/02 "Dynamic Response Behavior of Xiang Hong Dian Dam," by R.W. Clough, K.-T. Chang, H.-Q. Chen, R.M. Stephen, G.-L. Wang, and Y. Ghanaat - April 1984

UCB/EERC-84/03 "Refined Modelling of Reinforced Concrete Columns for Seismic Analysis," by S.A. Kaba and S.A. Mahin - April, 1984

UCB/EERC-84/04 "A New Floor Response Spectrum Method for Seismic Analysis of Multiply Supported Secondary Systems," by A. Asfura and A. Der Kiureghian - June 1984

UCB/EERC-84/05 "Earthquake Simulation Tests and Associated Studies of a 1/5th-scale Model of a 7-Story R/C Frame-Wall Test Structure," by V.V. Bertero, A.E. Aktan, F.A. Charney and R. Sause - June 1984

UCB/EERC-84/06 "R/C Structural Walls: Seismic Design for Shear," by A.E. Aktan and V.V. Bertero

UCB/EERC-84/07 "Behavior of Interior and Exterior Flat-Plate Connections subjected to Inelastic Load Reversals," by H.L. Zee and J.P. Moehle

UCB/EERC-84/08 "Experimental Study of the Seismic Behavior of a two-story Flat-Plate Structure," by J.W. Diebold and J.P. Moehle

UCB/EERC-84/09 "Phenomenological Modeling of Steel Braces under Cyclic Loading," by K. Ikeda, S.A. Mahin and S.N. Dermitzakis - May 1984

UCB/EERC-84/10 "Earthquake Analysis and Response of Concrete Gravity Dams," by G. Fenves and A.K. Chopra - August 1984

UCB/EERC-84/11 "EAGD-84: A Computer Program for Earthquake Analysis of Concrete Gravity Dams," by G. Fenves and A.K. Chopra - August 1984

UCB/EERC-84/12 "A Refined Physical Theory Model for Predicting the Seismic Behavior of Braced Steel Frames," by K. Ikeda and S.A. Mahin - July 1984

UCB/EERC-84/13 "Earthquake Engineering Research at Berkeley - 1984" - August 1984

UCB/EERC-84/14 "Moduli and Damping Factors for Dynamic Analyses of Cohesionless Soils," by H.B. Seed, R.T. Wong, I.M. Idriss and K. Tokimatsu - September 1984

UCB/EERC-84/15 "The Influence of SPT Procedures in Soil Liquefaction Resistance Evaluations," by H. B. Seed, K. Tokimatsu, L. F. Harder and R. M. Chung - October 1984

UCB/EERC-84/16 "Simplified Procedures for the Evaluation of Settlements in Sands Due to Earthquake Shaking," by K. Tokimatsu and H. B. Seed - October 1984

UCB/EERC-84/17 "Evaluation and Improvement of Energy Absorption Characteristics of Bridges under Seismic Conditions," by R. A. Imbsen and J. Penzien - November 1984

UCB/EERC-84/18 "Structure-Foundation Interactions under Dynamic Loads," by W. D. Liu and J. Penzien - November 1984

UCB/EERC-84/19 "Seismic Modelling of Deep Foundations," by C.-H. Chen and J. Penzien - November 1984

UCB/EERC-84/20 "Dynamic Response Behavior of Quan Shui Dam," by R. W. Clough, K.-T. Chang, H.-Q. Chen, R. M. Stephen, Y. Ghanaat and J.-H. Qi - November 1984

UCB/EERC-85/01 "Simplified Methods of Analysis for Earthquake Resistant Design of Buildings," by E.F. Cruz and A.K. Chopra - Feb. 1985

UCB/EERC-85/02 "Estimation of Seismic Wave Coherency and Rupture Velocity using the SMART 1 Strong-Motion Array Recordings," by N.A. Abrahamson - March 1985

UCB/EERC-85/03 "Dynamic Properties of a Thirty Story Condominium Tower Building," by R.M. Stephen, E.L. Wilson and N. Stander - April 1985

UCB/EERC-85/04 "Development of Substructuring Techniques for On-Line Computer Controlled Seismic Performance Testing," by S. Dermitzakis and S. Mahin - May 1985

UCB/EERC-85/05 "A Simple Model for Reinforcing Bar Anchorages under Cyclic Excitations," by F.C. Filippou - March 1985

UCB/EERC-85/06 "Racking Behavior of Wood-Framed Gypsum Panels under Dynamic Load," by M.G. Oliva - June 1985

UCB/EERC-85/07 "Earthquake Analysis and Response of Concrete Arch Dams," by K.-L. Fok and A.K. Chopra - June 1985

UCB/EERC-85/08 "Effect of Inelastic Behavior on the Analysis and Design of Earthquake Resistant Structures," by J.P. Lin and S.A. Mahin - June 1985

UCB/EERC-85/09 "Earthquake Simulator Testing of Base Isolated Bridge Deck Superstructures," by J.M. Kelly and I.G. Buckle

UCB/EERC-85/10 "Simplified Analysis for Earthquake Resistant Design of Concrete Gravity Dams," by G. Fenves and A.K. Chopra - September 1985

UCB/EERC-85/11 "Dynamic Interaction Effects in Arch Dams," by R.W. Clough, K.-T. Chang, H.-Q. Chen and Y. Ghanaat - October 1985

UCB/EERC-85/12 "Dynamic Response of Long Valley Dam in the Mammoth Lake Earthquake Series of May 25-27, 1980," by S. Lai and H.B. Seed - November 1985

UCB/EERC-85/13 "A Methodology for Computer-Aided Design of Earthquake-Resistant Steel Structures," by M.A. Austin, K.S. Pister and S.A. Mahin - December 1985